AUSTRALIA
University of Southern Queensland
Faculty of Health, Engineering and Sciences

MACHINABILITY OF NATURAL FIBRE REINFORCED POLYMERIC COMPOSITES

A Dissertation Submitted by

TALAL S. AL-SAEED
0061022931

For the Award of
Doctor of Philosophy
2014

Principle Supervisor: Dr B.F. Yousif

ABSTRACT

From an industrial perspective, there are some issues with the machinability of synthetic fibre/polymer composites (glass fibres), including hole accuracy, delamination, appearance and energy consumption. These are mainly due to the abrasive nature of the synthetic fibres. Introducing natural fibres as reinforcement to the polymeric composite may overcome some of these issues, as natural fibres have less abrasive effects compared to synthetic fibres. Moreover, natural fibres are becoming an attractive candidate to replace synthetic fibres for several applications.

In the current study, epoxy composites based on date palm fibres were developed. The interfacial adhesion of the date palm fibres with the matrix is first evaluated for optimum fibre diameter and NaOH concentrations through a single fibre pull out test. With regards to machinability of the composite, drilling experiments were conducted on neat epoxy, glass/epoxy and date/epoxy composites. A new dynamometer was developed and fabricated locally. The influence of the cutting speed, feed rate and drill diameter on the machinability of the composites was evaluated in terms of hole accuracy, inner and outer delamination, specific cutting pressure and machining power. Scanning electron microscopy and optical microscopy were used to examine the damaged features in the experiments of interfacial adhesion and machinability. The ANOVA approach was used to identify the most effective parameters on the machinability of the composites.

The results revealed that NaOH concentration in the treatment solution affects the strength and the interfacial adhesion of the fibre with the matrix. Six per cent NaOH concentration is the optimum concentration in which there was less damage to the strength of the fibre and enhancement to the interfacial adhesion of the fibre with the matrix. Tensile properties of the epoxy were found to be improved with the addition of either natural or synthetic fibres. However, glass fibres improved the tensile strength of the epoxy significantly compared to the date palm fibre, even though glass fibres suffered from detachment and a pull out mechanism during loading conditions.

In the drilling process for all materials, there were three regions observed: inner, intermediate and outer. The thrust and torque behaviour with the drilling time was divided into these three regions. The peak values were observed in the intermediate regions in which the shears occurred at a higher level with the thrust force. The presence of glass fibres in the epoxy composites assisted in reducing crack propagation at the inlet regions; however, it highly deteriorated the outlet region, as detachments and a decomposition mechanism were observed. For neat epoxy, cracks and fractures were the main damage features noticed. Meanwhile, the presence of date palm fibre in the epoxy improved the machinability of the composites, as it required similar values of torque and thrust to that of neat epoxy, while glass fibres needed more power. Date palm fibres assisted in reducing cracks in the inner and outer regions of the hole of the composites, even though pull out and detachments were observed.

Hole accuracy is highly controlled by the operating parameters, as an increase in the drilling speed and feed rate resulted in high error percentage of hole accuracy for all materials. The addition of date palm fibres had a lower error percentage to the hole accuracy compared to the glass fibres, and this was mainly due to the abrasive nature of the glass fibres. Micrographs show fragmentations and pull out of fibres for neat epoxy and glass/epoxy composites, respectively. Meanwhile, date/epoxy exhibited fragmentation at the edge of the holes, which was considered less damage compared to the glass/epoxy. The specific cutting pressure reduced significantly with an increase in the feed rate. However, there was no clear effect from the drilling speeds on the specific cutting pressure. The most influential parameter was the drill diameter, as there was a large increase in the specific cutting pressure with an increase of the drill diameter. Conversely, the drilling process for all materials resulted in high roughness values for the inner surface of the holes. The highest roughness for the inner surface was recorded when the glass/epoxy was drilled. Nevertheless, the addition of the date palm fibre also contributed to an increase of surface roughness of the composites. However, there was less of an increase in the roughness of the inner surface with the addition of date palm fibres to the composite compared to glass fibres. Machining power was influenced by the higher operating parameter values; however, for the intermediate and low range operating parameter values, there was not much difference in the machining power of all materials.

Interestingly, the machining power for the date/epoxy composite was competitive when compared to the neat epoxy, which is a promising result for the use of date palm fibre from a machinability perspective.

LIST OF PUBLICATIONS

1. T Alsaeed, H Ku and BF Yousif, 'Experimental investigation on the interfacial adhesion of date palm fibres with epoxy matrix', paper presented at *Composites Australia and the CRC for Advanced Composite Structures 2012 Conference – 'Diversity in Composites'*, March 2012, Sydney, Australia.
2. T Alsaeed, H Ku and BF Yousif 2013, 'A review on the mechanical properties and machinability of natural fibre reinforced composites', *International Journal of Precision Technology*, vol. 3, pp. 152–182.
3. T Alsaeed, H Ku and BF Yousif 2013, 'The potential of using date palm fibres as reinforcement for polymeric composites', *Materials and Design*, vol. 43, pp. 177–184.
4. T Alsaeed and BF Yousif, 'Machining performance of synthetic and natural fibre reinforced polymer composites', *Journal of Materials Processing Technology*, under review.
5. T Alsaeed and BF Yousif, 'Machinability of glass/date palm fibre epoxy composites', *International Journal of Machining and Machinability of Materials*, under review.

CERTIFICATION OF DISSERTATION

I certify that the ideas, designs and experimental work, results, analyses and conclusions set out in this dissertation are entirely my own effort, except where otherwise indicated and acknowledged.

I further certify that the work is original and has not been previously submitted for assessment in any other course or institution, except where specifically stated.

TALAL S. AL-SAEED
0061022931

__________________________ __________________________

Signature of Candidate Date

ENDORSEMENT

Signature of Principle Supervisor Signature of Associate Supervisor

Date Date

ACKNOWLEDGEMENTS

First, I express my thanks to Allah my lord who supports me all the time with this work. I would also like to express my most sincere appreciation to my PhD project supervisor Dr B.F. Yousif for all his support, encouragement, valuable input and guidance provided at every stage of this thesis. I would also like to extend my gratitude towards all departmental and technical staff at University of Southern Queensland for their assistance and support in using the facilities and materials for conducting the experimental work.

In addition, I wish to express my deepest appreciation to my mother, wife, friends and all of my family for their constant support throughout this study.

TABLE OF CONTENTS

LIST OF TABLES

LIST OF FIGURES

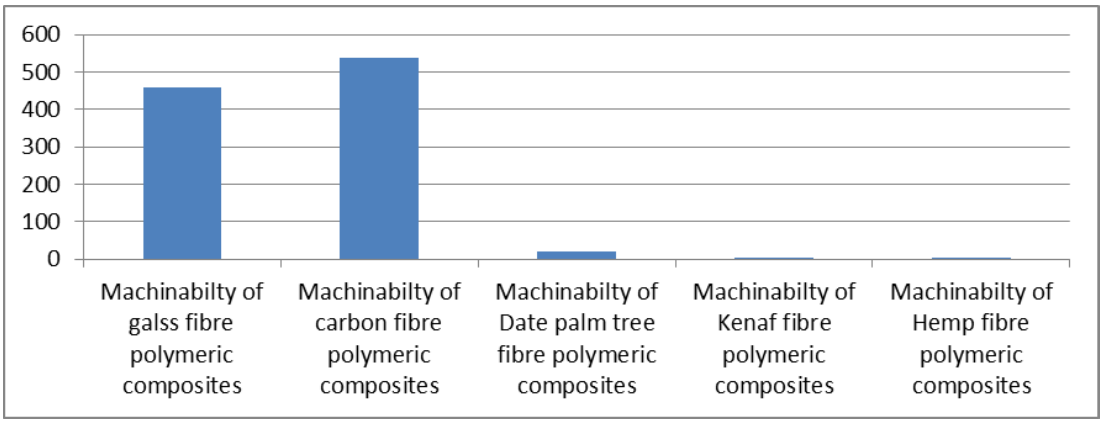

List of abbreviations

ANOVA	Analysis Of Variance
CO_2	Carbon Dioxide
DPFEC	date palm fibre reinforced epoxy composite
EDTA	ethylene diamante tetraacetic acid
FRP	fibre reinforced polymer
GFEC	glass fibre reinforced epoxy composites
GFRE	glass fibre reinforced epoxy
GFRP	glass fibre reinforced polyester
HCl	HydroChloric Acid
HDPE	high density polyestthline
HSS	high speed steel
kc	specific cutting force
L/D	length to diamter ratio
L_c	critical length
NaClO	*Sodium hypochlorite*
NaOH	*sodium hydroxide*
NE	neat epoxy
R_a	average roughness
SEM	scanning electron microscopy

T-DPFRE	Treated date palm fibre reinforced epoxy
UT-DPFRE	Untreated date palm fibre reinforced epoxy
V_f	volume fraction

CHAPTER 1: INTRODUCTION

1.1 Introduction

In recent years, an increased awareness of non-renewable resources becoming limited and a predictable reliance on renewable resources have been initiated due to environment and sustainability issues. This century has seen extraordinary achievements in green technology in the field of materials science through the growth of bio-materials. Natural fibres have become a promising alternative reinforcement fibre to replace synthetic fibres (Azwa et al., 2013, Heitzmann et al., 2013, Kwon et al., 2014). The use of natural fibres has many advantages compared with using synthetic fibres (glass or carbon fibres). They are low in cost because of their large quantity, are biodegradable, are flexible during processing with less resultant machine wear, have minimal health hazards, are low density, have a desirable fibre aspect ratio and have a relatively high tensile modulus. Natural fibres come from different sources, including wood, pulp, cotton, bark, nutshells, bagasse, corncobs, bamboo, cereal straw and vegetables. These fibres mainly consist of cellulose, lignin, hemicelluloses, pectins and extractives, depending on their origin. Previously, the applications of natural fibres were limited to home goods, light components and so on. This is because of the lack of understanding of the fibres' performance at severing loading conditions (i.e. mechanical, tribological and machining loads). The combination of environmental regulation and industrial demands motivates researchers to explore the potential for using natural fibres in new areas in industries. Despite this, the research in this area is still new and the need for further investigation is recommended by many recent reports (Kwon et al., 2014, Azwa et al., 2013, Alsaeed et al., 2013a). The candidate found that there is lack of studies on interfacial adhesion of the natural fibres and its effect on fibre/polymer composites for machinability purposes.

From industrial and academic points of view, there is always a major problem raised with regard to machining and/or fabricating synthetic fibre composites. This is that the inert nature of the common synthetic fibres means they are abrasive (Nirmal et al., 2012, Karnik et al., 2008, Shyha et al., 2010). The abrasiveness of the synthetic fibres damages the system components and may cause failure of even hard steel tools. In addition, the quality of machining synthetic fibre/polymer composites always suffers from a poor finish. That is, there is refractoriness of the fibres to machinability in terms of delamination size, surface roughness (R_a), cutting power, thrust force, material removal rate and bearing strength (Rajamurugan et al., 2012, Davim et al., 2011). Thus, proper selection of the cutting tool and cutting parameters are very important for the machining process. Further, little work on the machinability of natural fibre reinforced composite materials has been attempted.

The recent trend is to manufacture tribology components from engineering polymers and polymer-based composites. These materials have many applications, for instance, in the production of bearing components used in automobile industries, such as gears, wheels and bushes. Commonly, these tribo components are subjected to abrasive wear, either by sliding against a rough counter face or through abrasion by hard particles. Therefore, understanding abrasive wear behaviour is imperative from a tribological and commercial standpoint. Further, the majority of failures in designed parts have occurred because of an exposure to tribological loading conditions (Bhushan, 2013).

From the literature, many efforts are still expected in investigating the effect of synthetic fibres on the abrasive wear behaviour of polymers and, consequently, less attention is focused on natural fibres, since such fibres have only recently been utilised. Nevertheless, a few studies have been initiated to investigate the effects of jute, linen and cotton fibres on the adhesive wear performances of polymeric composites (Hashmi, Dwivedi & Chand 2007; (Bajpai et al., 2013a, Bajpai et al., 2013b, Bakry et al., 2013, Yousif, 2013), and the potential of other natural fibres (e.g. bamboo and date palm) is currently under investigation at the University of Southern Queensland (USQ). This has been the motivation for conducting a comprehensive investigation to study the effect of date palm fibres and a chopped strand mat of glass fibres on the two body abrasion of epoxy composites. Moreover, the current research intends to explore the possibility of replacing synthetic fibres with natural ones.

In light of the above, the candidate found it necessary to study the machinability and two body abrasion of epoxy composites based on date palm fibres and glass fibres. In this study, the project was divided into three stages: 1) studying the interfacial adhesion properties of date palm fibre with an epoxy matrix, 2) investigating the machinability of date palm or glass fibre/epoxy composites and 3) investigating the two body abrasive behaviour of the developed composites. To conduct the machining experiments, a new dynamometer adapted with a drilling machine was designed and manufactured to measure cutting pressure and cutting force at different operating parameters. An analysis of variance (ANOVA) approach was developed to discover the correlation between the operating parameters and the machinability of the epoxy composites in terms of the drilled hole accuracy. In terms of tribology, two body abrasive testing using a tribo-test machine was conducted using block on disk against various SiC at different applied loads in the range 5–20 N. The specific wear rate, friction coefficient and wear mechanism were studied and the surface morphology was examined using scanning electron microscopy (SEM) to observe the worn surfaces of the specimens after each test.

1.2 Objectives and Significance of this Research

The objectives of this research are:

1. to study the interfacial adhesion properties of date palm fibre with an epoxy matrix and to develop new environmentally friendly epoxy composites based on date palm fibres
2. to develop a new dynamometer adapted with a drilling machine to measure the output parameters (cutting pressure, cutting force and machining power)

3. to evaluate the machinability of glass fibre/epoxy composites considering different operating parameters
4. to investigate the machinability of epoxy composites based on date palm fibre and to compare the machinability of date palm fibre epoxy composite with machinability of glass fibre epoxy composites.

The significance of the project will have economic, environmental, industrial and scientific aspects. Some of the main significant outcomes of the project are:

1. Finding a new composite natural reinforcing material based on date palm fibres that can be compared to glass fibres with for the machining process is a significant approach to reduce the effect of polymeric composites production on the environment.
2. Synthetic fibre/polymers composites have poor machinability characteristics. In addition, applications based on natural fibre reinforced polymeric composites are found in numerous products. Enhancing the machinability of polymeric composites by replacing the synthetic reinforcement with comparable natural materials will be of interest to industrial and mechanical designers.
3. The development of a new prediction modelling system based on ANOVA theory is a new approach in machining and mechanical science. Such an approach helps to reduce the experimental efforts and cost in machining studies.
4. The development of a new dynamometer for experimental work paves the way for subsequent PhD students at USQ to conduct other machining experiments.
5. From this work, articles will be published in high-standard international journals. These will contribute to the science of mechanical and machining engineering.

1.3 Scope of the Study

The current study is divided into three stages (see Figure 1.1). In the first stage, a literature review was conducted to identify the main recent issues and develop the objectives of the study. In the second stage, perpetration, treatment and then chemical alkali optimisation for date palm fibres were conducted. In this stage, epoxy composites were developed and tests of the mechanical properties of the materials were conducted. Based on the outcomes of this stage, the optimum composites were selected for machining in the third stage.

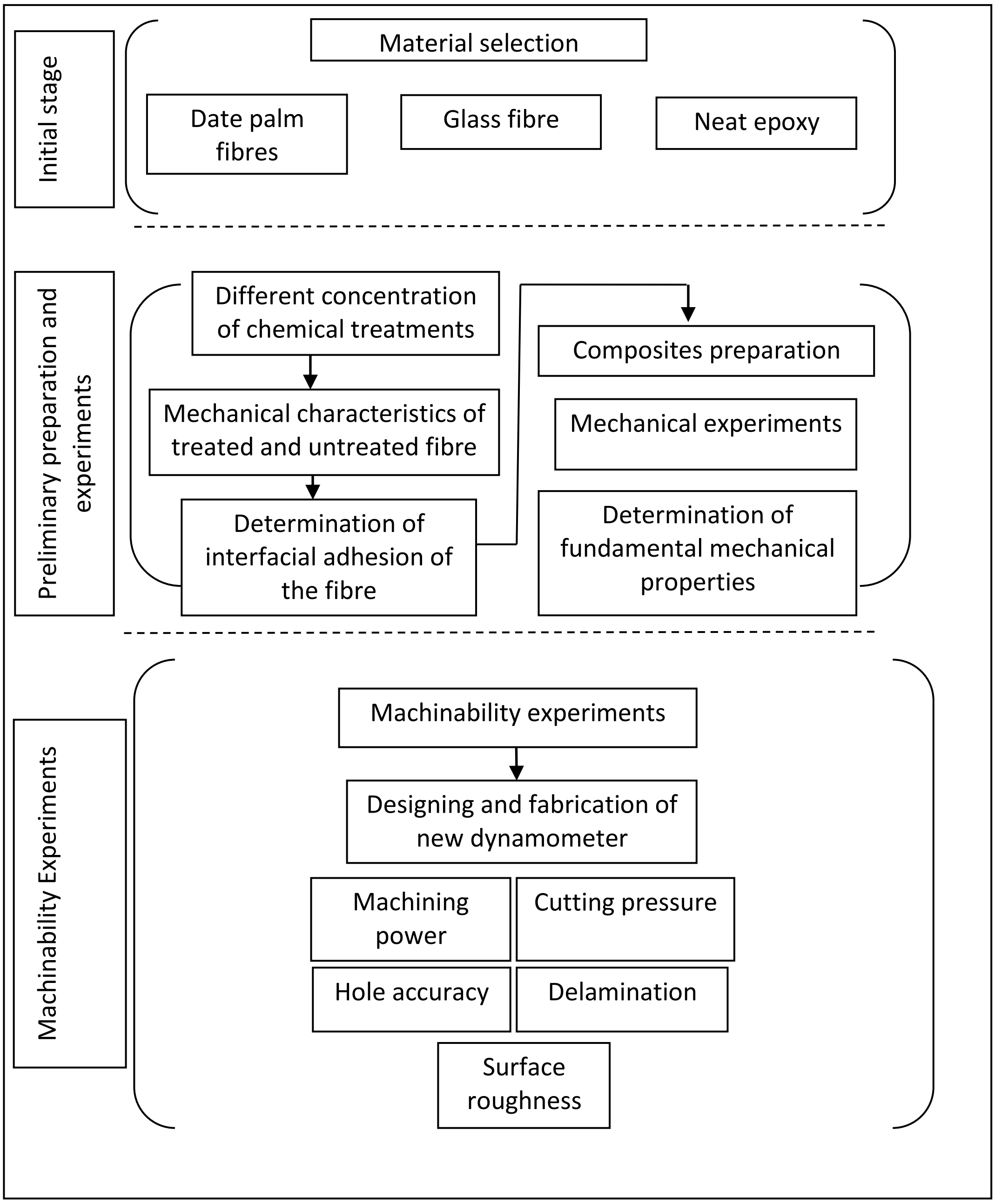

Figure 1.1: Scope of the study

1.4 Organisation of the Dissertation

This dissertation consists of six chapters covering the introduction, literature review, fundamental properties of the composites, machinability of the composites, two body abrasions of the composites and, finally, the conclusion and recommendations. A comprehensive literature review was conducted. This is presented in Chapter 2 and is published as a review article in International Journal of Precision Technology (Scopus Index). For the results and the discussion (Chapters 3–5), each chapter consists of a brief background on the topic, methodology, results, discussion and then a summary of the chapter. These chapters are either already published (Chapter 3—published in Materials and Design, impact factor 3) or under review. Chapter 6 summarises the main findings of the results and introduces future work as recommendations.

CHAPTER 2: A REVIEW OF THE MECHANICAL PROPERTIES AND MACHINABILITY OF FIBRE REINFORCED POLYMER COMPOSITES

2.1 Introduction

This chapter provides a review of the machinability and mechanical properties of natural fibre reinforced composites. Effects of chemical treatment, operating parameters and coupling agents on machinability of natural fibre reinforced composites are discussed. In addition, the effects of physical properties of the fibres on composite machinability are mentioned. Effects of chemical treatment, fibre orientation and volume fraction (V_f) on mechanical properties are described. Finally, the effect of physical properties of fibres on mechanical properties is also discussed.

2.1.1 Brief background on fibre polymer composites and recent issues

Nowadays, polymeric composites are increasingly used in several industrial applications to replace the metal and metal composites. For example, several metal parts in aircrafts have been replaced with parts made of carbon/epoxy materials. Also, fibre polymer composites found their ways in marines applications since many metal parts in ships are replaced with fibre/polymer composites. H(Hung et al., 1998) reported that tool requirements for machining metal matrix composites in a conventional machining process are essential. Conversely, machining of synthetic fibre composites, such as glass fibre and carbon fibres composites will create a major problem because of the inert nature, high hardness and refractoriness of the fibres to machinability in terms of delamination size, R_a, cutting power, thrust force, material removal rate and bearing strength. They are inhomogeneous and have anisotropic characteristics (Davim and Reis, 2004, Davim et al., 2011). Further, the abrasive nature of synthetic fibres causes rapid tool wear and poor surface finish (Wern et al., 1993). Thus, proper selection of the cutting tool and cutting parameters are very important for the machining process. Nevertheless, the effect of machining parameters such as feed, speed, drill diameter, fibre orientation and V_f have a great influence on the machinability of such materials, as reported by a large number of scientists during the past decade (Jain et al., 2002, Adam Khan and Senthil Kumar, 2011, Bouafif et al., 2009, Davim et al., 2011, Le Troëdec et al., 2011, Brahim and Cheikh, 2007, Mata et al., 2009, de Albuquerque et al., 2000, Nirmal et al., 2011b, Azmi, 2012, Ghidossi et al., 2006, Tsao and Chiu, 2011, Shyha et al., 2010, Palanikumar et al., 2006, Palanikumar, 2007, Hocheng and Tsao, 2003). It was found that less work had been undertaken on the machinability of natural fibre reinforced composite materials in terms of tool wear, R_a, cutting forces, material removal rate, cutting power, specific cutting force, tool life, specific cutting pressure and machining power than that done on the machinability of synthetic materials. Synthetic fibres were well known to be abrasive materials that caused significant damage to manufacturing machines and machining tools.

Fundamentally, fibres are a class of hair-like materials that can be continuous or in separate pieces. They can be divided into two types: natural and synthetic. Natural fibres come from three main sources, which are plant, animal and mineral. The early usage of natural plant fibres was more than 5,000 years ago, when humankind used them for warmth and protection. After World War II, the natural fibre industries lost most of their market share, mainly because of the increase in synthetic fibres (Jawaid and Abdul Khalil, 2011, Beg and Pickering, 2008, Ochi, 2008). In fact, synthetic fibres have serious negative aspects such as high cost, non-renewability, non-recyclability, high energy consumption in machining and manufacturing processes, CO_2 emission, highly abrasive nature and health issues when inhaled. These shortcomings have been exploited greatly by supporters of natural fibres (Beg and Pickering, 2008).

Now, the efforts of many researchers are put into substituting synthetic fibres with natural ones, to be compatible with new environmental regulations and depletion of petroleum resources (Jawaid and Abdul Khalil, 2011). In 2006, the Food and

Agriculture Organization of the United Nations declared the year 2009 as the international year of natural fibres, a yearlong campaign focusing on increasing global awareness of, and market demand for, natural fibres. In recent years (2005–2012), much effort has been directed towards the use of lignocellulosic fibres (natural fibres) as reinforcements for polymeric composites because of their superior properties, such as low environmental impact, biodegradability, non-abrasiveness, low weight, non-toxicity, low cost, abundance, renewability and neutrality with respect to CO_2 emissions (Rashkovan and Korabel'nikov, 1997, Ratna Prasad and Mohana Rao, 2011). Moreover, the natural fibres are a price-driven commodity that causes less damage to tools and moulding equipment, gives a relatively better finish, has a higher degree of flexibility (bend rather than fracture) and absorbs high-impact energy (Sever et al., 2012, Jawaid and Abdul Khalil, 2011, Shyha et al., 2010).

Moreover, specific surface micro-morphology of each natural fibre and low cost are the most important advantages that enhanced the natural market, which grew rapidly worldwide compared to synthetic fibres (Mylsamy and Rajendran, 2011, Jayabal et al., 2011, Alawar et al., 2009). Conversely, low melting point, low resistance to moisture absorption, poor wettability and the lack of good interfacial adhesion, which leads to debonding with age, are the main disadvantages that make use of natural fibres less attractive (Felix and Gatenholm, 1991b, Alawar et al., 2009, Beg and Pickering, 2008). In the following section, literature including the most recent and relevant articles studying the implementation of natural fibres as reinforcements in polymeric composites for mechanical and machinability applications is briefly addressed.

Many types of plant fibres extracted from different plants have been used as reinforcements for polymeric composites, for example, palm tree fibres (Alawar et al., 2009, Rao and Rao, 2007), flax (Jayabal et al., 2011), hemp (Medina et al., 2009, Le Troedec et al., 2008, Takeyama and Iijima, 1988), jute (Jayabal et al., 2011, Virk et al., 2010, Saha et al., 2010), wood fibre (Zafeiropoulos et al., 2002), rice husks (Coutinho and Costa, 1999), wheat (Wu et al., 2000, Colom et al., 2003), barley (Colom et al., 2003), oats (Colom et al., 2003), agave (Mylsamy and Rajendran, 2011), cane (sugar and bamboo) (Okubo et al., 2004, Bilba et al., 2003), vakka (Rao and Rao, 2007), kenaf (Liu et al., 2007, Medina et al., 2009, Edeerozey et al., 2007), ramie (Demir et al., 2006), oil palm empty fruit bunch fibre (Nam et al., 2011), sisal (Athijayamani et al., 2010), coir (Valadez-Gonzalez et al., 1999), bamboo (Mizobuchi et al., 2008, Rao and Rao, 2007), roselle (Athijayamani et al., 2010), banana fibre (Van de Weyenberg et al., 2006) and pineapple leaf fibre (Adam Khan and Senthil Kumar, 2011). Most of the above reported works have been conducted to study the effect of natural fibres on the physical, mechanical, tribological, dynamical, thermal, and electrical characteristics of polymeric composites. The mechanical properties of fibre composite depend on many parameters, such as fibre orientation, surface characteristics of the fibre (for interfacial adhesion), V_f of fibres, physical and mechanical properties of the fibre and the structure of the composite. It is therefore necessary to discuss in detail the effects of each parameter on the mechanical properties of the composites.

2.1.1.1 Effect of chemical treatment on machinability

One difficulty of machining natural fibre reinforced composites is a lack of good adhesion of the fibres to most polymeric matrices. The hydrophilic nature of natural fibres negatively affects adhesion to a hydrophobic matrix and, as a result, it may cause a lack of interlocking between the fibre and the matrix (Herrera-Franco and Valadez-González, 2004, Nam et al., 2011). To prevent this, the fibre surface must be modified to promote adhesion and, hence improve the machinability of the composites (Valadez-Gonzalez et al., 1999, Van de Weyenberg et al., 2006).

Adam Khan and Senthil Kumar (2011) investigated the machinability of short agave fibre reinforced epoxy composites in terms of fibre–matrix interaction for untreated and alkali-treated (five per cent) fibres. Rough surfaces were observed with the treated composites, which led to better interlocking between the fibre and the matrix and increased the area of contact. In contrast, voids were noticed in the untreated composites. These observations were qualitatively similar to those reported by

Valadez-Gonzalez et al. (1999) in their investigations of the effect of natural fibre surface treatment on the fibre–matrix bond strength of reinforced composites.
Athijayamani et al. (2010) studied the machinability of alkali-treated natural fibre (roselle and sisal) hybrid polyester composite in terms of weight loss. A 10 per cent sodium hydroxide (NaOH) solution treatment was used on the fibres for different durations (2, 4, 6 and 8 hours). Gradual weight loss was observed with increased wear test time (4, 8 and 12 minutes) and the alkali-treated composite samples showed superior wear performance when compared with the untreated composite samples. This could have resulted from the removal of the moisture of fibres with alkali treatment, which led to an increase in interfacial bonding strength between reinforcement and matrix.

Nam et al. (2011) studied machinability in terms of roughness average (R_a) of untreated and alkali-treated (five per cent NaOH) coir fibre reinforced poly (butylene succinate) biodegradable composites. It was reported that five per cent alkali treatment for a period of 72 hours increased R_a and the amount of cellulose exposed on the fibre surface, which enhanced the mechanical interlocking between the fibre and the matrix and led to better machinability. These observations are qualitatively similar to those reported by (Kabir et al., 2011) for their investigations of the effects of alkali treatment on the R_a of hemp fibre reinforced sandwich composites.

2.2 Mechanical Characteristics of Natural Fibre Polymer Composites

Previously natural fibres found their ways in some industries dealt with door inner panel, seat back and roof inner panel (Mallick, 2008). Recently, natural fibres have become a major area of interest for scientists, engineers and researchers as an optional material for the reinforcement of fibre reinforced polymer (FRP) compounds as reported by Mallick (2008) and Wahit et al. (2012). The use of natural fibres is gaining ground due to the advantages of using these compounds, including their low cost and non-abrasiveness. The influence of natural fibres on the properties of FRPs includes their use to improve tensile properties. Chemical modifications are used to improve interfacial bonding and increase the Young's modulus of the composite mixture. Natural fibres have taken a central role because of their favourable mechanical properties, low cost, non-abrasiveness, high specific strength, bio-degradability and eco-friendliness (Khondker et al., 2005). They are used as substitutes for conventional fibres, including carbon and glass fibre, because of their wide array of advantages (Panigrahy et al., 2006).

The effects of natural fibres on the nature of polymeric composites include alteration of the tensile properties of the polymers (Medina et al., 2009). Whether thermosets or thermoplastics are used, the tensile properties of the polymer are altered through changing the interfacial adhesion between the fibres and the matrix (Li et al., 2009). When using natural fibres, different chemical modifications are used to improve interfacial matrix–fibre bonding, which influences the tensile properties of the different composites (Herrera-Franco and Valadez-Gonzalez, 2005). Thus, when increasing the strength of the natural fibre is the desired effect, the natural fibre content used is increased to the maximum or optimum level (Herrera-Franco and Valadez-González, 2004). In cases where the engineers need to increase the Young's modulus of the given natural fibre composite, they increase the fibre loading in the mixture (Hu and Lim, 2007). For example, the tensile strength, as well as the Young's modulus of FRP, is increased considerably after the fibre loading is increased (Santos et al., 2009).

Mallick (2008) summarized the mechanical properties of hemp, flax sisal and jute fibres in his book showing the general information about the tensile strength, modulus and elongation of those fibres. For further information and discussion, the following sections discuss the influence of chemical treatments, volume fraction, and orientation of the fibres on the mechanical properties of the fibres and the composites.

2.2.1 Effect of chemical treatment

It is well known that natural fibres have an issue with regard to their compatibility with matrix (interfacial adhesion). This problem is mainly due to the presence of tissue on the fibre's surface, which weakens the interlocking of the fibres with the matrix. It has been reported by several works that untreated fibres lead to pull out mechanisms (e.g. tensile, tribology and flexural) during loading conditions. Some approaches, such as chemical treatments to the fibre, can overcome the issue of the interfacial adhesion of fibres with the matrix (Athijayamani et al., 2010, Alawar et al., 2009, Mylsamy and Rajendran, 2011, Takeyama and Iijima, 1988, Edeerozey et al., 2007, Saha et al., 2010, Le Troedec et al., 2008, Colom et al., 2003, Van de Weyenberg et al., 2003, Jayabal et al., 2011, Eichhorn et al., 2001).

Chemical treatment is the process of cleaning the surface of the fibre, removing the tissue, reducing the moisture absorption and increasing the R_a (Edeerozey et al., 2007, Mylsamy and Rajendran, 2011, Rokbi et al., 2011). There are numerous studies on the effect of chemical treatments (e.g. NaOH, polyethyleneimine, ethylenediaminetetraacetic acid, bleaching, acetylation, lime water, $Ca(OH)_2$ and $CaCl_2$) on the interfacial adhesion of the fibres with the matrix, which, in turn, influences the properties of the composites (Edeerozey et al., 2007, Alawar et al., 2009, Athijayamani et al., 2010, Takeyama and Iijima, 1988, Le Troedec et al., 2008, Van de Weyenberg et al., 2006, Mylsamy and Rajendran, 2011, Valadez-Gonzalez et al., 1999, Saha et al., 2010, Jayabal et al., 2011, Demir et al., 2006). The most common technique for treating the fibres chemically is immersion of the fibre in a chemical solution. The efficiency of the chemical treatment depends on the concentration of the solution, the duration of immersion, the surface characteristics of the fibres and the type of fibre (Athijayamani et al., 2010, Mamidi, 2012).

Athijayamani et al. (2010) investigated the effect of the immersion duration (2–8 hours) of roselle and sisal fibre in alkali (10 per cent) on the mechanical properties hybrid polyester composites. From that work, it was found that increasing immersion duration led to an increase in the tensile and flexural strength of the composite by 59 per cent and 47 per cent, respectively. This was due to the great improvement in the interfacial adhesion of the fibres with the matrix because of the removal of the outer layer of tissue on the fibre surface. This enhanced the adherence of the fibre to the matrix and assisted it to carry some of the load during tensile loading. In contrast, it was observed that the untreated fibres were not able to carry the load and a pull out mechanism occurred. Similar findings have been reported when short agave fibres were alkaline treated and used to reinforce epoxy composites (Mylsamy and Rajendran, 2011). However, increasing the duration of the treatment of the fibre led to lower tensile and flexural strengths. It can be argued that the tissue of the fibres was damaged by the increased treatment duration, resulting in weaker interfacial adhesion between the fibre and the matrix.

Kabir et al. (2011) used three different chemical treatments of hemp fibres (alkalisation, salination and acetylation) to study the mechanical properties of hemp fibre reinforced sandwich composites. It was reported that alkali-treated fibres pre-soaked with eight per cent NaOH showed greater tensile strength (111.05 MPa) than untreated fibres (84.06 MPa) (see Figure 2.1), and that this was due to the removal of hemicelluloses, lignin and cellulosic constituents from the fibre with treatment. SEM micrographs showed that the alkali-treated fibre surface was rough compared with that of the other treatments, thus leading to increased friction. Hence, better adhesion between the fibre and the matrix was achieved. In contrast, a coated fibre surface was noticed with the use of saline. This decreased the adhesion quality between the fibre and the matrix. Finally, the acetylated fibres showed a brittle surface. A number of authors have stated similar observations for chemically treated natural fibres (Athijayamani et al., 2010, Alawar et al., 2009, Mylsamy and Rajendran, 2011).

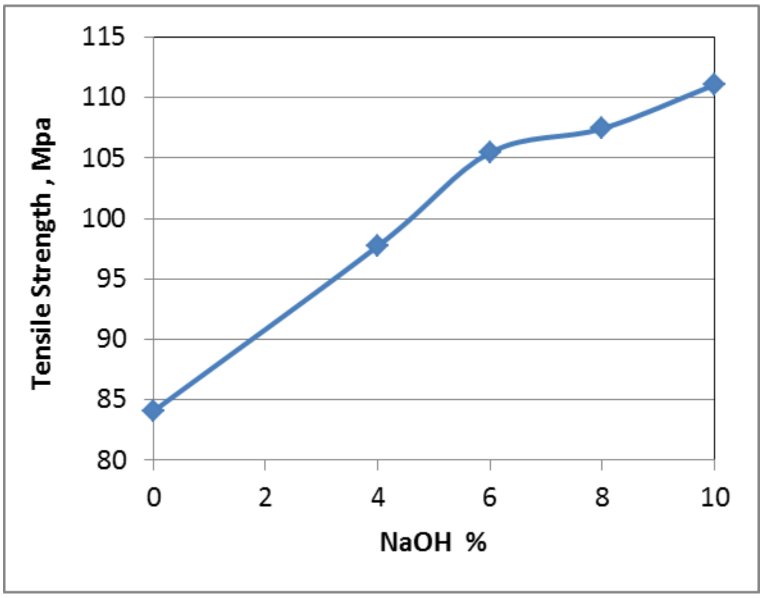

Figure 2.1: Tensile strength v. NaOH percentage (Athijayamani et al., 2010, Alawar et al., 2009, Mylsamy and Rajendran, 2011)

Edeerozey et al. (2007) studied the effect of modifying kenaf fibres with NaOH treatment at different concentrations (three to nine per cent) on the tensile strength of the fibre. It was concluded that three per cent NaOH was not effective in removing impurities. The best concentration for treating the fibre was six per cent NaOH, which completely removed the impurities. The higher NaOH concentration attacked the main structural components of the fibre and more grooves appeared on its surface. This resulted in further reduction in fibre strength. That is, tensile strength started to decrease with higher concentrations of NaOH (see Figure 2.2). The highest tensile test results of 239.3 N/mm^2 were seen with six per cent NaOH, while the tensile strength of untreated fibres was 215.4 N/mm^2. The increase in strength resulted from the removal of impurities. Similar findings were reported by (Eichhorn et al., 2001) when high concentration chemical treatment was used on kapok fibres.

Saha et al. (2010) investigated two methods of chemical treatment. The first was immersing fibres in 0.5–18 per cent NaOH at 30°C for a period ranging from 30 minutes to 24 hours. The other was immersing the fibres in 0.5–18 per cent NaOH 30°C for a period ranging from 30 minutes to 8 hours. Subsequently, the fibres were exposed to steam at 103 kPa pressure (gauged) and 125°C over a period ranging from 30 to 90 minutes. It was found that 0.5 per cent alkali/steam treatment showed an increase of 65 per cent in tensile strength (610 MPa) compared with untreated fibres (370 MPa) (see Figure 2.2) .This was due to fibre separation and removal of non-cellulosic materials which, consequently, resulted in an increased crystallinity. The successful removal of non-cellulosic materials (lignin, pectin or hemicelluloses) from the inner region of the fibre was also a factor in the improvement in tensile strength.

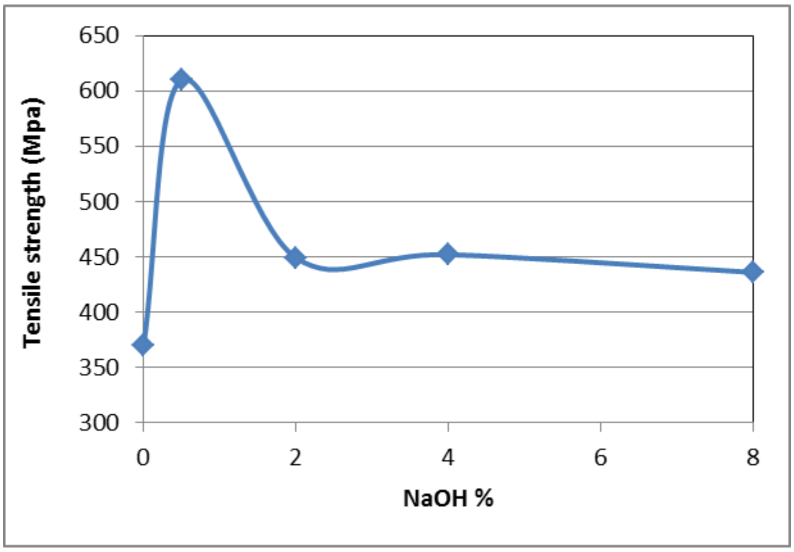

Figure 2.2: Tensile strength v. NaOH percentage (Saha et al., 2010)

Alawar, Hamed and Al-Kaabi (2009) investigated the mechanical properties, tensile strength, Young's modulus and elongation at break of date palm tree fibres subjected to different chemical treatments (0.5–5 per cent NaOH and 0.3–1.6 per cent HCl). It was concluded that one per cent NaOH treatment improved surface morphology by cleaning the fibre surface impurities. Tensile strength increased to 800 MPa, compared with the raw fibres' strength of 200 MPa, and Young's modulus increased to 160 GPa, compared with the raw fibres' value of eight GPa (see Figure 2.3). Conversely, distortion of surface morphology and a decrease in tensile strength to 105 MPa were noticed when HCl treatment was used. Finally, treated fibres showed higher resistance to degradation (42 per cent) compared with raw fibres (35 per cent). generally, the increase in concentration of HCl caused a decrease in fibre strength.

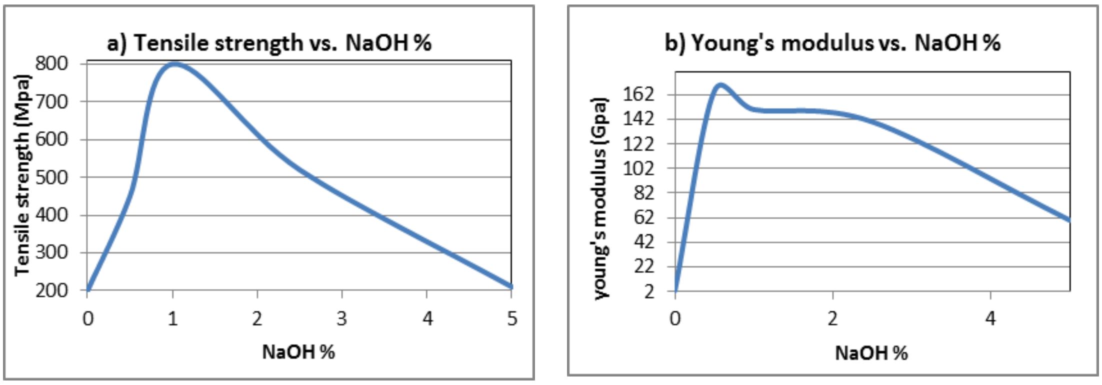

Figure 2.3: Influence of NaOH on the tensile strength and modulus of elasticity of palm tree fibres (Alawar, Hamed & Al-Kaabi 2009)

2.2.2 Effect of fibre orientation

For natural FRP composites, despite the large influence of fibre treatments on the mechanical properties of composites, as mentioned in the previous section, fibre orientation also plays an important role in controlling these (Jain et al., 2002, Khashaba et al., 2010b, Herrera-Franco and Valadez-González, 2004, Azmi, 2012, Tsao and Chiu, 2011, Yam et al., 1990, Yemele et al., 2010). Herrera-Franco and Valadez-González (2004) studied the effect of fibre orientation (transverse or longitudinal) and treatment with two per cent NaOH on the mechanical properties (tensile and flexural) of henequen fibre reinforced high density polyethylene (HDPE). That work showed that longitudinal orientation exhibited higher mechanical properties by approximately 90–95 per cent compared with the transverse orientation, in terms of tensile strength, modules of elasticity and flexural strength (see Figure 2.4). The longitudinal orientation of the fibre, associated with the chemical treatment, enhanced the interlocking of the fibres in the composite, which led to the better mechanical properties compared with the untreated fibres in transverse direction.

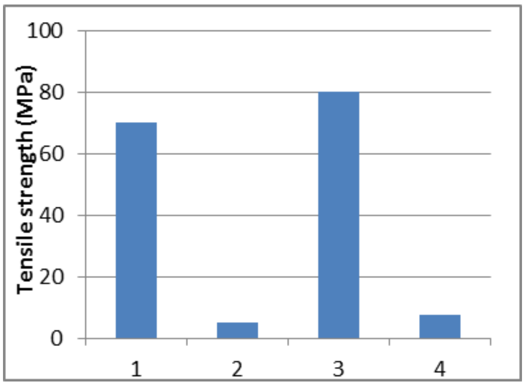

a)Tensile strength

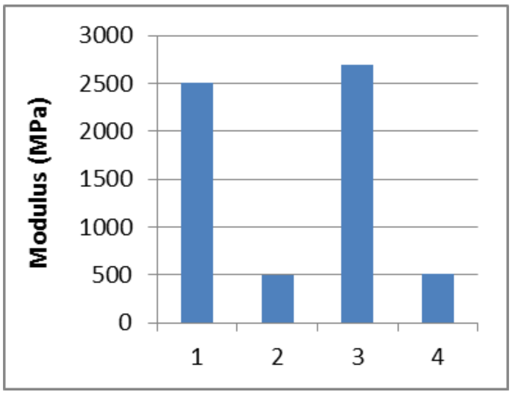

b) Modulus of elasticity

(1) Untreated Longitudinal, (2) Untreated Transverse, (3) Treated (two per cent NaOH) Longitudinal, (4) Treated (two per cent NaOH) Transverse

Figure 2.4: Influence of fibre orientation on mechanical properties of henequen fibre/HDPE composites

Brahim and Cheikh (2007) studied the influence of the fibre orientation (0°–90°) of unidirectional Alfa fibres in a polyester composite on mechanical properties (tensile stress and modulus of elasticity). The fibres had been extracted from the stem of the Alfa plant using the soda process, in which the plant stem was heated in a three per cent NaOH solution for two hours at a temperature of 100°C, after which the fibres were bleached for one hour using a 40 per cent NaClO solution. It was found that the mechanical properties (tensile stress and modulus of elasticity) of the composite decreased with increasing orientation angle, from 150 to 18 MPa and from 12.3 to 5 GPa, respectively (see Figure 12 and Figure 13. This could be explained because when the fibres were orientated in the load direction (0°) it would cause the load to be distributed along the entire length of the fibre. However, when the load directions were not parallel to the fibres, the load was not distributed along the entire fibre, giving lower values.

In similar work, (Jacob et al., 2004) investigated the influence of fibre orientation (0°–90°) on the tensile strength of sisal/oil palm hybrid fibre reinforced natural rubber composites. They concluded that the maximum tensile strength (8 MPa) was achieved when the fibres were longitudinally orientated (0°). In contrast, when the angle of the fibre orientation was increased to 90°, the tensile strength decreased to 4 MPa. When the fibres are aligned in the direction of force (longitudinally), the fibres transferred stress uniformly. However, when the fibres were aligned perpendicular to the direction of load (transversely) they could not distribute much stress.

De Albuquerque et al. (2000) investigated the effect of fibre orientation on the tensile strength of jute roving reinforced polyester composites. It was found that the tensile strength increased in the transverse direction from 40 MPa to 65 MPa with an increase in the fibre content from zero percentage by weight (wt%) to 30 wt%. Conversely, the tensile strength value decreased from 40 MPa to 10 MPa in the longitudinal direction with the same increase in the fibre content. These results could be due to the longitudinally orientated fibres acting like obstacles and preventing the distribution of stress throughout the matrix, thus causing a higher concentration of stress and poor mechanical properties.

2.2.3 Effect of volume fraction

The fibre V_f (i.e. concentration of the fibre in the composite) plays a significant role in the mechanical properties of composites. It has been reported that mechanical properties could be enhanced with certain increases in fibre V_f (Ku et al., 2011, Ratna Prasad and Mohana Rao, 2011, Brahim and Cheikh, 2007). Above a certain level, high V_f can cause fibre clotting and the applied loads cannot be distributed evenly, which leads to a decrease in the mechanical properties (Yousif, 2010). Hence, the optimisation of a fibre's V_f value is necessary for strengthening the composite (Ku et al., 2011, Lei et al., 2006, Ma et al., 2005, Beg and Pickering, 2008, Madsen and Lilholt, 2003, Mata et al., 2009, Migneault et al., 2009, Oda et al., 2012, Tarfaoui et al., 2008, Oksman et al., 2009). (Müller et al., 2009) and (Bras et al., 2010) investigated the effect of cellulose fibres V_f on the mechanical properties of starch-based composite. This work showed that an increase in volume of the fibre in the composite led to an increase in the tensile strength and elasticity modulus of reinforced composite compared with the neat composite.

The influence of fibre V_f (0–44 per cent) on the mechanical properties (longitudinal modulus and longitudinal stress) of Alfa/polyester composites was evaluated by (Brahim and Cheikh, 2007) and compared with synthetic composites based on glass fibres. The results revealed that mechanical properties of the composites increased with increase in V_f up to 44 per cent (see Figure 2.5), and were close to those of the composite reinforced with synthetic (glass) fibres at the same V_f.

Yousif (2010) studied the effect of V_f (0–60 per cent) on oil palm fruit fibres on the mechanical properties of polyester composites. It was concluded that increasing the volume fraction to 41 per cent resulted in an increase in tensile strength by around 110 per cent compared with neat polyester. Increasing the V_f to 38 per cent caused an increase in the compression strength of the composite by 30 per cent. These outcomes were due to uniform stress or strain distribution in the composite. However, at higher fibre loading, fibre clotting took place and the applied load could not be distributed evenly. Conversely, the tensile strength of the composite decreased with increasing V_f of fibres (see Figure 2.6).

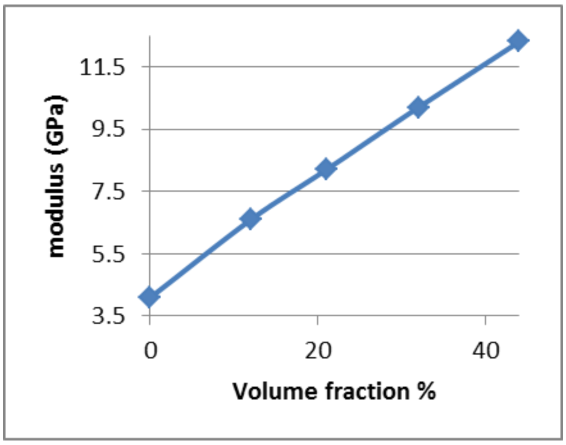

a) Fibre volume fraction effects on modulus of elasticity

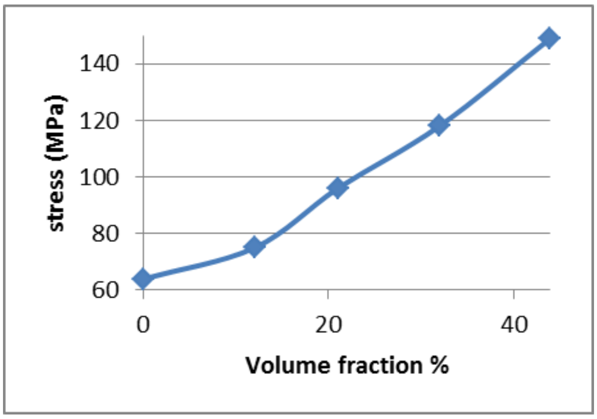

b) Fibre volume fraction effects on tensile stress

Figure 2.5: Fibre volume fraction effects on Alfa/polyester composites (Brahim and Cheikh, 2007)

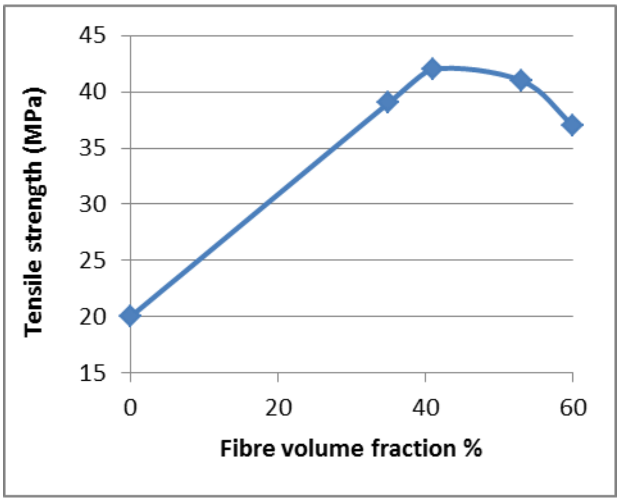

Figure 2.6: Fibre volume fraction effects on tensile strength of oil palm fruit fibres/polyester composites (Yousif 2010)

2.2.4 Effect of physical properties of fibres

Several studies have been conducted on physical properties of fibres that affect the final properties of natural fibre composites. These include quality of fibre distributed in the matrix; fibre size, length and diameter; moisture absorption; porosity and the way fibres break during compounding with the matrix (Tsao and Hocheng, 2008b, Yousif, 2010, Khashaba et al., 2010b, Palanikumar, 2011, Davim et al., 2004, Gaitonde et al., 2008, Mohan et al., 2005, Migneault et al., 2009). Throughout the mixing step, fibres are exposed to concentrated thermal and mechanical stresses, which lead to their breakage and, therefore, loss of some of their reinforcing action. Nevertheless, the aspect ratio of the fibre, which is the ratio between the length (L) and the diameter (D), also plays an important role in the mechanical properties of the composite, as mentioned by D(Duc et al., 2011).

(Brahmakumar et al., 2005) examined the effect of the fibre length (5–25 mm) and content (10–27 per cent) of coconut fibre reinforced polyethylene composites on mechanical properties (strength, modulus and elongation). It was reported that an increase in fibre length from 5 mm to 20 mm led to an increase in the tensile strength, tensile modulus and elongation by 52 per cent, 26 per cent and 31 per cent, respectively (see Figures 36–38). However, beyond the length of 20 mm, decreases in tensile strength and tensile modulus were noticed (by eight per cent and 13 per cent, respectively) and no change in the value of elongation was seen. It was also reported that an increase in fibre content from 10 per cent to 25 per cent caused an increase in the tensile strength and tensile modulus by 48 per cent and 53 per cent, respectively, whereas a 50 per cent decrease was noticed in the elongation value. However, beyond 25 per cent fibre content, decreases in the tensile strength and tensile modulus were noticed (by 14 per cent and five per cent, respectively) and no change in the elongation value was observed.

Beg and Pickering (2008) explored the influence of fibre length (0.95–3.07mm) on the mechanical properties (tensile strength, Young's modulus, failure strain and impact strength) of kraft fibre reinforced polypropylene composites. It was noticed that a decrease in fibre length led to increases in tensile strength from 37 MPa to 43 MPa, Young's modulus from 3.8 GPa to 4.6 GPa and impact strength from 5.6 kJ/m^2 to 6.5 kJ/m^2, whereas the failure strain value decreased from 2.47 per cent to 1.91 per cent. These changes in mechanical properties could be due to reduction in reinforcing efficiency, which was also mentioned by (Harper et al., 2006).

Yemele et al. (2010) investigated the effect of bark fibre (black spruce bark and trembling aspen bark) content (50 wt% and 60 wt%) and size (fine: 0.18–0.25 mm, medium: 0.25–0.50 mm, coarse: 0.50–1.00 mm) on tensile strength and flexural modulus of bark/HDPE composites according to a factorial design. The smallest L/D ratio was seen in black spruce bark and trembling aspen bark fine fibres (8.85 and 3.83, respectively), whereas the black spruce bark and trembling aspen bark coarse fibres showed the highest L/D ratio (13.83 and 10.68, respectively). The results of the experiments showed that increased fibre content led to increases in the tensile strength and flexural modulus. Moreover, fibre length improved strength and elasticity but led to a decrease in toughness and tensile strain at failure, that is, the fibre content effect on the mechanical properties was more significant than the size of the fibres.

Migneault et al. (2009) studied the effect of the L/D ratio (from 8.3–21.3) on the flexural and tensile modulus of wood–plastic composites with the use of two processing techniques (injection moulding and extrusion). For both processes, the effect of fibre L/D ratio on the flexural modulus and tensile was similar. Both increased, with different percentages, with increased fibre L/D ratio. However, the injection moulding method associated with increased fibre size led to better mechanical properties compared with the extrusion process. This drawback in the extrusion process can be explained by the fact that the process is generally associated with fibre fracture, as reported in other studies (Okubo et al., 2004, Grande and Torres, 2005).

2.3 Machinability of Synthetic Fibre/Polymer Composites

Machining of synthetic fibre composites, such as glass fibre and carbon fibre composites, is a major problem because of their inert nature, high hardness and refractoriness to machinability in terms of delamination size, R_a, cutting power, thrust force, material removal rate and bearing strength using drilling process, (Davim and Reis, 2004, Davim et al., 2011). Further, the abrasive nature of synthetic fibres causes rapid tool wear and poor surface finish. Thus, proper selection of the cutting tool and cutting parameters are very important for the machining process. Moreover, the effect of machining parameters such as feed, speed, drill diameter, fibre orientation and volume fraction (V_f) have a great influence on the machinability of materials such as (Jain et al., 2002, Adam Khan and Senthil Kumar, 2011, Bouafif et al., 2009, Davim et al., 2011, Le Troëdec et al., 2011, Brahim and Cheikh, 2007, Mata et al., 2009, de Albuquerque et al., 2000, Nirmal et al., 2011b, Arrakhiz et al., 2012, Tsao and Chiu, 2011, Shyha et al., 2010, Palanikumar et al., 2006, Palanikumar, 2007, Hocheng and Tsao, 2003, Ku et al., 2011, Faruk et al., 2012, Davim and Reis, 2004, Khashaba et al., 2010b, Bras et al., 2010, Kini and Chincholkar, 2010). A brief discussion of the effect of operating parameters on the machinability of composites based on synthetic fibres is provided in the following sections.

2.3.1 Effect of the operating parameters on thrust force

Hocheng and Tsao (2003) studied the effect of the machining parameters (feed, speed and drill diameter) on machinability in terms of thrust force of woven glass fibre reinforced epoxy (GFRE) composites using drill machine. It was reported that the cutting conditions used resulted in higher thrust force than predicted, while no obvious effect of cutting speed was observed. Further, high values for the correlation coefficient between thrust force and the machining parameters confirm the importance of reducing the thrust force in drilling GFRE composites.

(Khashaba et al., 2010b) studied the effect of the cutting parameters (cutting velocity and feed rate) under specific cutting pressure on machinability in terms of thrust force of glass fibre reinforced plastics (GFRPs) using a drill machine equipped with two different types of cemented carbide (K10) drills (Brad & Spur and Stub Length). The results showed that under the same cutting conditions, thrust forces for the two drilling sets increased with an increasing feed rate and that the Brad & Spur drill showed less thrust force values than the Stub Length drill. Similar work was carried out by (Ku et al., 2011), who tested the same reinforced material using different cutting speeds and different feed rates using drill machine. For neat epoxy, an insignificant effect on thrust force was noticed when cutting speed increased from 10 m/minute to 45 m/minute. This could have been the result of increased heat around the tool edge that destroyed the matrix and thus reduced the resistance forces. However, GFRE composites showed different results. The thrust force decreased by 29.4 per cent when cutting speed was increased from 5 m/minute to 45 m/minute. Further, thrust force increased by 62.5 per cent when drill diameter and fibre V_f was increased. Finally, both neat and GFRE composites' thrust force increased by 20 per cent when the feed rate was increased from 0.05 mm/revolution (rev) to 0.23 mm/rev. Similar work, material and results have been reported by Mata et al. (2009) using drill machine. A delay between the responses of thrust force was found and thrust force values were reduced because of the softening of the matrix caused by heat generation. Further, it was noticed that the effect of cutting speed on thrust force was insignificant.

(Jacob et al., 2004) used a glass fibre reinforced composite (glass/phenolic woven fabric) with high V_f (66 per cent) to study the effect of drilling variables (cutting speed and feed rate) and the number of holes (300) on machinability in terms of thrust force using a tipped carbide drill cutting tool using drill machine. It was noticed from the results that thrust force increased with increasing feed rate. This could have been because of the increase in the cross-sectional area of the undeformed chip. Further, a gradual, slow rise in thrust force with the number of holes drilled was noticed, which was generally related to steady state of wear of the cutting edge.

(El-Sonbaty et al.) studied the influence of two types of matrices (thermoplastics and thermoset) on machinability in terms of the thrust force of woven glass fibre composites by using drilling. It was concluded that with increasing the number of drilled holes, the thrust forces increased for both matrices but it was higher in thermoset composites. This could be because machining induced defects such as debonding and delamination. Tsao (2008) studied the effects of cutting parameters on machinability in terms of thrust forces using three kinds of step-core drills (twist, saw and candle) for carbon fibre reinforced plastic composites (CFRP) laminates. The cutting parameters used were diameter ratios of 5.5–7.4 mm/mm, feed rates of 8–16 mm/rev and spindle speeds of 800–1,200 revolutions per minute (RPM). It was found that increased drilling parameters led to an increase in thrust force. The highest thrust force was obtained by decreasing diameter ratio and spindle speed and increasing feed rate. Conversely, the lowest thrust force was recorded when both diameter ratio and spindle speed increased while decreasing feed rate. Further, the step-core saw drill offered the highest thrust force. The diameter ratio and feed rate were the major cutting parameters and the best experimental conditions were obtained by a combination of high diameter ratio (0.74 mm/mm), low feed rate (8 mm/rev) and spindle speed (1,200 RPM), but there were no clear reasons for these results.

(Bras et al., 2010) investigated the effect of machining parameters (feed, speed and drill diameter) on machinability in terms of thrust force when drilling woven GFRE composites using drill machine. The influence of cutting parameter on the thrust force was investigated using two drills with different diameters. The drilling processes were executed using a radial drill machine with cemented carbide drills. The results clearly showed that thrust force increased with an increase in cutting feed rates for both drill diameters. However, the drill with the larger diameter showed higher thrust forces. This was because of an increase in the resistance of chip formation and the axial thrust due to the increase in the cross-sectional area of the undeformed chip.

(Tsao and Chiu, 2011) studied the effect on machinability in terms of thrust forces for CFRPs of different drilling parameters . The parameters examined were spindle speed for inner (1,088–1,360 RPM) and outer (1,000–1,214 RPM) diameter, cutting velocity ratio (−2–2), feed rate (10–20 mm/min), stretch (−0.5–0.5 mm), inner drill diameter (5.6–6.8 mm) and two types of drill heads (outer drills and inner drills). It was found that cutting velocity, feed rate and inner drill type had the most effect on thrust force because of the chip clog in the drill head. However, stretch and outer drill diameter had a minimal effect on the thrust force of the composite when compared to other factors. Further, thrust forces were reduced when a smaller feed rate was used, resulting in smaller chips and delaminating.

(Eichhorn et al., 2001) investigated the effect of drilling parameters (spindle speed and feed rate) on machinability in terms of thrust force for thin CFRP laminates using a carbide (K20) drill. It was noticed that thrust forces increased with an increase in feed rate. This could be because of the increase in self-generated feed angle that considerably reduced the working clearance angle of the drill, resulting in rubbing against the work material and leading to higher thrust forces. Conversely, thrust forces have been found to decrease with increased spindle speed. This could be because the increase in temperature with spindle speed softens the composite.

2.3.2 Effect of the operating parameters on surface roughness

Hocheng and Tsao (2003) studied the effect of machining parameters (feed, speed and drill diameter) on machinability in terms of the R_a of woven GFRE composites using drill machine. It was reported that R_a increased with increased cutting feed rate, while no obvious effect of the cutting speed was observed. (Davim and Reis, 2004) studied the effect of cutting parameters (cutting velocity and feed rate) under specific cutting pressures on machinability in terms of R_a for GFRPs. A drill machine was used that was equipped with two different types of cemented carbide (K10) drills (Brad & Spur and Stub Length). The results showed high R_a values for both drills. Further, the Brad & Spur drill showed better performance than the Stub Length drill, in that it produced a smaller R_a. In addition, larger values were noticed at a high feed rate and smaller R_a values were obtained at high cutting speeds, that is, a better surface finishing was obtained at high cutting speed and low feed rate.

(Khashaba et al., 2010b) investigated the effect of drilling cutting parameters (cutting velocity and feed) drill on machinability in terms of specific cutting forces in FRPs with two different matrices (Viapal VUP 9731 and ATLAC 382-05) and using a Brad & Spur cemented carbide (K10). The results clearly indicated that R_a increased with increasing feed rate and decreased with increasing cutting speed.

El-Sonbaty, Khashaba and Machalyet (2004) studied the influence of cutting speed (218–1,850 RPM), feed rate (0.05–0.23 mm/rev) and drill size (8–13 mm) on GFRE composites. They tested different fibre V_f (0–23.7 per cent) on machinability in terms of R_a, using conventional drilling operations. For neat epoxy, the cutting speed and feed rate had no effect on R_a. However, GFRE composites showed different results. With increasing cutting speed, V_f and drill diameter, a 75 per cent decrease in the R_a (from 8 µm to 2 µm) was noticed. This was because of the increase in the reinforcing fibres supporting the matrix. Similar work, material and results have been reported by (Mata et al., 2009).

Palanikumar (2007) studied the effect of machining parameters (cutting speed, fibre orientation, depth of cut and feed rate) on machinability in terms of R_a for GFRE composites using drill machine. It was found that R_a decreased when cutting speed and depth of cut increased. Conversely, R_a increased as feed rate and fibre orientation increased.

(Bras et al., 2010) investigated the effect of machining parameters (feed, speed and drill diameter) on machinability in terms of R_a when drilling woven GFRE composites. The influence of cutting parameters on the R_a was investigated using two drills with different diameters. The drilling processes were executed using a radial drill machine with cemented carbide drills. The results showed that at low cutting feed rates, a complete shearing of the fibre occurred, resulting in a comparatively good surface finish. In contrast, R_a increased with increased cutting feed. This could be because of partially sheared fibres leading to relatively high R_a. However, no clear effect of the cutting speed was observed. Further, the cutting parameter that was found to have the highest physical influence on R_a for both composite materials was cutting speed.

Kini and Chincholkar (2010) studied the effect of machining parameters (speed, feed rate, depth of cut and tool nose radius) on machinability of GFRP in terms of R_a, using a turning lathe equipped with coated tungsten carbide inserts. Their study revealed that low values of feed rate (0.25 mm/rev) showed large values of R_a (2.48 µm) because at low feed rates there was a large quantity flow of fibres that caused the high R_a. Further, feed rate was found to be the most important factor affecting R_a.

2.3.3 Effect of the operating parameters on hole accuracy

Fixed dimensional and geometric tolerances have been sought by many researchers such as Jain et al. (2002), Beg and Pickering (2008) and Khashaba et al. (2010b). However, due to the nature of the composites, few worthwhile results have been achieved. Hole characteristics can cause stress concentration, especially at the fastener assemblies, leading to premature failure. The quality of the hole produced can be described in many ways (Jain et al., 2002). It can be classified as a geometrical error, or errors, regarding work piece material properties. The most important quality criteria emphasised by (Jain et al., 2002) were the errors in hole roundness and hole size. During drilling, the fibres were bent by the action of the cutting edge and then shear fractured. After the shear failure, the fibres attempt to reset, causing a tightening around the drill and, thus, the size of the drilled hole is less than the drill diameter. This phenomenon is commonly observed when drilling laminated GFRP composites. However, in the case of drilling higher percentage fibre content GFRP composites, such shrinkage is not found, since the woven fabric does not allow the fibres to bend greatly (Khashaba et al., 2010b). Machining, particularly drilling, of synthetic polymeric composites is widely used for producing riveted and bolted joints during assembly operations. It is well known that it is difficult to produce high quality holes with high efficiency by conventional drilling methods when using these polymeric composites (Demir et al., 2006). Thus, more expensive drilling techniques and special drill bits must be used to produce the most accurate holes.

(Beg and Pickering, 2008) conducted several drilling trials on woven glass fabric/epoxy using high speed steel (HSS) drills. Micrographs of the exit of the first and the last hole differed significantly. It could clearly be seen that the first hole possessed greater accuracy than the last one, and the accuracy of the holes decreased with an increase in the number of holes drilled. This was because of the progressive wear of the tool and the increased thrust force at the hole exit. The same results were reported by (Brahmakumar et al., 2005) when several drilling trials were carried out in CFRPs using carbide (K20) drills.

(Eichhorn et al., 2001) investigated the effect of drilling parameters (spindle speed and feed rate) on the machinability, in terms of accuracy, of drilled holes in thin CFRP laminates using a carbide (K20) drill. Variation in hole sizes was observed for all drilling parameters. Larger hole sizes were observed at lower cutting feeds and high spindle speed. There could be two reasons for this. First, the accumulated heat from friction could have caused cutting temperature to rise. Second, higher shear forces could have resulted from increased the specific cutting resistance because of smaller uncut chip thickness.

(Khashaba et al., 2010b) used a glass fibre reinforced composite (glass/phenolic woven fabric) with high V_f (66 per cent) to study the effect of drilling variables (cutting speed and feed) and the number of holes (300) on machinability in terms of the dimension of holes drilled using a tipped carbide drill cutting tool. Variation in hole sizes was noticed and a reduction in oversize was observed as the number of holes drilled increased, due to wear of the drill point. In addition, the change in hole sizes could have been due to the thermal shrinkage of the matrix material because of increase in temperature.

2.3.4 Effect of the operating parameters on cutting force using drill machine

(Khashaba et al., 2010b) investigated the effect of drilling cutting parameters (cutting velocity and feed) on machinability in terms of specific cutting force in FRPs with two different matrices (Viapal VUP 9731 and ATLAC 382-05) and using a Brad & Spur cemented carbide (K10) drill. The results clearly indicated that specific cutting force (kc) decreased when both cutting parameters decreased. The Viapal VUP 9731 matrix showed smaller values of kc when considering the same cutting parameters (cutting velocity and feed). Nevertheless, the cutting parameter that had greater influence on the specific cutting force was found to be feed rate, for both composite materials.

Davim, Gaitonde and Karniket (2011) analysed the interaction effects of machining parameters (cutting speed, feed) on the machinability of neat polyether ether ketone (PEEK) and reinforced PEEK (carbon fibre 30 per cent, glass fibre 30 per cent) in terms of cutting power and specific cutting force. A lathe equipped with cemented carbide tools (K10) was used. The results revealed that the addition of the reinforcements improved the mechanical properties (tensile modulus and tensile strength) by 42.8 per cent and 15.4 per cent, respectively. Despite the improvement in the mechanical properties of the reinforced PEEK, an increase in cutting power and cutting force by 90 per cent for all materials was observed when compared to neat PEEK. Therefore, the machinability of reinforced PEEK is relatively costly when compared to neat PEEK.

2.3.5 Effect of the operating parameters on delamination using drill machine

Polymeric composites are considered to be better materials for use as structural components because of their natural properties (Demir et al., 2006). However, composite materials are regarded as hard to machine materials, with low drilling efficiency and undesirable drilling-induced delamination (Bouafif et al., 2009). There are several kinds of damage that can occur while drilling holes. These can be classified into four categories: delamination at drill entry, geometric defects, temperature-related damages and delamination at drill exit (Lei et al., 2006).

Delamination or interlaminar cracking is considered one of the predominant modes of damage in polymeric composite materials. It is considered to be the main problem associated with drilling fibre reinforced composite materials. It is responsible for the rejection of approximately 60 per cent of the components produced in the aircraft industry (Ma et al., 2005). Delamination can be divided into two categories: peel-up delamination, which occurs around the periphery of drilled hole's entry and push-out delamination, which occurs around the periphery of the drilled hole's exit.

Delamination can result in reduction of the structural integrity of material, poor assembly tolerance, progressive stiffness and degradation and has the potential for long-term performance deterioration (Nam et al., 2011). Delamination is mainly the separation of the layers in the composite by a process of cell migration, which can be further defined as the movement of some cells in the composite due to an exterior force, such as drilling. The growth of delamination results in progressive stiffness, degradation and, eventually, failure of the polymeric composite structure. Several techniques have been employed to measure delamination after drilling composites. These are digital photography (Arib et al., 2006, Aziz and Ansell, 2004, Basu et al., 2012), S-Can (Adam Khan and Senthil Kumar, 2011) and shop microscope (Van de Weyenberg et al., 2006).

(Brahim and Cheikh, 2007) carried out a series of drilling experiments on woven-ply GFRP composite laminates using conventional drilling and vibration-assisted twist drilling to compare delamination for both techniques. Delamination was found in both techniques but conventional drilling induced more delamination than vibration-assisted drilling. This could be because of an increase in thrust force with the conventional drilling operation of composite laminates.

(Bras et al., 2010) studied the effect of machining parameters (feed, speed and drill diameter) on machinability in terms of delamination size of woven GFRE composites using cemented carbide drills. Delamination-free holes were not obtained and peel-up and push-out delaminations were obvious in photographs of all the machining parameters. Further, delamination size increased with increasing feed rate, spindle speed and drill diameter. This was due to increasing the cross-sectional area of the un-reformed chip, which leads to increasing thrust force and heat building up around the tool edge and destroying the matrix's stability.

The same results were obtained by (Ciftci et al., 2004) using different types of drills (twist, candlestick and saw drills) with thick carbon FRP. Ultrasonic scanning images clearly showed that delamination occurred with all drill types, but the twist drill showed more delamination than did the candlestick and saw drills. This was because of variations in the cutting edges of the drills. Similar findings were reported by D(de Albuquerque et al., 2000), where drilling strategies for hole making with two standard high speed drilling tools (8 mm standard three-fluted end and a combined process) were used on short GFRP composites.

(Harper et al., 2006) studied the effect on the number of holes drilled (3,750) and feed rate (0.2–0.4 mm/rev) of three prepreg types with unidirectional or woven forms, together with drill feed rate (0.2 and 0.4 mm/rev) on CFRPs on machinability according to delamination level. First, it was found that CFRP composites required fewer machining operations than standard materials because of near net shape fabrication techniques. Nonetheless, difficulties in machinability were present in relation to component and integrity. Second, the longest tool life was achieved at a feed rate of 0.4 mm/rev. Third, a typical worn lip of the drill head was obvious in

SEM images and a catastrophic failure was noticed for the majority of drilled holes at higher feed rates.

2.4 Machinability Performance of Natural Fibre/Polymer Composites

Interestingly, it was found that less work has been done on the machinability of such materials in terms of tool wear, tool life, R_a, cutting forces, material removal rate, cutting power, specific cutting force, specific cutting pressure and machining power than on the machinability of synthetic materials (see Figure 2.7 and Figure 2.8). This observation motivated the current work to investigate the machinability of polymeric composites based on natural fibres. In addition, synthetic fibres are well known to be abrasive materials that cause great damage to the manufacturing machines and machining tools.

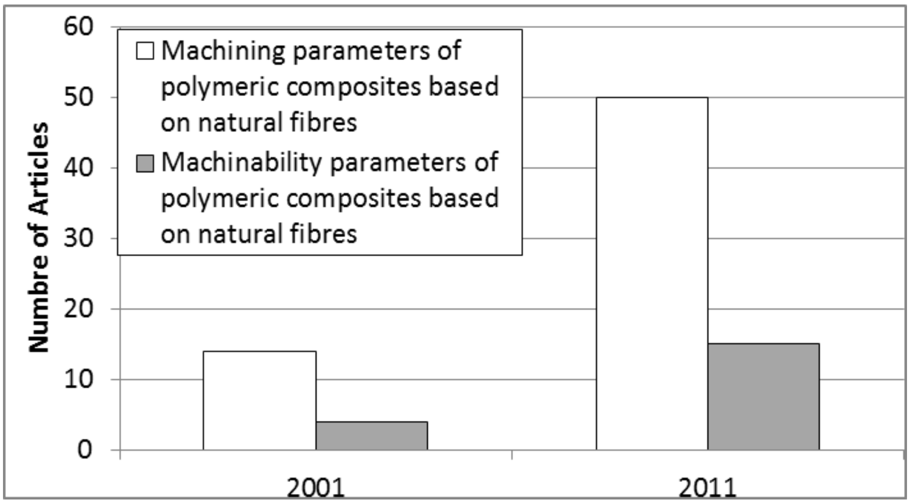

Figure 2.7: Comparison between the years 2001 and 2011 of the number of articles published on the machining and machinability of polymeric composites based on natural fibres

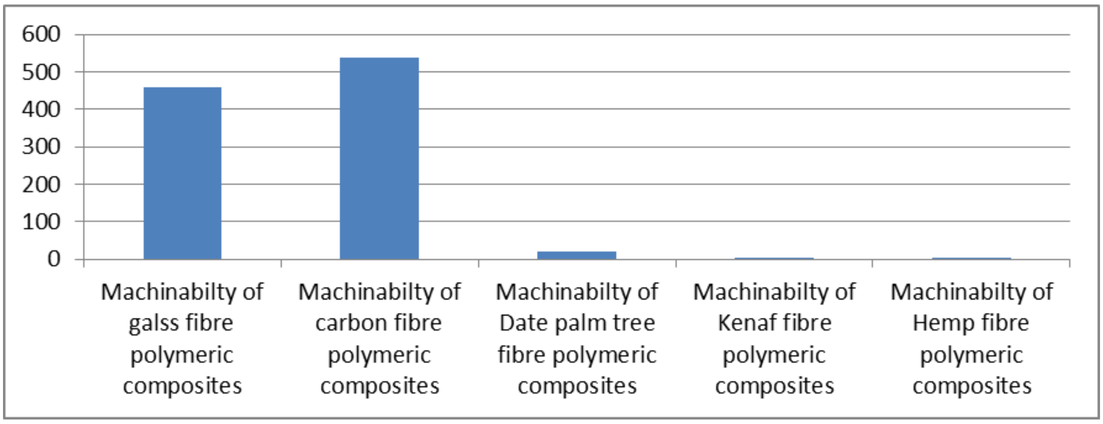

Figure 2.8: Comparison of the number of articles published on the machinability of polymeric composites based on natural and synthetic fibres

From those figures (2.7 and 2.8) one can see the limited literature on the machinability of the natural fibres polymer composites. However, with the available resources on different machining process took place on natural fibre polymer composites, the following sections addressed the main findings of the works and point out the main issues.

One difficulty that has limited the machinability of natural fibres as reinforcements of composites is the lack of a good adhesion to most polymeric matrices. The hydrophilic nature of natural fibres negatively affects adhesion to a hydrophobic matrix and, as a result, it may cause a lack of interlocking between the fibre and the matrix (Herrera-Franco and Valadez-González, 2004, Nam et al., 2011). To prevent this, the fibre surface must be modified to promote adhesion and, hence, improve the machinability of the composites (Valadez-Gonzalez et al., 1999, Van de Weyenberg et al., 2006).

Mylsamy and Rajendran (2011) investigated the influence of alkali treatment (five per cent) of short agave fibre reinforced epoxy composites on machinability in terms of fibre–matrix interaction for untreated and alkali-treated fibres using milling machine. Rough surfaces were observed with the treated composites, which led to better interlocking between the fibre and the matrix and increased the area of contact. In contrast, voids were noticed in the untreated (Herrera-Franco and Valadez-

González, 2004, Nam et al., 2011). To prevent this, the fibre surface must be modified to promote adhesion and, hence, improve the machinability of the composites (Valadez-Gonzalez et al., 1999, Van de Weyenberg et al., 2006). These observations were qualitatively similar to those reported by Valadez-Gonzalez et al. (1999), who investigated the effects of fibre surface treatment on the fibre–matrix bond strength of natural fibre reinforced composites.

Athijayamani et al. (2010) studied the effect of alkali treatment on machinability in terms of weight loss on natural fibre (roselle and sisal) hybrid polyester composite using drilling process. A 10 per cent NaOH solution treatment was used on the fibres for different durations (two, four, six and eight hours). Gradual weight loss was observed with increased wear test time (four, eight and 12 minutes) and the alkali-treated composite samples showed superior wear performance when compared with the untreated composite samples. This could be attributed to the removal of the moisture of fibres by the alkali treatment, which led to an increase in the interfacial bonding strength between the reinforcement and matrix.

(Nam et al., 2011) studied machinability in terms of the R_a of untreated and alkali-treated (five per cent NaOH) coir fibre reinforced poly (butylene succinate) biodegradable composites using drilling process. They reported that five per cent alkali treatment for a period of 72 hours increased R_a and the amount of cellulose exposed on the fibre surface. This enhanced the mechanical interlocking between the fibre and the matrix and led to better machinability.

2.4.1 Effect of fibre physical properties

Few reports have been made on the parameters that affect machinability of natural fibre composites (fibre distribution in the matrix, fibre length and diameter, moisture absorption, porosity and the way fibres break when compounding with the matrix) using milling machine. Mylsamy and Rajendran (2011) investigated the influence of fibre length (3, 7 and 10 mm) on machinability in terms of dimensional accuracy of drilled holes (4, 6, 8.5 and 12.5 mm) using drill machine. An HSS drill bit was used at 260 RPM on short agave fibre reinforced epoxy composites. From the drilled hole test, the composite with a 3 mm fibre length was found to be optimum, because it showed better dimensional accuracy than the other composites. As noted in the results, decreased fibre length helped to improve fibre wetting and impregnation. This, in turn, resulted in enhanced machinability.

Athijayamani et al. (2010) studied the effect of fibre content in hybrid polyester composites (5, 10, 20 and 30 wt% treated roselle and sisal fibres) on machinability in terms of drilled hole dimensional accuracy using drill machine. It was reported that composite specimens with 30 wt% fibre content showed better dimensional accuracy than composite specimens with 5 wt% fibre content. This could have been a result of the increased number of fibres around the drilled hole's surface, which helped hold it together.

2.4.2 Effect of operating parameters and conditions

Jayabal, Natarajan and Sekar (2011) investigated the effect of drilling parameters, such as drill bit diameter, spindle speed and feed rate, on machinability in terms of tool wear for hybrid composites, E-glass and natural coir fibre, using drill machine. It was reported that feed rate played an important role in the tool wear mechanism compared with other factors because of the size of the hole made and the counter force of fibres in composites. The insignificance of the effects of spindle speed and drill bit diameter parameters on machinability was due to the softness of the composite. The most effective interaction on machinability was found to be between drill bit diameter and feed rate. Further, optimum levels to attain a minimum value of tool wear were determined (diameter = 8 mm, spindle speed = 1,503 RPM and feed rate = 0.2 mm/rev).

2.4.3 Effect of coupling agents

There is no reported works on the influence of the coupling agent on the machinability of natural fibre/polymer composites. However, there are some reported works on the tribological behaviour of such materials and the roughness of the surface is considered in the studies which can be reported here. Coupling agents used to improve the interface between the fibre and the matrix have received considerable attention because of their effectiveness in modifying the interface by developing a bond between the components of the composite (Van de Weyenberg et al., 2003, Zafeiropoulos et al., 2002, Demir et al., 2006). Examples of coupling agents that have been used in recent research to change the fibre surface are γ-methacryloxypropyltrimethoxysilane and vinyl tris (2-methoxyethoxy) silane. The compatibility of the fibre with the polymeric matrix used can also be improved with these coupling agents (Yemele et al., 2010, Wu et al., 2000, Yam et al., 1990).

The effects of silane coupling agents of polypropylene–luffa fibre, namely aminopropyltriethoxy silane (AS) and mercapto silane (MS), on machinability in terms of R_a were investigated by Demir et al. (2006). They reported that AS and MS coupling agents exhibited lower R_a values (88 and 85 nm, respectively) than the untreated composite (138 nm) because of the increased coverage of fibre surfaces with a silane layer.

2.5 Recommendations and Main Points Extracted From the Literature

It was discovered that chemical treatment of natural fibres improved their compatibility with the matrix by removing their surface tissues, increasing the R_a and reducing moisture absorption. This resulted in improved mechanical properties of the composites (Athijayamani et al., 2010, Alawar et al., 2009, Mylsamy and Rajendran, 2011, Takeyama and Iijima, 1988, Edeerozey et al., 2007, Saha et al., 2010, Le Troedec et al., 2008, Colom et al., 2003, Van de Weyenberg et al., 2003, Jayabal et al., 2011, Eichhorn et al., 2001). The duration of chemical treatment was vital. The mechanical properties increased with longer duration of treatment but they would peak to a maximum and then fall. The usual chemical used was NaOH, at different concentrations.

Orientation of the fibre also plays an important role in controlling the mechanical properties of the composites (Jain et al., 2002, Khashaba et al., 2010b, Herrera-Franco and Valadez-González, 2004, Azmi, 2012, Tsao and Chiu, 2011, Yam et al., 1990, Yemele et al., 2010). Herrera-Franco and Valadez-González (2004) and Jacob, Thomas and Varughese (2004), respectively, found that longitudinal fibre orientation provided much higher tensile and flexural strengths that its traverse orientation counterpart.

It was also reported that mechanical properties could be enhanced by increasing fibre V_f (Ku et al., 2011, Rao and Rao, 2007, Brahim and Cheikh, 2007). However, V_f above a certain level causes fibre clotting, thus the applied loads cannot be distributed evenly, which leads to a decrease in mechanical properties (Yousif, 2010). Therefore, the optimisation of a fibre V_f value is necessary for strengthening the composite (Ku et al., 2011, Lei et al., 2006, Ma et al., 2005, Beg and Pickering, 2008, Madsen and Lilholt, 2003, Mata et al., 2009, Migneault et al., 2009, Oda et al., 2012, Tarfaoui et al., 2008, Oksman et al., 2009, Azmi, 2012).

Some physical properties of the fibres, including quality of fibre distributed in the matrix; fibre size, length and diameter; moisture absorption; porosity and the way fibres break during compounding with the matrix, were found to affect the mechanical properties of the composites formed (Tsao and Hocheng, 2008b, Yousif, 2010, Khashaba et al., 2010b, Palanikumar, 2011, Davim et al., 2004, Gaitonde et al., 2008, Mohan et al., 2005, Migneault et al., 2009). Moreover, the aspect ratio of the fibre (L/D) also plays an important role in the mechanical properties of the composite, as mentioned by D(Duc et al., 2011). (Beg and Pickering, 2008) found that a decrease in fibre length led to an increase in tensile strength, Young's modulus and impact strength of kraft fibre reinforced polypropylene composites.

From the above work and discussion, it can be concluded that the machinability and mechanical properties of natural FRP composites are affected not only by the interfacial adhesion between the fibres and the matrix, but also by the length and aspect ratio of the fibres and their V_f, orientation and dispersion in the composites. Moreover, fibre dispersion and length are correlated with the mixing number and shear levels in processing.

CHAPTER 3: CHARACTERISTICS OF DATE PALM FIBRE AND EPOXY COMPOSITES

3.1 Introduction

Interfacial adhesion of natural fibres as reinforcement for fibre polymeric composites is the key parameter in designing composites. In the current study, interfacial adhesion of date palm fibre with epoxy matrix is investigated experimentally using the single fibre pull out technique. The influence of NaOH treatment concentrations (zero per cent to nine per cent), fibre embedded length and fibre diameter on the interfacial adhesion property were considered in this study. SEM was used to observe the surface morphology and damage feature on the fibre and bonding area before and after conducting the experiments. The results revealed that six per cent concentration of NaOH is the optimum solution for treating date palm fibre to maintain high interfacial adhesion and strength with epoxy matrix. The embedded length of the fibre controlled the interfacial adhesion property, where 10 mm embedded length was the optimum fibre length.

3.1.1 Background of the research

In recent years, natural fibres have drawn considerable attention as substitutes for synthetic fibres, such as glass and carbon fibres. Natural fibre applications have been growing in many sectors, including automobiles, furniture, packing and construction industry parts where a high load carrying capacity is not required (Torres and Cubillas, 2005, Alawar et al., 2009, Edeerozey et al., 2007, Hepworth et al., 2000, Joshi et al., 2004, Rokbi et al., 2011). The attractive features of natural fibres over traditional counterparts include relatively low cost, low weight, high specific modulus, less hazards and abundant and renewable resources (Bledzki and Gassan, 1999, Haque et al., 2009, Rokbi et al., 2011, Rosa et al., 2009, Torres and Cubillas, 2005, Alawar et al., 2009). (Joshi et al., 2004) reported that low weight (20–30 wt%)

and high volume of natural fibres compared to synthetic fibres in polymeric composites have improved fuel efficiency and reduced emissions in automobile industries. Natural fibres can be disposed of at the end of their lifecycle via composting or recovery of their calorific value in a furnace, which is not possible with synthetic fibres (Torres and Cubillas, 2005, Joshi et al., 2004, Cantero et al., 2003). In contrast, natural fibres also exhibit some undesirable characteristics, such as high moisture absorption and highly anisotropic properties (Felix and Gatenholm, 1991a, Joseph et al., 1999, Cantero et al., 2003). Many studies on the mechanical properties of natural fibres and how these incorporate with various thermosets (epoxy, polyester and phenol formaldehyde) and thermoplastics (PE, PS and PEEK) have been attempted (Ben Difallah et al., 2012, Hepworth et al., 2000, Abdul Khalil et al., 2010, Virk et al., 2010, Torres and Cubillas, 2005, Haque et al., 2009, Rosa et al., 2009). These studies emphasised that the composited properties depend on the natural fibres' interfacial bonding with the synthetic matrices. In other words, adhesion between the reinforcing fibres and the matrix plays an important role in the final mechanical properties of the materials, as the stress transfer between matrix and fibres determines reinforcement efficiency. However, natural fibres tend to be strong polar and hydrophilic materials because of cellulose, hemicelluloses, pectins and lignin richness in natural fibres, while polymer materials are apolar and exhibit significant hydrophobicity (Hepworth et al., 2000, Cantero et al., 2003, Alawar et al., 2009, Haque et al., 2009, Saha et al., 2010). This means that there are significant problems of compatibility between the fibre and the matrix because of the weak interface. In general, poor interfacial interaction leads to internal strains, porosity, environmental degradation, moisture absorption, poor mechanical properties of composite parts and debonding over time. Therefore, surface modification of natural fibres by means of treatment is one of the largest areas of current research to improve compatibility and interfacial bond strength. It is worth mentioning that the chemical treatment of the fibres can either increase or decrease the strength of the fibres and, hence, a good understanding of what occurs structurally is required (Alawar et al., 2009, Bledzki and Gassan, 1999, Cantero et al., 2003, Edeerozey et al., 2007, Haque et al., 2009, Hepworth et al., 2000, Rokbi et al., 2011, Rosa et al., 2009, Saha et al., 2010, Torres and Cubillas, 2005).

Chemical treatments, such as bleaching, acetylation and alkali treatment, aim to improve fibre–matrix adhesion by increasing the surface roughness of the natural fibres through cleaning the fibre surface to remove impurities and disrupting the moisture absorption process through a coat of OH groups on the fibre (Cantero et al., 2003, Edeerozey et al., 2007, Haque et al., 2009, Rokbi et al., 2011, Rosa et al., 2009, Saha et al., 2010, Torres and Cubillas, 2005). Alawar et al. (2009) investigated the effects of chemical treatments on surface morphology and the mechanical properties of date palm fibre, considering two kind of treatments in deferent concentrations (NaOH 0.5–5 per cent and HCL 0.3–1.6 N). The results of that work revealed that HCL had high reduction in the tensile and huge distortions on the surface because of the acid attack on the surface of the fibre. However, NaOH treatment enhanced the surface morphology of the fibre and increased the number of grooves on the surface. In (Saha et al., 2010), the effect of alkali treatment (NaOH) under certain conditions (i.e., ambient temperatures, elevated temperatures and high pressure steaming treatment) on the tensile strength of jute fibres has been studied. The treatment resulted in a rough jute fibre surface and better separation by removing the surface impurities, non-cellulosic materials, inorganic substance and wax. In addition, the range representing O–H stretching of the hydrogen bond became less intense on alkali treatment. The optimum enhancing of tensile strength and elongation at break were 65 per cent and 38 per cent, respectively, for alkali-steam treatment compared to untreated fibres. In recent work (Rokbi et al., 2011), the influence of alkaline treatment on the flexural properties of polyester matrix composite reinforced with Alfa fibres (random orientation and 40 wt%) has been reported. The alkali treatment (NaOH) at one, five and 10 per cent concentrations for various socking periods of zero, 24 and 48 hours has been conducted. The flexural strength and flexural modulus improved by 60 per cent and 62 per cent, respectively, at 10 per cent NaOH consideration for 24 hours .The longer treatment time for Alfa fibres (48 hours with five per cent NaOH) decreased the flexural strength and flexural modulus because of excess delignification natural fibre that led to weakening of the fibre strength and damage to the fibre.

The date palm tree, a member of the palm tree family (phoenix dactylifera), is normally found in the Middle East, Northern Africa, the Canary Islands, Pakistan, India and the United States (California). The palm tree stem is covered with a mesh made of single fibres. Usually, these fibres create a natural woven mat of crossed fibres of different diameters. The possibility of finding a use for date palm fibres in fibre composite will open a new market for a fibre that is normally considered waste or is used in low value products.

3.2 Material Preparation and Experimental Procedure

3.2.1 Material selection and preparation

The resin used in this study was epoxy resin (R246TX), which was supplied by Australian Calibrating Services Pty Ltd. Date palm fibres were obtained from a date palm tree in a farm in Kuwait (see Figure 3.1a). All fibres were obtained from the outer layer of the tree stem. Only fibres from the same bunch were used to ensure consistency (see Figure 3.1b). The fibres were carefully extracted from the stem manually. Assuming that these fibres are of uniform cross-sectional geometry, the diameters and the shape of the fibres were selected using a Motic stereomicroscope (SMZ168 series). However, Figure 3.1b shows a waxy layer covering the fibre, which may be removed or cleaned with the assistance of the NaOH treatment (to be explained in the coming section). Three measurements were taken on each fibre. Glass fibre mats (see Figure 3.1c) with a density of 450 g/m2 were used for synthetic fibre epoxy composites and have similar geometry and arrangement to natural fibre mats for comparison purposes.

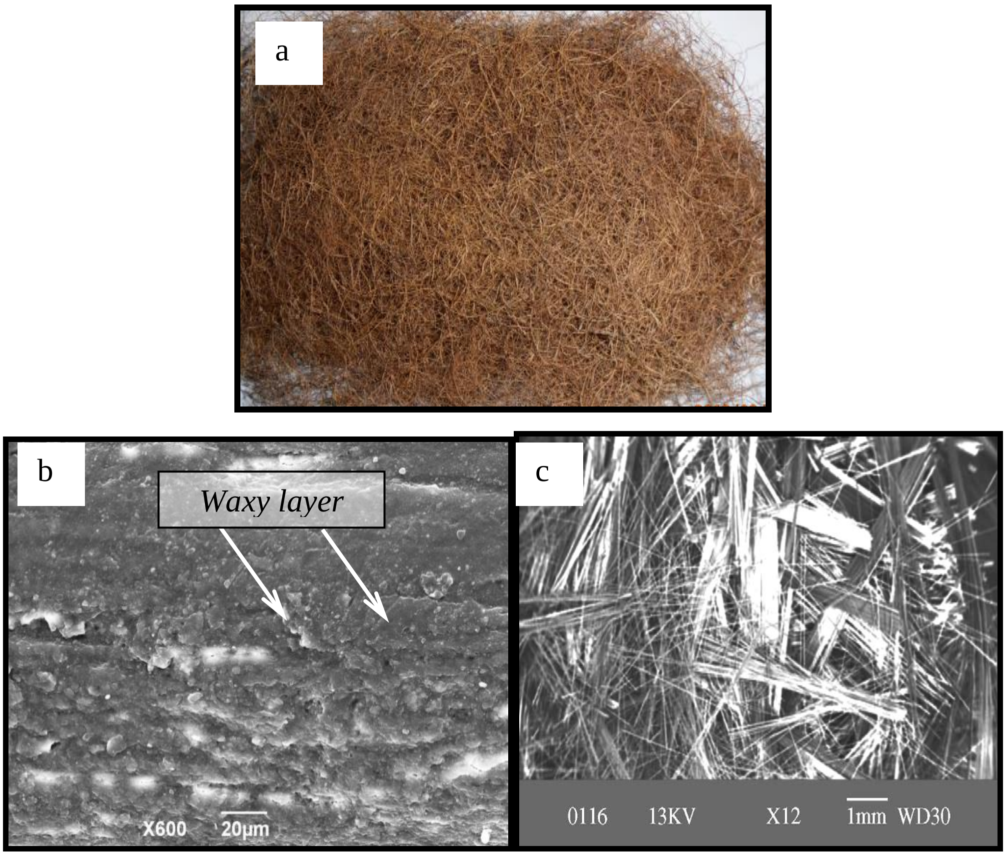

Figure 3.1: Micrographs of date palm and glass fibres

3.2.1.1 Alkali treatment

In the current work, selected date palm fibres were washed with tap water to remove all of the dirt and then left to dry at room temperature for 24 hours. The cleaned fibres were cut into an average length of 100 mm. Three different NaOH concentrations were prepared as 3, 6 and 9 wt%. The selected fibres were immersed in NaOH aqueous solution for 24 hours at room temperature. After treatment, the fibres were washed with tap water and then dried for 24 hours at room temperature. The influence of the treatment on the outer surface of the fibre will be presented in the results and discussion section of this chapter.

3.2.1.2 Samples preparation

To fabricate the single fibre pull out specimens, both ends of the selected fibres (treated with 3, 6 and 9 wt% NaOH) were adhered to two pieces of rubber to hold the ends of the fibres and also to prevent the resin from leaking during curing process. All the specimens were fixed to a gauge length of 10 mm. The gauge length was set to be short because longer fibres tend to have a higher possibility of flaws, which affects the consistency of results. Figure 3.1a shows the single fibre pull out sample preparation before pouring the resin mixture into the metal mould (90 mm × 10 mm × 10 mm). Before proceeding to specimen fabrication, a non-stick paper was placed into the mould to prevent the mixture from sticking and to ensure it was easy to remove after the curing process. The epoxy resin was mixed with hardener in a ratio of 3:1. The mixture was left for approximately five to 10 minutes and then poured carefully into the mould to avoid generating bubbles in the sample. Next, the mixture was poured into the mould and left to be cured at room temperature for 24 hours. Later, the sample was removed from the mould, as seen in Figure 3.1b. Finally, the composite was cut to desired fibre embedment lengths of 5, 10, 15 and 20 mm using a hand saw.

For tensile testing, a mould with a dog-bone shape and dimensions given in Figure 3.2 was used, according to American Society for Testing and Materials (ASTM) standard D638, which is one of the most commonly recommended standards for polymeric composites. The epoxy resin was mixed with hardener in a ratio of 3:1 and left for approximately five to 10 minutes. It was then poured carefully into the mould to avoid generating bubbles in the sample. Next, the mixture was poured into the mould and left to be cured at room temperature for 24 hours. Later, the sample was removed from the mould. For each set of experiments, five samples were prepared and tested. The average tensile strength, the modulus of elasticity and the strain at the fracture were determined.

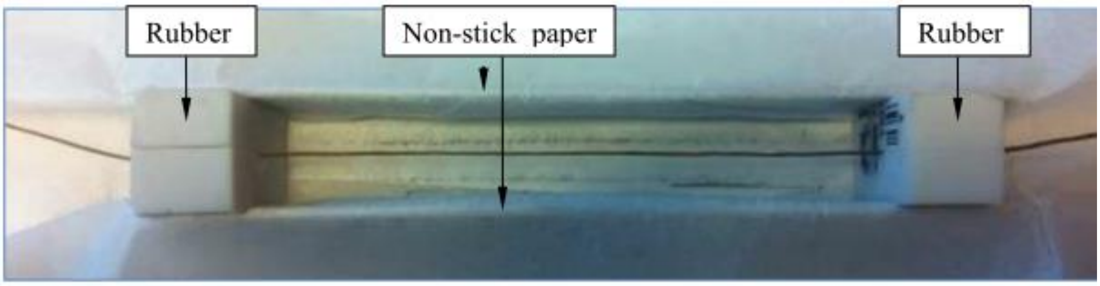

Mould for specimen fabrication

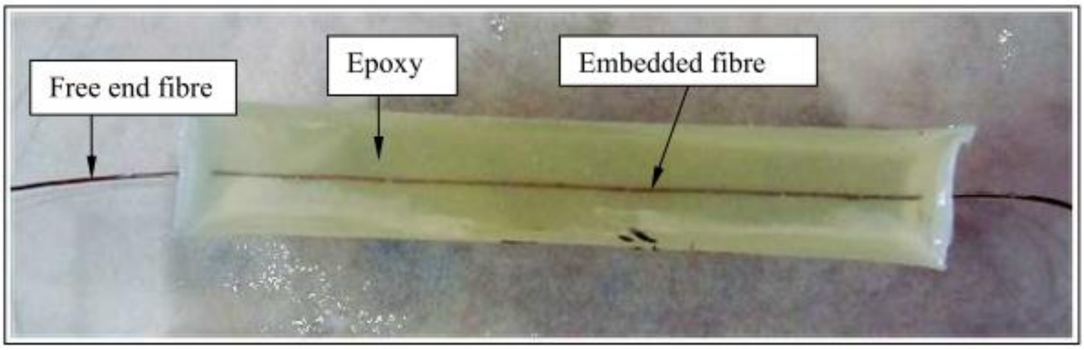

Specimen after removing from mould

Figure 3.2: Photos showing the single fibre in the mould and the sample after preparation

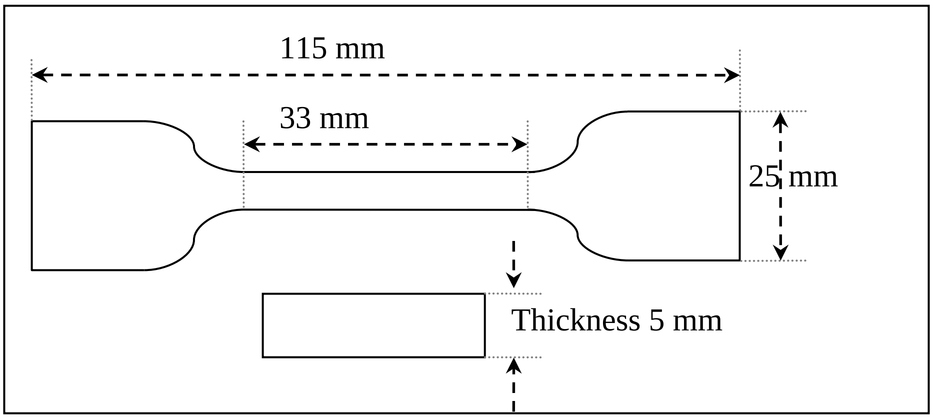

Figure 3.3: Specimen geometry and dimensions for tensile testing

3.2.2 Experimental procedure

3.2.2.1 Single fibre pull out experiments

For single fibre pull out tests, the specimen was clamped tightly on the Hounsfield tensometer (250 N–2500 N) system. The crosshead speed was set to 1 mm/min. Three test replicates were performed for each concentration of treatment (3–9 wt% NaOH) and the average values were determined. The single fibre pull out tests were performed based on the ASTM STP 452 (L.J. Broutman). The morphology of the fibres and matrix surfaces was studied under a scanning electron microscope. All specimens were gold sputtered before the examination.

3.2.2.2 Tensile experiments of the composites

The prepared tensile samples of neat epoxy, untreated and treated (six per cent NaOH) date palm fibre reinforced epoxy (UT-DPFRE and T-DPFRE) and glass fibre epoxy composites were tested according to ASTM D7205. The MTS 810 TestStar machine was used to conduct the tensile experiments. The machine was set to 1 mm/min loading speed. For each set of tests, five samples were tested and the averages of the data were determined. For all the prepared samples, an SEM was used to examine the samples after each test to study the morphology of the materials and categorise the damage features. The Neo-Jeol machine was used for SEM observation.

3.3 Results and Discussion

3.3.1 Effect of NaOH concentration on the surface characteristics of the fibres

The micrographs of the prepared fibres are shown in Figure 3.4a–d. Figure 3.4a represents the micrograph of the untreated date palm fibre. The figure shows that there is a layer covering the fibres (a waxy layer). This layer may decrease interfacial adhesion of the fibre with the matrix. Therefore, it is recommended to remove it via chemical treatment, such as NaOH. Since there are different findings regarding the effect of NaOH treatments on the surface characteristics of the natural fibres, the fibres were treated with three to nine per cent concentrations of NaOH. From Figure 3.4b–c, it is clear that NaOH treatment removes some of the waxy layer depending on the NaOH concentration. In Figure 3.4b (three per cent NaOH), a slight removal of the outer layer and appearance of the inner fibre can be noticed. At a higher NaOH concentration of six per cent NaOH, complete appearance of the inner fibres and exposure of the holes is evident. A rough surface on the fibre appears, which could assist in enhancing the interfacial adhesion of the fibre with the matrix. At a very high NaOH concentration of nine per cent (Figure 3.4d), complete removal of the outer layer and appearance of the inner fibres can be noticed. From above, it can be seen that an increase in NaOH concentrations boosts the removal of the waxy layer covering the natural fibre.

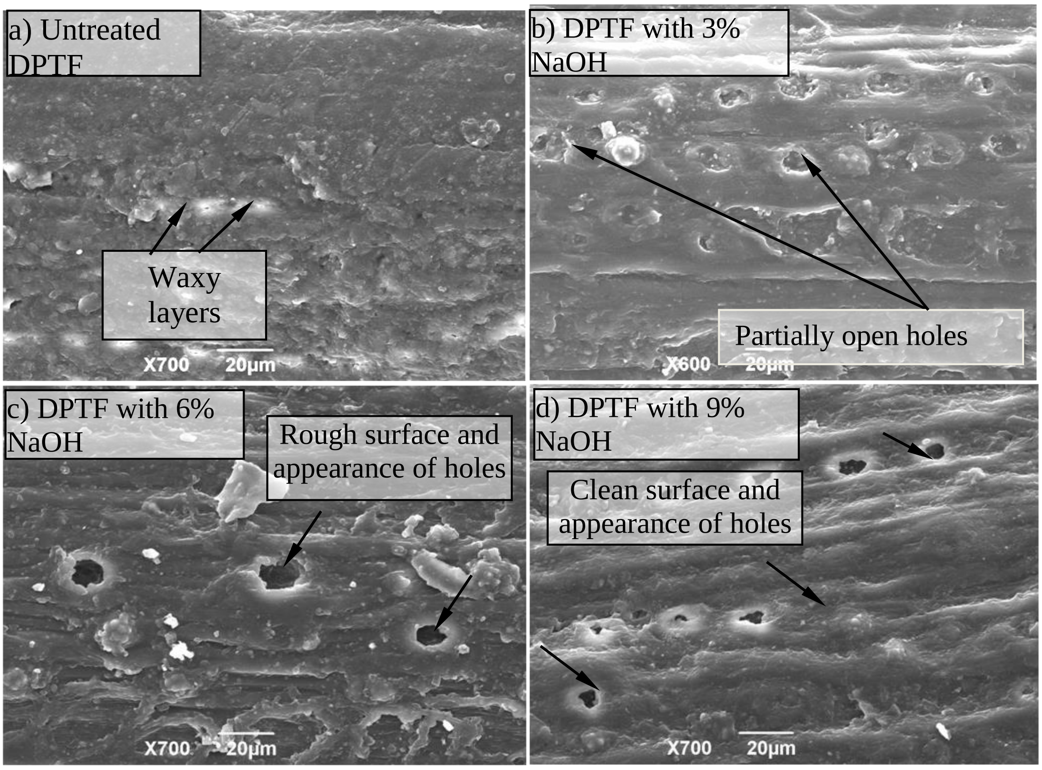

Figure 3.4: Micrographs of the untreated and treated date palm fibre surface with different NaOH concentrations

The NaOH treatment results are in agreement with the reported works that have been published on hemp (Le Troëdec et al., 2011, Sawpan et al., 2011), jute (Roy et al., 2012), oil palm (Yousif and El-Tayeb, 2007), coir (Yousif, 2009) and betel nut (Yousif et al., 2009). It has been found that NaOH is the most effective method in treating hemp fibres and enhancing interfacial adhesion properties. NaOH treatment acts on the middle lamella and on the primary cell wall, resulting in removal of the hemicelluloses and dissolving pectins. Conversely, bleaching (pure and followed by acetylation or alkalisation), pure acetylation, sodium sulphite and sulphuric acid with potassium permanganate have been used to treat okra fibres (De Rosa et al., 2011). In the study, all treatments tended to expose the lumens and the cleaning process occurred during treatment. Acetylate and bleach smoothed the surface of the fibre because of acetylation. Permanganate treated fibres showed small holes around the mid-section of the fibrils. An acid solution attacked the fibre and destroyed the main structure of the fibre. Similar results of acid solution treatment have been reported on hemp (Sawpan et al., 2011).

3.3.2 Tensile strength of single fibre

The tensile testing data of the date palm fibre treated with different NaOH concentrations (3, 6 and 9 wt%) are presented in Figure 3.5a–c. Each test was repeated three times and the results are displayed as strength against strain. In general, the tensile behaviour of the fibres exhibits ductile behaviour for all treated fibres, that is, elastic and elastic regions can be noticed in all curves presented. However, a higher concentration of NaOH (nine per cent) reduces the strain by approximately four per cent and 15 per cent compared to lower concentrations of NaOH (three and six per cent). The highest tensile strength (400 MPa) was exhibited when the fibre was treated with a low NaOH concentration (three per cent) (see Figure 3.5a). The lowest tensile strength (approximately 110 MPa) was evident in the treated fibre with a high concentration of NaOH (nine per cent) (see Figure 3.5c). In summary, it can be said that an increase in NaOH concentration worsens the tensile properties of the date palm fibre. Conversely, it is seen in Figure 3.4 that higher concentrations of NaOH enhance the surface characteristics of the fibre by removing the waxy layer from the surface. Therefore, there is optimum NaOH concentration through which good interfacial adhesion can be proposed. For the current study, it is proposed that six per cent NaOH is the optimum concentration, which provides acceptable fibre strength and surface characteristics. This can be further discussed with the single fibre pull out test in the following section.

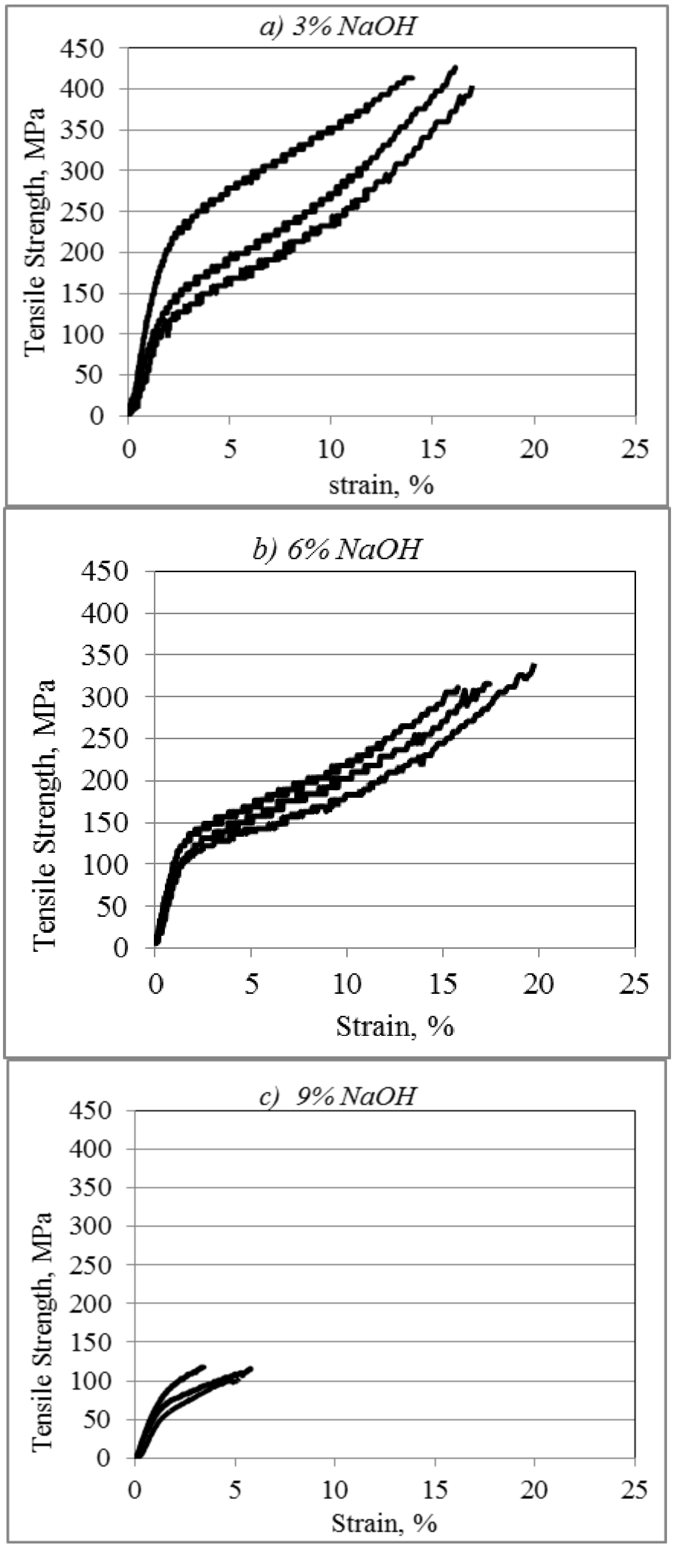

Figure 3.5: Tensile testing data of single fibre treated with different NaOH concentrations

3.3.3 Results and discussion of the interfacial adhesion tests

The single fibre pull out data are displayed as maximum stress and shear against NaOH concentrations of three, six and nine per cent with four different impeded lengths of 5 mm, 10 mm, 15 mm and 20 mm, as shown in Figure 3.6a and b. From Figure 3.6a, one can see that NaOH concentrations and the fibre embedded length influence the stress subjected on the fibre. There is an increase in the stress when the embedded length increases up to 15 mm, especially at NaOH concentrations of three per cent and six per cent. The longer imbedded length (20 mm) shows reduction in the stress at all NaOH concentrations. This is because of the differences in the tensile strength of the fibre and/or the interfacial adhesion property of the fibre with the matrix, that is, the ability of the fibre to carry the load and transfer it to the matrix. In terms of the fibre strength, it was mentioned in the previous section that a higher NaOH concentration (nine per cent) decreased the tensile strength of the fibre. It seems that the low stress subjected on the fibre during the pull out test was due to the breakage of the fibres rather than pull out. For the low stress generated on the fibre treated with three per cent NaOH treatment, it seems the interfacial adhesion is the most pronounced factor that affects the value of the stress during the pull out testing.

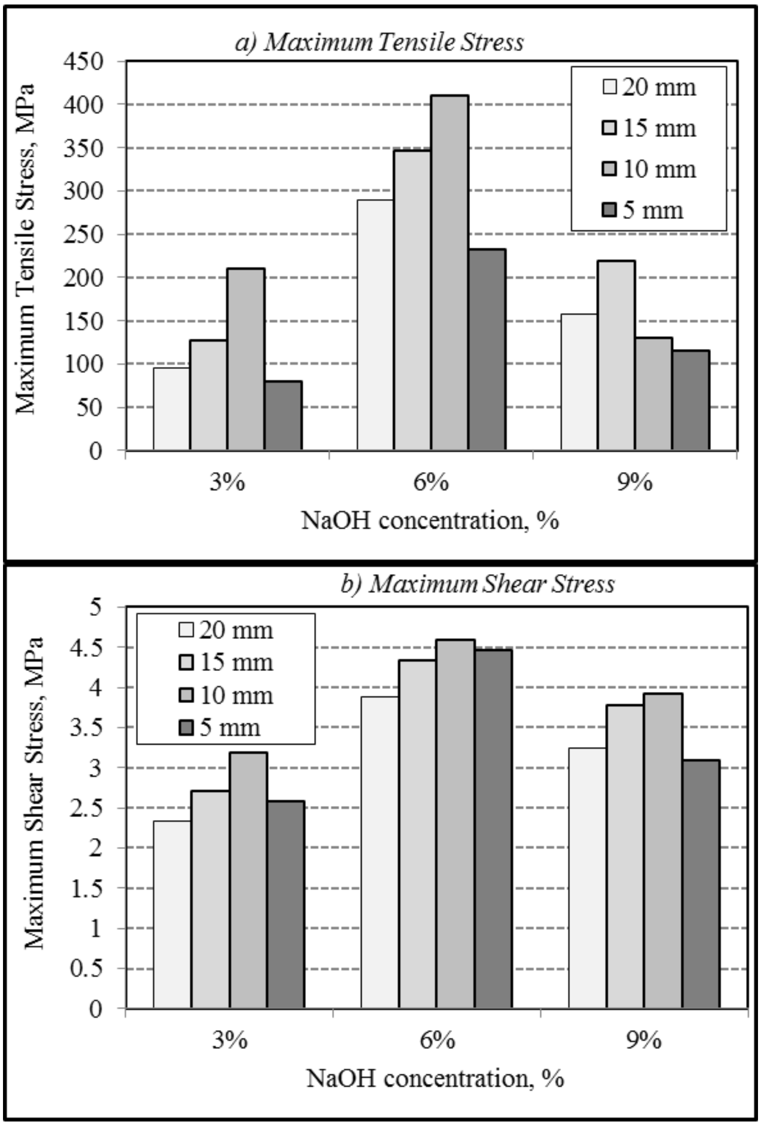

Figure 3.6: Single Fibre Pull out data showing the maximum tensile stress and maximum shear stress of the treated fibre with different NaOH concentrations

The interfacial adhesion of the fibre with matrix can be determined by measuring the shear stress generated in the bonding area (between the fibre and the matrix). Figure 3.6b displays the maximum shear stress in the interfacial area of the fibre with the matrix at different embedded lengths and NaOH concentrations. At a low NaOH concentration value of three per cent, the shear stress in the bonding area is relatively low compared to other concentrations. This could be due to the outer waxy layer surrounding the fibres, which lowers the interaction between the asperities of both epoxy and fibre surfaces. This could lead to a pull out process during the pull out testing. Further explanation will be given in the SEM observation section. Conversely, Figure 3.6b shows that the shear in the interfacial area is high when six per cent NaOH concentration was used in the fibre treatment. This means that there was high resistance to the pull out process during the loading despite the high tensile strength of the fibre at this concentration (Figure 3.5b). At a high NaOH concentration of nine per cent, it seems there is a reduction in the value of the shear in the bonding area. This is not because of poor interfacial adhesion of the fibre; rather, it is due to the weakness of the fibres that occurred because of the high concentration of NaOH, as evident in Figure 3.5c.

To clarify the above argument, schematic drawings showing the three treated fibre behaviours under pull out loading conditions are displayed in Figure 3.7a–c. For the fibre treated with three per cent NaOH, there was an outer layer covering the fibres. When the load was applied, the outer layer adhered to the epoxy and detachment between the inner fibres and the outer layer took place. At this stage, the pull out process occurred (see Figure 3.7a). Conversely, the outer layer was removed when the fibre was treated with six per cent NaOH, which, in turn, led to high interaction and adhesion of the inner fibres with the epoxy. Moreover, during the curing process, some of the epoxy resin can enter inside the fibre, which generates interlocking regions between the fibre surface and the epoxy matrix. Such behaviour prevents pull out of the fibres, which agrees with the high stress and shear results given in Figure 3.7 in the case of six per cent NaOH concentration (see Figure 3.7b). In the case of nine per cent NaOH treatment, the outer layer was removed; however, the fibre was weakened because of the high concentration of NaOH in the treatment process. It is suggested that there will be no pull out process; however, early breakage to the fibre will occur (see Figure 3.7c).

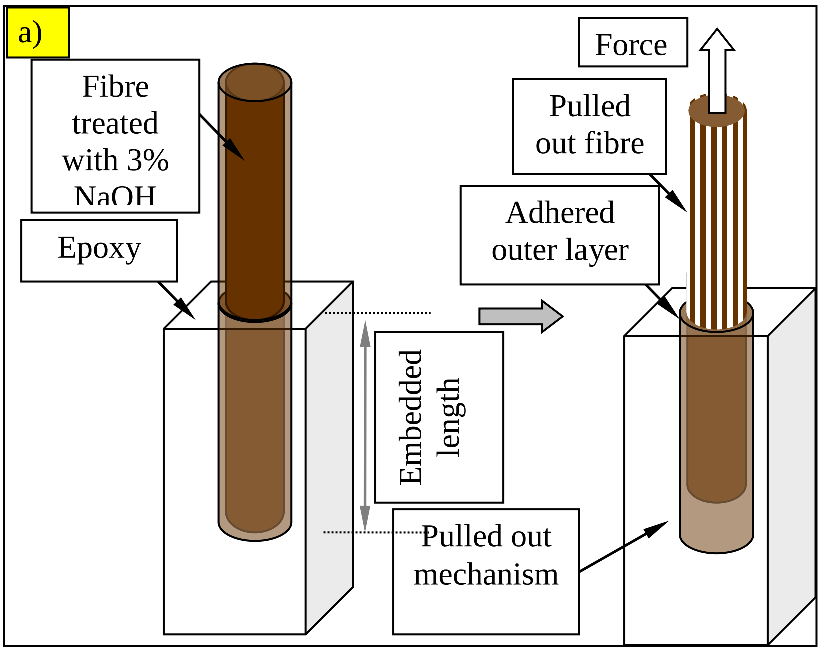
a)
Fibre treated with 3% NaOH
Epoxy
Force
Pulled out fibre
Adhered outer layer
Embedded length
Pulled out mechanism

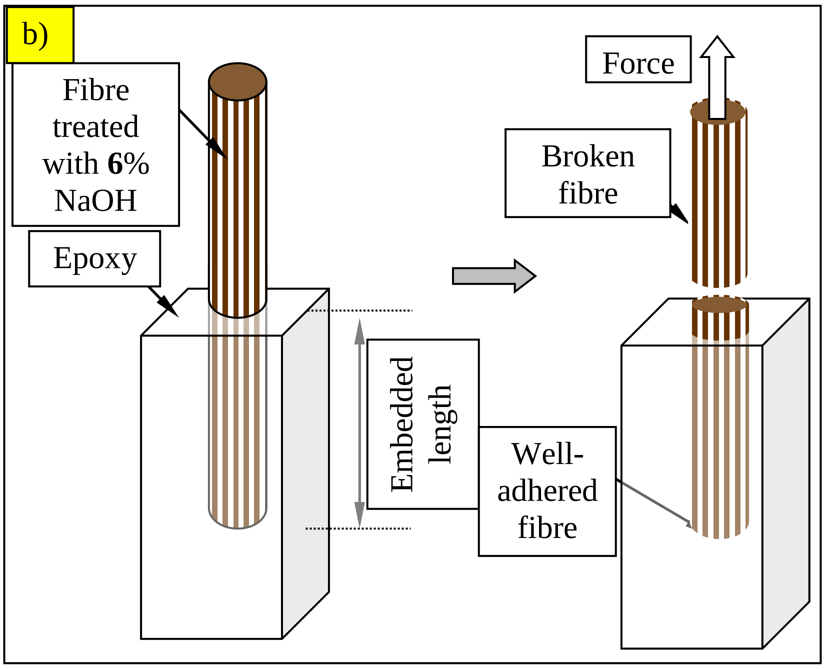
b)
Fibre treated with **6**% NaOH
Epoxy
Force
Broken fibre
Embedded length
Well-adhered fibre

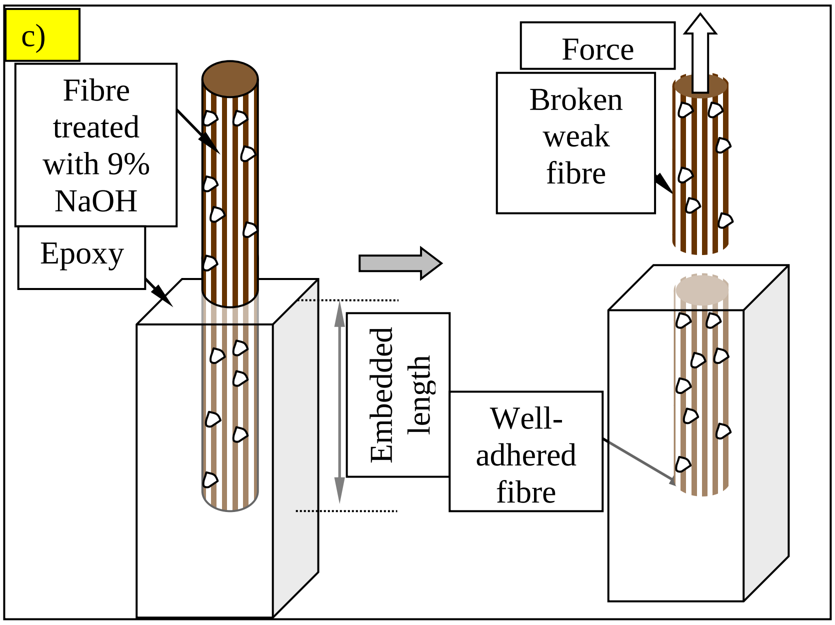

Figure 3.7: Schematic drawing showing the fibre behaviour under pull out testing for treated date palm fibre with different NaOH concentrations

3.3.4 SEM observation and discussion of the experimental results

To support the findings and the proposed mechanism, the tested samples were scanned using SEM. The micrographs of the tested samples are given in Figure 3.8 for the different NaOH concentrations. For three per cent NaOH treatment, the micrographs shown in Figure 3.8a–b indicate that the pull out mechanism took place during testing and the outer layer of the fibre seems to be adhered to the epoxy (c.f. Figure 3.8b). This supports the thought given in Figure 3.7a and is in agreement with the experimental results introduced in Figure 3.6a (i.e., low shear and stress of fibres at a low NaOH concentration of three per cent).

When the fibre was treated with six per cent NaOH, there was no evidence of the fibre pull out mechanism. However, tearing and breakage of fibres can be noticed, indicating high interfacial adhesion of the fibre with the matrix at this treatment condition (see Figure 3.8c). From the magnified micrograph (see Figure 3.8d), one can say that the bond between the date palm fibre treated with six per cent NaOH and the epoxy region is strong.

For the nine per cent NaOH treatment, it was not easy to examine the surface of the samples because of the deep allocation of the fibre breakage. Therefore, the sample was broken to observe the embedded part of the fibre. Figure 3.8e shows the micrograph of the embedded fibre (treated with nine per cent NaOH), indicating that the bond of the fibre with the matrix is very strong. However, there is clear damage to the fibres, that is, a weakening process took place on the fibre because of the high concentration of NaOH during the treatment process. Those micrographs support the experimental results (see Figure 3.6) and the thoughts in Figure 3.7.

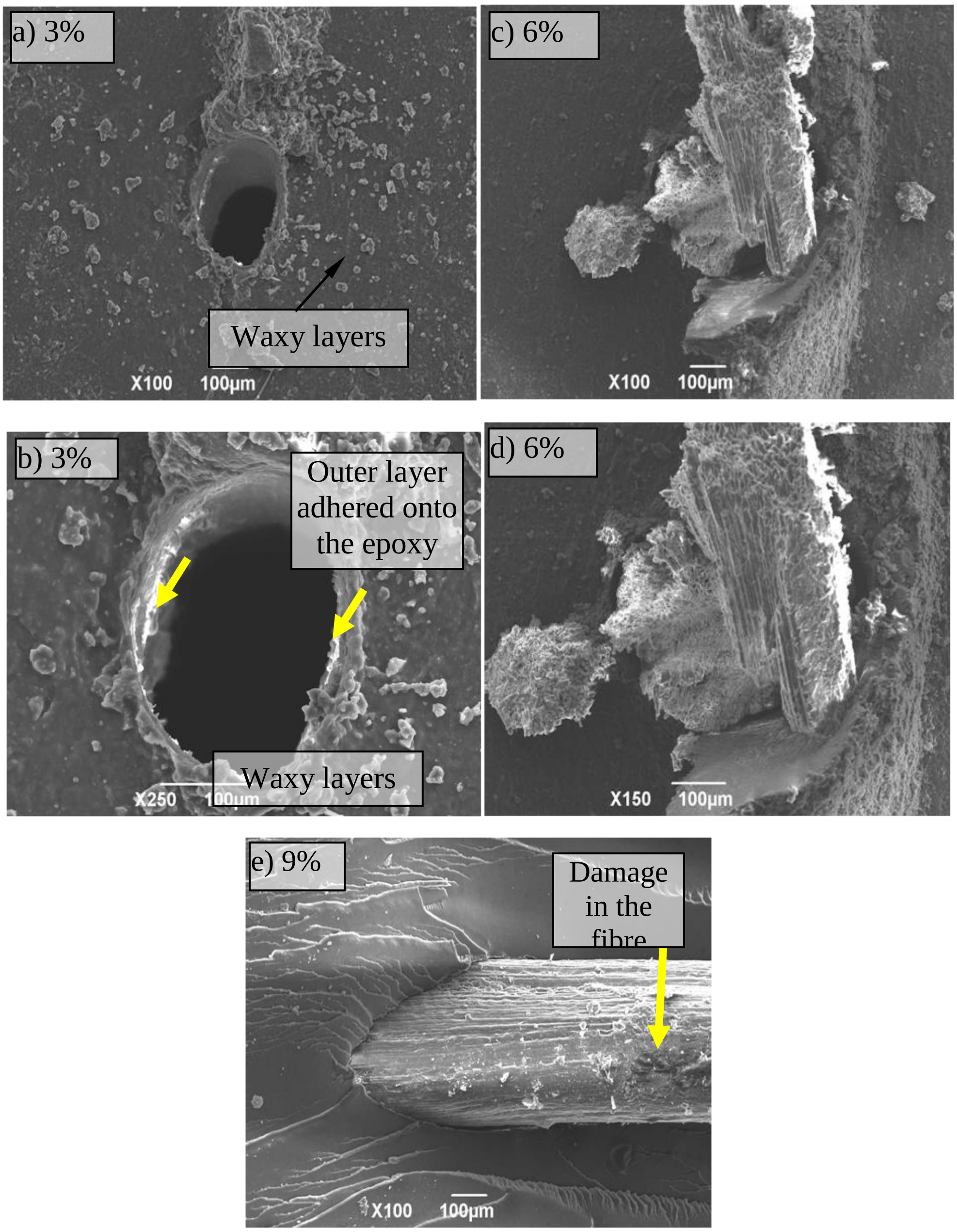

Figure 3.8: Micrographs of samples prepared with different NaOH percentage treatment fibre after single fibre pull out experiments

3.3.5 Correlation between experimental and theoretical data

To correlate the experimental finding with the theoretical ones, the critical length of fibres is determined based on Equation 3.1, (Folkes and Wong, 1987).

$$L_c = \frac{\sigma \, d}{\tau_c} \qquad \textbf{(Equation 3.1)}$$

where

L_c = critical length, σ = tensile strength of the fibre, d = diameter of the fibre and τ_c = shear strength of the bond between the matrix and the fibre. Simply, the critical length, L_c, is the minimum length that the fibres must have to strengthen a material to their maximum load. The experimental results obtained for the tensile and pull out tests are used to calculate the critical length of each fibre at its condition. Based on this, Figure 3.9 represents the relationship of the critical length with the diameter of the fibre at each NaOH concentration (three to nine per cent). The figure clearly indicates that increasing the diameter of the fibre requires longer fibre length for all NaOH concentrations. Further, the low and high NaOH concentrations (three per cent and nine per cent) require longer fibre lengths at all fibre diameters. This is mainly due to the poor interfacial adhesion of the fibre at low NaOH concentration and weakness of the fibre at high NaOH concentration. Therefore, six per cent NaOH is the most suitable percentage for date palm fibre treatment. It is recommended that this finding should be adopted with other types of fibres, that is, it is not necessarily that the higher the NaOH concentration the better the fibre's characteristics.

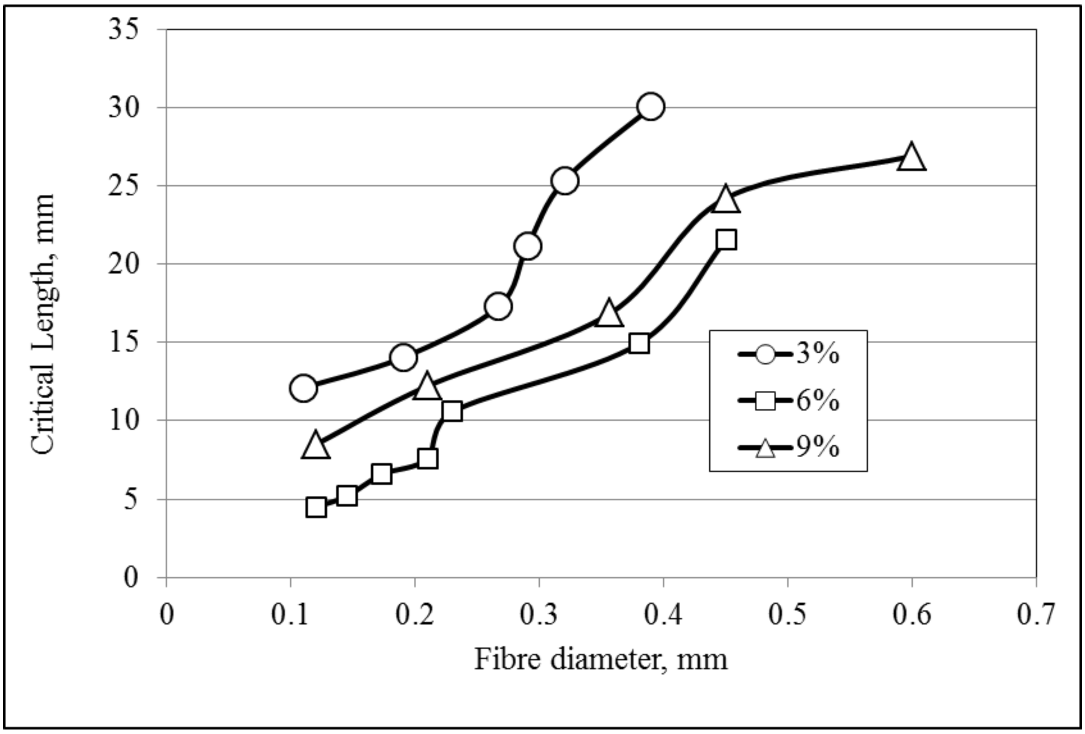

Figure 3.9: Critical length relationship with the fibre diameter and NaOH concentration

3.3.6 Comparison of interfacial adhesion results with previous published works

Table 3.1 summarises some of the most recent works that study the influence of interfacial adhesion of natural fibres with various matrices on the fibre and/or fibre/polymer composite properties in terms of mechanical (Le Troëdec et al., 2011, Sawpan et al., 2011, Merlini et al., 2011, Nirmal et al., 2011a), physical, chemical (Merlini et al., 2011) and tribological (Chin and Yousif, 2009, Yousif and El-Tayeb, 2007, Yousif, 2009, Yousif et al., 2009). All of these works showed significant influence of all chemical treatment on fibre and/or composite properties. However, it is not true that all types of chemical treatment and concentration improve the fibre and/or composite characteristics. For instance, ethylene diamine tetraacetic acid (1.35 x 10.3 mol/L) (EDTA) (Le Troëdec et al., 2011), polyethylene imine (2,000 g/mol) (PEI) (Abdelbary et al.), HCL (Nirmal et al., 2011b) and maleic anhydride (Sawpan et al., 2011) deteriorated the surface and the structure of the fibres. Despite enhancement of the interfacial adhesion of the fibre with the matrix, the fibre strength dramatically decreased after treatment. In other words, there was a negative effect and the treated fibre in the polymer matrix (i.e., neat polymer) showed better mechanical properties compared to treated fibre/polymer composites. This is in agreement with the current work, where a high NaOH concentration (nine per cent) enhanced the interfacial adhesion of the date palm fibre but decreased the tensile strength of the fibre itself. However, from the table, it is clear that NaOH chemical treatment is the most pronounced technique in enhancing interfacial adhesion of natural fibres and maintaining good tensile strength of the fibre, considering the optimum concentration of NaOH treatment. Conversely, the optimum percentage of NaOH varies for each type of fibre, which is dependent on the amount of OH group in the natural fibre. For example, 10 per cent NaOH concentration is needed to remove the waxy layer and tissues from banana fibres (Merlini et al., 2011). This amount of NaOH is not desired with other types of natural fibres, for example, date palm, coir (Yousif, 2009) and betel nut (Nirmal et al., 2011a, Nirmal et al., 2010).

Table 3.1: Summary of the previous works on interfacial adhesion of natural fibres

Fibre	Matrix	Treatment	Remarks
Hemp (Le Troëdec et al., 2011)	Silica colloid	1. ethylene diamine tetraacetic acid (1.35 x 10.3 mol/L) (EDTA) 2. polyethylene imine (2,000 g/mol) (PEI) 3. NaOH (1.6 mol/L)	1. EDTA decreased adhesion force by 33% 2. PEI decreased adhesion force by 26% 3. NaOH increased adhesion force by 130%
Coir (Arrakhiz et al., 2012)	Polyethylene	1. silane (0.5 wt%) 2. NaOH (1.6 mol/L) 3. Dodecane bromide (C12) (3 mL)	1. silane increased adhesion force by 12% 2. NaOH decreased adhesion by 4% 3. C12 increased adhesion force by 4%
Betel nut (Nirmal et al., 2011b)	1. Polyester 2. Epoxy	1. HCl 4% 2. HCl 6% 3. NaOH 4% 4. NaOH 6%	1. 6% NaOH with polyester increased adhesion force by 130% 2. 6% NaOH with epoxy increased adhesion force by 112%
Banana (Merlini et al., 2011)	Polyurethane	NaOH 10%	1. interfacial adhesion increased by 93%
Hemp (Sawpan et al., 2011)	Polyactide (PLA)	1. NaOH 5% 2. saline 0.5% 3. maleic anhydride 5% 4. acetic anhydride	1. 5% NaOH increased adhesion force by 100% 2. 0.5% saline increased adhesion force by 45% 3. acetic anhydride increased adhesion force by 9% 4. 5% maleic anhydride had no effect on adhesion force
Oil Palm (Yousif, 2010)	Polyester	1. 6% NaOH	1. highly enhanced the interfacial adhesion compared to the untreated fibres

3.4 Mechanical Properties of the Composites

Tensile data were obtained from the tensile machine and plotted in terms of stress versus strain, as shown in Figure 3.10 a–d, for neat epoxy, glass/epoxy composite and date/epoxy composite, respectively. In the first figure (see Figure 3.10a), it can be seen that the majority of the tensile strengths are reached, the ultimate value being between 40 MPa and 50 MPa. Despite the used epoxy in the current study being thermoset, it seems there is a slight plastic deformation region that can be seen after approximately 2.5 per cent of the strain. At some samples, the strain reached above four per cent, reflecting the ductility of the neat epoxy. Conversely, in Figure 3.10b, the addition of the glass fibres deteriorated the ductility of the epoxy because there was high reduction in the strain at the break of the composites to approximately 2.5 per cent in average for the five samples. This should be expected because of the high bristliness of the glass fibres compared to the epoxy. Despite this, one can see a significant improvement in the ultimate tensile strength, which reaches approximately 100 MPa compared to neat epoxy, which showed below 50 MPa, as seen in Figure 3.10a.

With the influence of the date palm fibre on the tensile behaviour of the epoxy, Figure 3.10c indicates intermediate improvement to the tensile strength of the epoxy compared with the glass fibres, that is, ultimate tensile strength increased from approximately 45 MPa (neat epoxy) to 78 MPa with the addition of the date palm. To show the differences between the effect of glass and the date palm fibres on the mechanical behaviour of the epoxy, Figure 3.10d was developed.

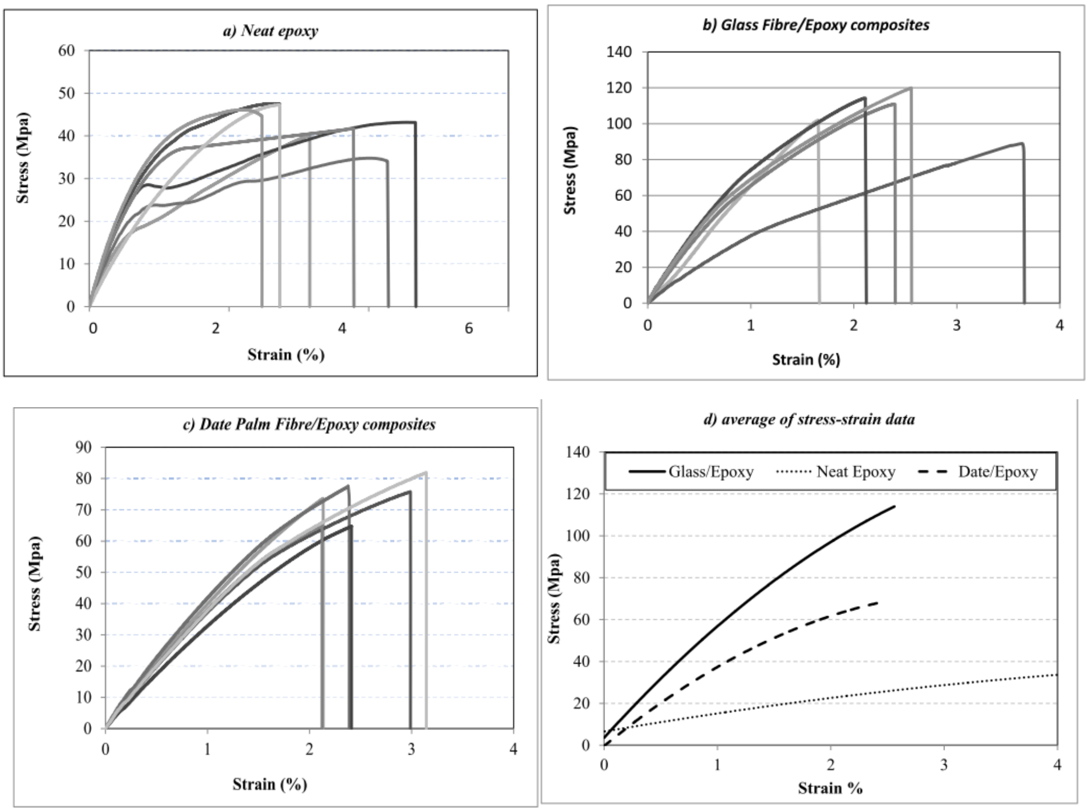

Figure 3.10: Stress v. strain of the different tests samples

In Figure 3.10d, one can see that both glass and date palm are able to enhance the ultimate tensile strength of epoxy; however, there is a slight reduction in the ductility of the epoxy. For modulus of elasticity, the values are determined for each set of data, plotted in Figure 3.11 and associated with the maximum and minimum values, as can be seen in the error bars. It seems that the addition of the fibres improves the modulus of the epoxy and further improvement can be seen when the date palm fibre is added to the epoxy. Twenty-seven per cent improvement in the modulus was achieved when the epoxy was reinforced with the date palm fibre and approximately 18 per cent was achieved with the glass fibres.

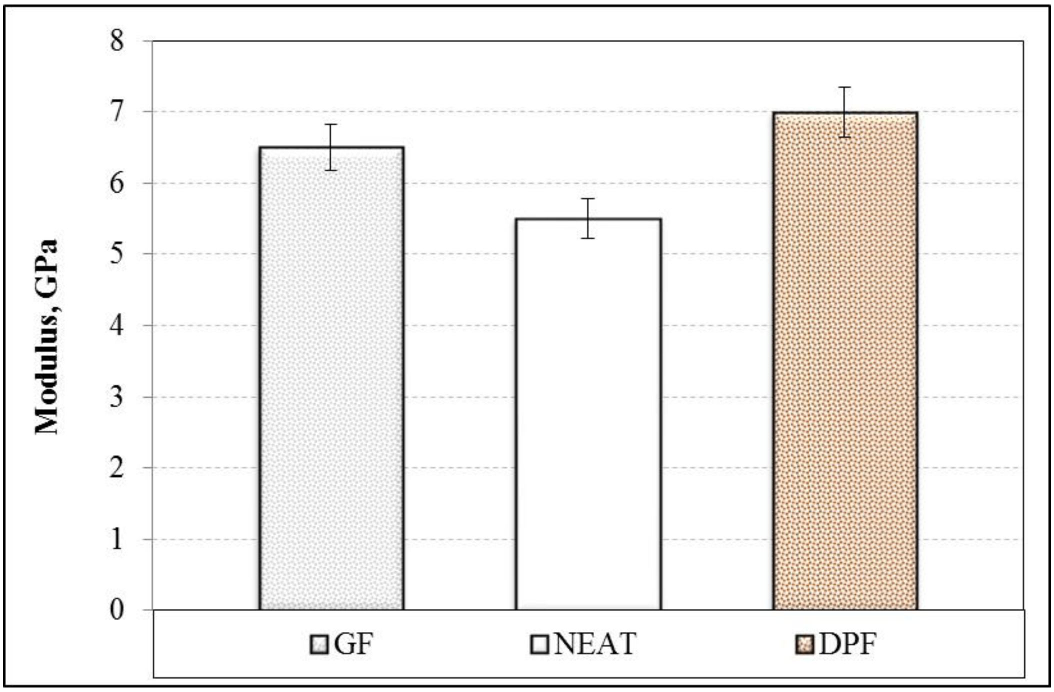

Figure 3.11: Modulus of elasticity for neat epoxy, glass fibre and date palm fibre epoxy composites

3.4.1 SEM observation on the fractured samples after tensile tests

The micrographs of the tensile samples after conducting the test are displayed in Figure 3.12a–c for neat epoxy, glass/epoxy and date/epoxy composites. In Figure 3.12a, a clear sign of the cleavage fracture mechanism is seen, which represents the high bristliness of the neat epoxy. River-like signs can also be seen, which indicates resistance to the fracture. Further, shear lip can be observed. These signs confirm that the failure of the sample occurred in cleavage form. For the glass/epoxy composites, a breakage to the end of the fibres can be seen and there are fibres exposed to the pull out mechanism during loading. Such a mechanism has been observed previously with glass/polyester (Yousif, 2008) and carbon/polymer composites (Al-Zubaidy et al., 2011, Feih and Mouritz, 2012).

In Figure 3.12c, it can be seen that there is good bonding between the date palm fibres and the epoxy matrix, which represents high interfacial adhesion achieved with six per cent NaOH (c.f. Figure 3.6). The majority of the fibres were exposed to breakage rather than detachment of the pull out mechanism. In such behaviour, the fibres were able to carry the load and the interface surfaces were able to transfer the load from the matrix to the fibres, leading to better tensile strength compared to the matrix alone. This could explain the mechanical results, which were presented in Figure 3.10.

When comparing the glass fibres and the date palm fibres, the strength of the glass fibre (> 2,000 MPa) is greater than the date palm fibre (320 MPa) (see Figure 3.5b). Since the volume fraction of both synthetic and natural fibre epoxy composites are kept the same, it is theoretically expected that the tensile strength of the glass/epoxy fibre will be greater than the date/epoxy composites by approximately 500 per cent. However, the current results show that the glass/epoxy strength (120 MPa) is greater than the date/epoxy (70 MPa) by approximately 42 per cent only. This can be explained by comparing the SEM of Figure 3.12b and Figure 3.12c, as the glass/epoxy composite suffered from debonding, delamination and the pull out process during loading, which weakened the composite, and the glass fibres were not able to carry the load. Conversely, the date palm fibres were exposed to breakage, which represents the ability to carry the load.

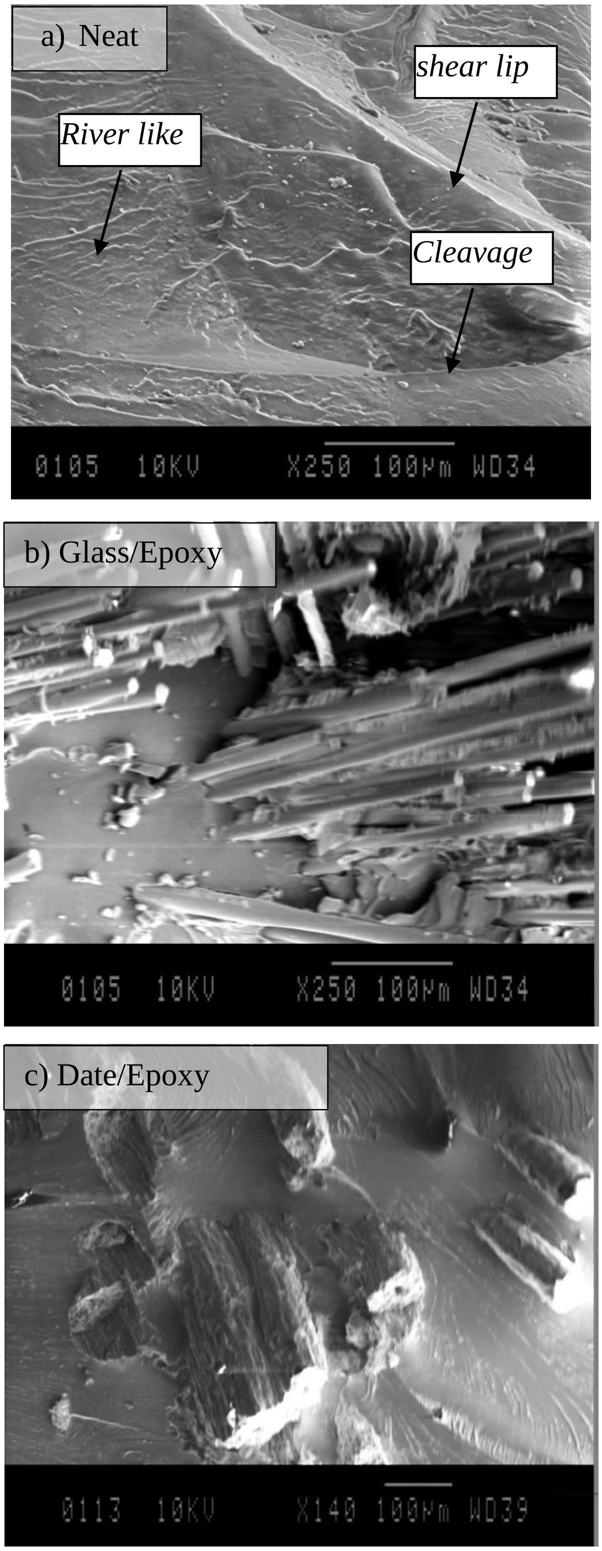

Figure 3.12: Micrographs of the different tensile samples of the epoxy composites

The previous published related works are summarised in Table 3.2 and the main findings are addressed. All of these works agree that alkali treatment is the key to enhancing the mechanical properties of the synthetic composites (thermoset, thermoplastic and elastomers) reinforced with natural fibres (sisal, kenaf and jute). In other words, the current findings are in agreement with the published works. Further, six per cent NaOH concentration was found to be the optimum for interfacial adhesion of the date palm fibres, which, in turn, resulted in good mechanical properties and comparable results to the synthetic fibre exhibited. The findings of this chapter may assist in understanding some of the results in the next chapter on the machinability of the epoxy composites.

Table 3.2: Summary of the previous work done on mechanical properties of natural fibre composites

Fibre	Mechanical testing	Matrix	Remarks
Sisal/oil palm hybrid fibre (Jacob et al., 2004)	• Tensile strength	• Natural rubber	• When fibres were aligned in the direction of force (longitudinal), the fibres transferred stress uniformly and, hence, the mechanical properties of the composites in the direction were superior. • Addition of fibres above optimum value led to decrease of tensile strength because of fibre clotting and, thus, not transferring the load uniformly. • Alkali-treated fibres exhibited better tensile properties than untreated composites because of the increase in the roughness of fibre surface, hence, increasing the surface area available for contact with the matrix.
Jute fibres and PPLSF (Shanmugam and Thiruchitrambalam, 2013)	• Tensile test	• Unsaturated polyester	• The rough surfaces and defibrillation that occurred on the fibre surfaces during alkali treatment resulted in a good fibre matrix adhesion and, hence, improved the tensile properties of the composites. • PPLSF/jute hybrid composites can be a potential replacement in place of synthetic fibres, such as glass fibres and some popular

			natural fibres. • Use of these composites will improve opportunity for growth of palm tree species.
Sisal/GFRP, jute/GFRP and sisal/jute/GFRP (Ramesh et al., 2013)	• Tensile test	• Polyester	• Maximum tensile strength of 229.54 MPa was obtained by jute composite.
Sisal fibre (Sangthong et al., 2009)	• Tensile	• Polymer	• Tensile properties increased with increasing fibre loading, up to an optimum level; after that, the tensile properties slightly decreased. It is more difficult for the resin to penetrate the decreasing spaces between the fibres at high levels of fibre content, leading to poor wetting; hence, a reduction occurred in the stress transfer efficiency across the composite.
Kenaf fibre (Anuar and Zuraida, 2011)	• Tensile	• Thermoplastic elastomer	• The presence of coupling agents improves fibre wetting and significantly increases the value of mechanical properties.

3.5 Summary of the Chapter

From the results obtained and observations made on the surface morphology, a few points can be concluded as follows:

1. The NaOH concentration in the treatment solution affects the strength and the interfacial adhesion of the fibre with the matrix. A low concentration of NaOH exhibited less influence on the strength of the fibre and surface interfacial adhesion. Conversely, a higher concentration (nine per cent) weakened and damaged the fibre. A six per cent NaOH concentration is the optimum concentration, as there was less damage to the strength of the fibre and higher enhancement of the interfacial adhesion of the fibre with the matrix.
2. The embedded length of the fibre controlled the interfacial adhesion property of the fibre. The optimum fibre length was 10 mm embedded length, which can transfer the load from the matrix to the fibre. The critical length was highly controlled by the diameter and the treatment of the fibre (concentration of NaOH). The lowest fibre critical length can be obtained at a lower fibre diameter and six per cent NaOH treatment.
3. The SEM observation indicated a pull out mechanism at a low NaOH concentration treatment of three per cent. At six per cent NaOH, there was breakage of the fibres, indicating high interfacial adhesion of the fibre with the matrix. Early breakage to the fibre was observed at a high level of NaOH concentration (nine per cent), which was due to the weakening process that occurred on the fibre during the treatment process.

The tensile properties of the epoxy were found to improve with the addition of either natural or synthetic fibres. However, glass fibres improved the tensile strength of the epoxy significantly compared to the date palm fibre, despite the fact that glass fibres suffered from detachment and a pull out mechanism during loading conditions. The NaOH treatment greatly improved the load transmission from the epoxy to the fibres, as there was no sign of pull out of date palm fibres during SEM observation.

CHAPTER 4: MACHINING PERFORMANCE OF SYNTHETIC AND NATURAL FIBRE REINFORCED POLYMER COMPOSITES

4.1 Introduction

From an industrial perspective, there are some issues with the machinability of synthetic fibre/polymer composites, such as hole accuracy, delamination, appearance and machining power. These are mainly due to the abrasive nature of the synthetic fibres. Introducing natural fibres as reinforcement to the polymeric composite may overcome some of these issues. In the current study, epoxy composites based on date palm or glass fibres composites are developed. The drilling process is performed to study the machining performance of the developed composites. A new dynamometer is developed and fabricated to study the machining behaviour of these composites in terms of thrust force and torque. SEM is used to observe the inner, intermediate and outer regions of the holes. The findings show that the thrust force and torque values are much less for natural fibres compared to synthetic fibres. In terms of accuracy and shape, the less abrasiveness nature of natural fibres resulted in better hole shape compared to the aggressive glass fibres, which suffered from breakage, delamination and decomposition, especially at the outer regions of the holes.

4.2 Background

Machining of synthetic fibre composites, such as glass fibre and carbon fibre composites, is a major problem because of their inert nature, high hardness and refractoriness to machinability in terms of delamination size, surface roughness and cutting power (Davim and Reis, 2004, Davim et al., 2011). The abrasive nature of synthetic fibres causes rapid tool wear and poor surface finish. Thus, proper selection of the cutting tool and cutting parameters are important for the machining process.

The machining parameters, such as feed, speed and drill diameter, greatly influence the machinability of such materials (Hocheng and Tsao, 2006, Liu et al., 2012, Davim et al., 2011, Schulze et al., 2011, Tsao and Hocheng, 2008a, Davim and Reis, 2004, Davim et al., 2004). (Tsao and Hocheng, 2008a) studied the effect of machining parameters (feed, speed and drill diameter) on machinability in terms of thrust force of GFRE composites. It was reported that the cutting conditions used resulted in higher thrust force than predicted, while no obvious effect of cutting speed was observed. Further, high values of the correlation coefficient between thrust force and the machining parameters confirm the importance of reducing the thrust force in drilling GFRE composites. In another work (Davim et al., 2004), the effect of cutting parameters (cutting velocity and feed rate) under specific cutting pressures on machinability in terms of thrust force in GFRPs using a drill machine equipped with two different types of cemented carbide (K10) drills (Brad & Spur and Stub Length) have been investigated. The results (under the same cutting conditions) showed that thrust forces for the two sets of drilling increased with an increasing feed rate and the Brad & Spur drill showed less thrust force values than the Stub Length drill. Similar findings were also reported by (El-Sonbaty et al., 2004) for the same materials. In (Tsao and Chiu, 2011), the effects of the cutting parameters—diameter ratio (5.5–7.4 mm/mm), feed rate (8–16 mm/rev) and spindle speed (800–1,200 rpm)—on machinability in terms of thrust forces using three kinds of step-core drills (twist, saw and candle) for CFRP laminates were tested. It was found that increased drilling parameters led to an increase in thrust force. The highest thrust force was obtained by decreasing the diameter ratio and spindle speed and increasing the feed rate. All of the above reported works confirmed that there is an essential issue with the machining of synthetic FRP composites and recommended further study to understand and improve the machinability of such important materials.

In addition to the above, it was found that there is less work involved in the machinability of natural FRP composites. This observation motivates the current work to study the machinability of polymeric composites based on natural fibres. In addition, synthetic fibres are well known abrasive materials that cause high damage to manufacturing machines and machining tools.

4.3 Material Fabrication and Experimental Procedure

4.3.1 Material fabrication

The composites were prepared using the hand lay-up technique because the fibres were in a mat form. To prepare the randomly orientated mat, the date palm fibres were first cut to a length of 200 mm and 5 g of the cut fibres were used for each layer of the mat. In preparing the mat, the fibres were distributed randomly on a flat mould and stretched out manually to ensure the rectangularity of the fibre distribution. Further, a steam iron was used to flatten the mats. Each mat was observed using optical microscopy and some adjustments to the fibre distribution were made for further assurance of the fibre distribution.

Natural and synthetic composites were prepared in the same way. A plastic mould with dimensions of 150 mm x 10 mm x 50 mm was used and non-stick paper was placed into the mould to prevent the mixture from sticking and to ensure easy removal after curing. The epoxy resin was mixed with hardener in a ratio of 3:1 and left for approximately five to 10 minutes. Next, it was poured carefully into the plastic mould to avoid bubbles generating in the mixture. Then, each mat was placed into the mould and a small quantity of the mixture was poured on top. A metal roller was applied to the mixture to remove the bubbles from the layer. This step was repeated for the remaining mats to create a final thickness of 1 cm. Next, a weight was put on top of the mixture to ensure homogeneity of the composite. Finally, the composite was left to be cured at room temperature for 24 hours and then removed from the mould to take its final shape. The prepared block was placed in the curing oven for the post-curing process at temperatures of 40ºC for 16 hours, 50ºC for 16 hours and 60ºC for eight hours. Glass fibre mats with a density of (450 g/cm^2) were used. The volume fractions of both composites were controlled at 40 to 45 per cent.

4.3.2 Experimental procedure

A commercial milling and drilling machine (GHD 30-V) was used to perform the machining process. The speed and feed was automatically controlled. HSS was used with drill bit diameters of 3 to 10 mm. This type of drill bit is commonly used in manufacturing composite industries. Since the main objectives of the current study are focusing on investigating the possibility of replacing the synthetic fibres with the natural fibres from machinability point of view, similar common tool used for drilling synthetic fibre polymer composites are used for the natural fibre polymer composites. However, for the future work, it is highly recommended to used different tool geometry and/or materials. Several parameters were considered in this study because of the significance of influencing the operating parameter on the machinability of polymeric composites and these are listed in Table 4.1. To analyse the results, the ANOVA method was used to correlate and find the most significant parameters on the machinability of both synthetic and natural fibre/epoxy composites. SPSS software was used in the statistical analysis. In the current study, a Motic stereomicroscope (SMZ168 series) microscopy was used for observation of the drilled holes. Micrographs were taken for each drilled hole. Four lines were drawn in the picture, as the measurements of the drawn lines were taken to obtain the mean diameter and, from that, the error was calculated.

Table 4.1: Drilling operating parameters

Material	Speed (rpm)	Feed Rate (mm/rev)
For each selected material	120	0.06
		0.09
		0.12
	690	0.06
		0.09
		0.12
	1450	0.06
		0.09
		0.12

4.4 Development of the New Dynamometer

Commercially, there are few international companies dealing with the development of dynamometers, especially for machining purposes. Investigating the machinability of materials demands the knowledge and understanding of the forces required and their trends in the machining process. This study establishes and initiates the first attempt of machining materials at the institute. The concept of measuring the forces on the worked pieces can be developed using new sensors and a new instrument for this purpose. For the current study, the work focuses on the machinability of the selected materials with regards to the drilling process. Therefore, an attempt is made to design and fabricate a new dynamometer to achieve the requirement of the research. Abacus software is used in the development of the system to design the component and visualise the final product.

4.4.1 Concept of the design

Basically, the drilling process takes places using two loads: torque and thrust force, as shown in Figure 4.1. The theory of drilling process have been extensively explained by (Armarego and Brown, 1969, Shaw, 1968). Similar approach have been adopted by Stephenson and Agapiou (2005) since shear force is developed by the torque for cutting purposes and feed of the cutting is generated by the thrust associated with shear loadings. Based on these approaches, the common dynamometers are developed to capture the torque and thrust force during the drilling process. In addition to that, using the CNC machine and control systems assisted to capture these parameters electronically using the reduction in the power during drilling, i.e. converting the electrical signal from the main supplier into torque. This technique suffers from several issues associated with the massive noise and lack of accuracy, which required extensive calibration. With the development in the instruments' technology, nowadays, there are available seniors, which can capture the torque and the thrust forces at high accuracy. In the light of this, the concept of the instrument is to capture these loads during the drilling process.

At the initial stage of development, several ideas were drawn to capture the torque using tensile or beam load cells. However, the concepts were omitted because of an accuracy issue. A newly commercialised torque sensor was found, which was developed by Besttech Sensors and Instrumentation in Germany and supplied by the Australian branch.

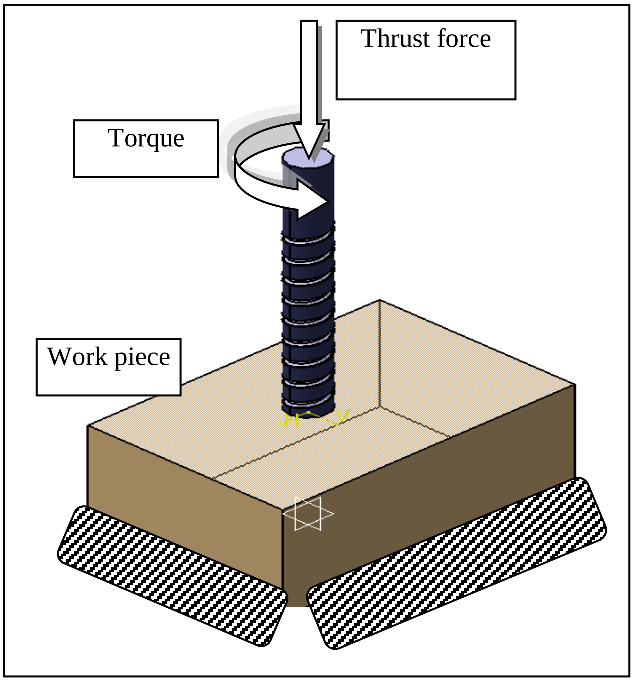

Figure 4.1: Loads during drilling process

4.4.2 Development of the dynamometer and selection of the instruments

In the previous section, the main idea was to measure the thrust force and the torque during the drilling process. The thrust load cell supplied by Besttech Sensors and Instrumentation was used to capture the thrust load. The load cell was connected to the computer using the data acquisition system. Three-dimensional drawings of the load cell are displayed in Figure 4.2. The small ball at the top of the load cell is the place on which to subject the thrust load. At the same time, there is a threaded hole at the centre of the load cell, which was used to connect the load cell with the sample holder to transfer the thrust load from the sample onto the load cell. The three holes in the load cell were used to fix the load cell on a component called a connector. The connector component was used to transfer the torque load from the upper part of the load cell to the lower part. This will be illustrated and clarified in the coming sections.

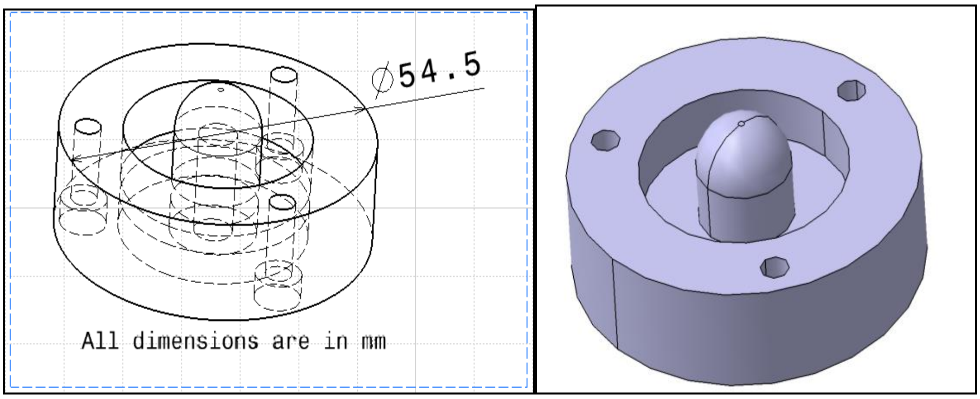

Figure 4.2: Thrust load cell

As mentioned previously, the thrust load cell was placed in a way to measure the thrust load subjected to the sample. The sample holder component was designed so that it could freely connect to the load cell. Figure 4.3 shows the sample holder on which the sample was fixed at the top for the drilling operation. The lower end of the holder was placed freely on another component, which is called the connector (see Figure 4.4). On the connector, the top end carried the thrust load cell using threaded holes. The thrust load cell was fixed rigidly. The sample holder (see Figure 4.3) was placed freely on top of the load cell to transfer the torque onto the connector.

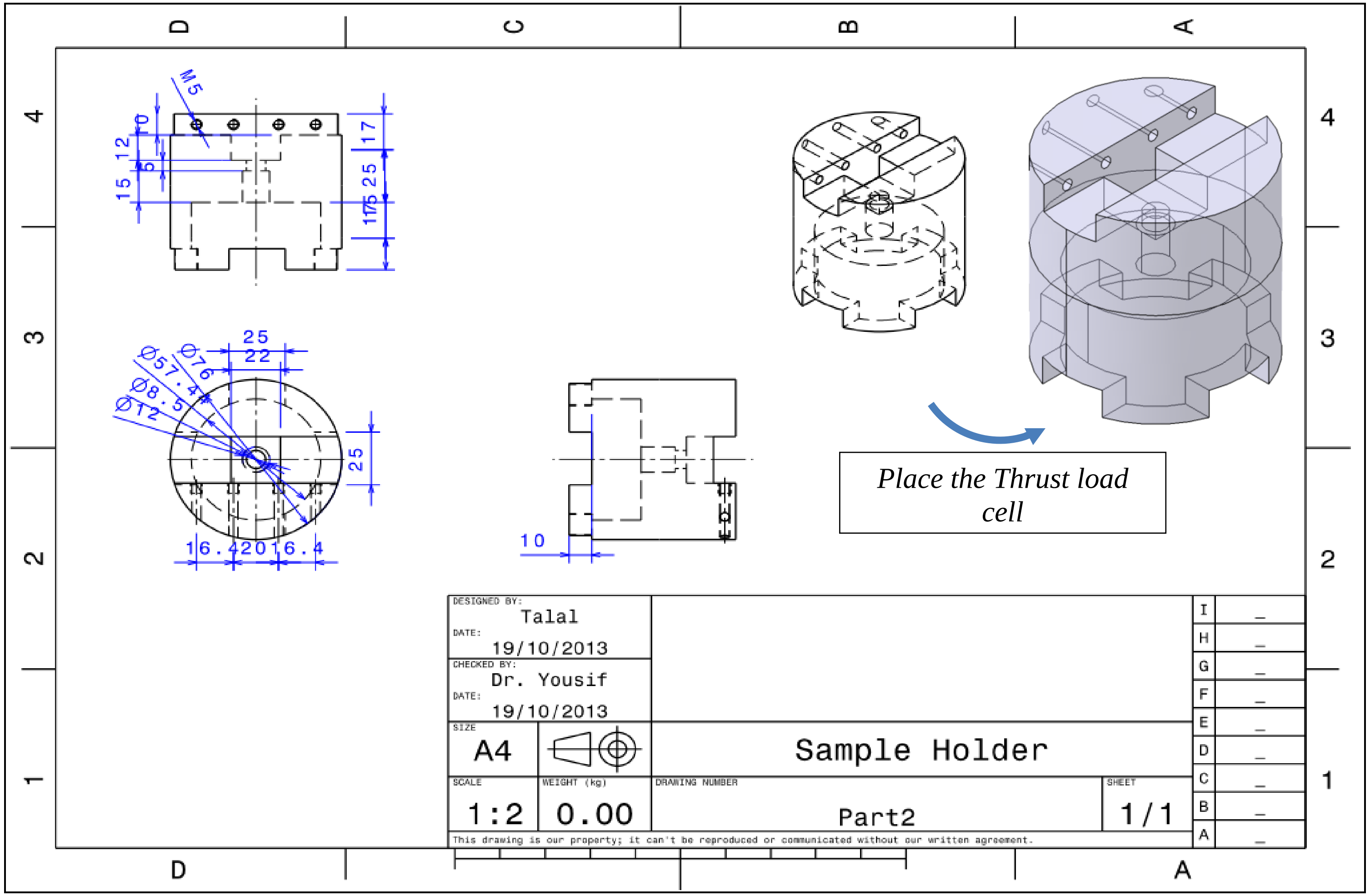

Figure 4.3: The developed sample holder

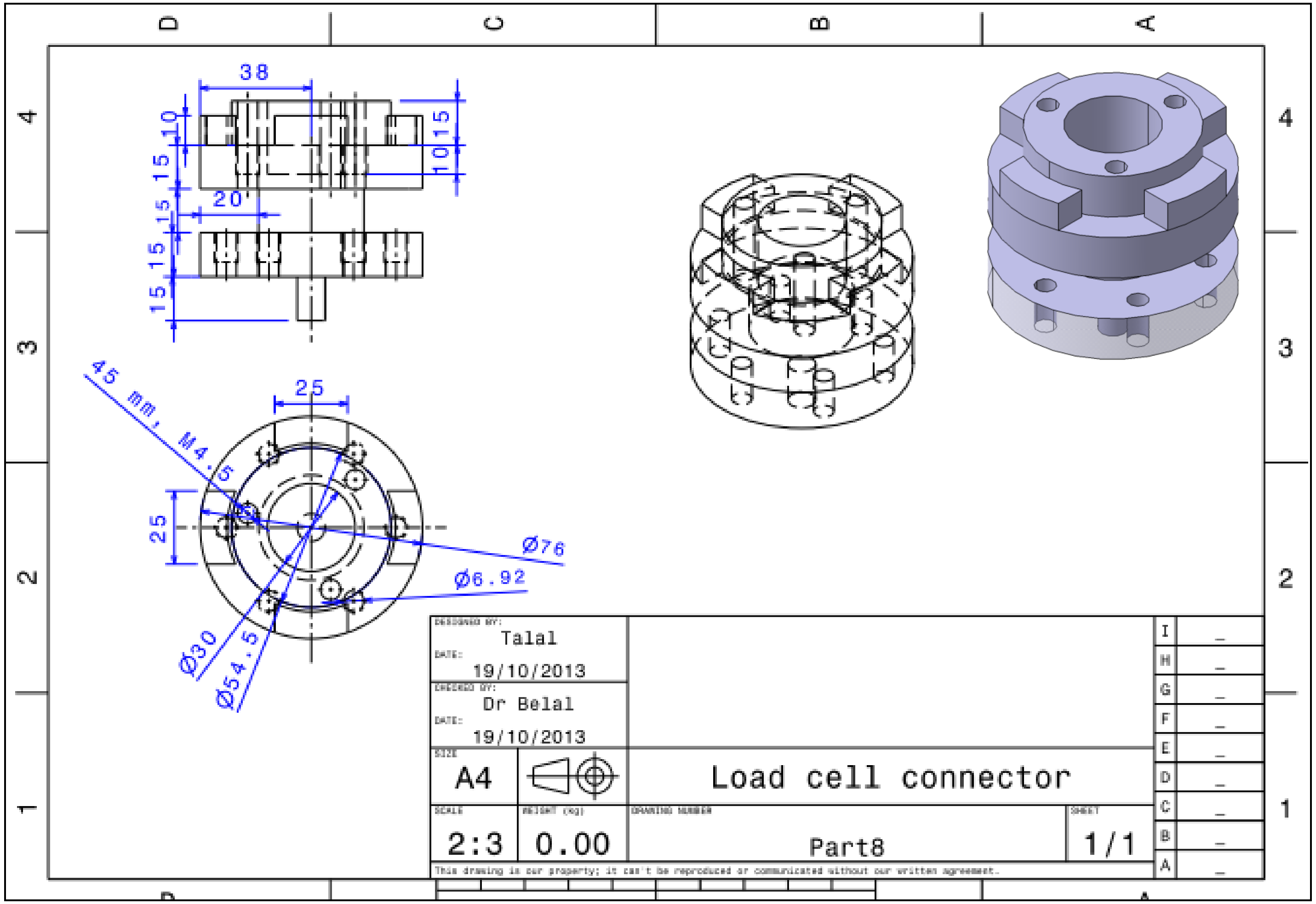

Figure 4.4: The developed load cell connector

To capture the torque generated by the drilling process, a dynamic dynamometer is commonly used. At the current innovated design, an attempt was made to use a highly sensitive stationary torque sensor. Three-dimensional drawings of the torque sensor are displayed in Figure 4.5. The senior can work in both directions by fixing one of the ends and connecting the other to the torque supplier, which is the connector in this system. The lower end of the torque was fixed to the drilling machine. At this stage, the upper part of the torque sensor was subjected to torsion via the connector, which was transferred from the sample folder and, in turn, supplied by the drilling tool. The strain gauges were placed inside the sensor and connected to the data acquisition system on a computer. Calibration was made for both sensors for each set of experiments. The calibration process will be explained later.

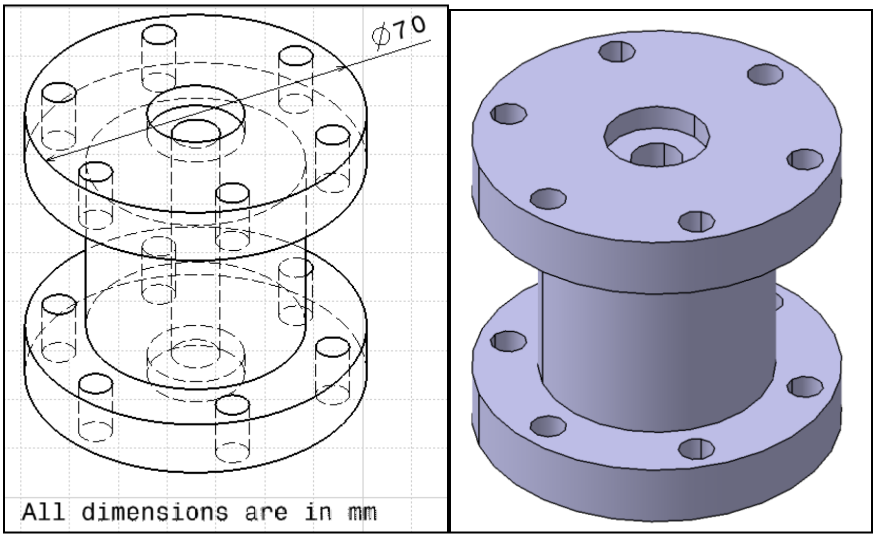

Figure 4.5: Thrust load cell

4.4.3 Dynamometer fabrication and assembly

To visualise the new dynamometer, Figure 4.6 shows the assembly process of the components and the order before conducting the experiments or the calibration. At the final stage, the new dynamometer looks like Figure 4.7. The dynamometry was placed on a CNN drilling machine and connected to a laptop to capture the thrust and torque values during the drilling process (see Figure 4.8).

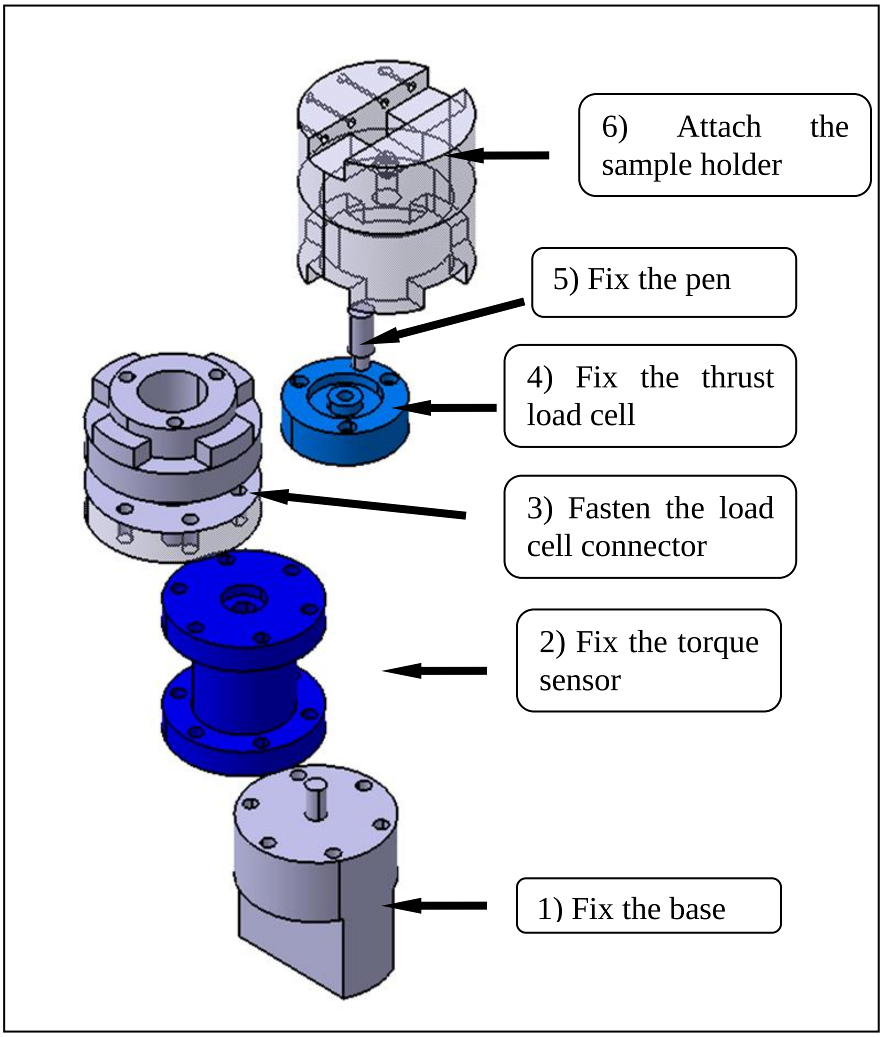

Figure 4.6: Assembly of the dynamometer components

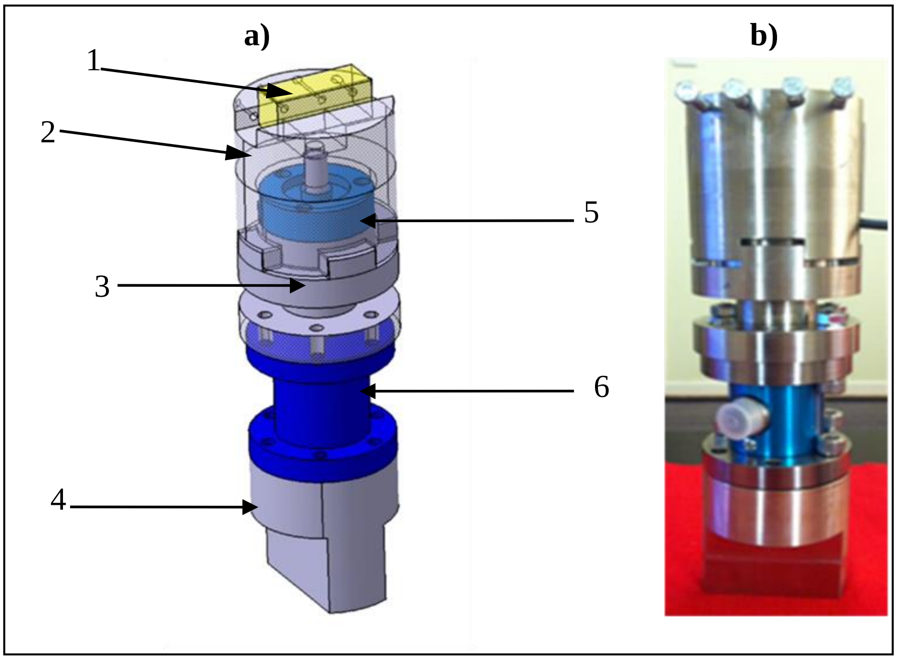

Note: 1 = sample, 2 = stainless steel sample holder, 3 = two load cells connecter, 4 = stainless steel bench bracket, 5 = compression load cell and 6 = torque load sensor

Figure 4.7: The new dynamometer after assembly—a) three-dimensional drawing of the new dynamometer and b) dynamometer after fabrication and assembly

•

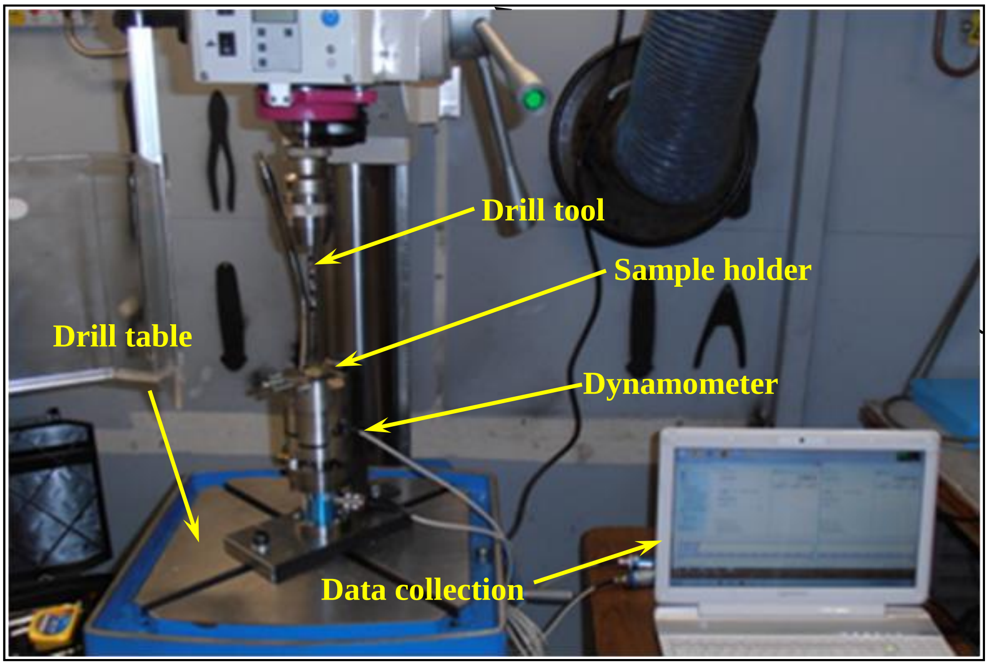

Figure 4.8: The new dynamometer attached to the drilling work table and the computer

4.4.4 Calibration of the dynamometer

Before each set of tests, the thrust load cell and the torque sensor were calibrated. In the calibration process, the whole dynamometer was fixed to a newly designed bench, while the load cell and the sensor were connected to the computer. For the torque sensor, the composite sample was replaced with a sample fixed with an arm for torque generation. Figure 4.9 shows the configuration of the dynamometer for both load cell and torque sensor calibration. It should be mentioned here that each procedure was conducted individually.

For the torque sensor calibration, different values of force were subjected in a horizontal direction on the fixed arm (see Figure 4.9) until the computer steadily read the value of the subjected torque. The real subjected torque can be calculated by multiplying the subjected force by the arm length (force point to the centre of the dynamometer, marked as '*l*'). The computer read each subjected torque and both real and computer readings were recorded and plotted (see Figure 10a). By using the line fitting in the Excel software, the calibration equation could be developed. The torque equation was then used to convert the captured date into the read data. The same procedure as the torque sensor was used for the thrust load cell calibration, as different thrust forces were subjected onto the dynamometer (see Figure 4.9). The computer also captured the thrust load. Both real and computer loads were recorded and plotted in Figure 4.10b. The developed equation was used to determine the real thrust load.

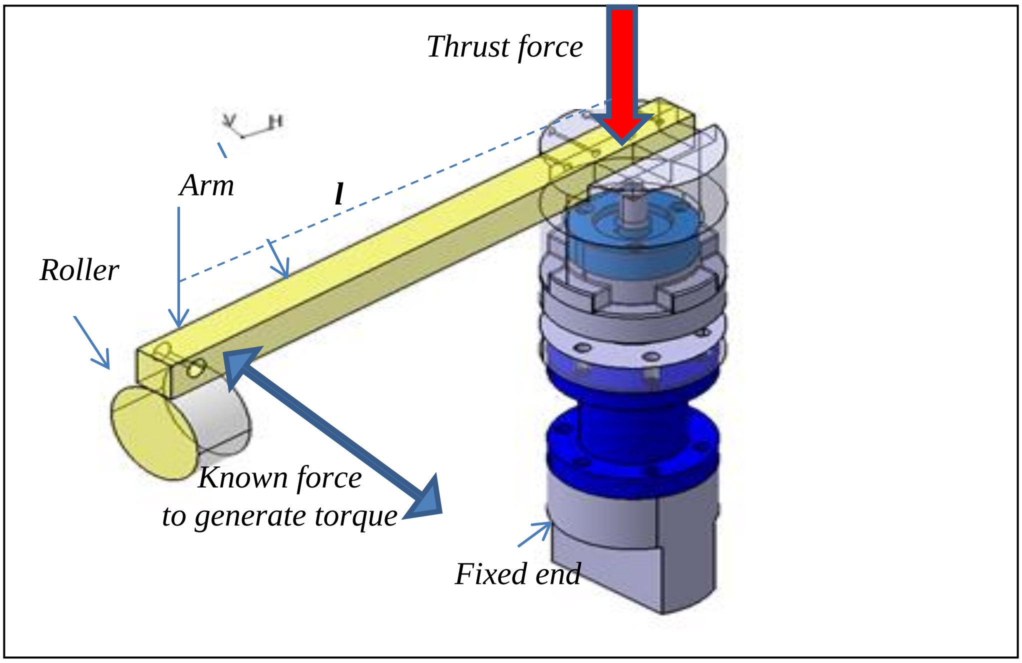

Figure 4.9: Calibration procedure for the torque sensor and the load cell

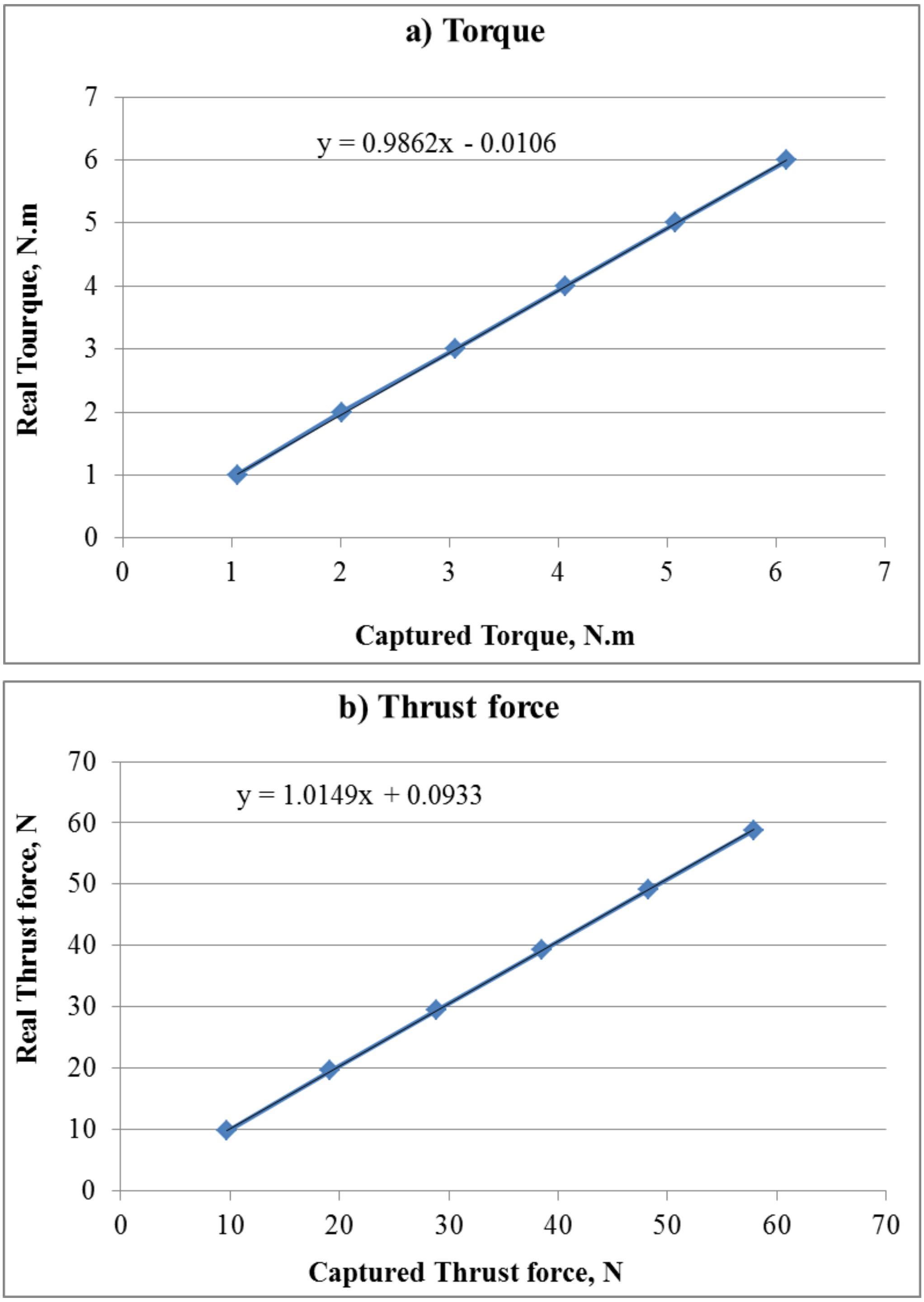

Figure 4.10: Calibration graphs for the new dynamometer for a) torque and b) compression load cells

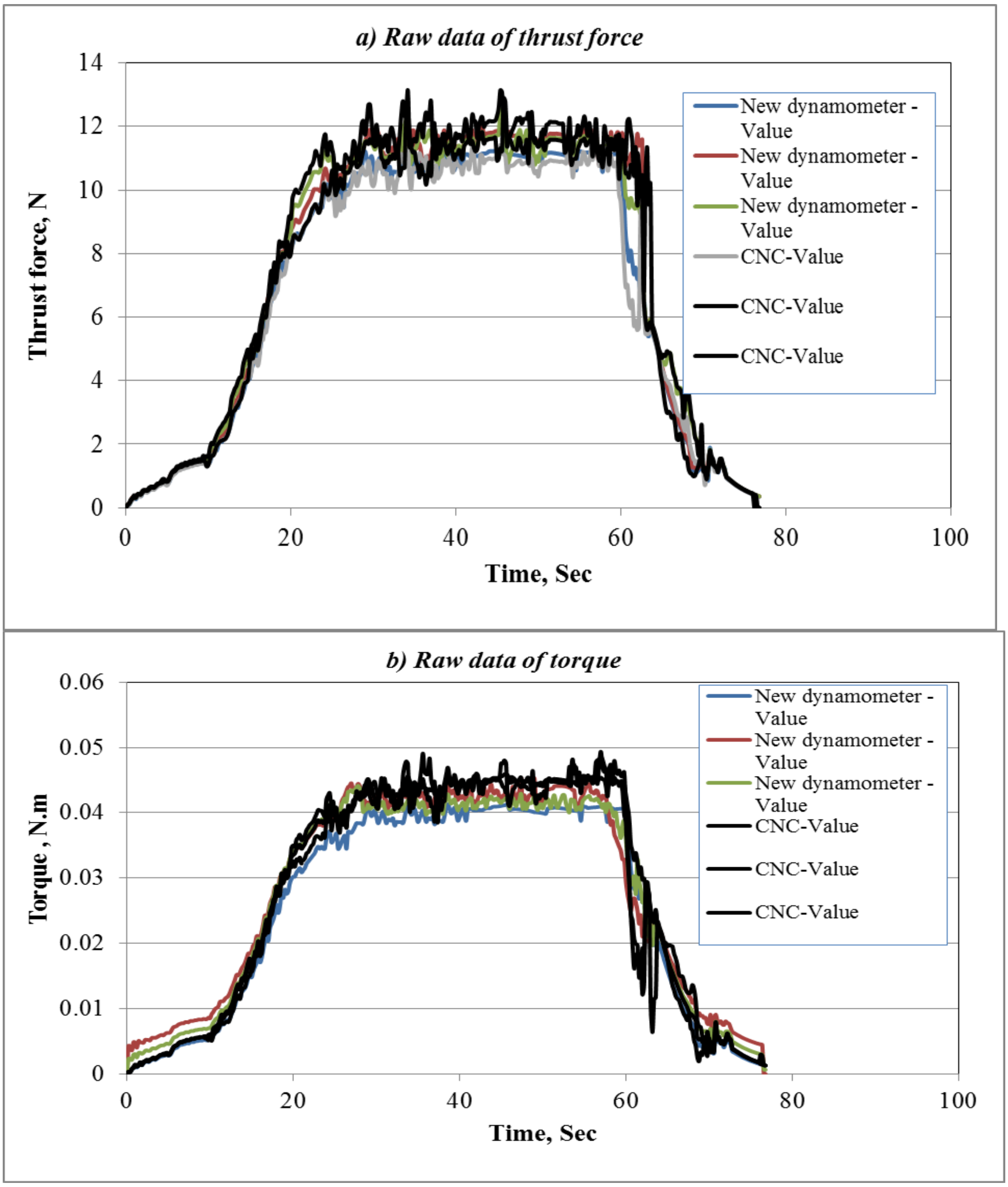

Figure 4.11: Collected raw date from the new dynamometer and the CNC machine

Due to the fluctuation in the data and the noise, the average function in excel software is used in presenting the data since a trend of 20 per average move adopted to plot the data. Sample of presenting the raw data in average form is given in Fig. 4.12 for both thrust force and the torque.

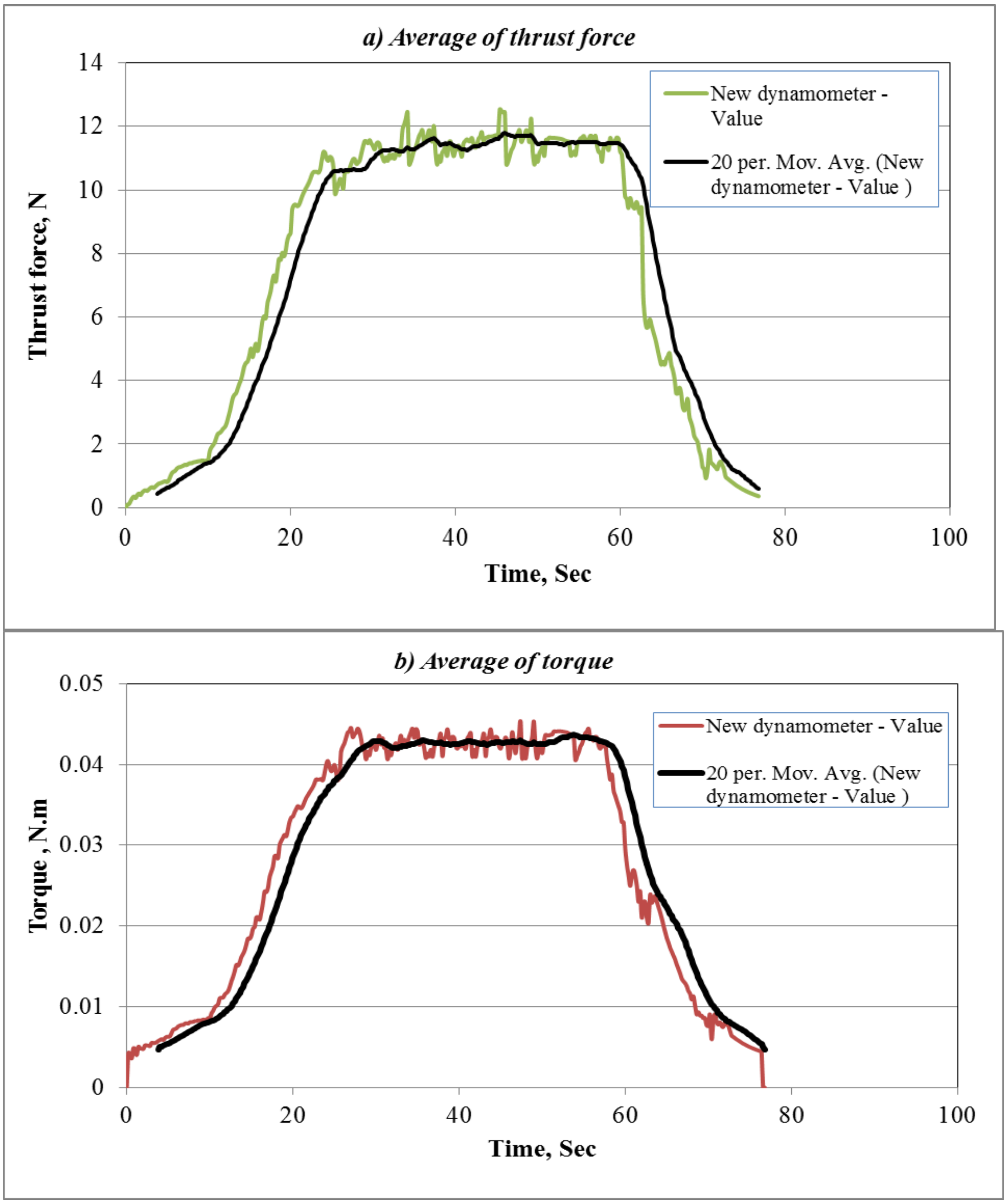

Figure 4.12: Presentation of the collected date from new dynamometer

4.5 Torque and Thrust Load Behaviour

In this section, samples of the data are given for each material for five tested samples. Further, this section covers the presentation of the raw data and the torque and thrust force behaviour of the composites under the operating condition of a cutting speed of 120 rpm, a feed rate of 0.06 mm/rev and a 3 mm drill diameter.

4.5.1 Torque behaviour

In Figure 4.11a–c, the value of the torque generated on the hole against the drilling time is presented for neat epoxy, glass/epoxy and date/epoxy composites. These samples are taken under the operating conditions of a cutting speed of 120 rpm, a feed rate of 0.06 mm/rev and a 3 mm drill diameter. Figure 4.11 shows that, during the drilling process, three regions of torque value are obvious. An initial stage is a dramatic increase in the torque value, representing an increase in the shear forces in the drilling process at this stage. Further, the contact area between the drilling tool and the surface of the composite increases with duration of the penetration of the drill inside the composite. The initial stage lasts for approximately twenty seconds on average for all composites. This region is followed by an almost steady region in which the torque value is the highest. This stage lasts for various times according to the material times. In this region of the drilling process, the shear force is at the peak and severe removal of material is taking place. The final stage is when the drill is about to leave the work piece. In this stage, there is a drop in the torque value until it reaches zero. This stage takes approximately ten to twenty seconds for a composite with a thickness of 10 mm.

Neat epoxy and date/epoxy composites consume approximately seventy seconds to drill a 10 mm thick plat. For the glass/epoxy composite, it seems that the drilling time is longer by ten second, as eighty seconds were needed to complete the drilling. This is an advantage for the natural fibre polymer composites because it consumes less time for machining compared to synthetic fibres. The higher times required for synthetic composites are due to the high resistance of the glass fibre to the cutting force (torque/radius). The figure shows that higher torque was exhibited when the glass/epoxy was machined compared to the neat epoxy and the date/epoxy composites.

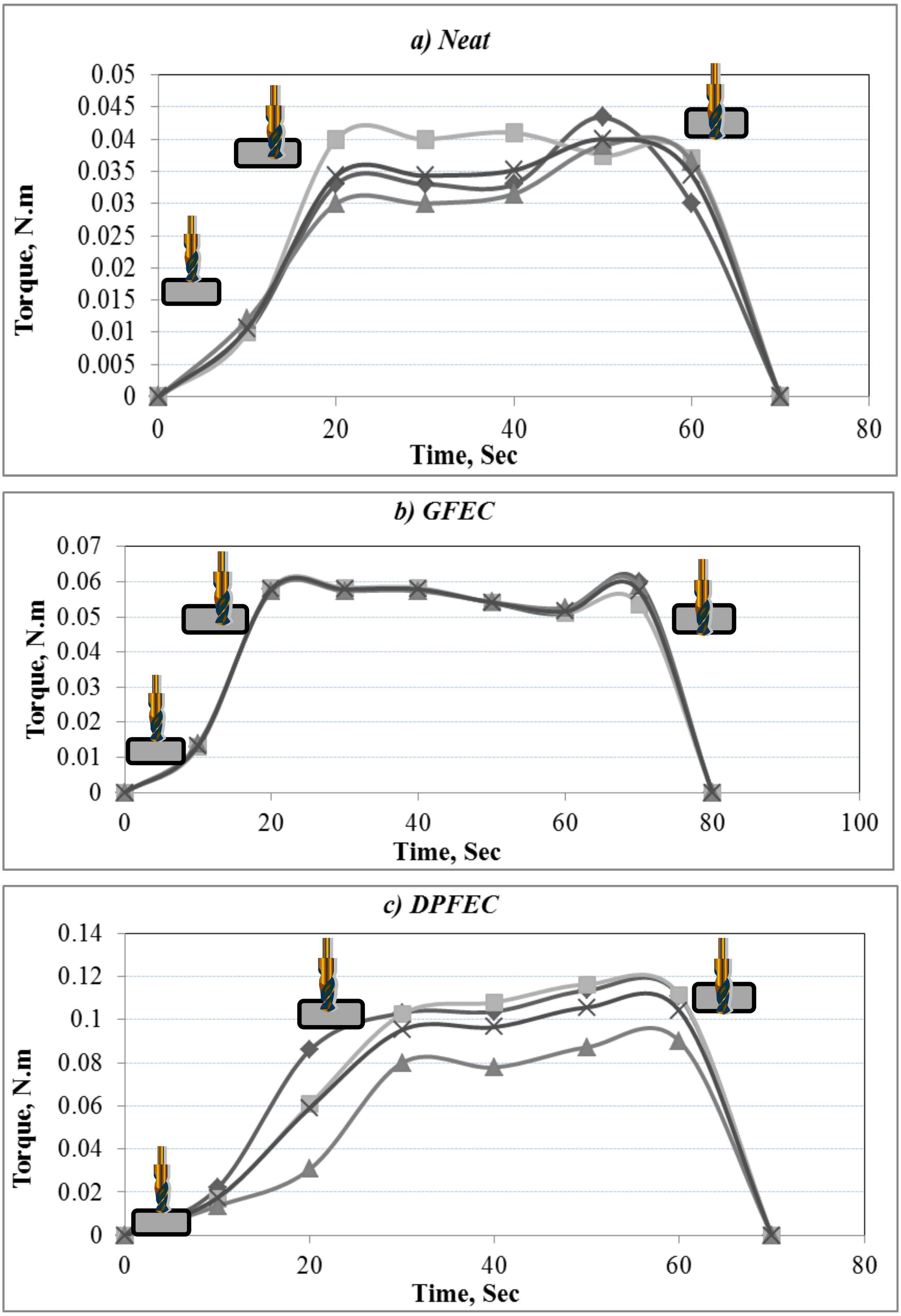
a) Neat
Torque, N.m
0.05
0.045
0.04
0.035
0.03
0.025
0.02
0.015
0.01
0.005
0
0
20
40
60
80
Time, Sec
b) GFEC
Torque, N.m
0.07
0.06
0.05
0.04
0.03
0.02
0.01
0
0
20
40
60
80
100
Time, Sec
c) DPFEC
Torque, N.m
0.14
0.12
0.1
0.08
0.06
0.04
0.02
0
0
20
40
60
80
Time, Sec

Figure 4.13: Drilling torque v. time for a) neat, b) glass fibre and c) date palm fibre composites at a cutting speed of 120 rpm, a feed rate of 0.06 mm/rev and a 3 mm drill diameter

For the glass/epoxy composites, maximum torque was found to be close to 0.06 N.m at the steady stage. Meanwhile, for the date/epoxy, the maximum torque was approximately 0.033 N.m. This indicates that the natural fibre/polymer composites demand less cutting force to complete the drilling compared to synthetic fibres and are comparable to neat epoxy.

The main reason for better machining performance of natural fibre polymer composites compared to synthetic fibres is that synthetic fibres, such as glass fibres, have a highly abrasive nature, which requires high energy for material removal. Further, the contact between the steel drill and the surface of the composites could be less, which would assist in reducing the torque. It has been reported that the adhesive frictional performance of natural fibre composites is always lesser than synthetic fibres (Yousif and Chin, 2012). Conversely, there could be another influential element, which is the way that chips (removed materials) exit the holes. Since the glass fibres have an abrasive nature, the chips will attack both the drill's surface and the hole's inner surface. However, since the neat epoxy and the date/epoxy composites attack the contacted surfaces less, it is suggested that a smoother surface and less damage to the drill tool may be observed. This proposal is illustrated in Figure 4.12. The damage features on the inner surface of the holes and the tool will be explained in the next section.

Similar results have been found by (Alam et al., 2011) using conventional and ultrasonically assisted drilling on a cortical bone, (Zarif Karimi et al., 2013) using a drill machine equipped with a twist drill on a composite laminate made of epoxy resin and reinforced with unidirectional E-glass fibre and (El-Sonbaty et al., 2004) using a drill machine to drill holes in randomly orientated GFRE. It has been mentioned that, after the initial engagement of the drill with the sample, the cutting force gradually increased with time and attained a stable reading for several seconds when the drill was fully engaged with the sample. The force then disappeared suddenly when the drill pierced the entire thickness of the sample.

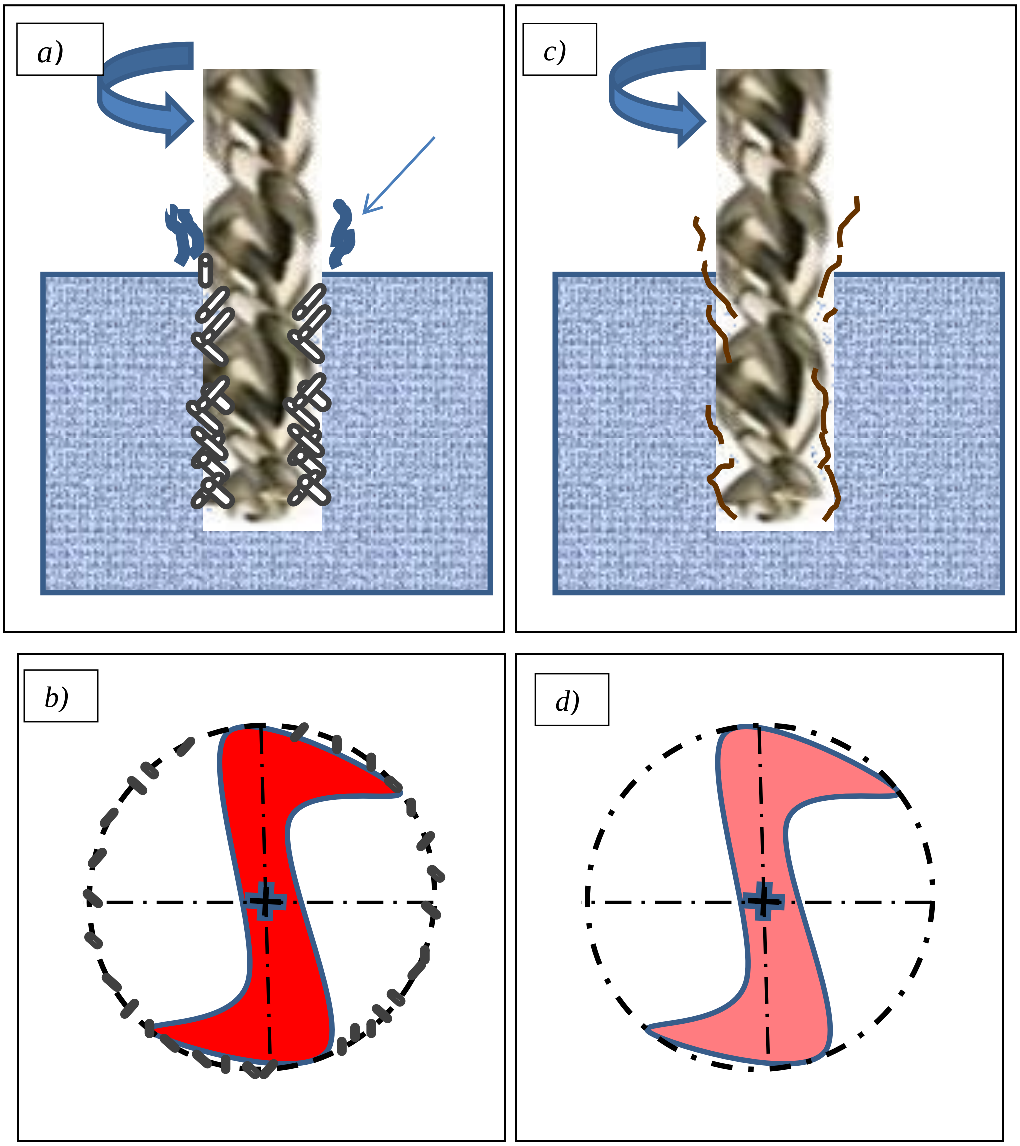

Figure 4.14: Mechanisms of material removal from glass/epoxy (a & b) and date/epoxy (c & d) composites

The torque values at the steady cutting state at different operating parameters are presented in Figure 4.13a–c for neat epoxy, glass/epoxy and date/epoxy composites. For the neat epoxy, there was a clear increase in the torque value with an increase in drill diameter for all drilling speeds. This was expected for all materials since higher shear force is required for cutting the materials from the hole. For the influence of the feed rate on the torque, it seems the torque increases with an increase in feed rate (i.e., $torque_{120, 0.06}$ = 0.04 N.m; $torque_{120, 0.12}$ = 0. 05 N.m) when a 3 mm drill diameter is used. In other words, there is an increase in the torque value by approximately 20 per cent with an increase in feed rate. However, the drilling speed has a different influence because low torque is required at the intermediate speed value of 690 rpm. The lowest value torque (0.04) was introduced when the 3 mm drill diameter was used with a feed rate of 0.06 mm/rev and drilling speed of 120 rpm. The highest value was recorded when the largest drill diameter (10 mm) was used at a higher feed rate (0.12 mm/rev) and speed (1450 rpm), which was 0.446 N.m.

In Figure 4.13b, a similar effect to that of the neat epoxy for the feed rate, drilling speed and drill diameter on the torque of the glass/epoxy composites can be seen. However, the torque values were greater than for neat epoxy and this has been clarified previously with the argument that glass fibres have a highly abrasive nature and require more energy to remove them. The highest value was recorded when the largest drill diameter (10 mm) was used at a higher feed rate (0.12 mm/rev) and speed (1450 rpm), which was 0.7 N.m. In comparison to the neat epoxy, there was an increase in the torque by about 42 per cent when the epoxy was reinforced with glass fibres. However, with the addition of date palm fibres, no such increase occurred in the torque values for all operating parameters (see Figure 4.13c). The trends of the torque value were similar to the glass/epoxy and neat epoxy materials.

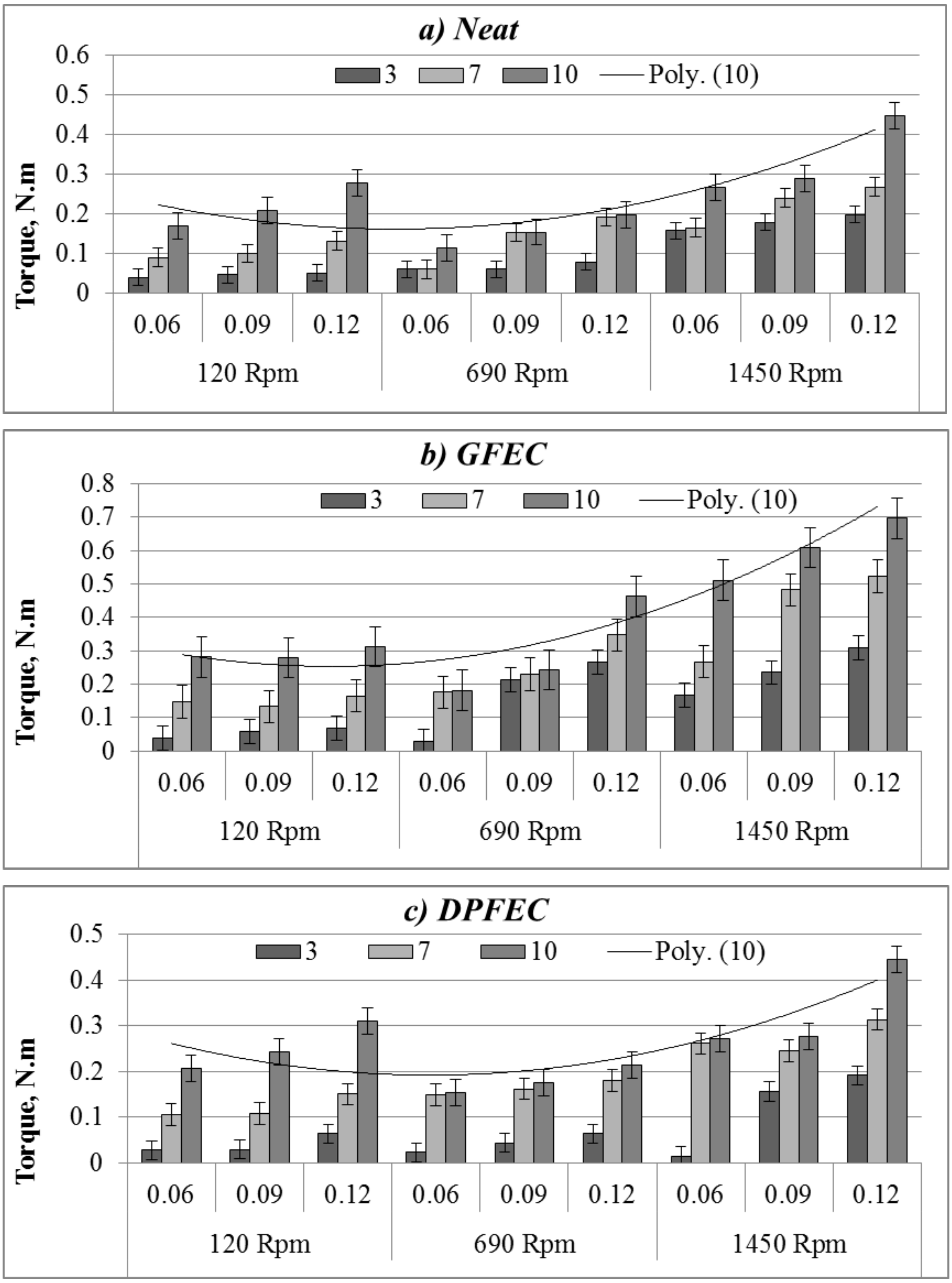

Figure 4.15: Torque values of neat epoxy, glass/epoxy and date/epoxy composites at different drill diameters, cutting speeds and feed rates

4.5.2 Thrust force behaviour

Thrust force versus time for all tested materials is presented in Figure 4.14a–c for a cutting speed of 120 rpm, a feed rate of 0.06 mm/rev and a 3 mm drill diameter. For all materials, there is similarity in the thrust force for various times. Moreover, the trends are similar to the torque results presented in Figure 4.14 under the same conditions. It seems that there is a dramatic increase in the thrust force at the initial stage and a dramatic drop at the end of the process. For thrust force values, neat epoxy and date/epoxy composites have similar values of approximately 12 N at the steady drilling process. Conversely, glass/epoxy composites demand a higher thrust force during the process, as the recorded maximum thrust force is approximately 19 N, as shown in Figure 4.14b.

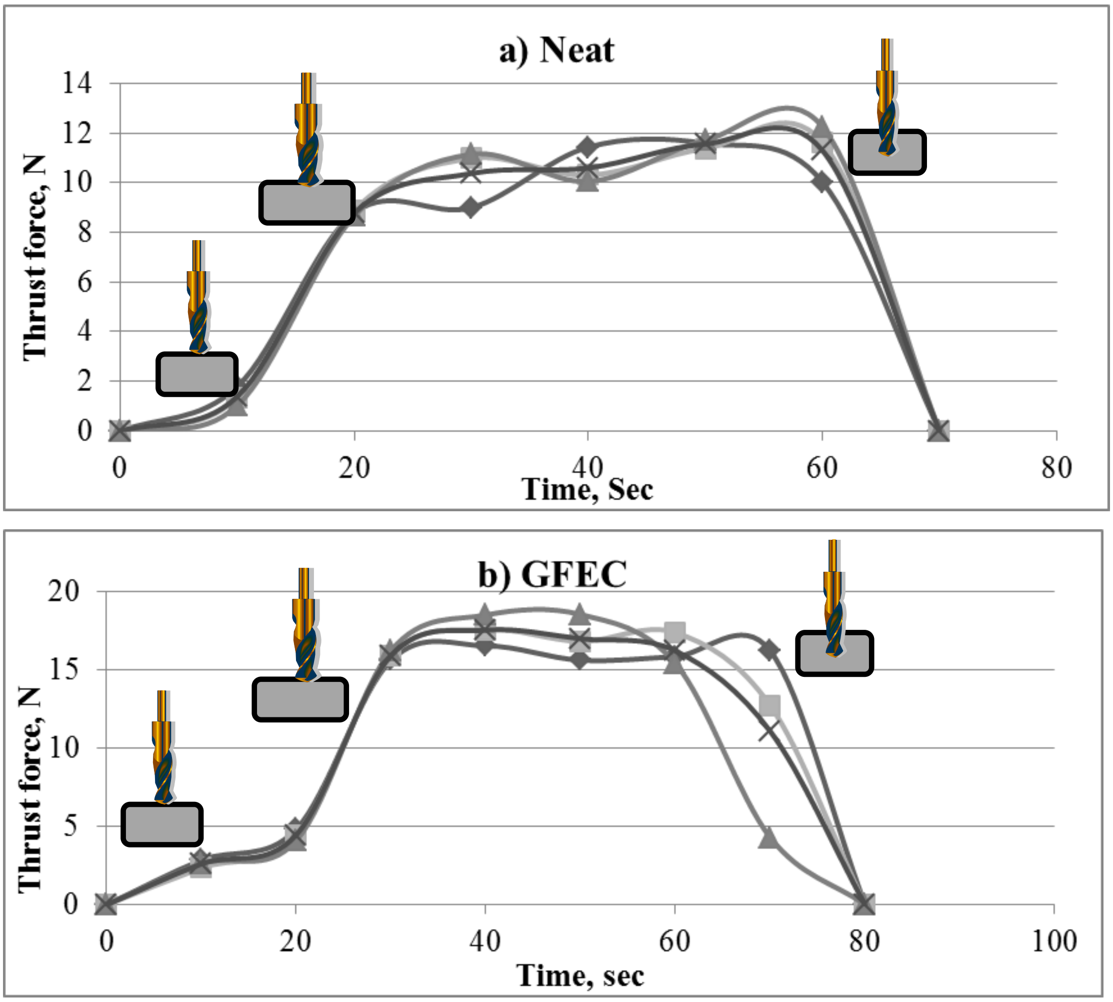

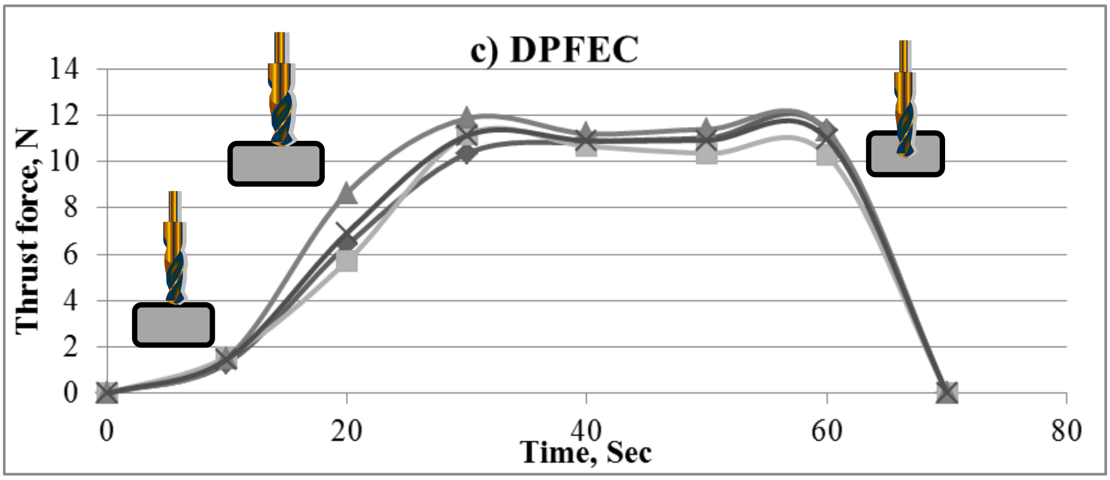

Figure 4.16: Drilling thrust force v. time for a) neat, b) glass fibre and c) date palm fibre composites at a cutting speed of 120 rpm, a feed rate of 0.06 mm/rev and a 3 mm drill diameter

A similar argument and proposal as that used in the previous section (see Figure 4.12) can be used here to explain the higher value of the thrust force when the glass/epoxy was drilled compared to the neat epoxy and the date/epoxy composites. The presence of abrasive glass fibre in the drilling area significantly prevented the penetration of the drill, causing high resistance in the area that demands high force.

Comparable results were declared by (Khashaba et al., 2010a) using two sizes of drills with different cutting parameters on a woven GFRE composites, (Zarif Karimi et al., 2013) using a conventional drilling machine with a unidirectional glass/epoxy resin, Davim et al. (2004) using a drilling process on a GFRP and (Krishnaraj et al., 2012) using a drill machine on thin CFRP laminates. There were extreme increases in the thrust forces, up to a maximum value, just before the drill approached the exit side of the hole. It stayed at that position for a few seconds before dropping to zero. In addition, it has been mentioned that increasing the feed rate results in higher thrust forces. Further, increasing the drill diameter results in an increase in the time needed for the drill to exit the work piece. Conversely, thrust forces have been found to decrease with an increase in spindle speed, and this could be due to the increase in temperature with spindle speed that leads to softening of the composite.

The thrust values at the steady cutting state at different operating parameters are presented in Figure 4.15a–c for neat epoxy, glass/epoxy and date/epoxy composites. For the neat epoxy, there was a clear increase in thrust values with an increase in the drill diameter for all drilling speeds. This was expected for all materials since higher shear force is required to cut materials from the hole. For the influence of the feed rate and cutting speed on the thrust, it seems the thrust force increases with an increase in feed rate (i.e., $thrust_{120,\ 0.06}$ = 4.89 N, $thrust_{1,450,\ 0.06}$ = 7.4 N and $thrust_{120,\ 0.12}$ = 7.227 N) when a 3 mm drill diameter is used. In other words, there is an increase in the thrust force value by approximately 28 per cent with an increase in the feed rate and 32 per cent with an increase in the cutting speed. The lowest value of the thrust force (4.89 N) was introduced when the 3 mm drill diameter was used with a feed rate of 0.06 mm/rev and a drilling speed of 120 rpm. The highest value was recorded when the largest drill diameter (10 mm) was used at a higher feed rate (0.12 mm/rev) and speed (1450 rpm), which was 41.1 N.

In Figure 4.15b, a similar effect to that of the neat epoxy for feed rate, drilling speed and drill diameter on the thrust of the glass/epoxy can be seen. However, the thrust force values were greater than those for the neat epoxy, and this has been clarified previously with the argument that glass fibres have a highly abrasive nature and require more energy to remove them. The highest value was recorded when the largest drill diameter (10 mm) was used at a higher feed rate (0.12 mm/rev) and speed (1450 rpm), which was 143.75 N. In comparison to the neat epoxy, there was an increase in the thrust force by approximately 71 per cent when the epoxy was reinforced with glass fibres. Conversely, the addition of date palm fibres increased the thrust force values by 55 per cent compared to the neat epoxy composite, using a drill diameter (10 mm), feed rate (0.12 mm/rev) and cutting speed (1,450 rpm) as seen in Figure 4.15c. Further, the trends of the thrust value of date/epoxy are similar to the glass/epoxy and neat epoxy materials.

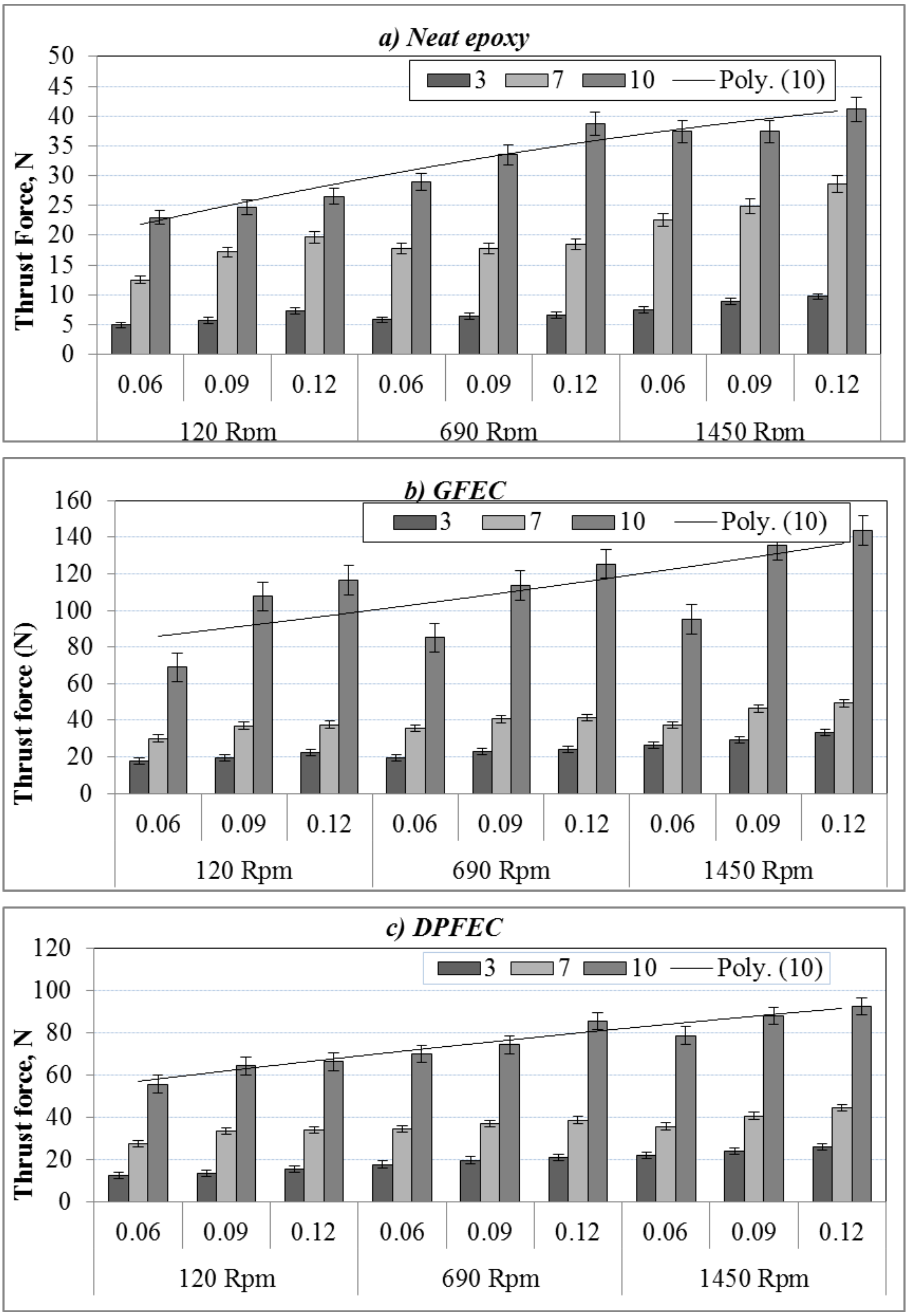

Figure 4.17: Thrust force for neat epoxy, glass/epoxy and date/epoxy at different cutting speeds and feed rates

4.5.3 Drilling progress observations

To understand the drilling process for the three materials, the inner, intermediate and outer regions of the hole on the samples were observed for a cutting speed of 120 rpm, a feed rate of 0.06 mm/rev and a 3 mm drill diameter. Before presenting the micrographs of the samples, the torque and thrust trends presented in Figure 4.11 and Figure 4.15 suggest that the drilling process took place in three regions. Figure 4.16 suggests that there were three damaged areas with different damage features, which could explain the torque and thrust force trends that have been presented previously.

The figure suggests that, at the initial stage of the drilling, the inlet regions suffered from a high cutting force, as the contacted area was less than the onwards process area. Moreover, the contact at the outer layer of the samples may lead to detachment and fractures at the edges, which leads to a larger hole diameter in the inlet. This means that the inner diameter of the hole is commonly greater than the diameter of the tool. With the case of the fibre/polymer composites, there may be great distortion in the shape of the hole in the inner area compared to the neat epoxy. At the inner area, there may be debonding, pull out, breakage and detachment of fibres. However, for neat epoxy, the fracture mechanism may take place at the inner area.

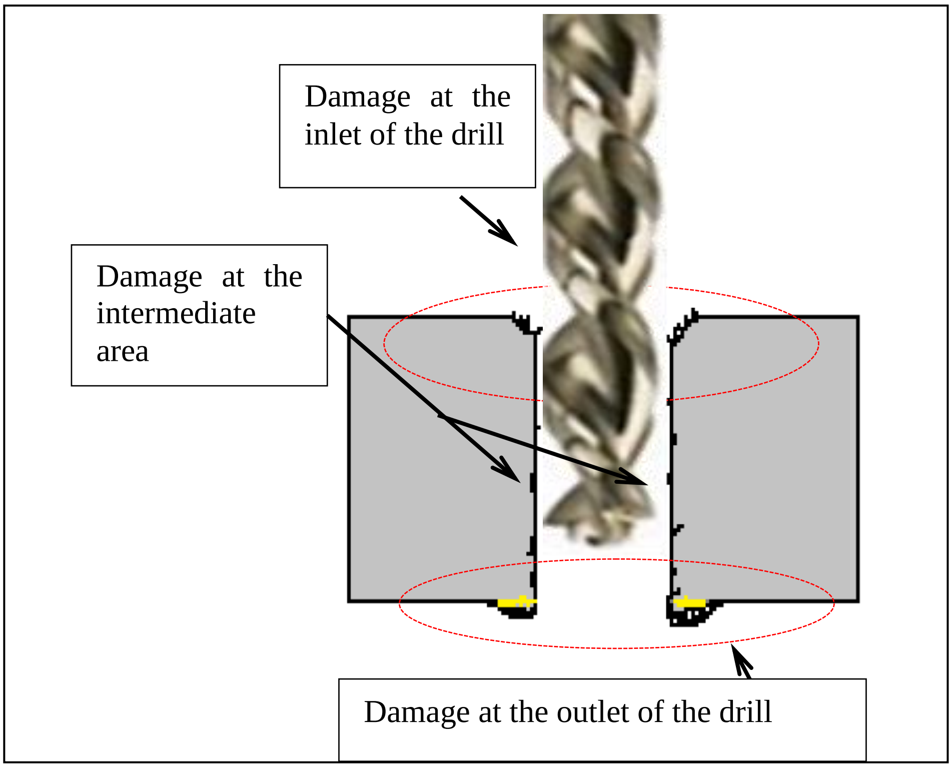

Figure 4.18: Damage on the inner, intermediate and outer regions during the drilling process

4.5.4 Neat epoxy

The micrographs of the drilled neat epoxy sample showing the inner intermediate and outer regions are displayed in Figure 4.17a–c. In Figure 4.17a–b, the inner regions contain many micro cracks, debris and signs of fracture. The direction of the material removal is in line with the direction of the drill. However, massive removal of material seems to be at the edge of the hole and distortion can be seen. This results in poor hole accuracy. Once the tip of the drill penetrates the bulk of the material, there is a uniform surface on the neat epoxy (see Figure 4.17c) despite the fact that there are some fracture failures and pitting phenomenon can be observed. At the outer regions of the hole, accumulation of the material can be seen and generation of a hump can be found. However, the removed materials adhered again weakly to the surface of the hole. Therefore, a detachment sign can be seen, which resulted from the removed materials. It seems the proposed idea in Figure 4.16 agrees with the

SEM observation for the neat epoxy. Further, the accuracy and the delamination of the hole should be considered from the inner and the outer regions. It is highly recommended that the fracture mechanism is studied and the damages on both the inlet and outlet of the holes is understood, as any damage to those areas could be an initiation for micro or macro cracks, leading to failure of the materials. For the neat epoxy, some cracks at the inlet of the holes and in the design of the components made of this material were observed, and it is highly recommended to consider the crack in the design.

The above recommendation with regards to crack propagation at the inlet or outlet of the holes is important in the case of the composites because it is well known that the reinforcements are the initiatives of the cracks and micro cracks (Krishnaveni et al., 2005, Wieleba, 2002, Bonny et al., 2010). The following section will focus on this matter with the assistance of micrographs of glass or date palm fibre reinforced epoxy composites.

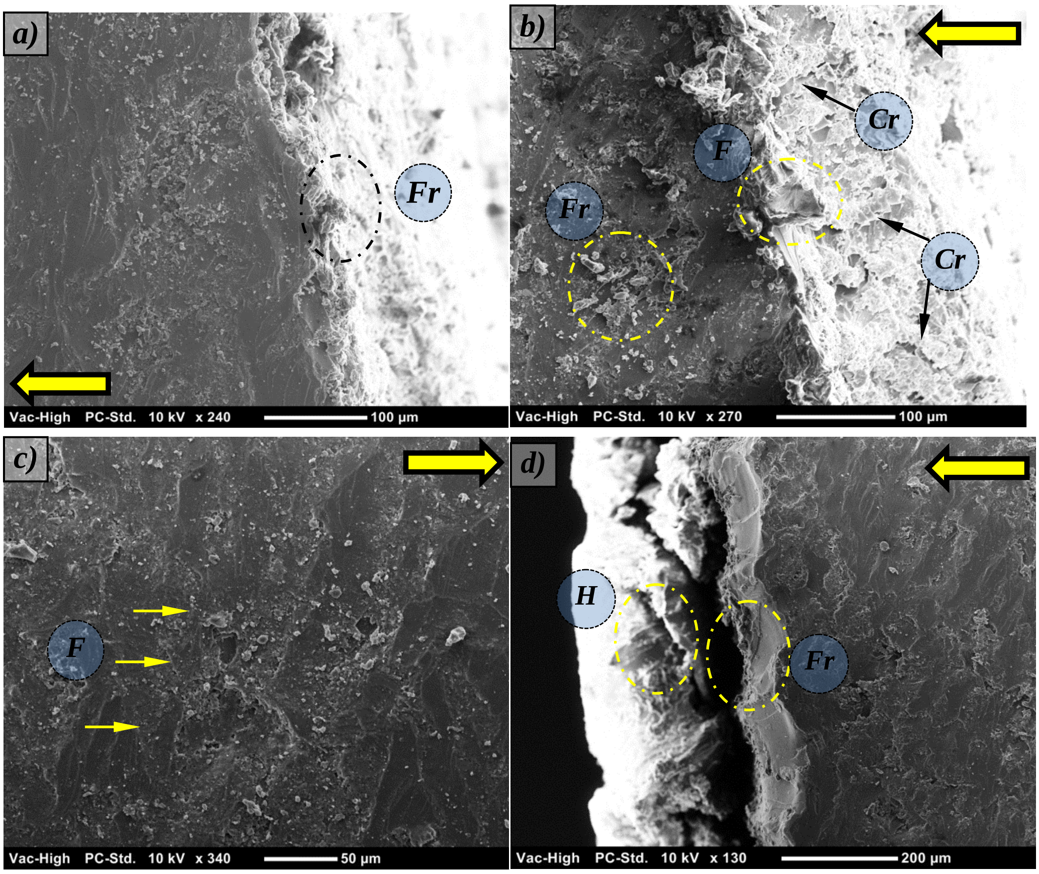

Note: F = fracture, Fr. = fragmentation, Cr. = crack and H. = hump

Figure 4.19: SEM photographs for neat epoxy using a 3 mm drill diameter, cutting speed of 120 rpm and feed rate of 0.06 mm/rev

4.5.5 Glass/Epoxy

Figure 4.18a–f displays the micrographs of the GFRE holes using a 3 mm drill diameter, a cutting speed of 120 rpm and a feed rate of 0.06 mm/rev for inlet, intermediate and outlet regions, respectively. At the inlet regions, there are signs of fragmentation, especially in the resinous regions, and this could be due to the fatigue loading during the drilling process. Moreover, the pitting process can be observed, which led to a larger hole at the outer regions compared to the intermediate, as can be seen in Figure 4.18a. Non-uniform edges can also be seen at the outer regions, indicating poor hole accuracy. Despite these features, there are no signs of crack at the inlet of the hole, which is due to the presence of reinforcements (glass fibres) in the composites. In other words, the presence of glass fibres assisted prevention of crack generation on the outer region of the hole. Such a strengthening mechanism and presentation of crack generation could be the region of high torque and thrust force generated on this composite, as introduced previously in Figure 4.11 and 4.15. Further, in the intermediate regions (see Figure 4.18c), there are signs of fibreglass breakage and detachments associated with pitting and fractures in the resinous regions. However, the glass fibres are still well adhered to the composite surface, which could lead to highly rough surface. At the outer regions and edge, Figure 4.18d shows signs of fracture and pitting and the generation of a hump. Moreover, at the inner surface of the outlet regions, there are signs of detachment and decomposition of the composites. This weakens the composites block significantly and may lead to failure of the designed composites without it being realised. This research recommends further study on how to present detachments and decomposition of fibre polymer composites at such regions, and improvements of interfacial adhesion of fibres with the matrix or orientations of the fibres could be the key. It seems that this edge requires polishing before it can be used. In other words, the finishing is poor, representing a lack of machinability of this composite.

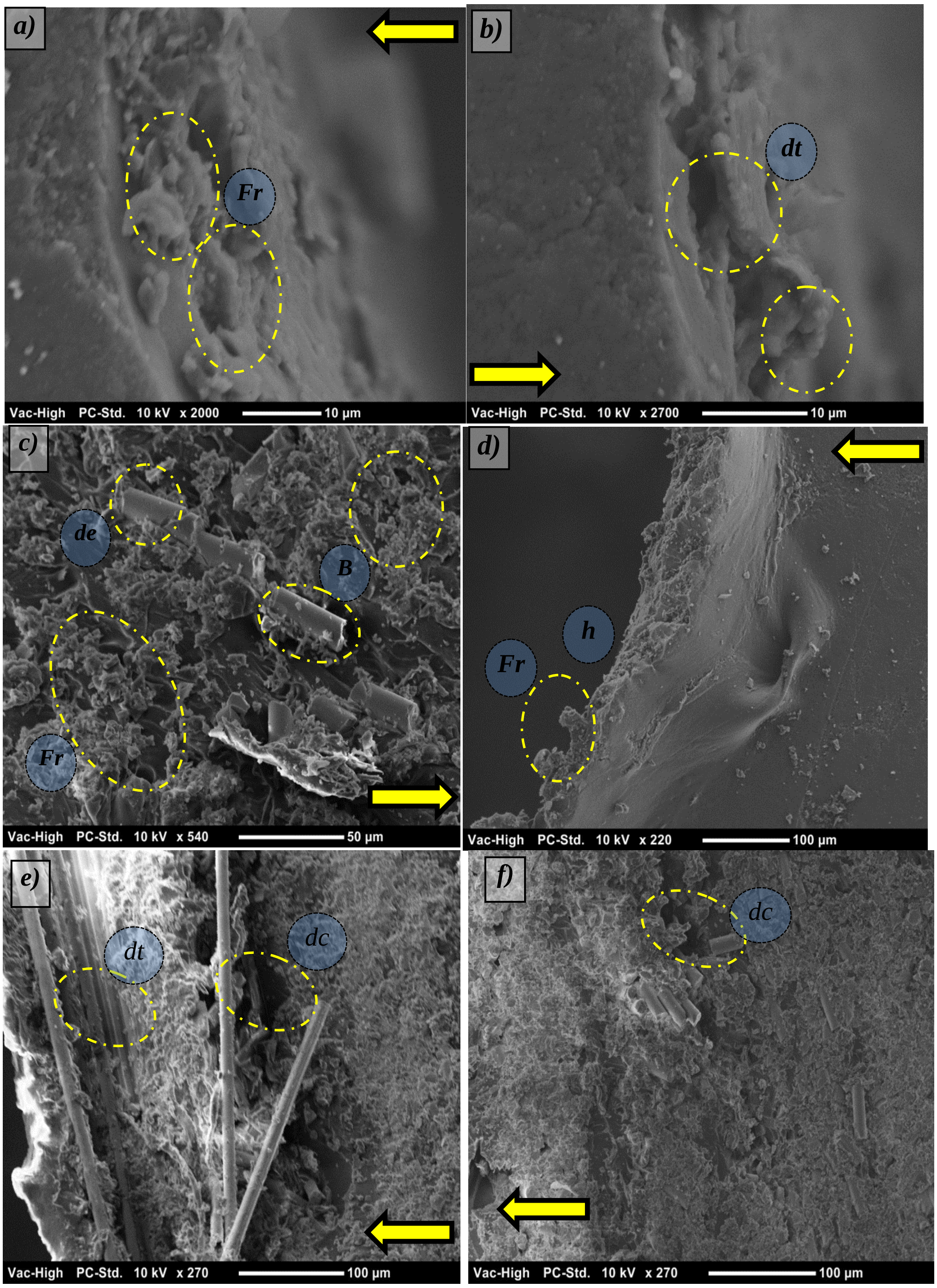

Note: F = fracture, Fr. = fragmentation, H. = hump, de. = debonding, dt. = detachment, B. = broken fibre and dc = decomposition

Figure 4.20: SEM photographs for glass/epoxy using a 3 mm drill diameter, cutting speed of 120 rpm and feed rate of 0.06 mm/rev

4.5.6 Date/Epoxy

For date/epoxy composite, Figure 4.19 shows the micrographs of the inner, intermediate and outer regions of a hole using a 3 mm drill diameter, a cutting speed of 120 rpm and a feed rate of 0.06 mm/rev. At the inner edges, Figure 4.19a shows that a fracture process took place during the drilling just below the edge. This reflects the brittleness of the composites. At a larger zoom, Figure 4.20b shows a relatively smooth edge compared to the one shown on the glass/epoxy composite (see Figure 4.19a and b). Interestingly, there are no signs of cracks on the edge and/or detachment or delamination. However, deeper in the hole, one can see that pull out of fibre and detachment took place (see Figure 4.20c and d). This is associated with a river-like fracture pattern. The study suggests that the fracture leads to the detachment of the fibres, which can also result in pull out of the fibre. In (Alsaeed et al., 2013b), it is confirmed that six per cent NaOH introduces the optimum interfacial adhesion to the date palm fibre to be adhered with the epoxy matrix. In other words, the pull out of the detachment mechanism, which is taking place during the drilling, is due to the fracture in the resinous regions, which weaken the bonding area. In Figure 4.20d, there are signs of debonding, which can explain this. At the outer regions of the hole, there are signs of fracture and sharp edges can be noticed (see Figure 4.20e and f). Bending of fibres can be seen at the edges. In Figure 4.20e, the inner surface close to the edge of the hole does not indicate any detachment, decomposition or failure signs, as seen before when the glass/epoxy was observed (see Figure 4.18e and f). This introduces interesting and comparative results to the natural fibres compared to the synthetic fibres in terms of machinability.

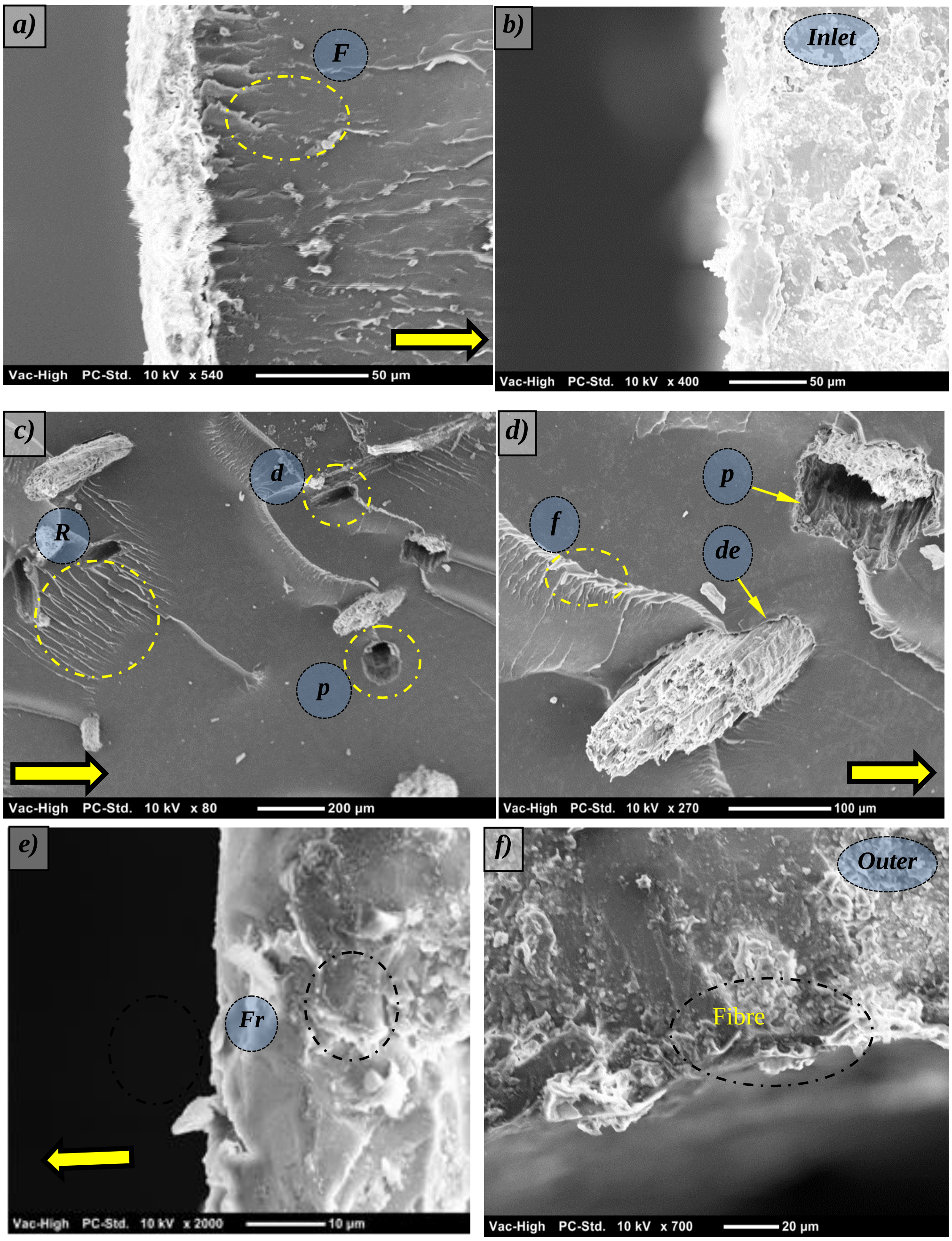

Note: F. = fracture, Fr. = fragmentation, Cr. = crack, P. = pull out, de. = debonding, dt. = detachment and R. = river-like

Figure 4.21: SEM photographs for date/epoxy using a 3 mm drill diameter, cutting speed of 120 rpm and feed rate of 0.06 mm/rev

4.6 Conclusion

This study presents the new dynamometer, detailing its design, fabrication, calibration and testing. The main findings of this work are:

- When drilling the materials, regions can be classified as inner, intermediate and outer. The thrust and torque behaviour was examined for a particular drilling time and divided into these three regions for neat epoxy, glass/epoxy and date/epoxy composites. The peak values were observed in the intermediate regions in which shears occurred at a higher level with the thrust force. The peak region can be considered the steady state region, as the others regions (inlet and outlet) offer less resistance to the material removal process.
- The presence of the glass fibres in the epoxy composites assisted in reducing the crack propagation at the inlet regions; however, the outlet region was highly deteriorated, as detachments and the decomposition mechanism were observed. For neat epoxy, cracks and fractures were the main damage features noticed.
- The presence of the date palm fibre in the epoxy improved the machinability of the composites, as it required similar values of torque and thrust to the neat epoxy, while the glass fibres needed more power. Further, it assisted in reducing the cracks in the inner and outer regions of the hole of the composites, despite pull out and detachments being observed.
- It is strongly recommended to observe the inner and outer regions of the hole because those regions could be an initiator for failure of the designed components.

CHAPTER 5: MACHINABILITY OF GLASS/DATE PALM FIBRE EPOXY COMPOSITES AND THEIR INFLUENCE ON THE DRILL TOOL

5.1 Introduction

In this chapter, a brief background on the machining of syntactic FRP composites and the issues in this area will be introduced. The results of the current study on delamination, hole accuracy, surface roughness and specific cutting pressure will be presented for neat epoxy, glass/epoxy and date/epoxy composites. The results will be compared with previous recent published works. For influence of machining on the tool, microscopy of the tool will be displayed and discussed to show and categorise damage. The ANOVA table and a summary of the chapter will be given at the end because the parameters and the experimental data are large.

5.2 Background

The majority of the works determined the machinability performance of materials based on hole accuracy, delamination, surface roughness and machining power (Hocheng & Tsao 2003(Davim and Reis, 2004); (Khashaba et al., 2010b). For instance, Hocheng and Tsao (2003) studied the effect of machining parameters (feed, speed and drill diameter) on machinability in terms of surface roughness of GFRE composites. It was reported that surface roughness increased with an increased cutting feed rate, while no obvious effect of the cutting speed was observed. (Davim and Reis, 2004) studied the effect of cutting parameters (cutting velocity and feed rate) for specific cutting pressures on machinability in terms of surface roughness in GFRPs. The results showed high values of surface roughness for both drills. Further, the Brad & Spur drill showed better performance than the Stub Length drill (i.e., produced smaller value of surface roughness). Similar findings have been reported previously for different synthetic FRP composites, such as GFRE (Mata et al., 2009, El-Sonbaty et al., 2004); Palanikumar 2007; (Bras et al., 2010)).

For the effect of the operating parameters on hole accuracy, fixed dimensional and geometric tolerances have been sought by many researchers cutting polymeric composite materials. The quality of the hole produced can be described in many ways (Jain et al., 2002). It can be classified as a geometrical error or errors regarding work piece material properties. The most important quality criteria emphasised are the error in hole roundness and hole size. Machining synthetic polymeric composites, particularly drilling, is widely used for producing riveted and bolted joints during assembly operations. It is well known that it is difficult to produce good quality holes with high efficiency using those polymeric composites by conventional drilling methods (Demir et al., 2006) and, thus, more expensive drilling techniques and special drill bits must be used to produce the most accurate holes. (Beg and Pickering, 2008) conducted several drilling trials on woven glass fabric/epoxy using HSS drills. (Khashaba et al., 2010b) studied the effect of drilling variables (cutting speed and feed) on machinability in terms of the dimension of holes drilled using a tipped carbide drill cutting tool and a glass fibre reinforced composite (glass/phenolic woven fabric). A variation in hole size was noticed and a reduction in oversize was observed as the number of holes drilled increased because of wear on the drill point. Similar concerns have been considered by many recent researchers on delamination and specific cutting power and most of the reported works agreed with the use of synthetic fibres in polymer composites because the machinability of the polymers worsens with the addition of synthetic fibres. It is suggested that the issue is mainly due to the highly abrasive nature of the synthetic fibres. In this work, an attempts to study the influence of natural fibres on the machinability of epoxy composites and compare such effects to the addition of glass fibres in epoxy is made. Several operating parameters are considered in the drilling process.

5.3 Determination of Material Machinability

5.3.1 Determination of hole accuracy

Chapter 4 explained the material preparation, experimental procedure and results for the thrust force and torque for composites at various operating parameters. In Chapter 5, the machinability of the composites will be determined according to hole accuracy, inner and outer delamination and specific cutting pressure. To determine the hole accuracy and, from the reported work in the literature, during drilling of fibre polymer composites, fibres are initially exposed to a bending process by the action of the cutting edge and then to shear fracturing. The remaining fibres try to reset. This causes tightening around the drill, resulting in the size of the drilled hole being less or greater than the drill diameter. This phenomenon is commonly observed in the drilling of laminated GFRP composites (Davim and Reis, 2004). Figure 5.1 presents a diagrammatic representation of the drilled hole scheme. Four lines should be drawn on the picture. The measurements of the drawn lines are taken to obtain the mean diameter and, from that, the error is calculated using Equation 5.1.

$$\text{Error} = \frac{\text{real diameter - mean diameter}}{\text{real diameter}} \times 100 \qquad \textbf{(Equation 5.1)}$$

In the current study, a Motic stereomicroscope (SMZ168 series) microscopy is used for observation of the drilled holes. Samples of the determination of hole accuracy procedure are given in Figure 5.2 for neat epoxy, glass/epoxy and date/epoxy composites machined with a 3 mm drill diameter at different cutting speeds (120 rpm, 690 rpm and 1450 rpm) and feed rate of 0.06 mm/rev. It should be mentioned here that, for each set of drilling, the average of the hole accuracy is determined for at least five samples and the average results are presented with the maximum and minimum values.

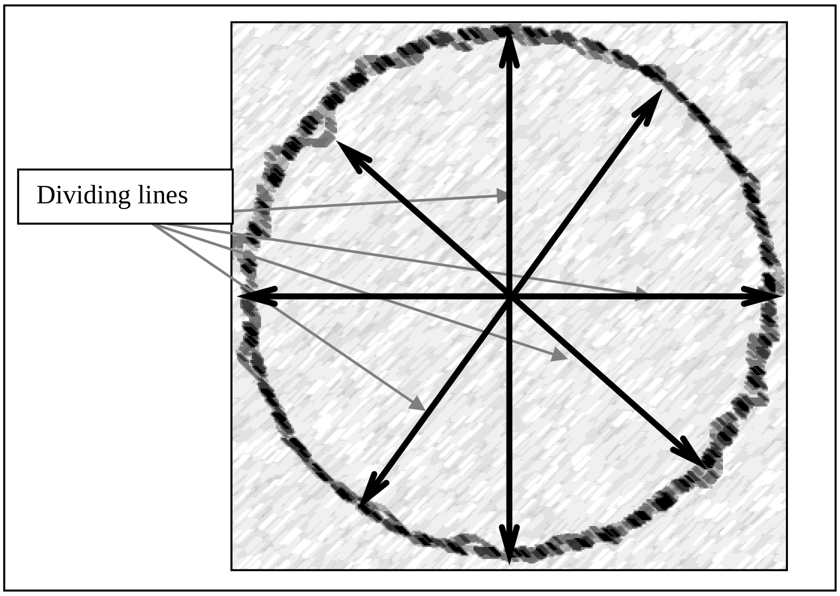

Figure 5.1: A diagrammatic representation of the drilled hole and the drawn lines to determine the error percentage representing the hole accuracy

<table>
<tr><td></td><td>3 mm, 120 rpm,
0.06 mm/rev</td><td>3 mm, 690 rpm,
0.06 mm/rev</td><td>3 mm, 1450 rpm,
0.06 mm/rev</td></tr>
<tr><td>Neat</td><td>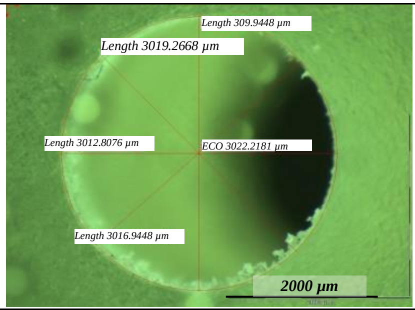
</td><td>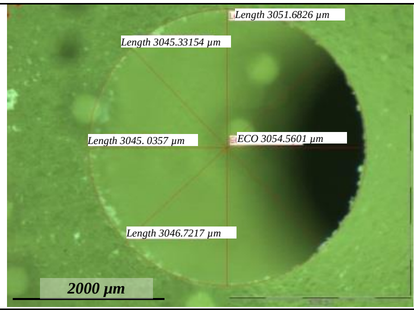
</td><td>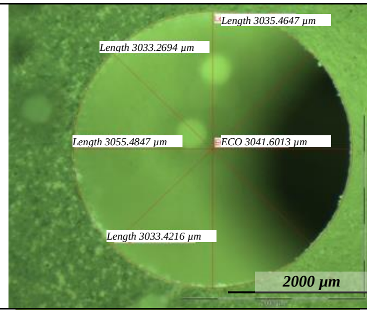
</td></tr>
<tr><td>GFEC</td><td>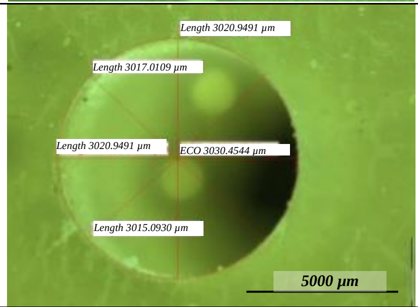
</td><td>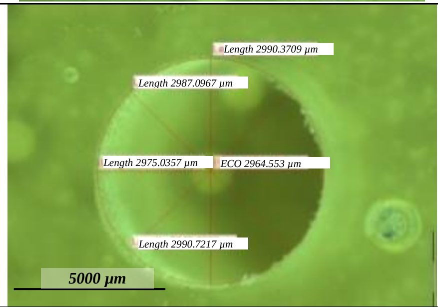
</td><td>
</td></tr>
<tr><td>DPFEC</td><td>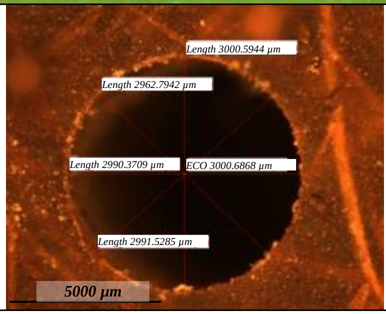
</td><td>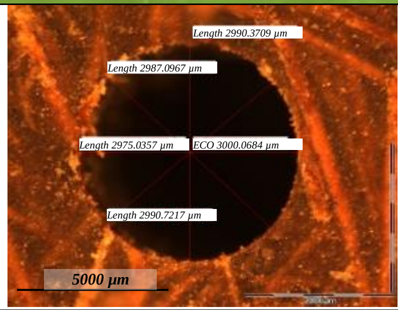
</td><td>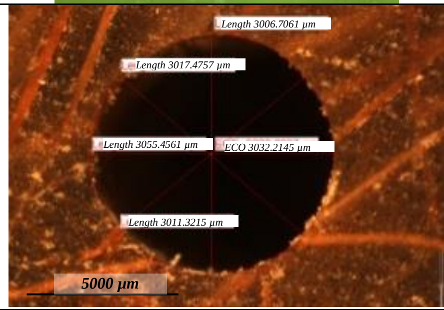
</td></tr>
</table>

Figure 5.2: Micrographs of drilled hole size accuracy after being drilled at different cutting speeds for the three composites

5.3.2 Determination of inner and outer delamination in the composites

Delamination in drilling is one of the important aspects affecting the drilled hole surface and strength. It is mainly due to the thrust force developed during drilling. In the literature review, feed rate, cutting speed and material thickness were found to be the drilling parameters that most influence delamination in the drilling of polymeric composites. Pictures of each drilled hole should be taken to determine the delamination factor. The delamination factor can be expressed as Equation 5.2 (Davim et al., 2007).

$$F_d = \frac{D_{\max}}{D} + \frac{A_d}{(A_{\max} - A_d)}(Fd^2 - Fd) \qquad \textbf{(Equation 5.2)}$$

where

F_d = delamination factor, D_{max} = maximum diameter of the damaged area, D = drill diameter, A_d = hole diameter, A_{max}, = $\pi D^2_{max}/4$ and A_d = damaged area. Figure 5.3 presents a diagrammatic representation of the delamination scheme. Figure 5.3a shows the maximum diameter that can be detected with the use of optical microscopy. The difficult part was how to determine the damaged area outside the hole (see Figure 5.3b). Some authors suggested using software and converting the hole image to greyscale and then determining the damaged area. However, in the current work, the microscopy is connected to a computer, which is equipped with software that allows the area on the image to be determined (see Figure 5.3c). This was extremely helpful for determining the damaged area in most cases. A sample of the maximum diameter determination for the inner area of the hole is given in Figure 5.4. The delamination at the inlet and outlet of the hole is determined and presented in this chapter.

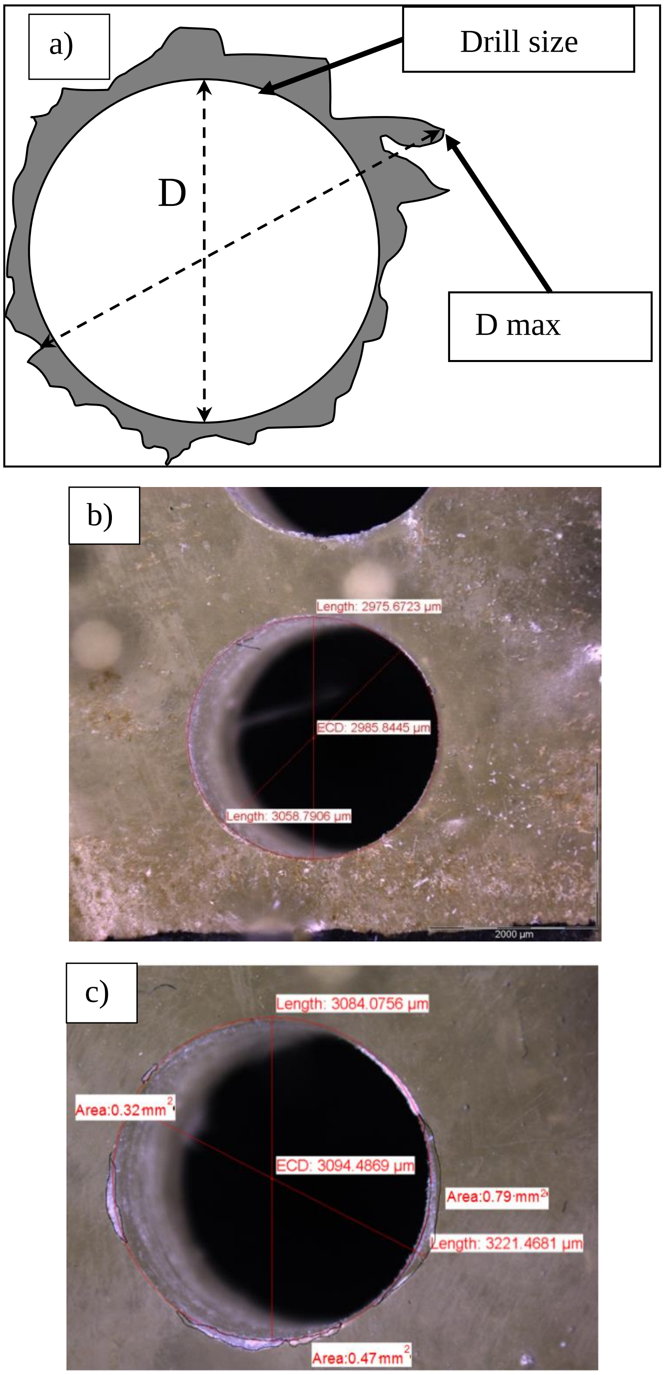

Figure 5.3: Maximum drill diameter and damaged area outside the hole

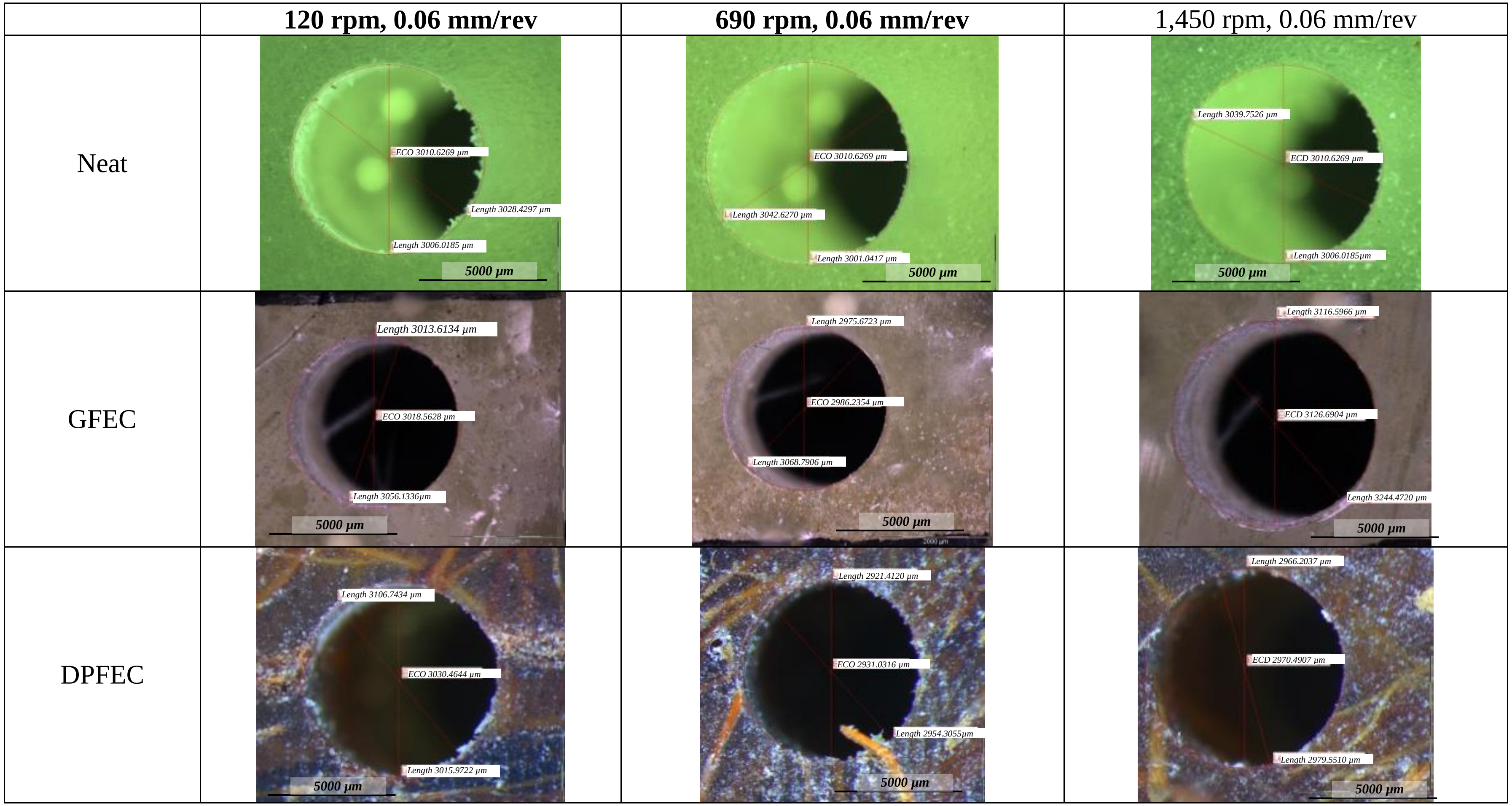

Figure 5.4: Micrographs of inner delamination on drilled hole surfaces after being drilled at different cutting speeds for the three composites

5.3.3 Other outputs

The specific cutting pressure will be calculated using Equation 5.3.

$$Ks = \frac{8 \times T}{f \times d^2} \qquad \textbf{(Equation 5. 3)}$$

where

T = torque in N.m, f = feed rate in mm/rev and d = diameter of the hole in mm.

Surface roughness is an important characteristic that describes the quality of the machined hole surface. In the current work, the surface roughness for each drilled hole was measured using the MarSurf PS1 surface roughness tester. In addition, SEM was used to examine the inner surface of the hole, as it was not possible with optical microscopy. Further, SEM was used to examine the tool after the experiments to check for damage. This assisted in understanding the effect of each material on the life of the tool and the severity of the damage.

5.4 Machinability of Selected Materials

Hole accuracy, inner delamination, outer delamination and specific cutting pressure at different operating parameters are presented in this section for all materials (see Figure 5.5–5.15). The data averages are determined and presented with the maximum and minimum values.

5.4.1 Hole accuracy under different operating parameters

The influence of the operating parameters on the hole accuracy of the neat epoxy, glass/epoxy and date/epoxy composites are presented in terms of error percentages in Figure 5.5a–c. In general, the figure shows that the operating parameters have a significant influence on hole accuracy of all materials. In most cases, an increase in the feed rate exhibits relatively high error rates for all materials. In other words, the hole is not highly uniform at higher feed rates, resulting in poor hole accuracy for the materials. For instance, error increased by approximately 60 per cent when the neat epoxy was machined with a high feed rate and a 10 mm drill diameter at a speed of 1,450 rpm. At the same operating conditions, error for glass/epoxy and date/epoxy increased by 350 per cent and 100 per cent, respectively. An increase in error with an increase of feed rate could be expected, as there is not enough time to finish the drilling of the hole edges when compared to a low feed rate. Such a trend has been reported previously for carbon fibre reinforced plastic (Shyha et al., 2010, Krishnamoorthy et al., 2012, Shyha et al., 2009) and glass fibre reinforced polyester (Rajamurugan et al., 2013).

Similarly, the drilling speed also influences hole accuracy for all materials. In other words, high drilling speeds result in high error hole accuracy in most cases. However, for glass/epoxy, there are some cases in which low error in hole accuracy occurs, for example, when the drill speed is intermediate (690 rpm), refer to the feed rate of 0.09 and drill diameter of 10 mm.

An increase in the error of hole accuracy when the drill speed increases could be due to the brittle nature of the epoxy. From the reported works, thermosets exposed to impact result in high fracture modes and possible fragmentation (Bagwell and Wetherhold, 2005, Kanchanomai et al., 2005). In the current study, it is suggested that the shear loading on the edge of the hole results in high fragmentation material removal, which results in high error hole accuracy. This is supported by the micrographs displayed in Figure 5.6 for the three materials. The micrographs clearly show damaged edges, especially in the case of glass/epoxy composites. For all materials, it seems the removal of the material occurs in fracture mode at the initial stage, showing signs of fracture and sometimes a pitting mechanism, indicating fatigue loading may take place during drilling.

In some reported works, it has been found that spindle speed is the main parameter affecting the circularity error and this is followed by feed rate. (Campos Rubio et al., 2013) used a drilling machine on PA6 and PA66GF30 composites with three carbide drills (K20). (Krishnaraj et al., 2012) used high speed drilling on CFRP laminates. It has been reported that feed rate has a greater influence on diameter of the hole. Further, higher feed rates result in holes closer to the nominal diameter. Conversely, spindle speed was found to be one of the major determinants of the circularity of the drilled hole and the best results were obtained at high speeds. According to (Inoue et al., 1997), when a small amount of drilled holes must be produced with great quality, then low feed rates should be used. Conversely, higher feed rates should be used for huge quantity production with less quality.

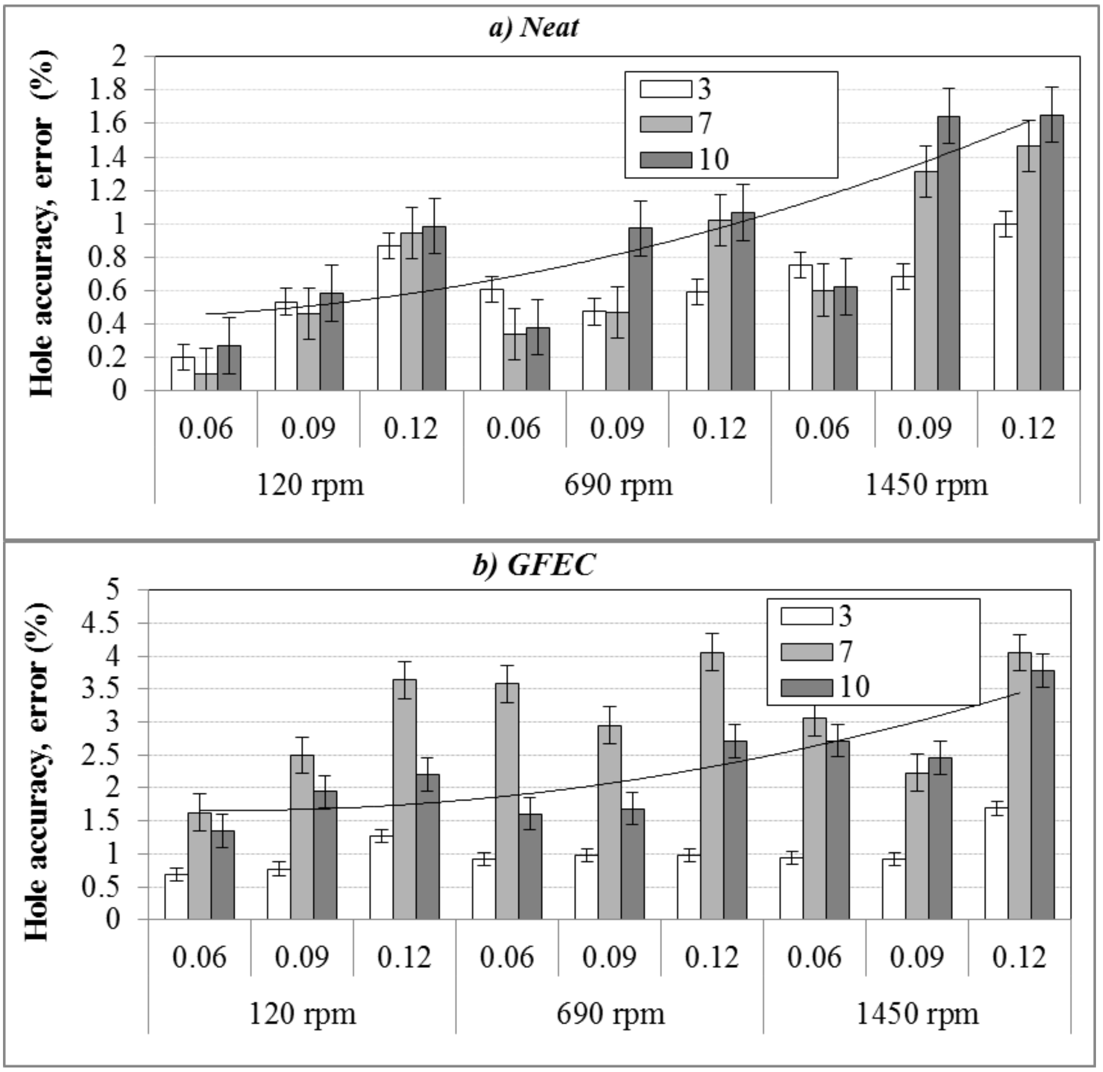

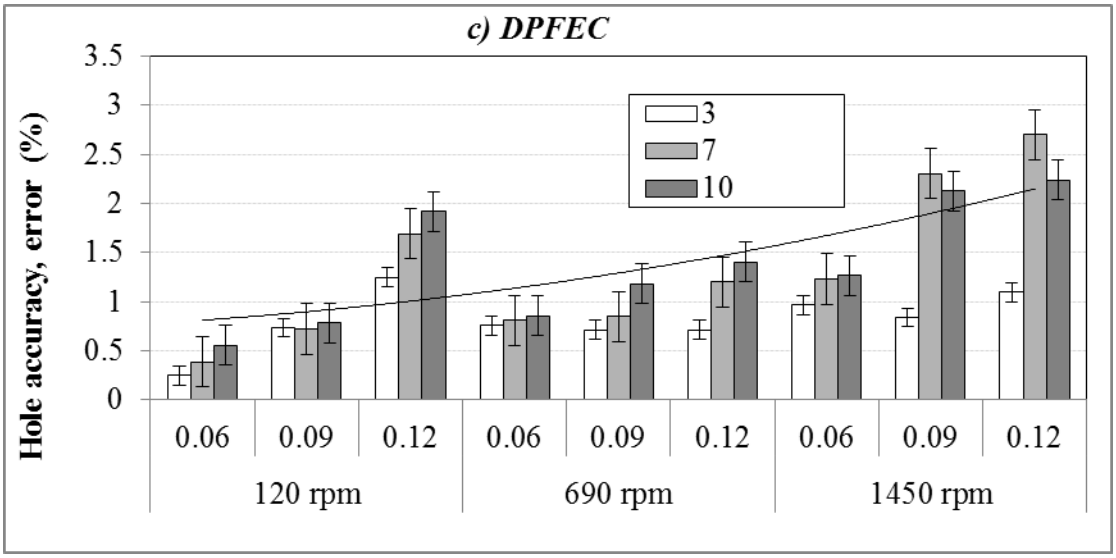

Figure 5.5: Hole accuracy for the three materials at different operating parameters

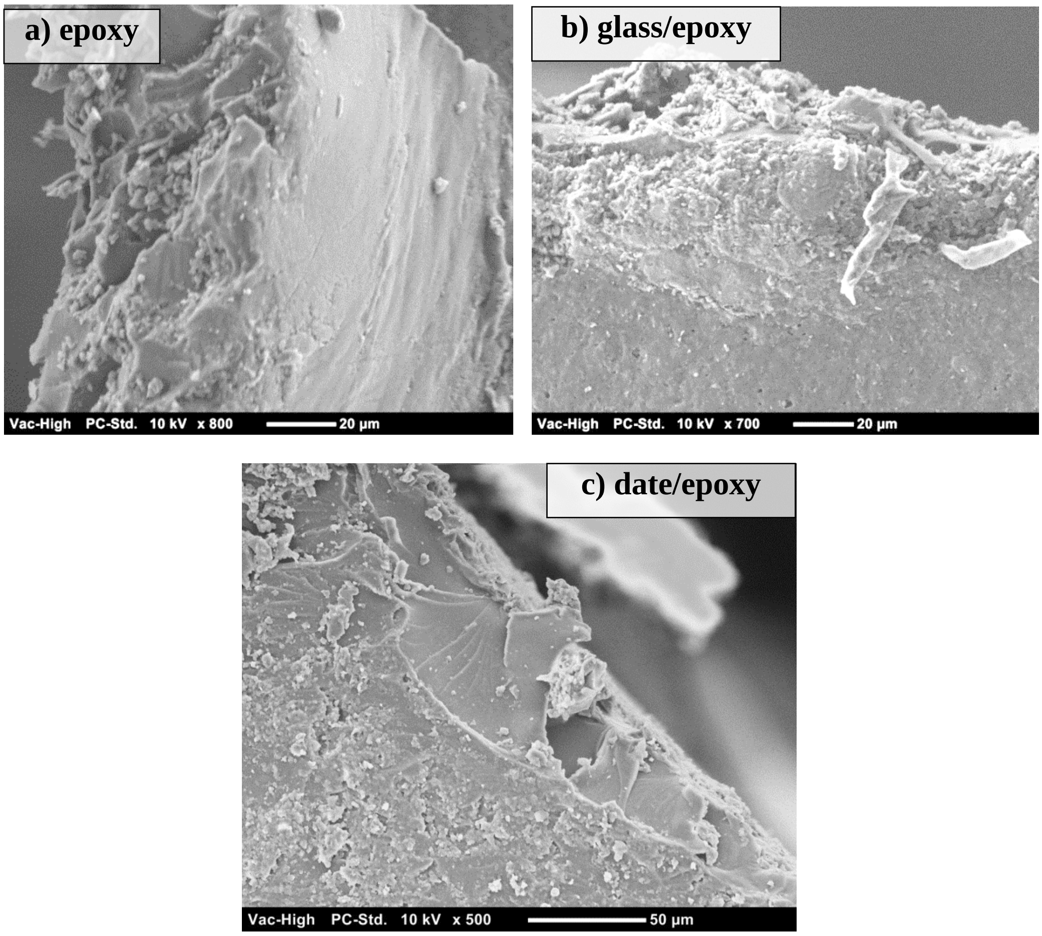

Figure 5.6: Micrographs of the hole edges at higher feed rate (0.12 mm/rev) and high speed (1,450 rpm) of neat epoxy, glass/epoxy and date/epoxy composites

For comparison purposes between neat epoxy, glass/epoxy and date/epoxy composites in terms of hole accuracy, the data in Figure 5.5 are extracted and represented in Figure 5.7 for the drill diameter of 10 mm only. For other drill diameters, the main findings are the same and are excluded. From this figure, it can be seen that the addition of either glass or date palm fibre worsens hole accuracy of the epoxy, as neat epoxy exhibited the lowest error in hole accuracy for all tested parameters. Conversely, it is obvious that the addition of date palm fibre to epoxy introduces less error compared to the addition of glass fibre for all tested parameters. This is a promising result for the composites based on natural fibres compared to synthetic fibres. This assists in the component design, as the high error percentage in hole accuracy could indicate a high tolerance in the hole, which makes the hole a critical area for stress concentrations and/or crack propagation. The micrographs of the edges from the inside of the hole for both composites may help in understanding the results and the arguments here (see Figure 5.8).

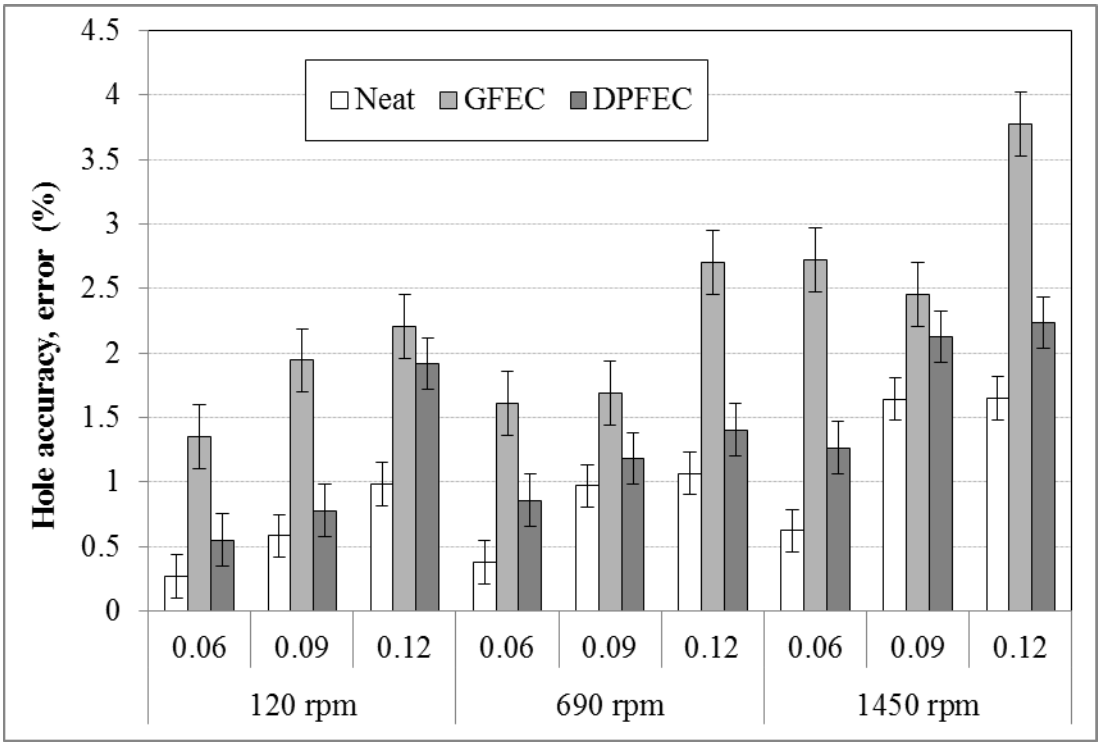

Figure 5.7: Comparison of hole accuracy for the three materials at 10 mm drill diameter

For glass/epoxy composites, the fibres are pulled out towards the outside when the tool is removed (i.e., the fibre is resting at this stage). Moreover, it seems the resinous regions are exposed to high fracture loadings, which distort the shape of the edge. Conversely, date palm fibres introduce more uniform edges compared to glass fibres and result in low error in terms of hole accuracy compared to glass fibres.

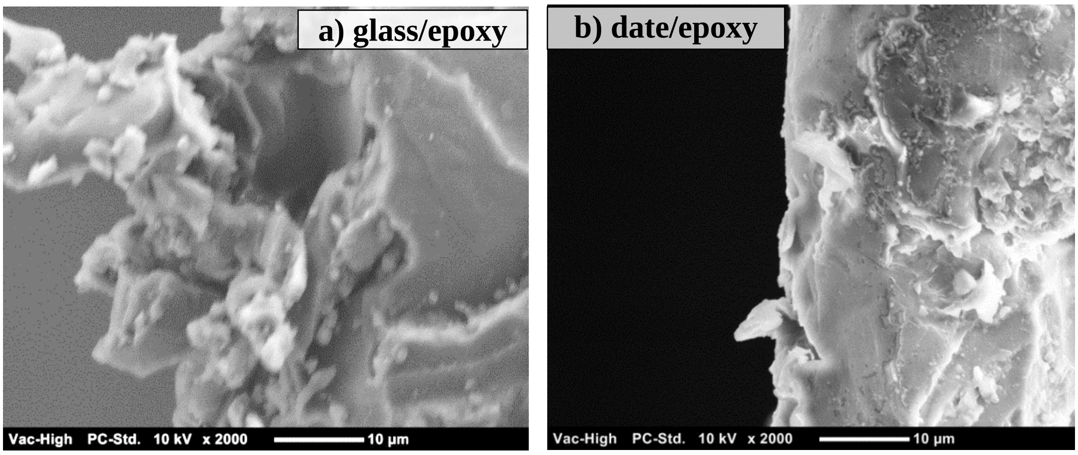

Figure 5.8: Micrographs of hole edges from the inside at higher feed rate (0.12 mm/rev) and high speed (1,450 rpm) of glass/epoxy and date/epoxy composites

Table 5.1 summarises the ANOVA table to show the influence of each operating parameter on hole accuracy. The table indicates that the most influential parameter is the feed rate because it contributes approximately 40 per cent, which is followed by drilling speed at 32 per cent. In other words, the drill diameter shows no significant influence on hole accuracy.

Table 5.1: ANOVA analysis of operating parameters on hole accuracy

Source	**Sum of Squares**	***df***	**Mean Square**	***F***	**Sig.**	**Contribution (%)**
Diameter	1.023	2	.511	4,683.4	.000	7.6
Speed	4.279	2	2.139	19,593.7	.000	31.8
Feed	5.479	2	2.740	25,091.3	.000	40.7
Diameter * Speed	.467	4	.117	1,068.6	.000	3.5

Diameter * Feed	1.127	4	.282	2,581.1	.000	8.4
Speed * Feed	.443	4	.111	1,014.8	.000	3.3
Diameter * Speed * Feed	.645	8	.081	738.5	.000	4.8
Error	.006	54	.000			0.0
Total	13.469	80				100.0

5.4.2 Inner delamination at different operating parameters

The delamination factor for the inlet of the hole was determined using (Davim et al., 2007) approach for all materials under different operating parameters. The average of at least three readings is presented in Figure 5.9 with the maximum and minimum obtained values included. In general, one can see much less influence from the operating parameters on the delamination factor of all materials, especially for the neat epoxy; in most cases, the range of hole accuracy is approximately 1.15. The consistency in the delamination factor of the neat epoxy compared to its composites is due to the presence of the fibres, which resulted in high delamination at the edge of the hole, as seen in Figure 5.8 for the micrographs of the composites. For glass/epoxy, it seems there is a slight reduction in the delamination factor with an increase in feed rate, which is in agreement with reported works by (Davim et al., 2007), when a low feed rate is used. Increasing the cutting speed results in a slight increase in the delamination factor, which is also in agreement with (Davim et al., 2007, Nagarajan et al., 2012). It is found that the addition of glass fibre worsens hole quality and the machinability of the composites because the delamination factor reaches 1.2, which is considered high for such operating parameters. For date/epoxy composites, Figure 5.9c shows fewer disturbances within the delamination factor of the composites for all of the operating parameters, which are in range of 1.15.

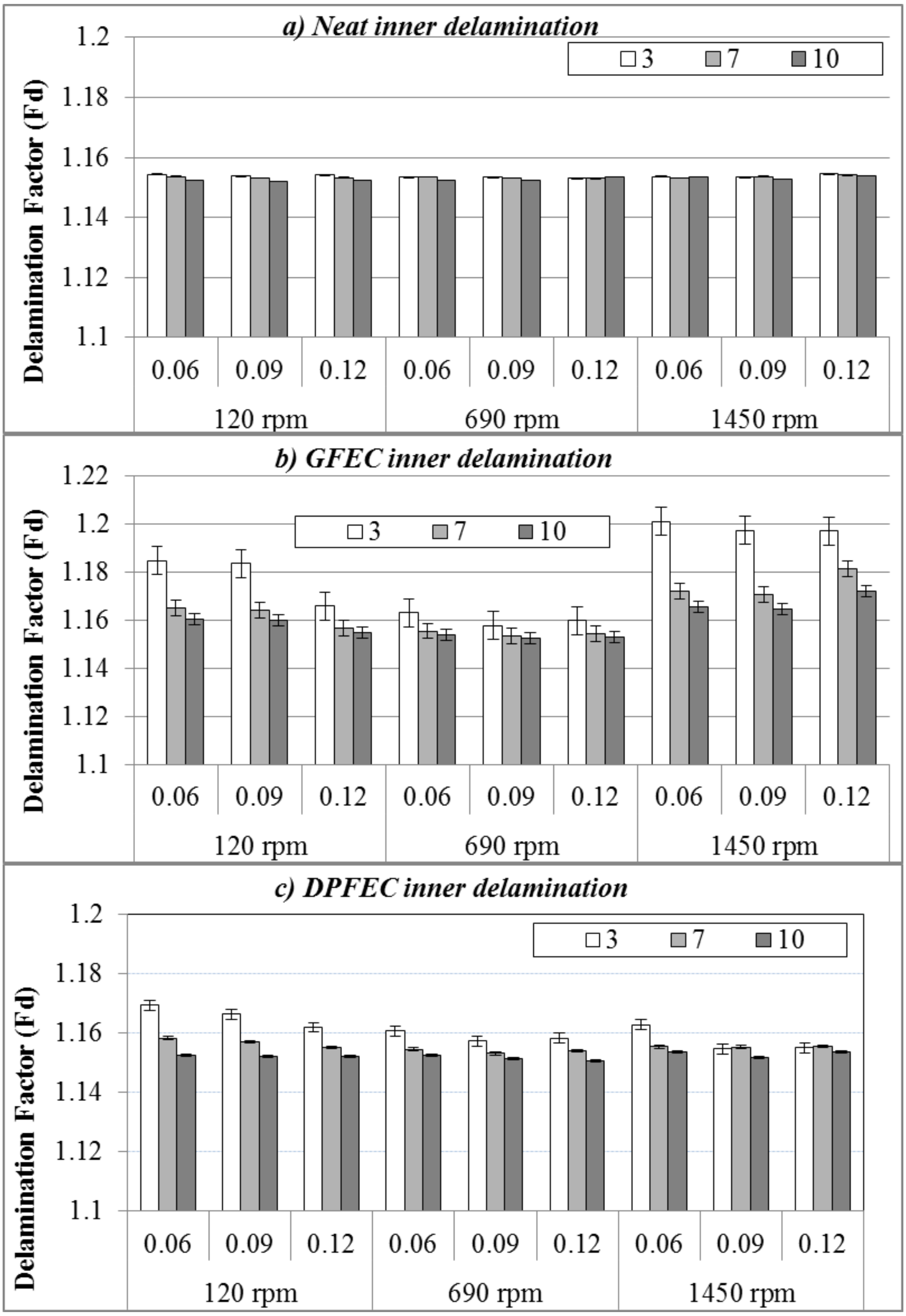

Figure 5.9: Inner delamination for the three materials at different operating parameters

To show the inner delamination factor of all materials under the same conditions, the above data are plotted for a drill diameter of 10 mm and presented in Figure 5.10. For all operating parameters with a 10 mm drill diameter, the inner delamination factor for neat epoxy and date/epoxy composites is comparable to glass/epoxy, which exhibits a higher delamination factor. These findings are mainly due to the abrasive nature of glass fibres compared to the date palm fibres and the damage caused by the glass fibres compared to the date palm fibres. Figure 5.11 may support this claim, as removal of the glass fibres from the bulk of the materials could act as a third body between the tool and the inner surface of the hole, causing the high delamination factor. For date/epoxy, such a scenario could be less predictable, as date palm fibre is natural and not brittle like glass fibre. This will assist in maintaining good hole quality with less delamination factor.

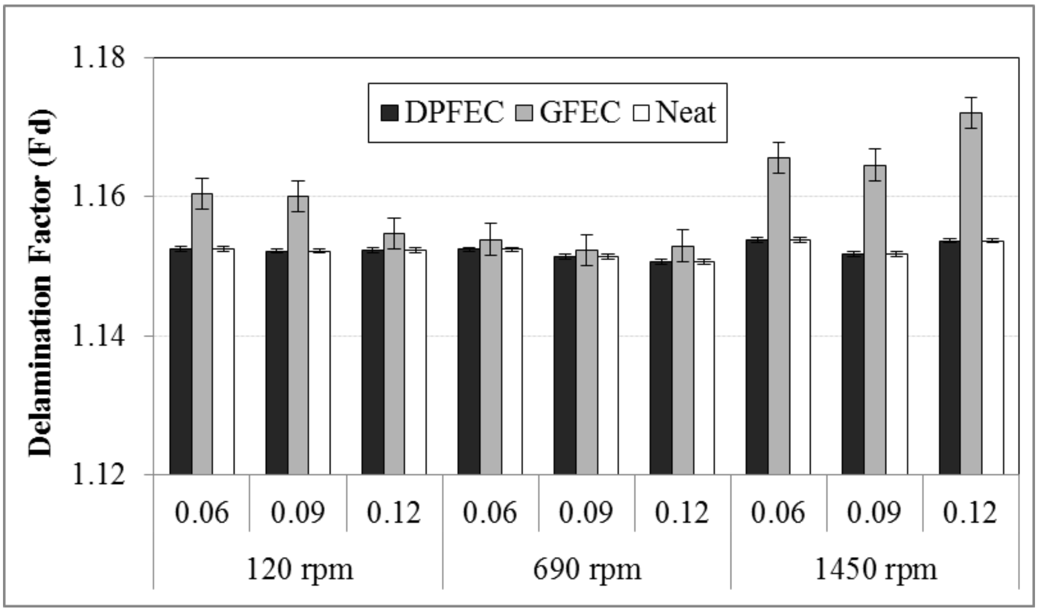

Figure 5.10: Comparison of inner delamination for the three materials at a 3 mm drill diameter

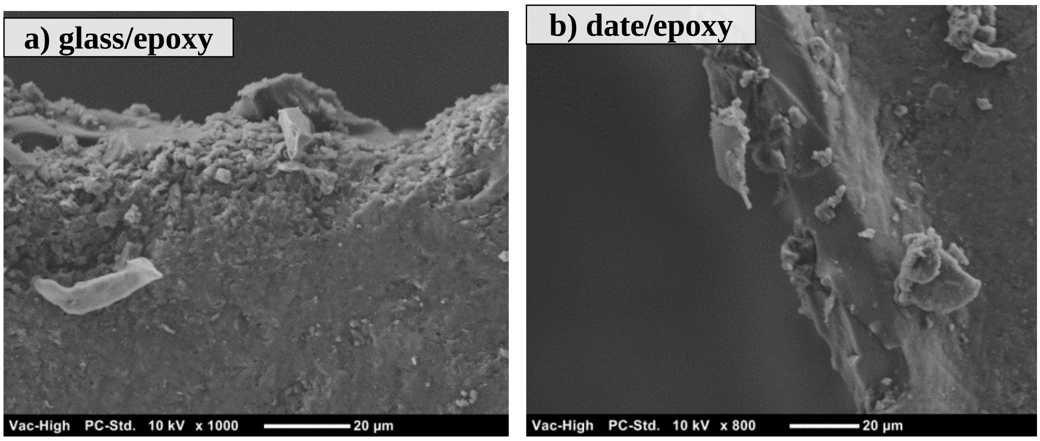

Figure 5.11: Micrographs of the inner side of the hole of the composites drilled at 120 rpm, 0.06 mm/rev and with a 3 mm drill diameter.

An ANOVA table may assist in understanding the most influential parameter on the inner delamination factor. Table 5.2 lists all operating parameters and their effect on the inner delamination factor. It seems the drill diameter is the key rule in controlling the inner delamination of the composites and is followed by the feed rate and the drilling speed.

Table 5.2: ANOVA analysis of operating parameters on inner delamination factor

Source	Sum of Squares	*df*	Mean Square	*F*	Sig.	Contribution (%)
Diameter	0.001868	2.00	0.00093	447.61	0.00	40.0
Speed	0.000522	2.00	0.00026	124.98	0.00	11.2
Feed	0.001042	2.00	0.00052	249.79	0.00	22.3
Diameter * Speed	0.000000	4.00	0.00000	0.02	1.00	0.0
Diameter * Feed	0.000000	4.00	0.00000	0.01	1.00	0.0
Speed * Feed	0.001129	4.00	0.00028	135.23	0.00	24.1
Diameter * Speed * Feed	0.000000	8.00	0.00000	0.02	1.00	0.0
Error	0.000113	54.00	0.00000			2.4
Total	0.004674	80.0000				100.0

5.4.3 Outer delamination at different operating parameters

The outer delamination is represented by the delamination factor for the outlet of the hole. The results of the delamination factor for the materials at different operating parameters are displayed in Figure 5.12. For neat epoxy, the delamination factor is less sensitive to the operating parameters because it maintains its value at approximately 1.17 in most cases. The homogeneity of the neat epoxy resulted in such a delamination factor. Conversely, for glass/epoxy composites, an increase in either the feed rate, drill speed or drill diameter reduces the outer delamination factor. It seems the massive loading in terms of shear and/or thrust at the outlet of the hole leads to better hole quality. This is in agreement with (Nagarajan et al., 2012). A similar reduction in the delamination factor can be seen for date palm fibre in Figure 5.12c.

(Davim et al., 2008) investigated the effect of the cutting parameters on drilling medium density fibreboard (MDF). They declared that the delamination factor (inner and outer) decreases with an increase of cutting speed and feed rate. The effect of the feed rate on the delamination of a GFRP has been investigated by (Capello, 2004), and it was found that delamination does not take place at low feed rates. Nevertheless, when the feed rate increases, the actual back rake angle becomes negative, which will push the work material instead of shearing and causing delamination.

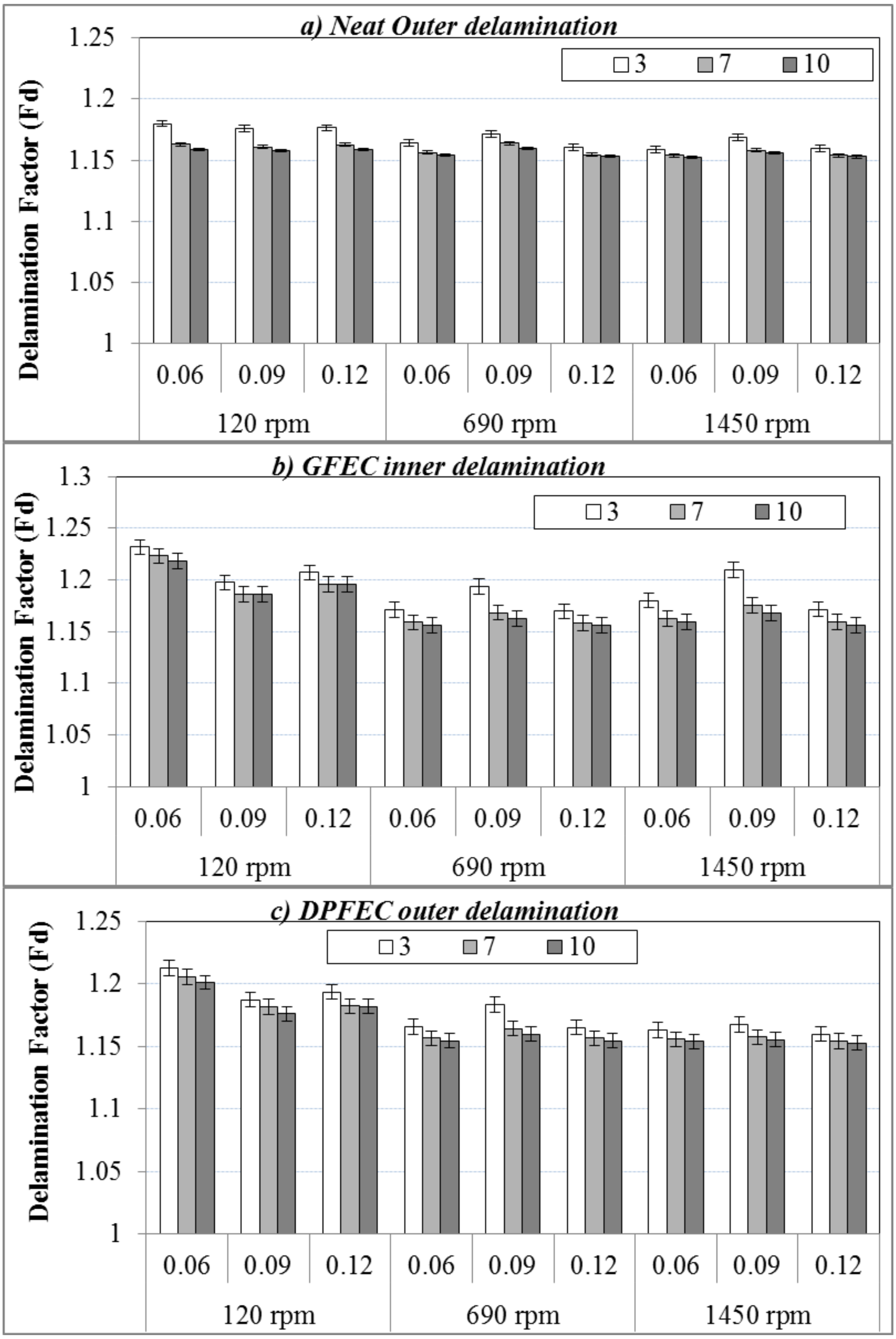

Figure 5.12: Outer delamination for the three materials at different operating parameters

For comparison purposes, the delamination factor for all materials that underwent the drilling process with a 10 mm drill diameter is plotted in Figure 5.13. From this figure, it seems the neat epoxy maintains the lowest delamination factor for all operating parameters, especially at low loading parameters of 0.06 mm/rev and 120 rpm. At severe loading condition of high speed and feed, neat epoxy and its composites exhibit a similar delamination factor of slightly higher than 1.15.

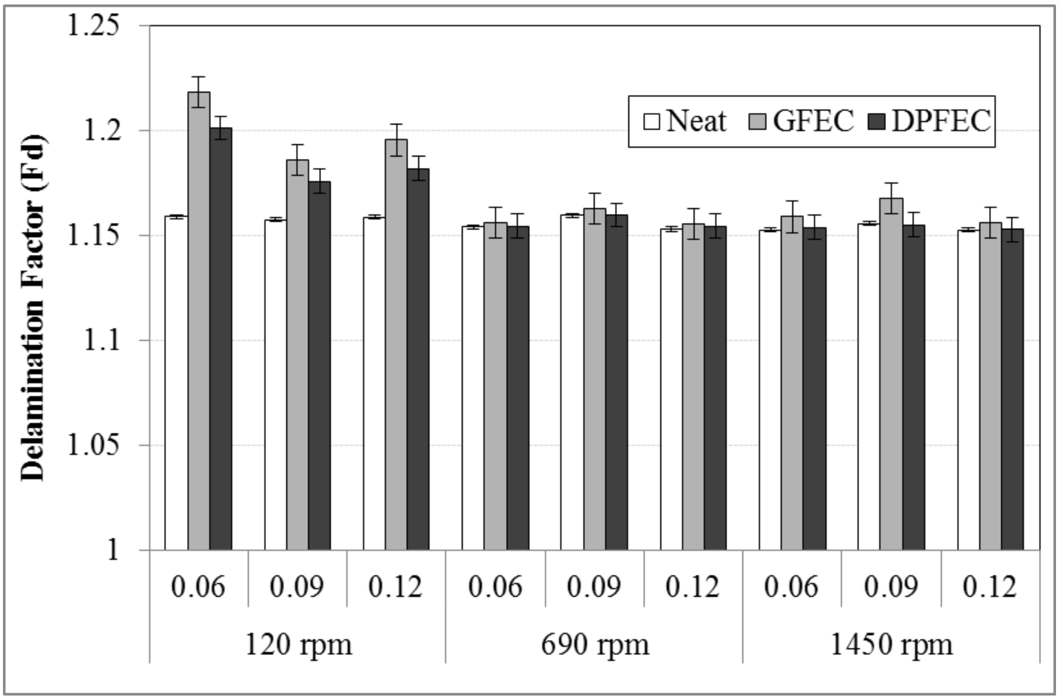

Figure 5.13: Comparison of outer delamination for the three materials at 10 mm drill diameter

For the composites, it seems the operating parameters influence outer delamination. This can be confirmed with the ANOVA table in Table 5.3, showing that drill diameter followed by drill speed and then feed rate significantly influence the outer delamination factor.

Table 5.3: ANOVA analysis of operating parameters on outer delamination factor

Source	Sum of Squares	*df*	Mean Square	*F*	Sig.	Contribution (%)
Diameter	0.001840	2	0.000920	441.0	0.000	36.86
Speed	0.001218	2	0.000609	291.9	0.000	24.40
Feed	0.001153	2	0.000577	276.4	0.000	23.10
Diameter * Speed	0.000000	4	0.000000	0.0	1.000	0.00
Diameter * Feed	0.000000	4	0.000000	0.0	1.000	0.00
Speed * Feed	0.000667	4	0.000167	79.9	0.000	13.37
Diameter * Speed * Feed	0.000000	8	0.000000	0.0	1.000	0.39
Error	0.000113	54	0.000002			2.26
Total	0.004992	80				100.00

5.4.4 Specific cutting pressure at different operating parameters

Specific cutting pressure is an important measurement involved in determining the machinability of materials. The influence of the operating parameters on the specific cutting pressure of all materials is presented in Figure 5.14. The figure shows that the increase in the feed rate results in a reduction in the specific cutting pressure. However, the increase in the drill speed and or drill diameter increases the specific cutting pressure. In other words, the lowest values can be found with a 3 mm drill diameter at a low drilling speed, which is in agreement with (Paulo Davim and Mata, 2007).

To show the influence of the fibre addition on the machinability of the composite in terms of specific cutting pressure, Figure 5.15 is plotted for the drilled composite at different operating parameters with a 10 mm drill diameter.

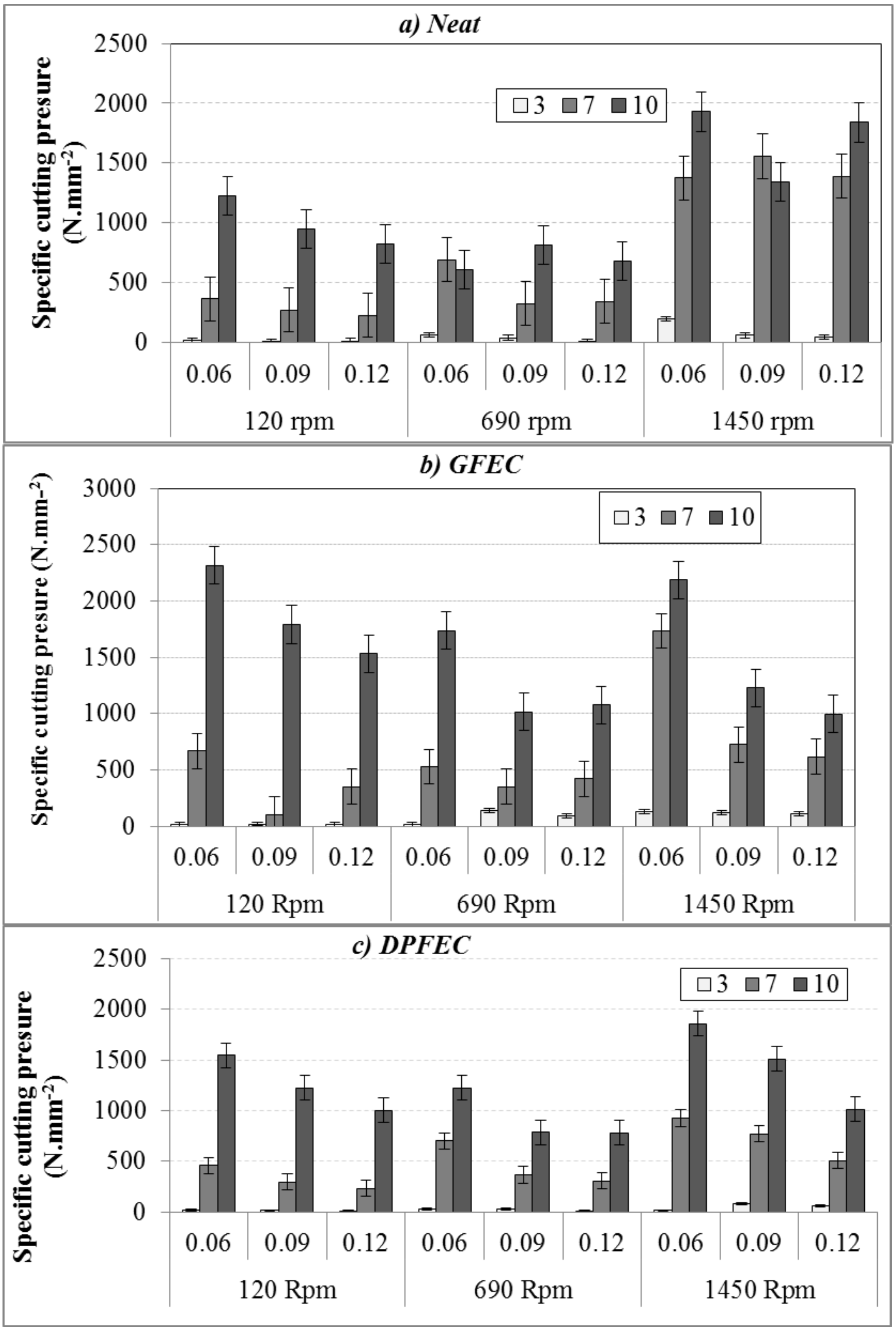

Figure 5.14: Specific cutting pressure for neat epoxy, glass/epoxy and date/epoxy at different drill diameters, cutting speeds and feed rates

5.5 Influence of Machining on Inner Surface Roughness

In addition to the above results, the roughness of the inner surface could be another term needing consideration in machinability. The roughness of the inner surface of all holes was measured and the average determined. However, the roughness of the inner surface was less affected when a different diameter was used for the same operating conditions. In this section, the roughness of the holes drilled with a 10 mm drill diameter is presented in Figure 5.15a for all materials under different operating parameters. An increase in the feed rate relatively reduces the roughness; however, an increase in the drill speed increases the roughness for all materials.

The initial roughness of the outer surface of the plate before drilling was measured and an average of 0.9 µm was determined. The figure shows that the roughness of all materials increased compared to the initial surface roughness value. The least effected material was the neat epoxy, as the maximum roughness can be seen at approximately 5 µm. The roughness of the glass/epoxy represents the highest among the materials and the maximum reached with a high feed rate and high drilling speed was approximately 9.5 µm. The roughness of the date/epoxy materials showed intermediate values compared to the others, as the roughness was approximately 6 µm in most cases. The relative increase in the inner surface of the composite compared to the neat epoxy is given in Figure 5.15b. The figure clearly shows that the increase in the inner surface roughness of the glass/epoxy is much higher than the date/epoxy composite.

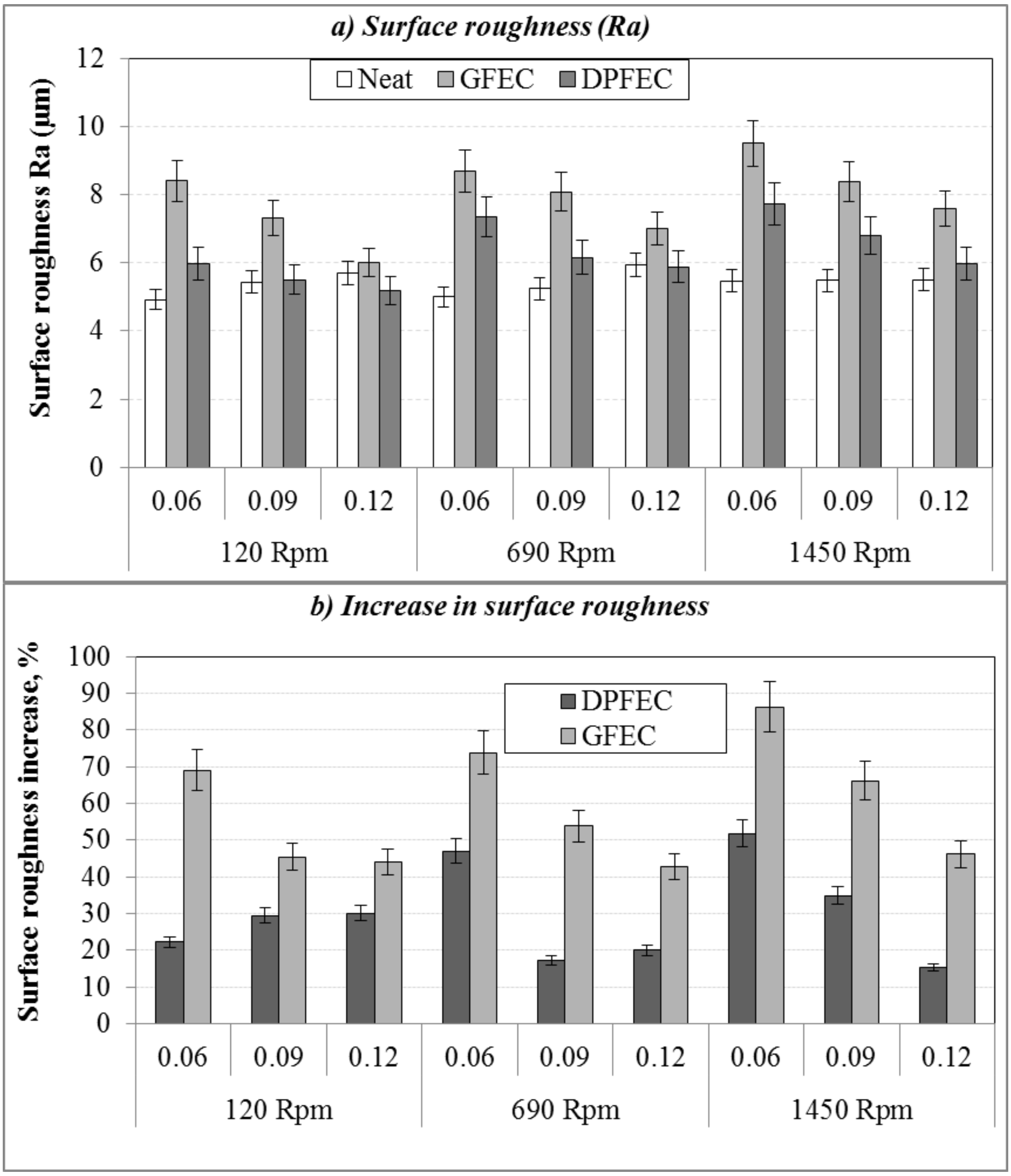

Figure 5.15: Surface roughness of all materials and roughness increase of composites compared to neat epoxy

It seems that the damage on the inner surface of the glass/epoxy is much high than on the date/epoxy. Figure 5.16 shows some micrographs of the inner surface for both glass/epoxy and date/epoxy composites. The figures show much damage to both surfaces of the composites, which could explain the increase in the roughness of the inner surface of the composites compared to neat epoxy. At higher magnifications (see Figure 5.16b and d), the ends of the glass fibres are not polished and this resulted in high roughness compared to date palm fibre, which showed a fracture on the surface, resulting in a smooth surface. However, according to Figure 5.16c, at the fibrous regions, the detachments could be the main reason for high roughness of the composites. In previous sections, it is suggested that the material removal mechanism could centriole the delamination and the hole accuracy. Similarly, the removal of abrasive glass fibres from the hole could result in pitting and an attack on the inner surface of the composites, which could result in higher roughness compared to date palm fibres. This could explain the current results. However, further investigation using different natural fibres and synthetic fibres could confirm these findings.

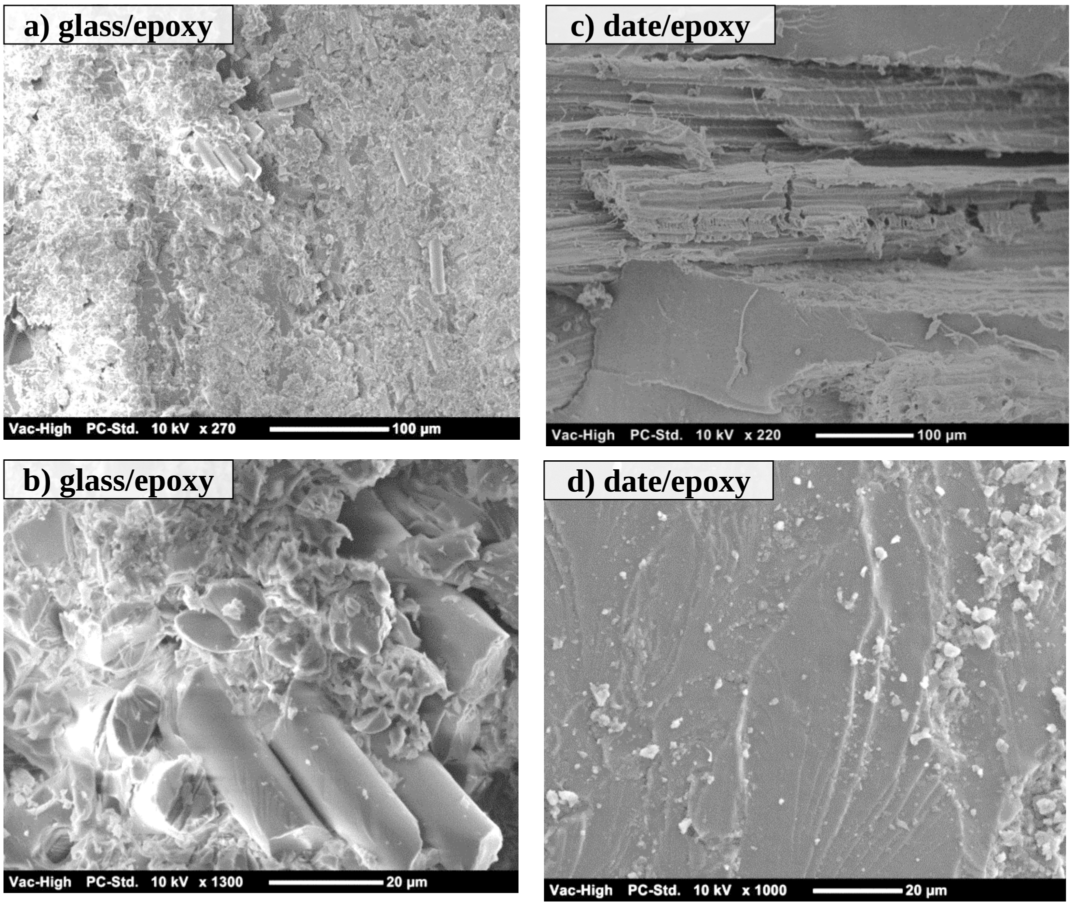

Figure 5.16: Micrographs of the inner surface of the composites drilled with a drill speed of 1,450 rpm, feed rate of 0.12 mm/rev and a 10 mm drill diameter

5.6 Influence of Machining on Power

The power combination of torque and thrust force was determined for all composites under different operating parameters and displayed in Figure 5.17. The effect of the operating parameters on the machining power is not clear at lower values, as the power is extremely low compared to those given at a higher drilling speed. With a 1,450 rpm drilling speed, an increase in the drill diameter increases the machining power for all materials. By comparing the three materials, Figure 5.18 shows the machining power of all materials at different feed rates and cutting speeds with a 10 mm drill diameter. The figure clearly shows that the machining power for neat epoxy is quite similar to that consumed for the date/epoxy composite. In other words, the addition of the date palm fibre had no effect on the cost of the drilling process compared to the neat epoxy. Conversely, the addition of glass fibre resulted in higher machining power compared to neat and date/epoxy materials. This presents an advantage in using natural fibres compared to synthetic fibres. At high operating parameter values for drill speed and feed rate, there was a reduction in the machining power by approximately 40 per cent when date palm fibre replaced glass fibre.

The low power required to machine the date/epoxy composites was due to low torque and thrust force needed in the drilling process, which was explained in the previous sections and in Chapter 4. In light of the above, it can be said that date palm fibres have several advantages compared to glass fibres for machinability, as they result in good quality holes with less machining power compared to glass fibres. However, further study is required to investigate and confirm these findings by considering different natural fibres and/or different matrices.

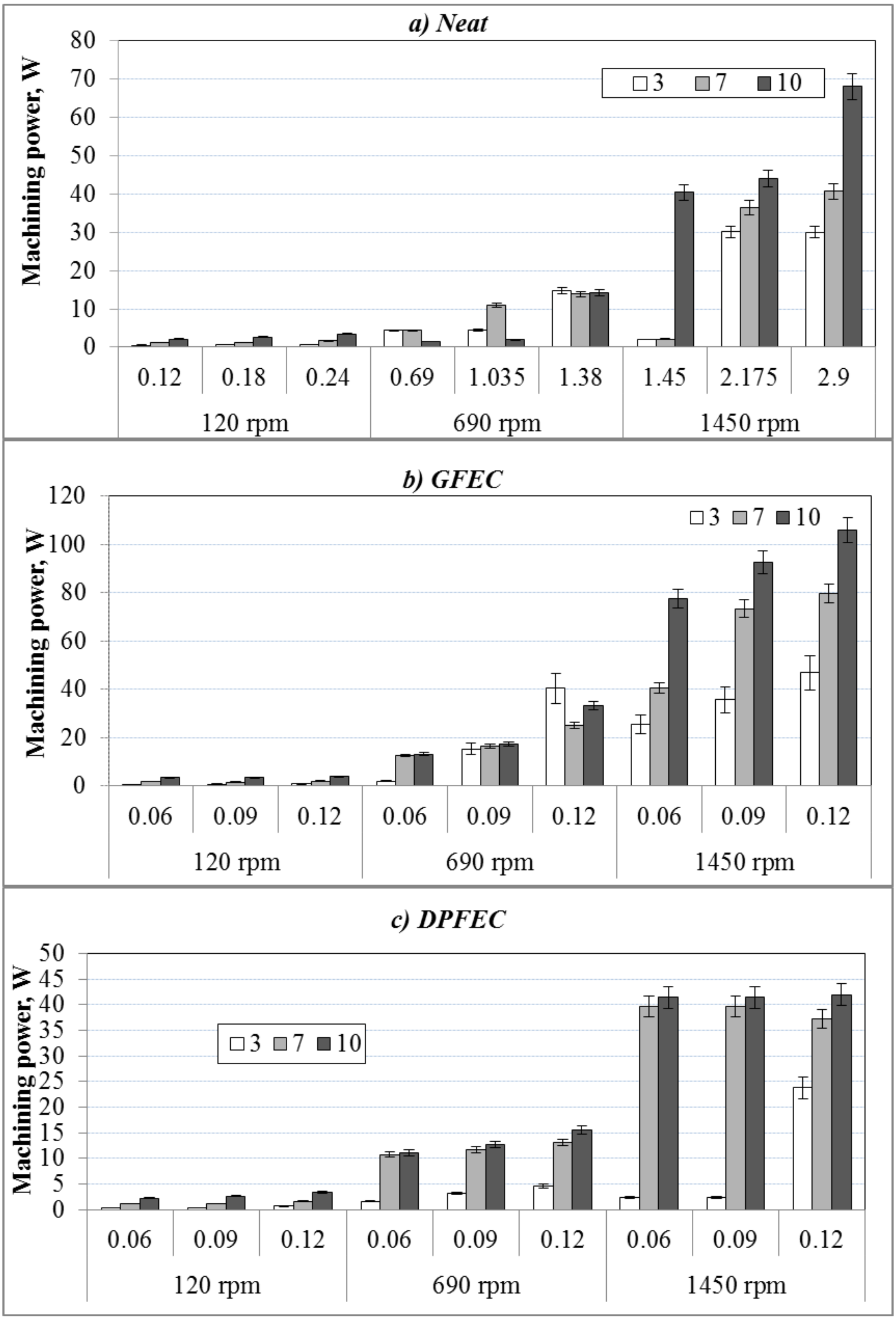

Figure 5.17: Machining power of all materials at different operating parameters

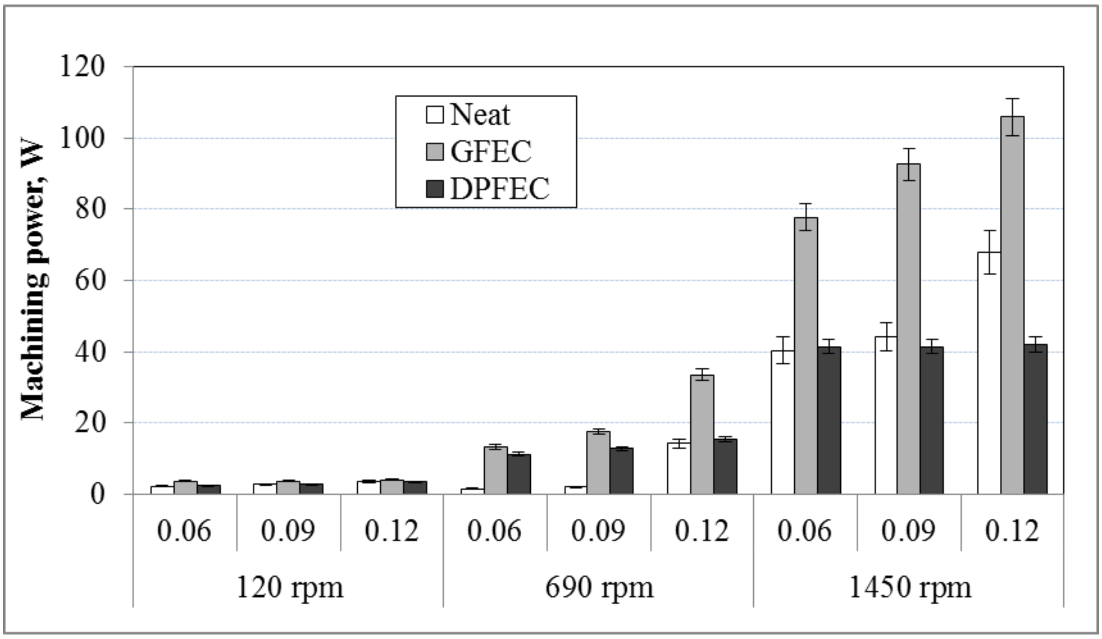

Figure 5.18: Machining power of all materials at different feed rates and cutting speeds with a 10 mm drill diameter

The ANOVA table in Table 5.4 indicates that the drilling speed controls the machining power for the composites, which contributes at approximately 57 per cent and is followed by the feed rate at 10.9 per cent and the drill diameter at 5.7 per cent. This confirms the above presented results.

Table 5.4: ANOVA analysis of operating parameters on machining power

Source	Sum of Squares	*df*	Mean Square	*F*	Sig.	Contribution (%)
Diameter	1,476.32	2	738.16	439,120.35	0.00	5.77
Speed	14,602.26	2	7,301.13	4,343,325.37	0.00	57.05
Feed	2,795.38	2	1,397.69	831,463.87	0.00	10.92
Diameter * Speed	3,224.73	4	806.18	479,585.69	0.00	12.60
Diameter * Feed	421.38	4	105.35	62,668.47	0.00	1.65
Speed * Feed	2,485.17	4	621.29	369,596.59	0.00	9.71
Diameter * Speed * Feed	588.43	8	73.55	43,756.29	0.00	2.30
Error	0.09	54	0.00			0.00
Total	25,593.77	80				100.00

5.7 Influence of Machining on the Drill Tool

The influence of the operating parameters and the drilling material on the tips and edges of the drill tool is an interesting and vast area of research in the machining sciences. The current research evaluates the influence of the drilling process for different materials on the HSS drill via SEM only. Figure 5.19 displays the micrographs of the 3 mm drill diameter after conducting 500 drill holes at 1,450 rpm and 0.12 mm/rev before and after cleaning. The tip of the drill seems to be affected significantly by the process of the glass fibres, as there was high distortion at the edges of the tips, especially before cleaning (see Figure 5.19a–c). After cleaning, the edges suffered from high abrasive wearing, as shown in Figure 4.19d and e. This confirms the suggestion given in the previous section (see Figure 4.12 and 4.16 in Chapter 4). Some of the deformed debris had adhered to the surface of the drill, which roughened the tool. This could explain the delamination and the hole accuracy findings, as rough surfaces may also result in abrasive wear at the edges of the hole. Further, there is fatigue loading at the edges, which has caused a fracture in some places (see Figure 5.19d and e).

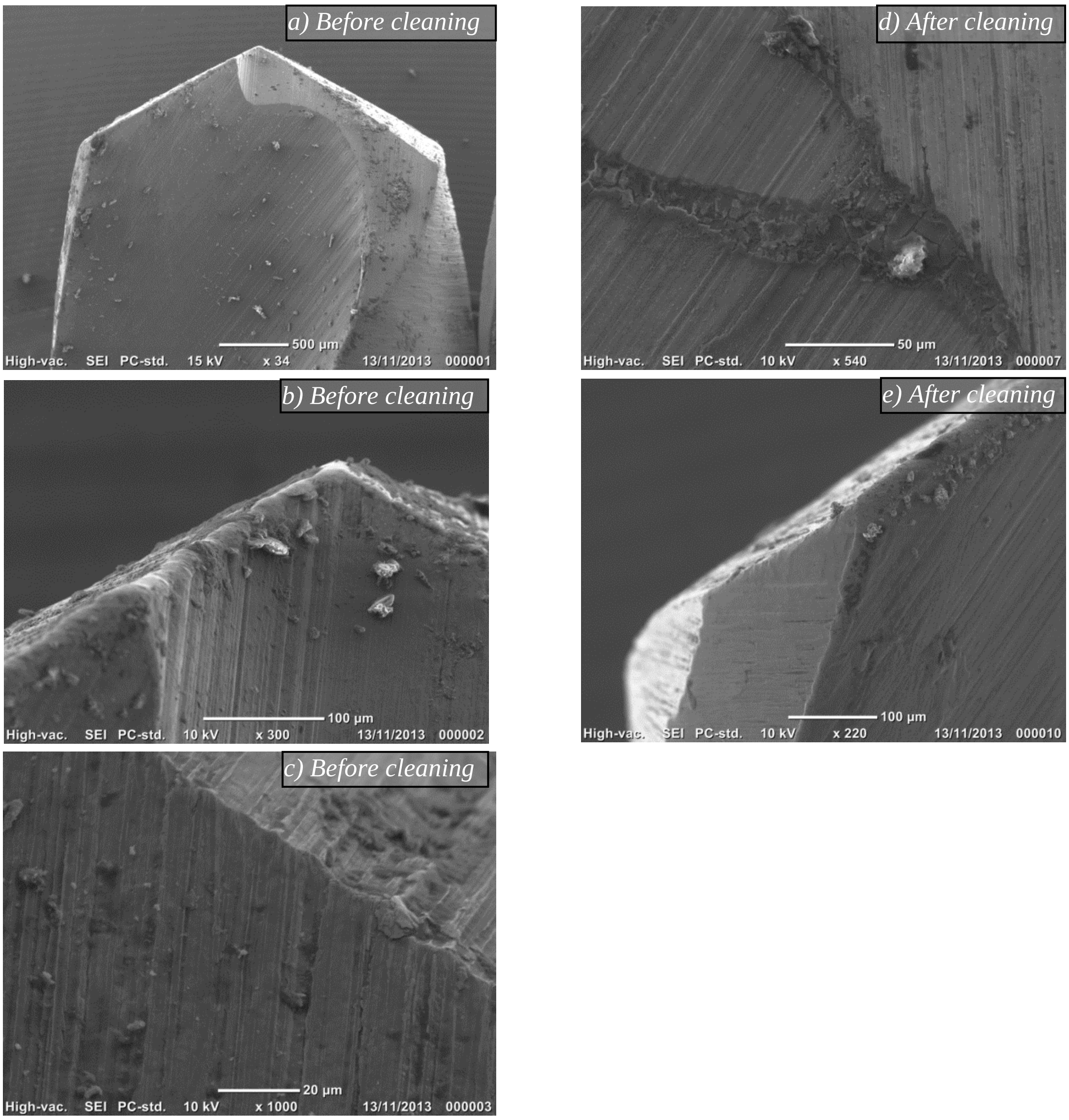

Figure 5.19: Micrographs of the HSS drill after glass/epoxy composites have been machined with a 3 mm drill diameter, 1,450 rpm drill speed and 0.12 mm/rev 500 times

The micrographs of the drill tool used for the date/epoxy drilling process are displayed in Figure 5.20. One can see that the damage on the tool is lesser than that seen in Figure 5.19. Although there is adhered materials on the surface of the drill (see Figure 5.20a–c), there is no damage on either the edges or the tip of the tool. After cleaning, the sharp edges of the tool can be seen and there is no sign of fracture of abrasive nature, as seen earlier in Figure 4.19.

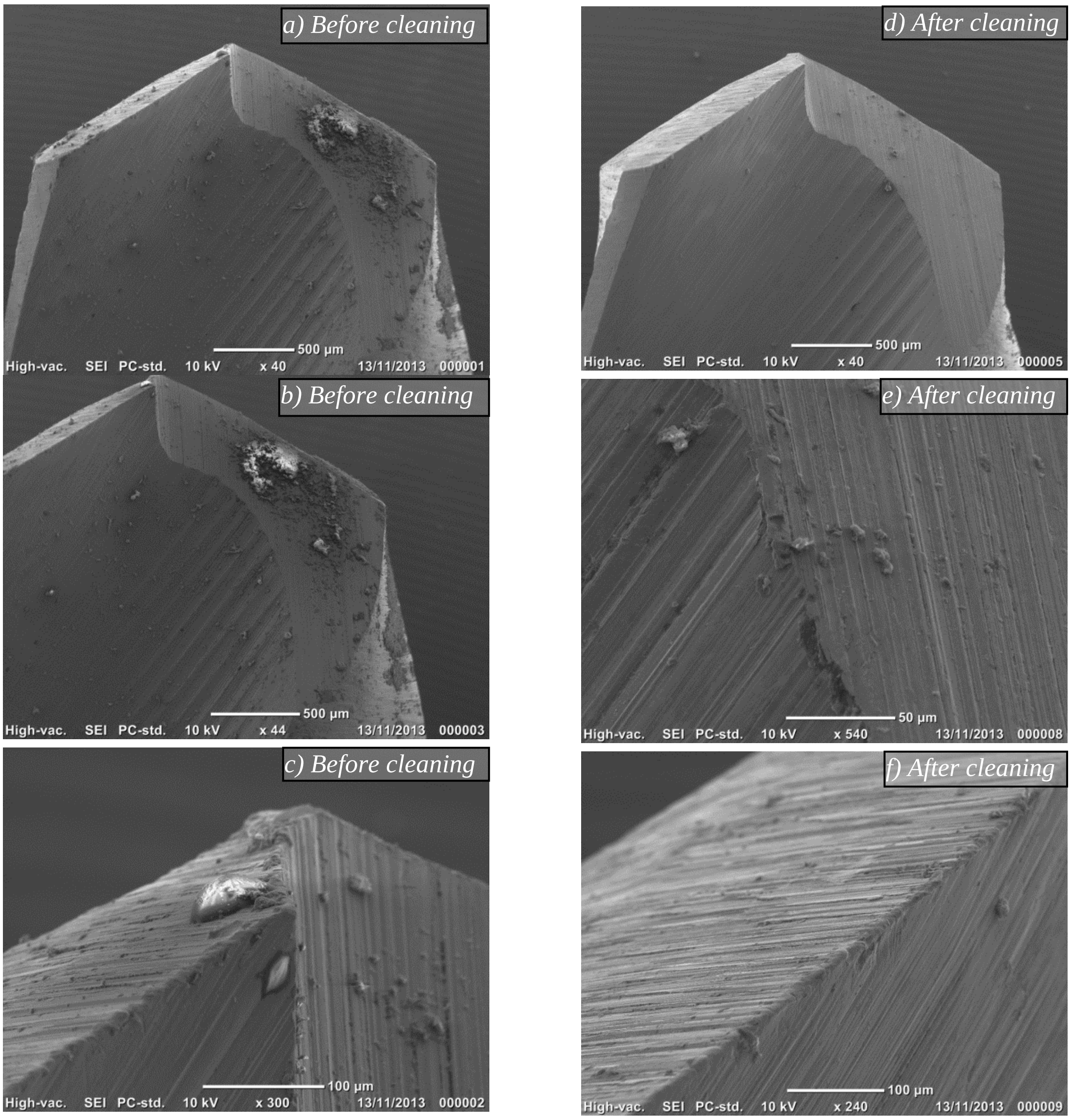

Figure 5.20: Micrographs of the HSS drill after date/epoxy composites have been machined with a 3 mm drill diameter, 1,450 rpm drill speed and 0.12 mm/rev 500 times

This is a promising result and is an advantage that can be added to the list of advantages for natural fibres. In other words, there is less wear to the drill tool when natural FRP composites are used instead of synthetic fibre/polymer composites. At a higher magnification and after clearing, Figure 5.20f shows that the tool is still in good condition and can be used further.

5.8 Summary of the Chapter

This chapter covers the machinability of neat epoxy, glass/epoxy and date/epoxy composites under different operating parameters. Operating parameters have a significant influence on most of the machinability measurements, such as hole accuracy, delamination and specific cutting pressure. In general, it can be said that higher operating parameter values for feed rate, drilling speed and drill diameter result in low quality holes. The main points of the chapters are summarised as follows:

- Hole accuracy is highly controlled by operating parameters, as an increase in drilling speed and feed rate resulted in high error percentage of hole accuracy for all materials. The addition of date palm fibres had less error percentage for hole accuracy compared to glass fibres, and this was mainly due to the abrasive nature of the glass fibres compared to the date palm fibres. Micrographs showed fragmentation and pull out of fibres for neat epoxy and glass/epoxy composites, respectively. Meanwhile, date/epoxy exhibited fragmentation at the edge of the holes, which was considered less damage compared to glass/epoxy.
- There was no remarkable effect from the operating parameters on the delamination factor of all materials. Conversely, the inner delamination factor of neat epoxy and date/epoxy composite was comparative, while the glass fibre showed high values of the delamination factor. This was due to the same reason as above, that is, the abrasive nature of the glass fibre. In addition, it was proposed that, during material removal, the glass debris acted as a third body, which, in turn, attacked the inner surface and the inner edge.

- The outer delamination factor was slightly influenced by the operating parameters, especially for the neat epoxy. For the composites, there was a slight reduction in the value of the delamination factor when the operating parameters increased to a higher level. There was not much difference in the delamination factor of all materials. In other words, both glass and date palm fibres had no remarkable effect on the outer delamination factor.
- The specific cutting pressure significantly reduced with an increase in the feed rate. However, there is no clear effect from the drilling speeds on the specific cutting pressure. The most influential parameter is the drill diameter, as there was a large increase in the specific cutting pressure with an increase in the drill diameter.
- The drilling process for all materials resulted in high roughness values for the inner surface of the holes. The highest roughness for the inner surface was recorded when the glass/epoxy was drilled. Nevertheless, the addition of the date palm fibres also contributed to an increase in surface roughness of the composites. However, there was less of an increase in the roughness of the inner surface with the addition of date palm fibres to the composite compared to glass fibres.
- Machining power was influenced by higher operating parameter values; however, for intermediate and low range values, there was not much difference in the machining power of all materials. Interestingly, the machining power for the date/epoxy composite was competitive when compared to the neat epoxy, which is a promising result for the use of date palm fibre from a machinability perspective.

CHAPTER 6: CONCLUSIONS AND RECOMMENDATIONS

6.1 Conclusion

The machinability of epoxy composites has been evaluated in the current study and two different types of fibres have been considered: synthetic (glass) and natural (date palm). Different operating parameters were used in the experiments. Moreover, the interfacial adhesion of the date palm and the epoxy was investigated using single fibre pull out testing. The main findings of this research are concluded in the following points:

- NaOH concentration influences the strength of the fibres significantly, as well as the interfacial adhesion of the fibre with the matrix. The lower the concentration of the NaOH displayed the lower the effect on the strength of the fibre and interfacial adhesion between the fibres and the matrix. Nevertheless, a higher concentration of NaOH (nine per cent) damaged the fibre and weakened it. Six per cent NaOH was found to be the optimum concentration, as it offers enhancement to the interfacial adhesion of the fibre with the matrix and less damage to the fibres, hence, more fibre strength. The interfacial adhesion property of the fibre with the matrix was controlled by the embedded length of the fibre into the matrix. The optimum fibre embedded length was found to be 10 mm, which can transfer the load from the matrix to the fibre. The lowest fibre critical length can be obtained at a lower fibre diameter and six per cent NaOH treatment. The critical length of the fibre in the matrix was highly controlled by the diameter and the treatment of the fibre (concentration of NaOH). A pull out mechanism was observed by SEM at low NaOH concentration treatment (three per cent). Conversely, there was a breakage of fibres at six per cent NaOH, indicating the high interfacial adhesion of the fibre with the matrix. Nevertheless, early breakage of the fibre was observed at a high NaOH concentration level of nine per cent, which was due to the weakening process that occurred on the fibre during the treatment process.

- The tensile properties of the epoxy were found to improve with the addition of either natural or synthetic fibres. However, glass fibres improved the tensile strength of the epoxy significantly compared to date palm fibres, even though glass fibres suffered from detachment and a pull out mechanism during loading conditions. The NaOH treatment greatly improved the load transmission from the epoxy to the fibres, as there was no sign of pull out of date palm fibre during the SEM observation.
- During the drilling process, regions were observed and classified as inner, intermediate and outer. The thrust and torque behaviour with the drilling time was divided based on these three regions for neat epoxy, glass/epoxy and date/epoxy composites. Peak values were observed in the intermediate regions in which shears occurred at a higher level with the thrust force. The peak region can be considered the steady state region, as less resistance to the material removal took place in the inlet and outlet regions. The presence of glass fibres in the epoxy composites assisted in reducing crack propagation at the inlet regions; however, it highly deteriorated the outlet region, as detachments and the decomposition mechanism were observed. For neat epoxy, cracks and fractures were the main damage features noticed. The presence of date palm fibres in the epoxy improved the machinability of the composites, as it required similar values of torque and thrust to that of neat epoxy, while glass fibres needed more power. Further, it assisted in reducing cracks in the inner and outer regions of the hole, even though pull out and detachments were observed. It is strongly recommended to observe the inner and outer regions of the hole, as those regions could initiate the failure of the designed components.
- Hole accuracy is highly controlled by the operating parameters, as an increase in the drilling speed and feed rate resulted in a high error percentage for hole accuracy for all materials. The addition of the date palm fibres had a lower error percentage for hole accuracy compared to glass fibres and this was

mainly due to the abrasive nature of the glass fibres compared to the date palm fibres. Micrographs showed fragmentation and pull out of fibres for neat epoxy and glass/epoxy composites, respectively. Meanwhile, date/epoxy exhibited fragmentation at the edge of the holes, which was considered less damage compared to glass/epoxy.

- For the inner delamination, there was no remarkable effect from the operating parameters on the delamination factor of all materials. Conversely, the inner delamination factor of neat epoxy and date/epoxy composites was comparative, while the glass fibre showed high values for the delamination factor. This was due to the same reason as above, that is, the abrasive nature of the glass fibre. In addition, it was proposed that, during material removal, the glass debris acted as a third body, which, in turn, attacked the inner surface and the inner edge.
- The outer delamination factor was slightly influenced by the operating parameters, especially for neat epoxy. For the composites, there was a slight reduction in the value of the delamination factor when the operating parameters increased to a higher level. There was not much difference in the delamination factor of all materials. In other words, both glass and date palm fibres had no remarkable effect on the outer delamination factor.
- The specific cutting pressure reduced significantly with an increase in the feed rate. However, there was no clear effect from the drilling speeds on the specific cutting pressure. The most influential parameter is the drill diameter, as there was a large increase in the specific cutting pressure with an increase in the drill diameter.
- The drilling process for all materials resulted in high roughness values for the inner surface of the holes. The highest roughness for the inner surface was recorded when the glass/epoxy was drilled. Nevertheless, the addition of the date palm fibres also contributed to an increase in surface roughness of the composites. However, there was less of an increase in roughness of the inner surface with the addition of date palm fibres to the composite compared to glass fibres.

- Machining power was influenced by higher operating parameter values; however, for intermediate and low range operating parameter values, there was not much difference in the machining power of all materials. Interestingly, the machining power for the date/epoxy composites was competitive when compared to neat epoxy, which is a promising result for the use of date palm fibre from a machinability perspective.

6.2 Recommendations

As the current research focused on the effect of date palm fibres on machinability of epoxy composites and was considered an initiator for future work on different materials, some recommendations can be given to assist other researchers in their work. These are as follows:

- It is highly recommended that interfacial adhesion of the fibre with the matrix is studied before conducting the machining experiments, as it assists in understanding some of the damage features related to delamination and hole accuracy.
- Considering different materials may help to establish a good database to study the correlation between the mechanical and machinability of such materials.
- A comprehensive study on cost effectiveness could be conducted to evaluate the influence of replacing natural fibres with synthetic fibres. Such a study will help to motivate industries to take further steps towards using such sustainable reinforcements.
- The tool geometry and the damages on the tool can be observed using large SEM machine, which will highly contribute to understanding the wear occur on the tool during the drilling process. This will assist in explain some of the phenomenon took place on the surfaces of the holes since the drilling is the response of the surfaces of both tool and the materials.

REFERENCES

ABDELBARY, A., ABOUELWAFA, M. N., EL FAHHAM, I. M. & HAMDY, A. H. The effect of surface defects on the wear of Nylon66 under dry and water lubricated sliding. *Tribology International*.

ABDUL KHALIL, H. P. S., FIROOZIAN, P., BAKARE, I. O., AKIL, H. M. & NOOR, A. M. 2010. Exploring biomass based carbon black as filler in epoxy composites: Flexural and thermal properties. *Materials & Design,* 31**,** 3419-3425.

ADAM KHAN, M. & SENTHIL KUMAR, A. 2011. Machinability of glass fibre reinforced plastic (GFRP) composite using alumina-based ceramic cutting tools. *Journal of Manufacturing Processes,* 13**,** 67-73.

AL-ZUBAIDY, H., ZHAO, X.-L. & AL-MIHAIDI, R. 2011. Mechanical Behaviour of Normal Modulus Carbon Fibre Reinforced Polymer (CFRP) and Epoxy under Impact Tensile Loads. *Procedia Engineering,* 10**,** 2453-2458.

ALAM, K., MITROFANOV, A. V. & SILBERSCHMIDT, V. V. 2011. Experimental investigations of forces and torque in conventional and ultrasonically-assisted drilling of cortical bone. *Medical Engineering & Physics*, 33**,** 234-239.

ALAWAR, A., HAMED, A. M. & AL-KAABI, K. 2009. Characterization of treated date palm tree fiber as composite reinforcement. *Composites Part B: Engineering,* 40**,** 601-606.

ALSAEED, T., YOUSIF, B. & KU, H. 2013a. A review on the mechanical properties and machinability of natural fibre reinforced composites. *International Journal of Precision Technology,* 3**,** 152-182.

ALSAEED, T., YOUSIF, B. F. & KU, H. 2013b. The potential of using date palm fibres as reinforcement for polymeric composites. *Materials and Design,* 43**,** 177-184.

ANUAR, H. & ZURAIDA, A. 2011. Improvement in mechanical properties of reinforced thermoplastic elastomer composite with kenaf bast fibre. *Composites Part B: Engineering,* 42**,** 462-465.

ARIB, R. M. N., SAPUAN, S. M., AHMAD, M. M. H. M., PARIDAH, M. T. & ZAMAN, H. M. D. K. 2006. Mechanical properties of pineapple leaf fibre reinforced polypropylene composites. *Materials & Design,* 27**,** 391-396.

ARMAREGO, E. J. A. & BROWN, R. H. 1969. *The machining of metals,* Prentice-Hall.

ARRAKHIZ, F. Z., EL ACHABY, M., KAKOU, A. C., VAUDREUIL, S., BENMOUSSA, K., BOUHFID, R., FASSI-FEHRI, O. & QAISS, A. 2012. Mechanical properties of high density polyethylene reinforced with chemically modified coir fibers: Impact of chemical treatments. *Materials & Design,* 37**,** 379-383.

ATHIJAYAMANI, A., THIRUCHITRAMBALAM, M., NATARAJAN, U. & PAZHANIVEL, B. 2010. Influence of Alkali-Treated Fibers on the Mechanical Properties and Machinability of Roselle and Sisal Fiber Hybrid Polyester Composite. *Polymer Composites,* 31**,** 723-731.

AZIZ, S. H. & ANSELL, M. P. 2004. The effect of alkalization and fibre alignment on the mechanical and thermal properties of kenaf and hemp bast fibre composites: part 2 – cashew nut shell liquid matrix. *Composites Science and Technology,* 64, 1231-1238.

AZMI, A. I. 2012. *Machinability Study of Fibre-reinforced Polymer Matrix Composites.* Mechanical Engineering)--University of Auckland.

AZWA, Z. N., YOUSIF, B. F., MANALO, A. C. & KARUNASENA, W. 2013. A review on the degradability of polymeric composites based on natural fibres. *Materials & Design,* 47, 424-442.

BAGWELL, R. M. & WETHERHOLD, R. C. 2005. Fiber pullout behavior and impact toughness of short shaped copper fibers in thermoset matrices. *Composites Part A: Applied Science and Manufacturing,* 36, 683-690.

BAJPAI, P. K., SINGH, I. & MADAAN, J. 2013a. Frictional and adhesive wear performance of natural fibre reinforced polypropylene composites. *Proceedings of the Institution of Mechanical Engineers Part J-Journal of Engineering Tribology,* 227, 385-392.

BAJPAI, P. K., SINGH, I. & MADAAN, J. 2013b. Tribological behavior of natural fiber reinforced PLA composites. *Wear,* 297, 829-840.

BAKRY, M., MOUSA, M. O. & ALI, W. Y. 2013. Friction and wear of friction composites reinforced by natural fibres. *Materialwissenschaft Und Werkstofftechnik,* 44, 21-28.

BASU, G., ROY, A. N., SATAPATHY, K. K., ABBAS, S. M. J., MISHRA, L. & CHAKRABORTY, R. 2012. Potentiality for value-added technical use of Indian sisal. *Industrial Crops and Products,* 36, 33-40.

BEG, M. D. H. & PICKERING, K. L. 2008. Mechanical performance of Kraft fibre reinforced polypropylene composites: Influence of fibre length, fibre beating and hygrothermal ageing. *Composites Part A: Applied Science and Manufacturing,* 39, 1748-1755.

BEN DIFALLAH, B., KHARRAT, M., DAMMAK, M. & MONTEIL, G. 2012. Mechanical and tribological response of ABS polymer matrix filled with graphite powder. *Materials & Design,* 34, 782-787.

BHUSHAN, B. 2013. *Principles and applications of tribology,* John Wiley & Sons.

BILBA, K., ARSENE, M. A. & OUENSANGA, A. 2003. Sugar cane bagasse fibre reinforced cement composites. Part I. Influence of the botanical components of bagasse on the setting of bagasse/cement composite. *Cement and Concrete Composites,* 25, 91-96.

BLEDZKI, A. K. & GASSAN, J. 1999. Composites reinforced with cellulose based fibres. *Progress in Polymer Science,* 24, 221-274.

BONNY, K., DE BAETS, P., PEREZ, Y., VLEUGELS, J. & LAUWERS, B. 2010. Friction and wear characteristics of WC–Co cemented carbides in dry reciprocating sliding contact. *Wear,* 268, 1504-1517.

BOUAFIF, H., KOUBAA, A., PERRÉ, P. & CLOUTIER, A. 2009. Effects of fiber characteristics on the physical and mechanical properties of wood plastic composites. *Composites Part A: Applied Science and Manufacturing,* 40, 1975-1981.

BRAHIM, S. B. & CHEIKH, R. B. 2007. Influence of fibre orientation and volume fraction on the tensile properties of unidirectional Alfa-polyester composite. *Composites Science and Technology,* 67, 140-147.

BRAHMAKUMAR, M., PAVITHRAN, C. & PILLAI, R. M. 2005. Coconut fibre reinforced polyethylene composites: effect of natural waxy surface layer of the fibre on fibre/matrix interfacial bonding and strength of composites. *Composites Science and Technology,* 65, 563-569.

BRAS, J., HASSAN, M. L., BRUZESSE, C., HASSAN, E. A., EL-WAKIL, N. A. & DUFRESNE, A. 2010. Mechanical, barrier, and biodegradability properties of bagasse cellulose whiskers reinforced natural rubber nanocomposites. *Industrial Crops and Products,* 32, 627-633.

CAMPOS RUBIO, J. C., SILVA, L. J. D., LEITE, W. D. O., PANZERA, T. H., FILHO, S. L. M. R. & DAVIM, J. P. 2013. Investigations on the drilling process of unreinforced and reinforced polyamides using Taguchi method. *Composites Part B: Engineering,* 55, 338-344.

CANTERO, G., ARBELAIZ, A., LLANO-PONTE, R. & MONDRAGON, I. 2003. Effects of fibre treatment on wettability and mechanical behaviour of flax/polypropylene composites. *Composites Science and Technology,* 63, 1247-1254.

CAPELLO, E. 2004. Workpiece damping and its effect on delamination damage in drilling thin composite laminates. *Journal of Materials Processing Technology,* 148, 186-195.

CHIN, C. W. & YOUSIF, B. F. 2009. Potential of kenaf fibres as reinforcement for tribological applications. *Wear,* 267, 1550-1557.

CIFTCI, I., TURKER, M. & SEKER, U. 2004. Evaluation of tool wear when machining SiCp-reinforced Al-2014 alloy matrix composites. *Materials & Design,* 25, 251-255.

COLOM, X., CARRASCO, F., PAGÈS, P. & CANAVATE, J. 2003. Effects of different treatments on the interface of HDPE/lignocellulosic fiber composites. *Composites Science and Technology,* 63, 161-169.

COUTINHO, F. M. B. & COSTA, T. H. S. 1999. Performance of polypropylene-wood fiber composites. *Polymer Testing,* 18, 581-587.

DAVIM, J. P., CLEMENTE, V. C. & SILVA, S. 2008. Drilling investigation of MDF (medium density fibreboard). *Journal of Materials Processing Technology,* 203, 537-541.

DAVIM, J. P., GAITONDE, V. N. & KARNIK, S. R. 2011. Erratum: Machinability evaluation in unreinforced and reinforced PEEK composites using response surface models (Journal of Thermoplastic Composite Materials (2010) 23:1 DOI: 10.1177/0892705709093503). *Journal of Thermoplastic Composite Materials,* 24, 299.

DAVIM, J. P. & REIS, P. 2004. Machinability study on composite (polyetheretherketone reinforced with 30% glass fibre-PEEK GF 30) using polycrystalline diamond (PCD) and cemented carbide (K20) tools. *International Journal of Advanced Manufacturing Technology,* 23, 412-418.

DAVIM, J. P., REIS, P. & ANTÓNIO, C. C. 2004. A study on milling of glass fiber reinforced plastics manufactured by hand-lay up using statistical analysis (ANOVA). *Composite Structures,* 64, 493-500.

DAVIM, J. P., RUBIO, J. C. & ABRAO, A. M. 2007. A novel approach based on digital image analysis to evaluate the delamination factor after drilling composite laminates. *Composites Science and Technology,* 67**,** 1939-1945.

DE ALBUQUERQUE, A. C., JOSEPH, K., HECKER DE CARVALHO, L. & D'ALMEIDA, J. R. M. 2000. Effect of wettability and ageing conditions on the physical and mechanical properties of uniaxially oriented jute-roving-reinforced polyester composites. *Composites Science and Technology,* 60**,** 833-844.

DE ROSA, I. M., KENNY, J. M., MANIRUZZAMAN, M., MONIRUZZAMAN, M., MONTI, M., PUGLIA, D., SANTULLI, C. & SARASINI, F. 2011. Effect of chemical treatments on the mechanical and thermal behaviour of okra (Abelmoschus esculentus) fibres. *Composites Science and Technology,* 71**,** 246-254.

DEMIR, H., ATIKLER, U., BALKÖSE, D. & TıHMıNLıOĞLU, F. 2006. The effect of fiber surface treatments on the tensile and water sorption properties of polypropylene–luffa fiber composites. *Composites Part A: Applied Science and Manufacturing,* 37**,** 447-456.

DUC, A. L., VERGNES, B. & BUDTOVA, T. 2011. Polypropylene/natural fibres composites: Analysis of fibre dimensions after compounding and observations of fibre rupture by rheo-optics. *Composites Part A: Applied Science and Manufacturing,* 42**,** 1727-1737.

EDEEROZEY, A. M. M., AKIL, H. M., AZHAR, A. B. & ARIFFIN, M. I. Z. 2007. Chemical modification of kenaf fibers. *Materials Letters,* 61**,** 2023-2025.

EICHHORN, S. J., BAILLIE, C. A., ZAFEIROPOULOS, N., MWAIKAMBO, L. Y., ANSELL, M. P., DUFRESNE, A., ENTWISTLE, K. M., HERRERA-FRANCO, P. J., ESCAMILLA, G. C., GROOM, L., HUGHES, M., HILL, C., RIALS, T. G. & WILD, P. M. 2001. Current international research into cellulosic fibres and composites. *Journal of Materials Science,* 36**,** 2107-2131.

EL-SONBATY, I., KHASHABA, U. A. & MACHALY, T. Factors affecting the machinability of GFR/epoxy composites. *Composite Structures,* 63**,** 329-338.

EL-SONBATY, I., KHASHABA, U. A. & MACHALY, T. 2004. Factors affecting the machinability of GFR/epoxy composites. *Composite Structures,* 63**,** 329-338.

FARUK, O., BLEDZKI, A. K., FINK, H.-P. & SAIN, M. 2012. Biocomposites Reinforced with Natural Fibers: 2000-2010. *Progress in Polymer Science*.

FEIH, S. & MOURITZ, A. P. 2012. Tensile properties of carbon fibres and carbon fibre–polymer composites in fire. *Composites Part A: Applied Science and Manufacturing,* 43**,** 765-772.

FELIX, J. M. & GATENHOLM, P. 1991a. The nature of adhesion in composites of modified cellulose fibers and polypropylene. *Journal of Applied Polymer Science,* 42**,** 609-620.

FELIX, J. M. & GATENHOLM, P. 1991b. Nature of adhesion in composites of modified cellulose fibers and polypropylene. *Journal of Applied Polymer Science,* 42**,** 609-620.

FOLKES, M. & WONG, W. 1987. Determination of interfacial shear strength in fibre-reinforced thermoplastic composites. *Polymer,* 28**,** 1309-1314.

GAITONDE, V. N., KARNIK, S. R., RUBIO, J. C., CORREIA, A. E., ABRÃO, A. M. & DAVIM, J. P. 2008. Analysis of parametric influence on delamination in high-speed drilling of carbon fiber reinforced plastic composites. *Journal of Materials Processing Technology,* 203**,** 431-438.

GHIDOSSI, P., MANSORI, M. E. & PIERRON, F. 2006. Influence of specimen preparation by machining on the failure of polymer matrix off-axis tensile coupons. *Composites Science and Technology,* 66**,** 1857-1872.

GRANDE, C. & TORRES, F. G. 2005. Investigation of fiber organization and damage during single screw extrusion of natural fiber reinforced thermoplastics. *Advances in Polymer Technology*, 24**,** 145-156.

HAQUE, M. M., HASAN, M., ISLAM, M. S. & ALI, M. E. 2009. Physico-mechanical properties of chemically treated palm and coir fiber reinforced polypropylene composites. *Bioresource Technology,* 100**,** 4903-4906.

HARPER, L. T., TURNER, T. A., WARRIOR, N. A. & RUDD, C. D. 2006. Characterisation of random carbon fibre composites from a directed fibre preforming process: The effect of fibre length. *Composites Part A: Applied Science and Manufacturing,* 37**,** 1863-1878.

HEITZMANN, M. T., VEIDT, M., NG, C. T., LINDENBERGER, B., HOU, M., TRUSS, R. & LIEW, C. K. 2013. Single-Plant Biocomposite from Ricinus Communis: Preparation, Properties and Environmental Performance. *Journal of Polymers and the Environment,* 21**,** 366-374.

HEPWORTH, D. G., VINCENT, J. F. V., JERONIMIDIS, G. & BRUCE, D. M. 2000. The penetration of epoxy resin into plant fibre cell walls increases the stiffness of plant fibre composites. *Composites Part A: Applied Science and Manufacturing,* 31**,** 599-601.

HERRERA-FRANCO, P. & VALADEZ-GONZALEZ, A. 2005. A study of the mechanical properties of short natural-fiber reinforced composites. *Composites Part B: Engineering,* 36**,** 597-608.

HERRERA-FRANCO, P. J. & VALADEZ-GONZÁLEZ, A. 2004. Mechanical properties of continuous natural fibre-reinforced polymer composites. *Composites Part A: Applied Science and Manufacturing*, 35**,** 339-345.

HOCHENG, H. & TSAO, C. C. 2003. Comprehensive analysis of delamination in drilling of composite materials with various drill bits. *Journal of Materials Processing Technology,* 140**,** 335-339.

HOCHENG, H. & TSAO, C. C. 2006. Effects of special drill bits on drilling-induced delamination of composite materials. *International Journal of Machine Tools and Manufacture,* 46**,** 1403-1416.

HU, R. & LIM, J.-K. 2007. Fabrication and Mechanical Properties of Completely Biodegradable Hemp Fiber Reinforced Polylactic Acid Composites. *Journal of Composite Materials,* 41**,** 1655-1669.

HUNG, N. P., VENKATESH, V. C. & LOH, N. L. 1998. Cutting tools for metal matrix composites.

INOUE, H., AOYAMA, E., HIROGAKI, T., OGAWA, K., MATUSHITA, H., KITAHARA, Y. & KATAYAMA, T. 1997. Influence of tool wear on internal damage in small diameter drilling in GFRP. *Composite Structures,* 39**,** 55-62.

JACOB, M., THOMAS, S. & VARUGHESE, K. T. 2004. Mechanical properties of sisal/oil palm hybrid fiber reinforced natural rubber composites. *Composites Science and Technology,* 64, 955-965.

JAIN, V. K., CHOUDHURY, S. K. & RAMESH, K. M. 2002. On the machining of alumina and glass. *International Journal of Machine Tools and Manufacture,* 42, 1269-1276.

JAWAID, M. & ABDUL KHALIL, H. P. S. 2011. Cellulosic/synthetic fibre reinforced polymer hybrid composites: A review. *Carbohydrate Polymers,* 86, 1-18.

JAYABAL, S., NATARAJAN, U. & SEKAR, U. 2011. Regression modeling and optimization of machinability behavior of glass-coir-polyester hybrid composite using factorial design methodology. *International Journal of Advanced Manufacturing Technology,* 55, 263-273.

JOSEPH, P. V., JOSEPH, K. & THOMAS, S. 1999. Effect of processing variables on the mechanical properties of sisal-fiber-reinforced polypropylene composites. *Composites Science and Technology,* 59, 1625-1640.

JOSHI, S. V., DRZAL, L. T., MOHANTY, A. K. & ARORA, S. 2004. Are natural fiber composites environmentally superior to glass fiber reinforced composites? *Composites Part A: Applied Science and Manufacturing,* 35, 371-376.

KABIR, M. M., WANG, H., LAU, K. T., CARDONA, F. & ARAVINTHAN, T. 2011. Mechanical properties of chemically-treated hemp fibre reinforced sandwich composites. *Composites Part B: Engineering,* In Press, Corrected Proof.

KANCHANOMAI, C., RATTANANON, S. & SONI, M. 2005. Effects of loading rate on fracture behavior and mechanism of thermoset epoxy resin. *Polymer Testing,* 24, 886-892.

KARNIK, S., GAITONDE, V., RUBIO, J. C., CORREIA, A. E., ABRÃO, A. & DAVIM, J. P. 2008. Delamination analysis in high speed drilling of carbon fiber reinforced plastics (CFRP) using artificial neural network model. *Materials & Design,* 29, 1768-1776.

KHASHABA, U. A., EL-SONBATY, I. A., SELMY, A. I. & MEGAHED, A. A. 2010a. Machinability analysis in drilling woven GFR/epoxy composites: Part I – Effect of machining parameters. *Composites Part A: Applied Science and Manufacturing,* 41, 391-400.

KHASHABA, U. A., EL-SONBATY, I. A., SELMY, A. I. & MEGAHED, A. A. 2010b. Machinability analysis in drilling woven GFR/epoxy composites: Part II – Effect of drill wear. *Composites Part A: Applied Science and Manufacturing,* 41, 1130-1137.

KHONDKER, O. A., ISHIAKU, U. S., NAKAI, A. & HAMADA, H. 2005. Fabrication mechanical properties of unidirectional jute/PP composites using jute yarns by film stacking method. *Journal of Polymers and the Environment,* 13, 115-126.

KINI, M. V. & CHINCHOLKAR, A. M. 2010. Effect of machining parameters on surface roughness and material removal rate in finish turning of ±30° glass fibre reinforced polymer pipes. *Materials & Design,* 31, 3590-3598.

KRISHNAMOORTHY, A., RAJENDRA BOOPATHY, S., PALANIKUMAR, K. & PAULO DAVIM, J. 2012. Application of grey fuzzy logic for the optimization of drilling parameters for CFRP composites with multiple performance characteristics. *Measurement,* 45**,** 1286-1296.

KRISHNARAJ, V., PRABUKARTHI, A., RAMANATHAN, A., ELANGHOVAN, N., SENTHIL KUMAR, M., ZITOUNE, R. & DAVIM, J. P. 2012. Optimization of machining parameters at high speed drilling of carbon fiber reinforced plastic (CFRP) laminates. *Composites Part B: Engineering,* 43**,** 1791-1799.

KRISHNAVENI, K., SANKARA NARAYANAN, T. S. N. & SESHADRI, S. K. 2005. Electroless Ni–B coatings: preparation and evaluation of hardness and wear resistance. *Surface and Coatings Technology,* 190**,** 115-121.

KU, H., WANG, H., PATTARACHAIYAKOOP, N. & TRADA, M. 2011. A review on the tensile properties of natural fiber reinforced polymer composites. *Composites Part B: Engineering,* 42**,** 856-873.

KWON, H. J., SUNTHORNVARABHAS, J., PARK, J. W., LEE, J. H., KIM, H. J., PIYACHOMKWAN, K., SRIROTH, K. & CHO, D. 2014. Tensile properties of kenaf fiber and corn husk flour reinforced poly(lactic acid) hybrid bio-composites: Role of aspect ratio of natural fibers. *Composites Part B: Engineering,* 56**,** 232-237.

L.J. BROUTMAN, M. O. T. F.-P. M. I. S., INTERFACES IN COMPOSITES, ASTM STP 452 (2ND EDITION), AMERICAN SOCIETY FOR TESTING AND MATERIALS, PHILADELPHIA, PA (1969), P. 2741. .

LE TROËDEC, M., RACHINI, A., PEYRATOUT, C., ROSSIGNOL, S., MAX, E., KAFTAN, O., FERY, A. & SMITH, A. 2011. Influence of chemical treatments on adhesion properties of hemp fibres. *Journal of Colloid and Interface Science,* 356**,** 303-310.

LE TROEDEC, M., SEDAN, D., PEYRATOUT, C., BONNET, J. P., SMITH, A., GUINEBRETIERE, R., GLOAGUEN, V. & KRAUSZ, P. 2008. Influence of various chemical treatments on the composition and structure of hemp fibres. *Composites Part A: Applied Science and Manufacturing,* 39**,** 514-522.

LEI, W., LEI, W.-G. & REN, C. 2006. Effect of volume fraction of ramie cloth on physical and mechanical properties of ramie cloth/UP resin composite. *Transactions of Nonferrous Metals Society of China,* 16, Supplement 2**,** s474-s477.

LI, X., PANIGRAHI, S. & TABIL, L. 2009. A study on flax fiber-reinforced polyethylene biocomposites. *Applied Engineering in Agriculture,* 25**,** 525.

LIU, D., TANG, Y. & CONG, W. L. 2012. A review of mechanical drilling for composite laminates. *Composite Structures,* 94**,** 1265-1279.

LIU, W., DRZAL, L. T., MOHANTY, A. K. & MISRA, M. 2007. Influence of processing methods and fiber length on physical properties of kenaf fiber reinforced soy based biocomposites. *Composites Part B: Engineering,* 38**,** 352-359.

MA, X., YU, J. & KENNEDY, J. F. 2005. Studies on the properties of natural fibers-reinforced thermoplastic starch composites. *Carbohydrate Polymers,* 62**,** 19-24.

MADSEN, B. & LILHOLT, H. 2003. Physical and mechanical properties of unidirectional plant fibre composites—an evaluation of the influence of porosity. *Composites Science and Technology,* 63, 1265-1272.

MALLICK, P. K. 2008. *Fiber-reinforced composites: materials, manufacturing, and design,* CRC Press.

MAMIDI, S. V. S. 2012. *Manufacturing an involute spline cutting tool on wire EDM using SolidWorks and ESPRIT.* CALIFORNIA STATE UNIVERSITY.

MATA, F., GAITONDE, V. N., KARNIK, S. R. & DAVIM, J. P. 2009. Influence of cutting conditions on machinability aspects of PEEK, PEEK CF 30 and PEEK GF 30 composites using PCD tools. *Journal of Materials Processing Technology,* 209, 1980-1987.

MEDINA, L., SCHLEDJEWSKI, R. & SCHLARB, A. K. 2009. Process related mechanical properties of press molded natural fiber reinforced polymers. *Composites Science and Technology,* 69, 1404-1411.

MERLINI, C., SOLDI, V. & BARRA, G. M. O. 2011. Influence of fiber surface treatment and length on physico-chemical properties of short random banana fiber-reinforced castor oil polyurethane composites. *Polymer Testing,* 30, 833-840.

MIGNEAULT, S., KOUBAA, A., ERCHIQUI, F., CHAALA, A., ENGLUND, K. & WOLCOTT, M. P. 2009. Effects of processing method and fiber size on the structure and properties of wood–plastic composites. *Composites Part A: Applied Science and Manufacturing,* 40, 80-85.

MIZOBUCHI, A., TAKAGI, H., SATO, T. & HINO, J. Drilling machinability of resin-less green composites reinforced by bamboo fiber. 2008 Algarve. 185-194.

MOHAN, N. S., RAMACHANDRA, A. & KULKARNI, S. M. 2005. Influence of process parameters on cutting force and torque during drilling of glass–fiber polyester reinforced composites. *Composite Structures,* 71, 407-413.

MÜLLER, C. M. O., LAURINDO, J. B. & YAMASHITA, F. 2009. Effect of cellulose fibers addition on the mechanical properties and water vapor barrier of starch-based films. *Food Hydrocolloids,* 23, 1328-1333.

MYLSAMY, K. & RAJENDRAN, I. 2011. Influence of alkali treatment and fibre length on mechanical properties of short Agave fibre reinforced epoxy composites. *Materials & Design,* 32, 4629-4640.

NAGARAJAN, V. A., SELWIN RAJADURAI, J. & ANNIL KUMAR, T. 2012. A digital image analysis to evaluate delamination factor for wind turbine composite laminate blade. *Composites Part B: Engineering,* 43, 3153-3159.

NAM, T. H., OGIHARA, S., TUNG, N. H. & KOBAYASHI, S. 2011. Effect of alkali treatment on interfacial and mechanical properties of coir fiber reinforced poly(butylene succinate) biodegradable composites. *Composites Part B: Engineering,* 42, 1648-1656.

NIRMAL, U., LOW, K. & HASHIM, J. 2012. On the effect of abrasiveness to process equipment using betelnut and glass fibres reinforced polyester composites. *Wear,* 290, 32-40.

NIRMAL, U., SINGH, N., HASHIM, J., LAU, S. T. W. & JAMIL, N. 2011a. On the effect of different polymer matrix and fibre treatment on single fibre pullout test using betelnut fibres. *Materials & Design,* 32, 2717-2726.

NIRMAL, U., SINGH, N., HASHIM, J., LAU, S. T. W. & JAMIL, N. 2011b. On the effect of different polymer matrix and fibre treatment on single fibre pullout test using betelnut fibres. *Materials & Design,* 32, 2717-2726.

NIRMAL, U., YOUSIF, B. F., RILLING, D. & BREVERN, P. V. 2010. Effect of betelnut fibres treatment and contact conditions on adhesive wear and frictional performance of polyester composites. *Wear,* 268, 1354-1370.

OCHI, S. 2008. Mechanical properties of kenaf fibers and kenaf/PLA composites. *Mechanics of Materials,* 40, 446-452.

ODA, S., LEOMAR FERNANDES JR, J. & ILDEFONSO, J. S. 2012. Analysis of use of natural fibers and asphalt rubber binder in discontinuous asphalt mixtures. *Construction and Building Materials,* 26, 13-20.

OKSMAN, K., MATHEW, A. P., LÅNGSTRÖM, R., NYSTRÖM, B. & JOSEPH, K. 2009. The influence of fibre microstructure on fibre breakage and mechanical properties of natural fibre reinforced polypropylene. *Composites Science and Technology,* 69, 1847-1853.

OKUBO, K., FUJII, T. & YAMAMOTO, Y. 2004. Development of bamboo-based polymer composites and their mechanical properties. *Composites Part A: Applied Science and Manufacturing,* 35, 377-383.

PALANIKUMAR, K. 2007. Modeling and analysis for surface roughness in machining glass fibre reinforced plastics using response surface methodology. *Materials & Design,* 28, 2611-2618.

PALANIKUMAR, K. 2011. Experimental investigation and optimisation in drilling of GFRP composites. *Measurement,* 44, 2138-2148.

PALANIKUMAR, K., KARUNAMOORTHY, L. & KARTHIKEYAN, R. 2006. Assessment of factors influencing surface roughness on the machining of glass fiber-reinforced polymer composites. *Materials & Design,* 27, 862-871.

PANIGRAHY, B., RANA, A., CHANG, P. & PANIGRAHI, S. 2006. Overview of flax fibre reinforced thermoplastic composites. *Can Biosyst Eng J,* 06-165.

PAULO DAVIM, J. & MATA, F. 2007. New machinability study of glass fibre reinforced plastics using polycrystalline diamond and cemented carbide (K15) tools. *Materials & Design,* 28, 1050-1054.

RAJAMURUGAN, T., SHANMUGHAM, K. & PALANIKUMAR, K. 2012. Analysis of delamination in drilling glass fiber reinforced polyester composites. *Materials & Design*.

RAJAMURUGAN, T. V., SHANMUGAM, K. & PALANIKUMAR, K. 2013. Analysis of delamination in drilling glass fiber reinforced polyester composites. *Materials & Design,* 45, 80-87.

RAMESH, M., PALANIKUMAR, K. & REDDY, K. H. 2013. Mechanical property evaluation of sisal–jute–glass fiber reinforced polyester composites. *Composites Part B: Engineering,* 48, 1-9.

RAO, K. M. M. & RAO, K. M. 2007. Extraction and tensile properties of natural fibers: Vakka, date and bamboo. *Composite Structures,* 77, 288-295.

RASHKOVAN, I. A. & KORABEL'NIKOV, Y. G. 1997. The effect of fiber surface treatment on its strength and adhesion to the matrix. *Composites Science and Technology,* 57, 1017-1022.

RATNA PRASAD, A. V. & MOHANA RAO, K. 2011. Mechanical properties of natural fibre reinforced polyester composites: Jowar, sisal and bamboo. *Materials & Design,* 32**,** 4658-4663.

ROKBI, M., OSMANI, H., IMAD, A. & BENSEDDIQ, N. 2011. Effect of Chemical treatment on Flexure Properties of Natural Fiber-reinforced Polyester Composite. *Procedia Engineering,* 10**,** 2092-2097.

ROSA, M. F., CHIOU, B.-S., MEDEIROS, E. S., WOOD, D. F., WILLIAMS, T. G., MATTOSO, L. H. C., ORTS, W. J. & IMAM, S. H. 2009. Effect of fiber treatments on tensile and thermal properties of starch/ethylene vinyl alcohol copolymers/coir biocomposites. *Bioresource Technology,* 100**,** 5196-5202.

ROY, A., CHAKRABORTY, S., KUNDU, S. P., BASAK, R. K., BASU MAJUMDER, S. & ADHIKARI, B. 2012. Improvement in mechanical properties of jute fibres through mild alkali treatment as demonstrated by utilisation of the Weibull distribution model. *Bioresource Technology,* 107**,** 222-228.

SAHA, P., MANNA, S., CHOWDHURY, S. R., SEN, R., ROY, D. & ADHIKARI, B. 2010. Enhancement of tensile strength of lignocellulosic jute fibers by alkali-steam treatment. *Bioresource Technology,* 101**,** 3182-3187.

SANGTHONG, S., PONGPRAYOON, T. & YANUMET, N. 2009. Mechanical property improvement of unsaturated polyester composite reinforced with admicellar-treated sisal fibers. *Composites Part A: Applied Science and Manufacturing,* 40**,** 687-694.

SANTOS, E. F., MAULER, R. S. & NACHTIGALL, S. M. 2009. Effectiveness of maleated-and silanized-PP for coir fiber-filled composites. *Journal of Reinforced Plastics and Composites,* 28**,** 2119-2129.

SAWPAN, M. A., PICKERING, K. L. & FERNYHOUGH, A. 2011. Effect of fibre treatments on interfacial shear strength of hemp fibre reinforced polylactide and unsaturated polyester composites. *Composites Part A: Applied Science and Manufacturing,* 42**,** 1189-1196.

SCHULZE, V., BECKE, C., WEIDENMANN, K. & DIETRICH, S. 2011. Machining strategies for hole making in composites with minimal workpiece damage by directing the process forces inwards. *Journal of Materials Processing Technology,* 211**,** 329-338.

SEVER, K., SARIKANAT, M., SEKI, Y., ERKAN, G., ERDOĞAN, Ü. H. & ERDEN, S. 2012. Surface treatments of jute fabric: The influence of surface characteristics on jute fabrics and mechanical properties of jute/polyester composites. *Industrial Crops and Products,* 35**,** 22-30.

SHANMUGAM, D. & THIRUCHITRAMBALAM, M. 2013. Static and dynamic mechanical properties of alkali treated unidirectional continuous Palmyra Palm Leaf Stalk Fiber/jute fiber reinforced hybrid polyester composites. *Materials & Design,* 50**,** 533-542.

SHAW, C. 1968. *Metal Cutting Principles. 3rd Ed,* M.I.T. Press.

SHYHA, I., SOO, S. L., ASPINWALL, D. & BRADLEY, S. 2010. Effect of laminate configuration and feed rate on cutting performance when drilling holes in carbon fibre reinforced plastic composites. *Journal of Materials Processing Technology,* 210**,** 1023-1034.

SHYHA, I. S., ASPINWALL, D. K., SOO, S. L. & BRADLEY, S. 2009. Drill geometry and operating effects when cutting small diameter holes in CFRP. *International Journal of Machine Tools and Manufacture,* 49**,** 1008-1014.

STEPHENSON, D. A. & AGAPIOU, J. S. 2005. *Metal Cutting Theory and Practice,* Taylor & Francis.

TAKEYAMA, H. & IIJIMA, N. 1988. Machinability of Glassfiber Reinforced Plastics and Application of Ultrasonic Machining. *CIRP Annals - Manufacturing Technology,* 37**,** 93-96.

TARFAOUI, M., CHOUKRI, S. & NEME, A. 2008. Effect of fibre orientation on mechanical properties of the laminated polymer composites subjected to out-of-plane high strain rate compressive loadings. *Composites Science and Technology,* 68**,** 477-485.

TORRES, F. G. & CUBILLAS, M. L. 2005. Study of the interfacial properties of natural fibre reinforced polyethylene. *Polymer Testing,* 24**,** 694-698.

TSAO, C. C. & CHIU, Y. C. 2011. Evaluation of drilling parameters on thrust force in drilling carbon fiber reinforced plastic (CFRP) composite laminates using compound core-special drills. *International Journal of Machine Tools and Manufacture,* 51**,** 740-744.

TSAO, C. C. & HOCHENG, H. 2008a. Evaluation of thrust force and surface roughness in drilling composite material using Taguchi analysis and neural network. *Journal of Materials Processing Technology,* 203**,** 342-348.

TSAO, C. C. & HOCHENG, H. 2008b. Evaluation of thrust force and surface roughness in drilling composite material using Taguchi analysis and neural network. *Journal of Materials Processing Technology,* 203**,** 342-348.

VALADEZ-GONZALEZ, A., CERVANTES-UC, J. M., OLAYO, R. & HERRERA-FRANCO, P. J. 1999. Effect of fiber surface treatment on the fiber–matrix bond strength of natural fiber reinforced composites. *Composites Part B: Engineering,* 30**,** 309-320.

VAN DE WEYENBERG, I., CHI TRUONG, T., VANGRIMDE, B. & VERPOEST, I. 2006. Improving the properties of UD flax fibre reinforced composites by applying an alkaline fibre treatment. *Composites Part A: Applied Science and Manufacturing,* 37**,** 1368-1376.

VAN DE WEYENBERG, I., IVENS, J., DE COSTER, A., KINO, B., BAETENS, E. & VERPOEST, I. 2003. Influence of processing and chemical treatment of flax fibres on their composites. *Composites Science and Technology,* 63**,** 1241-1246.

VIRK, A. S., HALL, W. & SUMMERSCALES, J. 2010. Failure strain as the key design criterion for fracture of natural fibre composites. *Composites Science and Technology,* 70**,** 995-999.

WAHIT, M. U., AKOS, N. I. & LAFTAH, W. A. 2012. Influence of natural fibers on the mechanical properties and biodegradation of poly (lactic acid) and poly (ε-caprolactone) composites: A review. *Polymer Composites,* 33**,** 1045-1053.

WERN, C. W., RAMULU, M. & COLLIGAN, K. 1993. A study of the surface texture of composite drilled holes. *Journal of Materials Processing Technology,* 37**,** 373-389.

WIELEBA, W. 2002. The statistical correlation of the coefficient of friction and wear rate of PTFE composites with steel counterface roughness and hardness. *Wear,* 252**,** 719-729.

WU, J., YU, D., CHAN, C. M., KIM, J. & MAI, Y. W. 2000. Effect of Fiber Pretreatment Condition on the Interfacial Strength and Mechanical Properties of Wood Fiber/PP Composites. *Journal of Applied Polymer Science,* 76**,** 1000-1010.

YAM, K. L., GOGOI, B. K., LAI, C. C. & SELKE, S. E. 1990. Composites from compounding wood fibers with recycled high density polyethylene. *Polymer Engineering and Science,* 30**,** 693-699.

YEMELE, M. C. N., KOUBAA, A., CLOUTIER, A., SOULOUNGANGA, P. & WOLCOTT, M. 2010. Effect of bark fiber content and size on the mechanical properties of bark/HDPE composites. *Composites Part A: Applied Science and Manufacturing,* 41**,** 131-137.

YOUSIF, B. & EL-TAYEB, N. 2007. The effect of oil palm fibers as reinforcement on tribological performance of polyester composite. *Surface Review and Letters,* 14**,** 1095-1102.

YOUSIF, B. F. 2008. Replacing of glass fibres with seed oil palm fibres for tribopolymeric composites. *Tribology - Materials, Surfaces and Interfaces,* 2**,** 99-103.

YOUSIF, B. F. 2009. Frictional and wear performance of polyester composites based on coir fibres. *Proceedings of the Institution of Mechanical Engineers, Part J: Journal of Engineering Tribology,* 223**,** 51-59.

YOUSIF, B. F. 2010. Effect of oil palm fibres volume fraction on mechanical properties of polyester composites. *International Journal of Modern Physics B,* 24**,** 4459-4470.

YOUSIF, B. F. 2013. Editorial for SI: Materials, design and tribology. *Materials and Design*.

YOUSIF, B. F. & CHIN, C. W. 2012. Epoxy composite based on kenaf fibers for tribological applications under wet contact conditions. *Surface Review and Letters,* 19.

YOUSIF, B. F., DEVADAS, A. & YUSAF, T. F. 2009. ADhesive wear and frictional behavior of multilayered polyester composite based on Betelnut fiber mats under wet contact conditions. *Surface Review and Letters,* 16**,** 407-414.

ZAFEIROPOULOS, N. E., BAILLIE, C. A. & HODGKINSON, J. M. 2002. Engineering and characterisation of the interface in flax fibre/polypropylene composite materials. Part II. The effect of surface treatments on the interface. *Composites Part A: Applied Science and Manufacturing,* 33**,** 1185-1190.

ZARIF KARIMI, N., HEIDARY, H., MINAK, G. & AHMADI, M. 2013. Effect of the drilling process on the compression behavior of glass/epoxy laminates. *Composite Structures,* 98**,** 59-68.

APPENDIX A: EQUIPMENT'S SPECIFICATIONS

A.1 The drill machine

A.1.1 Drill machine specification

ORDER CODE	D176
Model	GHD-30V
Drilling Capacity	31.5mm
Thread Tapping Capacity	M20
Spindle Taper	3MT
Spindle Travel	125mm
Throat Depth	285mm
Quill Diameter	62mm
Column Diameter	115mm
Spindle To Table	790mm
Spindle To Base	1270mm
Table Type	Rectangle
Table Size	426 x 400mm
T-Slot Size	14mm
Automatic Quill Feed	0.06, 0.09, 0.12mm/rev
Work Light	Yes
Coolant System	Yes
Spindle Speed Steps	3 (Variable)
Spindle Speed Range	50-2850rpm
Motor Power	2.2kW / 3hp
Voltage	240V - 15amp
Full Height	1940mm
Weight (Nett)	368kg

A.1.2 Drill machine features

A.1.3 Drill machine technical data

Technical data

The following information gives the dimensions and weight and is the manufacturer's authorised machine data.

2.1	**Power connection**		
Total connection rate	230V; 2,5 kW ~50Hz		
Cooling pump	230V; 40 W		
2.2	**Drill capacity**		
Drill capacity in steel [mm]	30		
Working radius [mm]	285		
Spindle sleeve travel [mm]	125		
2.3	**Spindle seat**		
Spindle seat	MK3		
Spindle sleeve feed [mm / rev]	Speed		
	1	2	3
	0,1	0,15	0,2
	☞ „Automatic spindle sleeve feed“ on page 30		
2.4	**Drilling table**		
Table measurements [mm] Length x width	400 x 500		
Size of T-slots [mm]	14		
Maximum distance [mm] Spindle - table	780		
Dimension base [mm] Length x width	420 x 643		
Maximum distance [mm] Spindle - base	1320		
2.5	**Working area**		
Height [mm]	2500		
Depth [mm	1700		
Width [mm	1500		
2.6	**Revolutions**		
Gear	L	M	H
Spindle rotating speeds [min^{-1}]	80 - 700	170 - 1500	400 - 3000
2.7	**Floor load**		
Ground resistance	14 kN/m^2		
2.8	**Ambient conditions**		
Temperature	5 - 35 °C		
Rel. humidity	25 - 80 %		

2.9	**Operating material**
Gear oil for spindle sleeve gear 2.5 liters	Mobilgear 627 or equivalent oil ☞ „Recommended working materials“ on page 42
Rack and upright of the drill	Commercial heavy grease
2.10	**Coolant system**
Max. height of pressure [m]	3
Tank capacity [ccm]	4500
Max. rate of flow	2 l / min

A.1.4 Drill machine dimensions

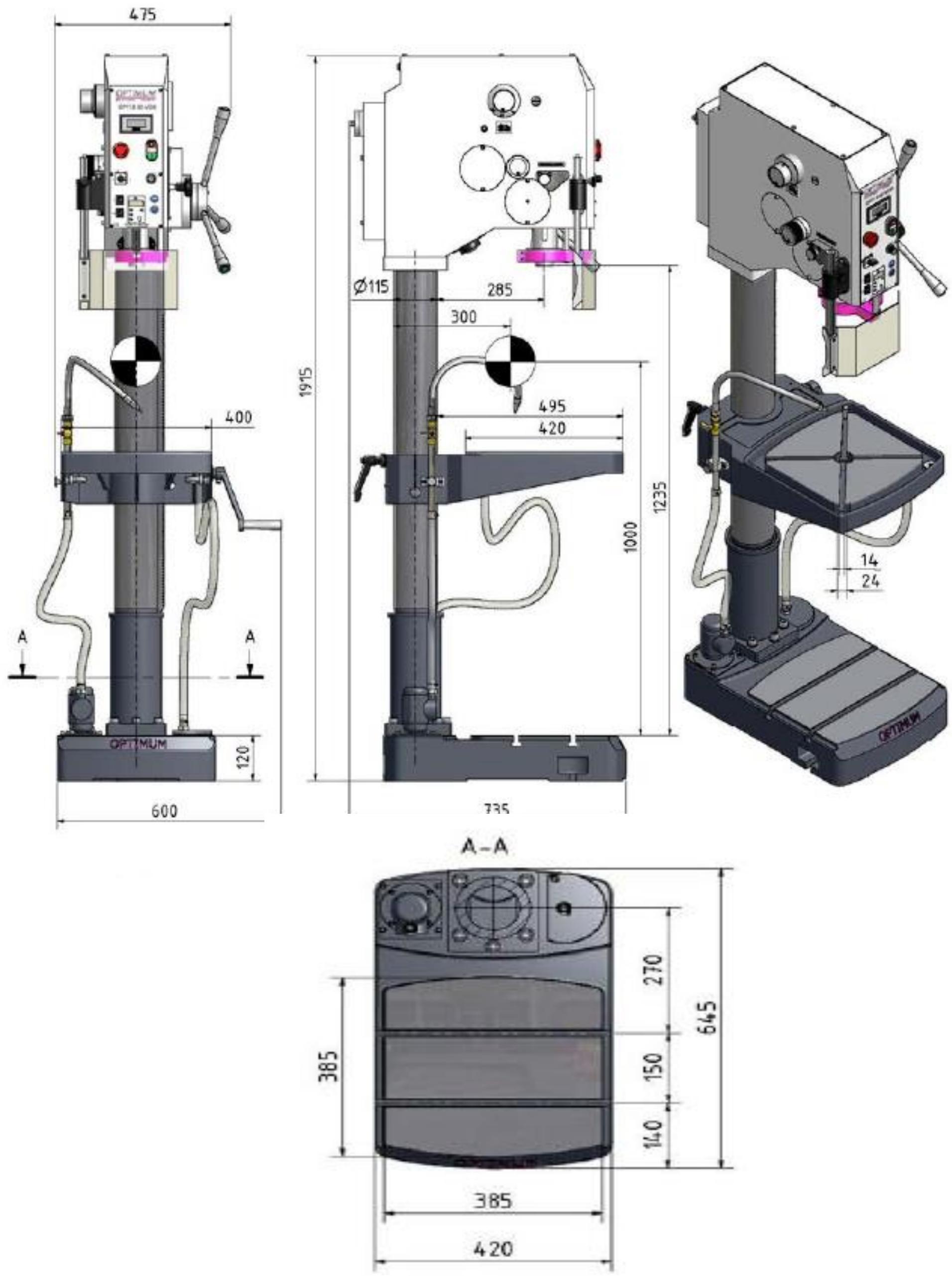

A.2 Sensors

A.2.1 Tension – Compression sensor

A.2.1.1 Sensor technical data

Technical Data

Dim. tolerances acc. ISO 2768-f

Order Code	Load Range	Accuracy[1)] [%v.E].	Sensitivity [mV/V]		ø D [mm]	H [mm]	Natural Frequency [kHz]	Weight [kg]	Wrench Torque for Mounting Screw 12.9
8523-20	0 ... 20 N	≤ ± 0.5	nominal [4)]	1.0	54.5	16	0.5	0.15	3 Nm
8523-50	0 ... 50 N	≤ ± 0.5	nominal [4)]	1.0	54.5	16	0.75	0.15	3 Nm
8523-100	0 ... 100 N	≤ ± 0.5	standardized	1.5 ± 0.5 %	54.5	16	0.80	0.15	3 Nm
8523-200	0 ... 200 N	≤ ± 0.2	standardized	1.5 ± 0.2 %	54.5	16	1.1	0.15	3 Nm
8523-500	0 ... 500 N	≤ ± 0.2	standardized	1.5 ± 0.2 %	54.5	16	2.3	0.15	3 Nm
8531-1000	0 ... 1000 N	≤ ± 0.25	standardized	1.5 ± 0.2 %	89.5	22	1.0	0.35	6 Nm
8531-2000	0 ... 2000 N	≤ ± 0.15	standardized	1.5 ± 0.2 %	99.5	30	1.8	0.35	6 Nm
8531-5000	0 ... 5000 N	≤ ± 0.15	standardized	1.5 ± 0.2 %	99.5	30	3.0	0.35	6 Nm

A.2.1.2 Sensor dimensions

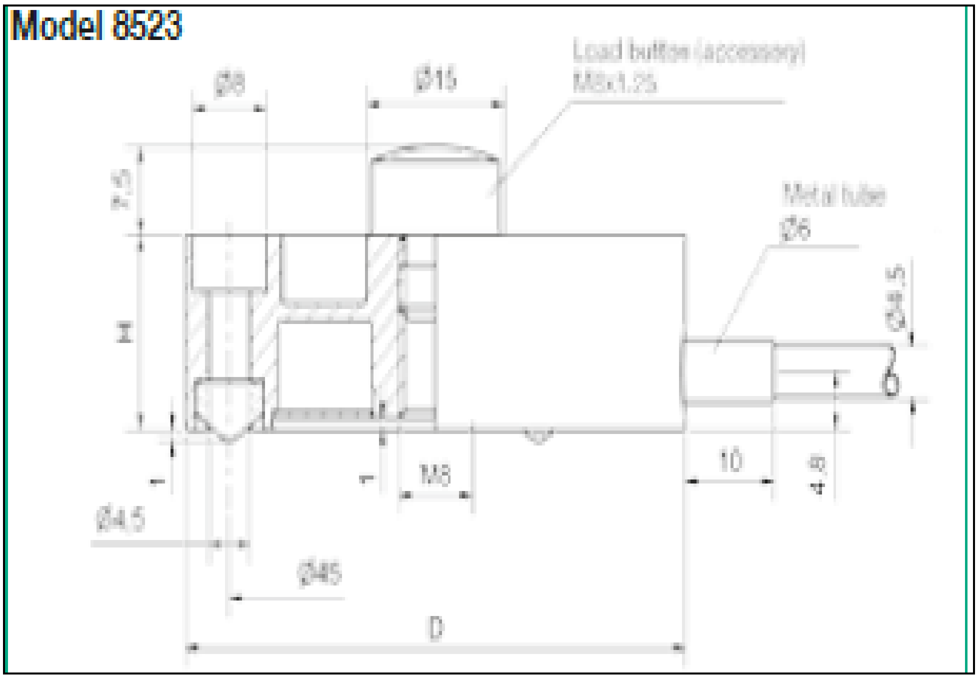

A.2.2 Torque sensor

A.2.2.1 Sensor technical data

Order Code	Measurement Range	Dimensions [mm]								Number of Bore Holes T	P
		øA	øB	øD	F	G	L	øT	øQ		
8627-5010	0 ... ± 10 Nm	20^{H7}	10	70	12	M8	65	58	45	6x60°	33
8627-5025	0 ... ± 25 Nm	20^{H7}	10	70	12	M8	65	58	45	6x60°	33
8627-5050	0 ... ± 50 Nm	20^{H7}	10	70	12	M8	65	58	45	6x60°	33
8627-5100	0 ... ± 100 Nm	20^{H7}	10	70	12	M8	65	58	45	6x60°	33
8627-5200	0 ... ± 200 Nm	20^{H7}	10	70	12	M8	65	58	45	6x60°	33
8627-5500	0 ... ± 500 Nm	20^{H7}	18	100	15	M10	80	82	60	8x45°	39.5
8627-6001	0 ... ± 1000 Nm	20^{H7}	18	100	15	M10	80	82	60	8x45°	39.5
8627-6002	0 ... ± 2000 Nm	75^{H7}	20	130	20	M12	100	100	80	12x30°	45
8627-6005	0 ... ± 5000 Nm	75^{H7}	-	130	20	M12	100	100	80	12x30°	45

A.2.2.2 Sensor dimensions

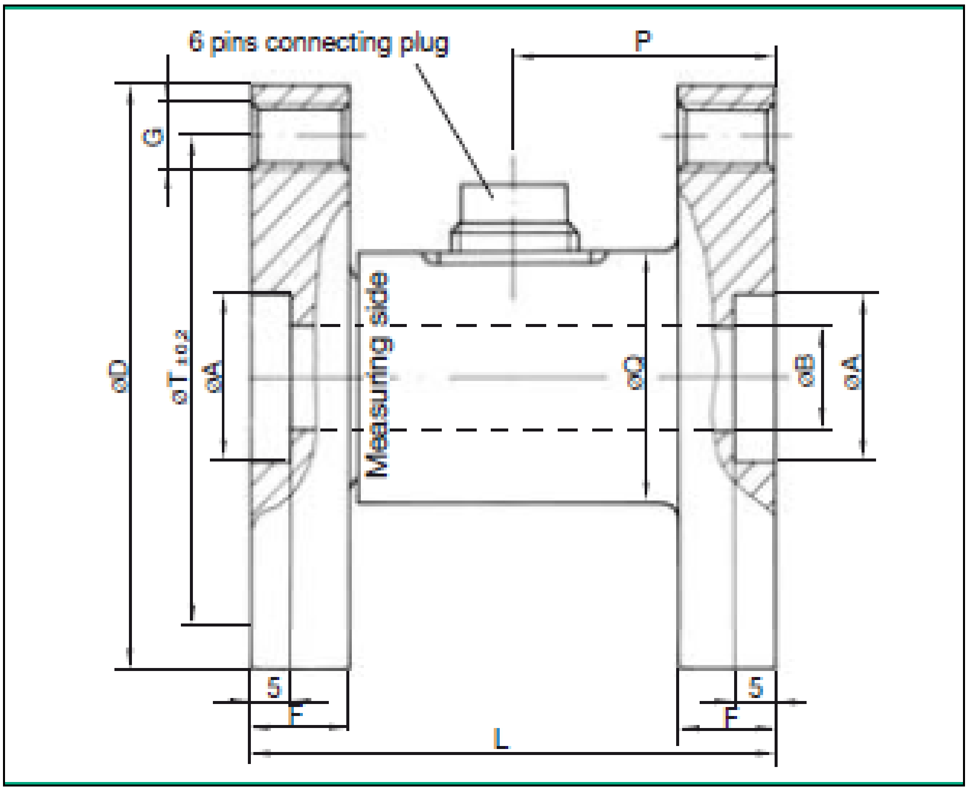

6 pins connecting plug
P
G
ØD
ØT±0.2
ØA
Measuring side
ØQ
ØB
ØA
5
F
L
5
F

A.2.3 USB sensor interface sensor

A.2.3.1 Sensor technical data

TECHNICAL DATA

Type	LCV-USB2-SG	LCV-USB2-U5	LCV-USB2-U10	LCV-USB2-I20
Art.-No.	112311	112312	112705	112313
Input Range	±3 mV/V	±5 V	±10 V	0/4…20 mA

Supply	from USB	4…6 V DC ≤350 mA
Excitation	SG U5/U10 I20	4 V ≤20 mA 12 V ≤80 mA 12 V ≤80 mA
Measured Values	SG U5/U10 I20	±3 mV/V = ±30,000 digits ±5 V/±10 V = ±25,000 digits 0…20 mA = 0…+20,000 digits
Resolution	SG U5 U10 I20	1 mV/V = 10,000 digits 1 V = 5000 digits 1 V = 2500 digits 1 mA = 1000 digits
Zero Point	SG/U5/U10/I20	0 digits
Output Format		16bit signed int.
Input Resistance	SG U5/U10 I20 burden	>1 MΩ >1 MΩ 62 Ω
Measuring Rate		max. 5000 meas./s
Temperature Drift		4 Bit/10 K
Linearity Error		±32 digits
Accuracy		±32 digits

Miscellaneous

Cable Length LCV-USB2-Evaluation	2 m
Cable Length LCV-USB2-Sensor	1m (max.3 m)
Nominal Temperature Range	+10…+40 °C
Service Temperature Range	0...+50 °C
Storage Temperature Range	-10...+70 °C
Dimensions (Ø x L)	25 x 115 mm (incl. screw joint)
Level of Protection	IP67

Art.-No.	Options	Description
110564	mV/V	mV/V adjusted sensitivity
110120	LCV-USB2/TR-EXT	Digital input at channel B

APPENDIX B: RAW COLLECTED DATA

B.1 Neat epoxy

B.1.1 Raw collected Thrust forces data

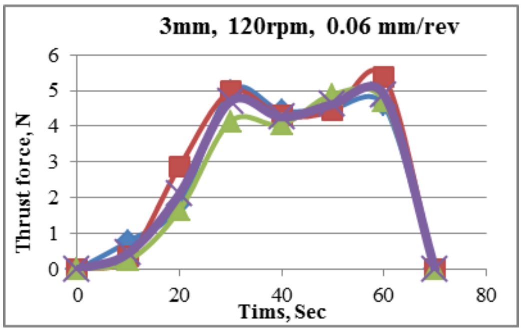

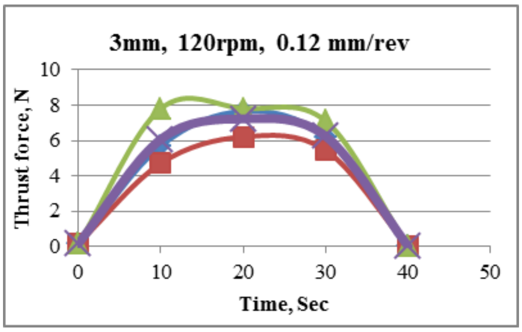

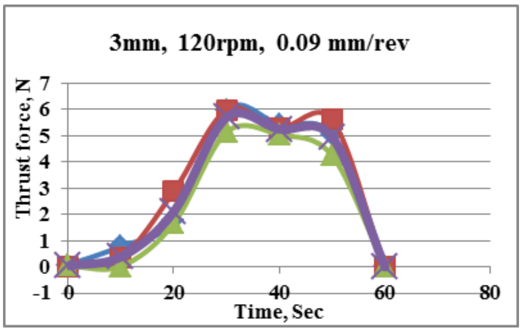

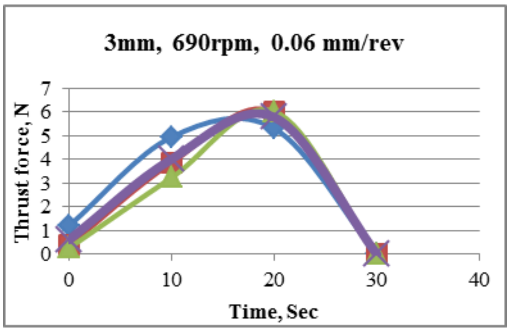

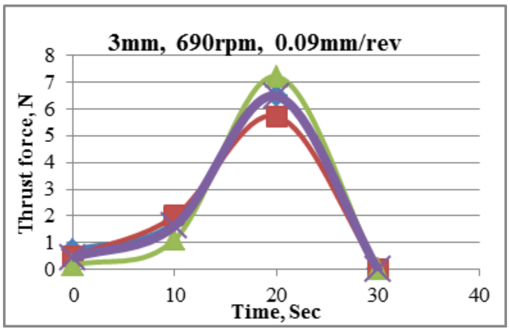
3mm, 690rpm, 0.09mm/rev
Thrust force, N
Time, Sec

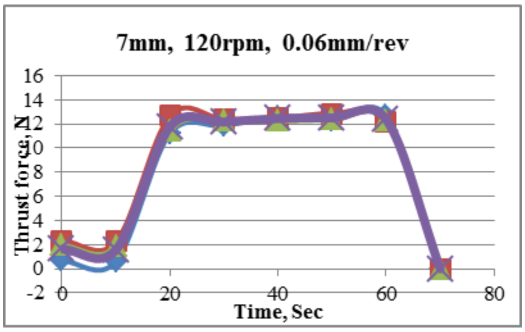
7mm, 120rpm, 0.06mm/rev
Thrust force, N
Time, Sec

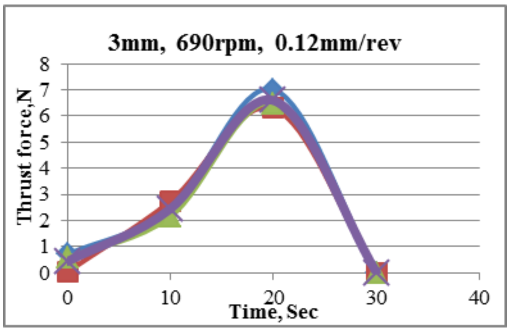
3mm, 690rpm, 0.12mm/rev
Thrust force,N
Time, Sec

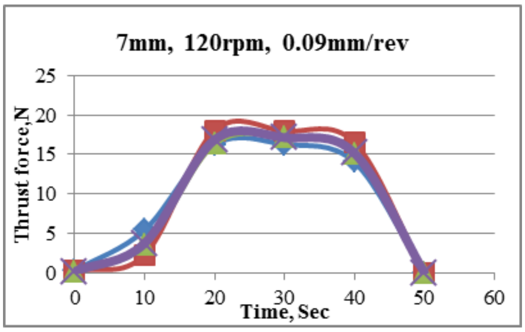
7mm, 120rpm, 0.09mm/rev
Thrust force,N
Time, Sec

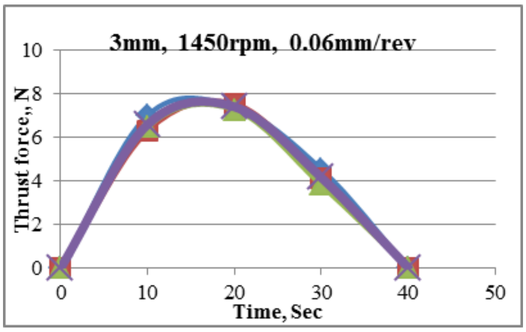
3mm, 1450rpm, 0.06mm/rev
Thrust force,, N
Time, Sec

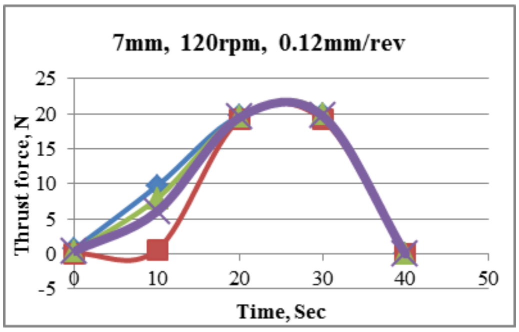
7mm, 120rpm, 0.12mm/rev
Thrust force, N
Time, Sec

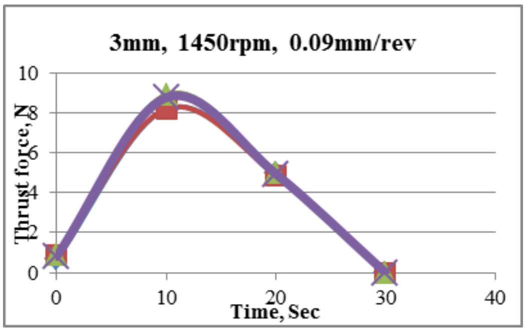
3mm, 1450rpm, 0.09mm/rev
Thrust force, N
Time, Sec

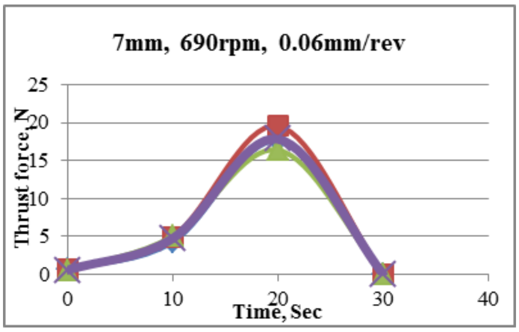
7mm, 690rpm, 0.06mm/rev
Thrust force, N
Time, Sec

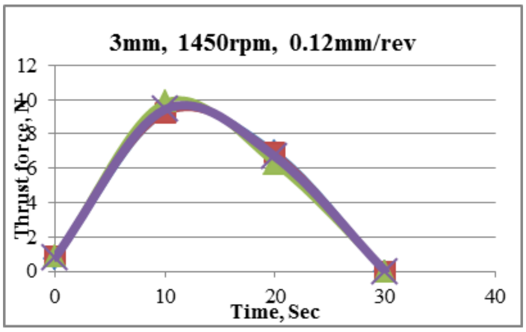
3mm, 1450rpm, 0.12mm/rev
Thrust force, N
Time, Sec

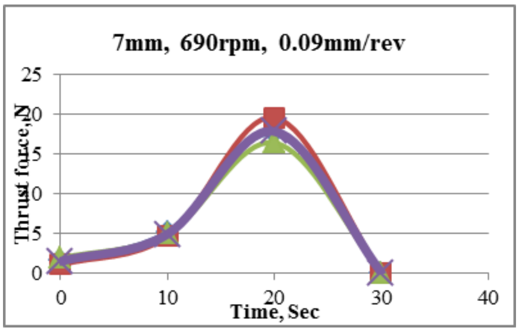
7mm, 690rpm, 0.09mm/rev
Thrust force,N
Time, Sec

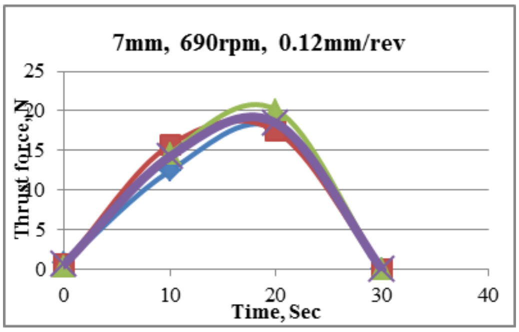
7mm, 690rpm, 0.12mm/rev
Thrust force, N
Time, Sec

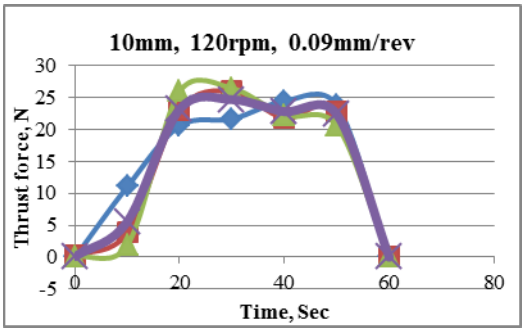
10mm, 120rpm, 0.09mm/rev
Thrust force, N
Time, Sec

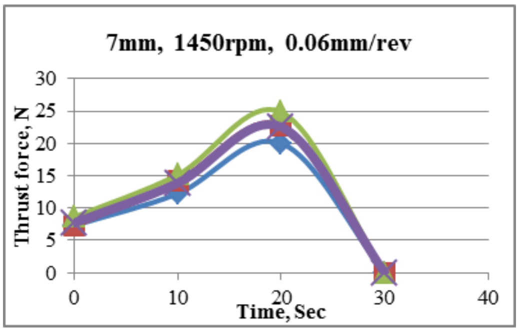
7mm, 1450rpm, 0.06mm/rev
Thrust force, N
Time, Sec

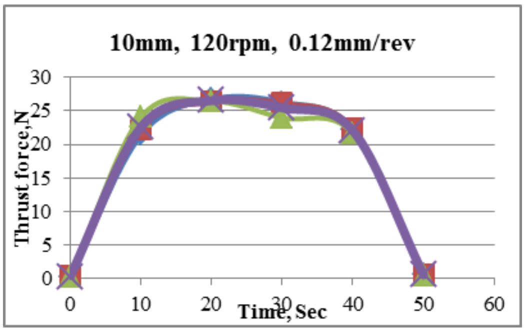
10mm, 120rpm, 0.12mm/rev
Thrust force, N
Time, Sec

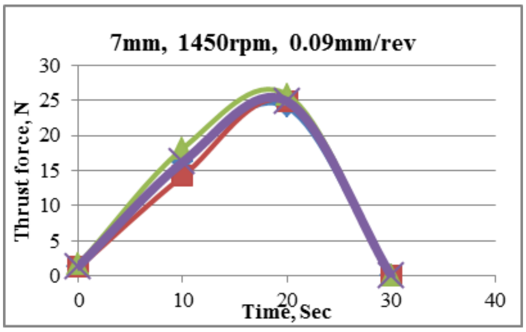
7mm, 1450rpm, 0.09mm/rev
Thrust force, N
Time, Sec

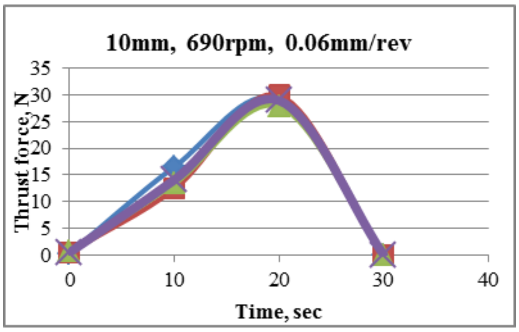
10mm, 690rpm, 0.06mm/rev
Thrust force, N
Time, sec

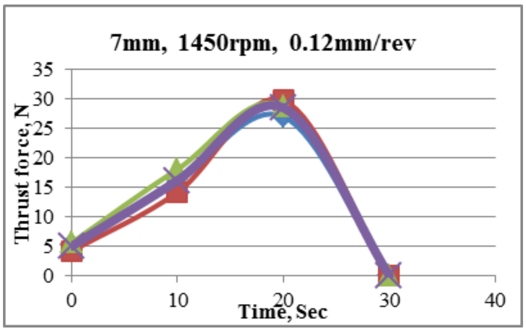
7mm, 1450rpm, 0.12mm/rev
Thrust force, N
Time, Sec

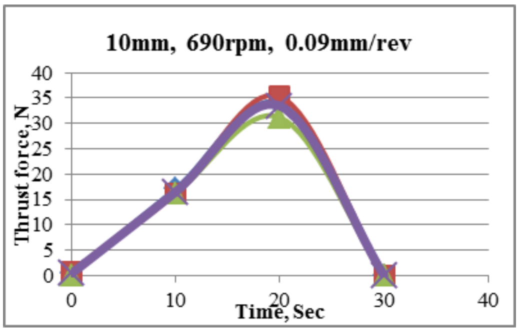
10mm, 690rpm, 0.09mm/rev
Thrust force, N
Time, Sec

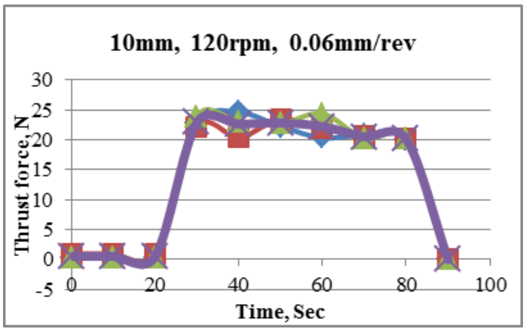
10mm, 120rpm, 0.06mm/rev
Thrust force, N
Time, Sec

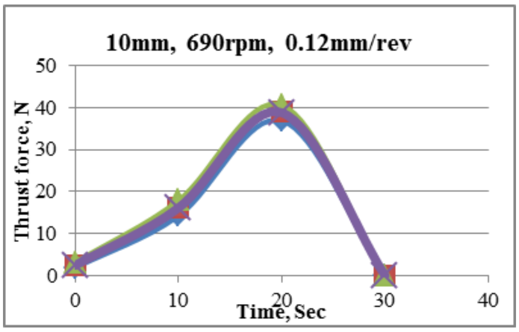
10mm, 690rpm, 0.12mm/rev
Thrust force, N
Time, Sec

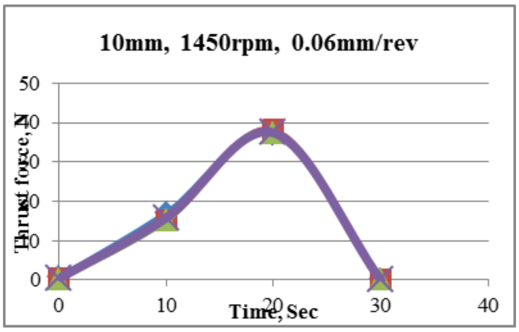

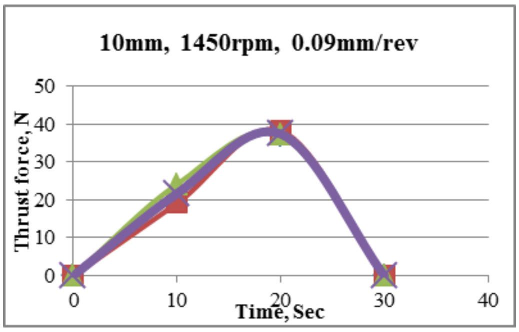

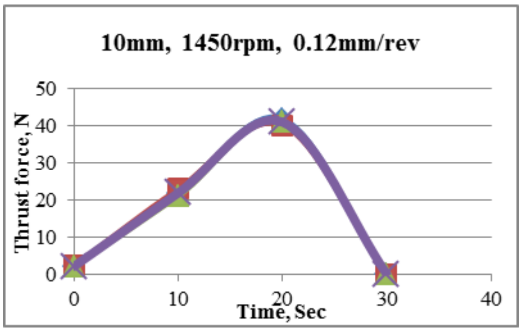

B.1.2 Raw collected Torque data

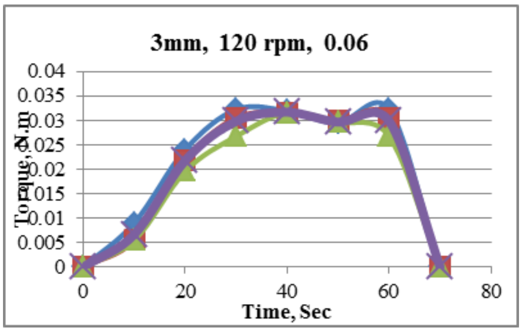

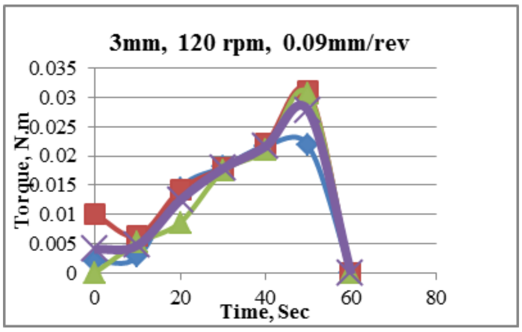

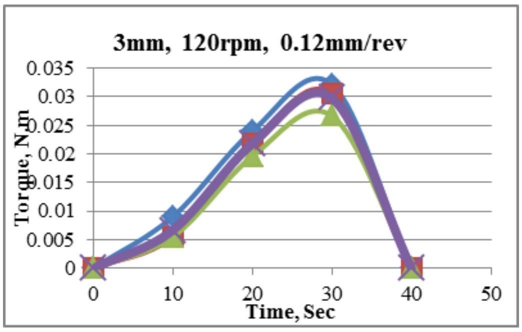

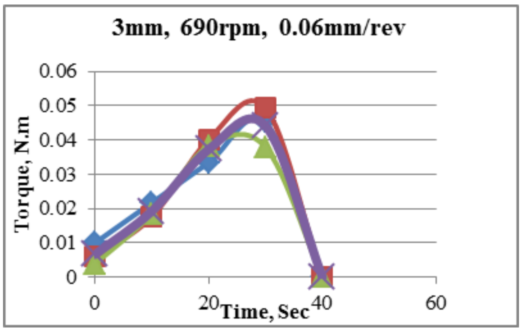

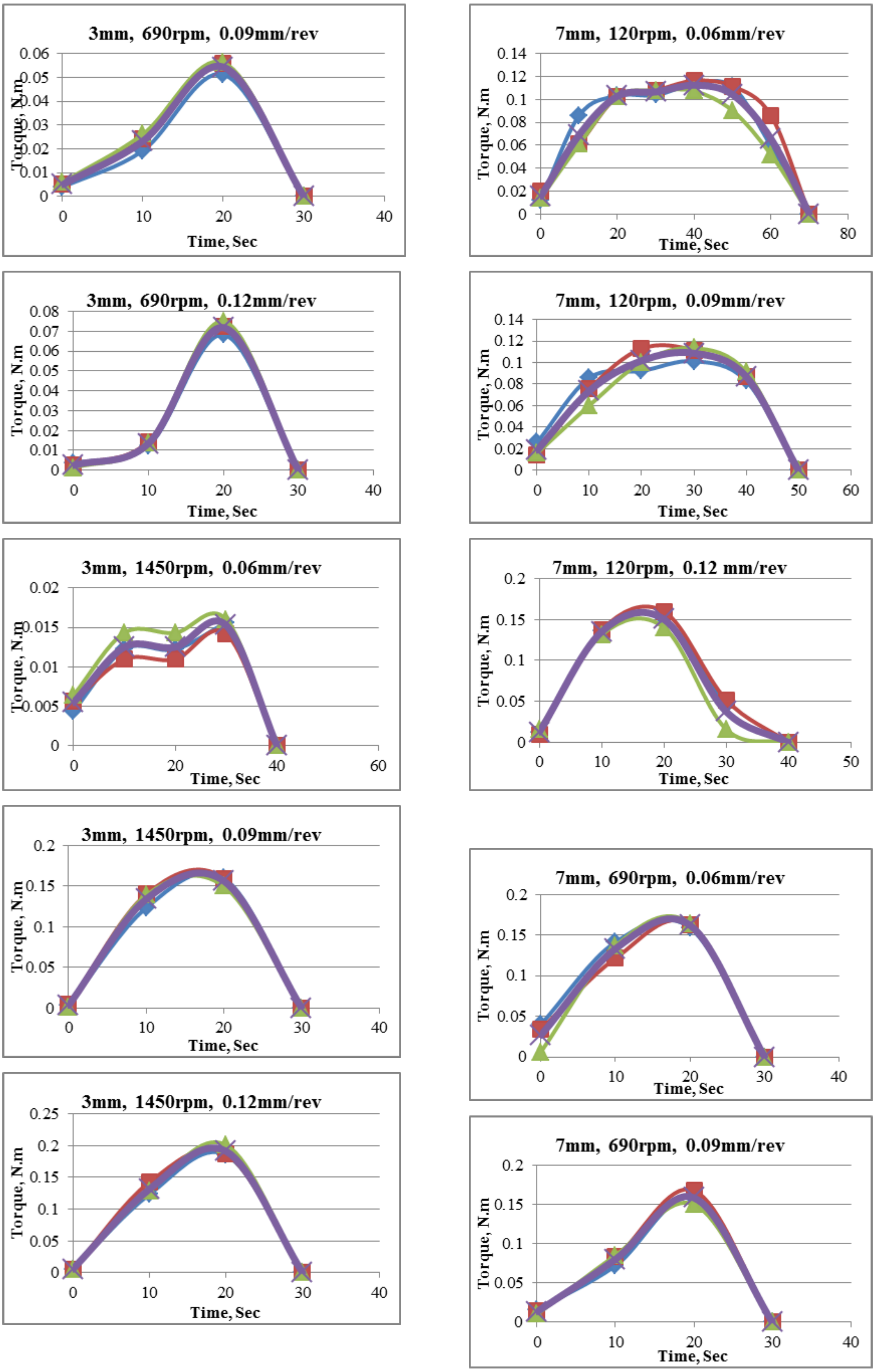

3mm, 690rpm, 0.09mm/rev
Torque, N.m
Time, Sec
3mm, 690rpm, 0.12mm/rev
Torque, N.m
Time, Sec
3mm, 1450rpm, 0.06mm/rev
Torque, N.m
Time, Sec
3mm, 1450rpm, 0.09mm/rev
Torque, N.m
Time, Sec
3mm, 1450rpm, 0.12mm/rev
Torque, N.m
Time, Sec
7mm, 120rpm, 0.06mm/rev
Torque, N.m
Time, Sec
7mm, 120rpm, 0.09mm/rev
Torque, N.m
Time, Sec
7mm, 120rpm, 0.12 mm/rev
Torque, N.m
Time, Sec
7mm, 690rpm, 0.06mm/rev
Torque, N.m
Time, Sec
7mm, 690rpm, 0.09mm/rev
Torque, N.m
Time, Sec

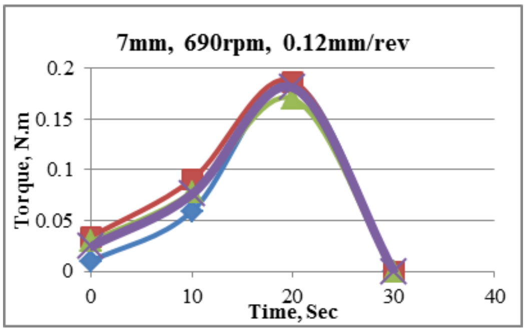
7mm, 690rpm, 0.12mm/rev
Torque, N.m
0 0.05 0.1 0.15 0.2
0 10 20 30 40
Time, Sec

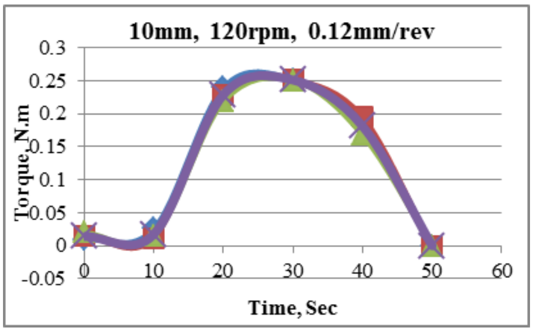
10mm, 120rpm, 0.12mm/rev
Torque, N.m
-0.05 0 0.05 0.1 0.15 0.2 0.25 0.3
0 10 20 30 40 50 60
Time, Sec

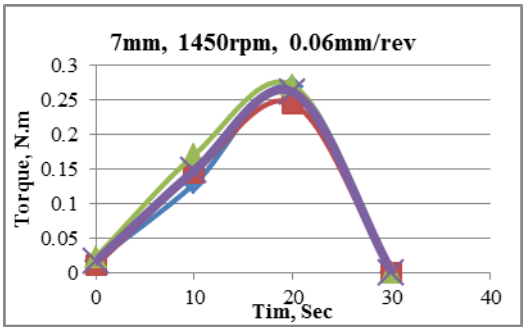
7mm, 1450rpm, 0.06mm/rev
Torque, N.m
0 0.05 0.1 0.15 0.2 0.25 0.3
0 10 20 30 40
Tim, Sec

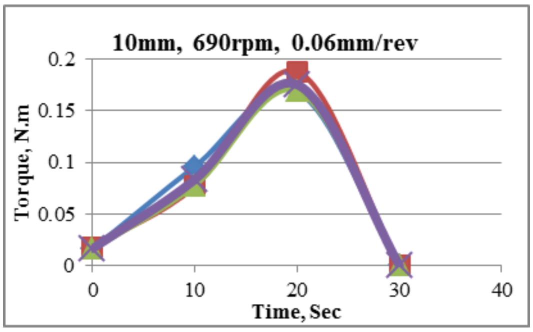
10mm, 690rpm, 0.06mm/rev
Torque, N.m
0 0.05 0.1 0.15 0.2
0 10 20 30 40
Time, Sec

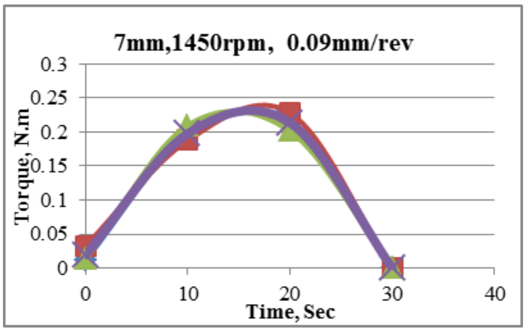
7mm,1450rpm, 0.09mm/rev
Torque, N.m
0 0.05 0.1 0.15 0.2 0.25 0.3
0 10 20 30 40
Time, Sec

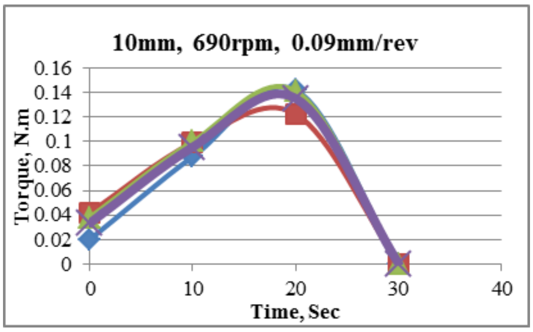
10mm, 690rpm, 0.09mm/rev
Torque, N.m
0 0.02 0.04 0.06 0.08 0.1 0.12 0.14 0.16
0 10 20 30 40
Time, Sec

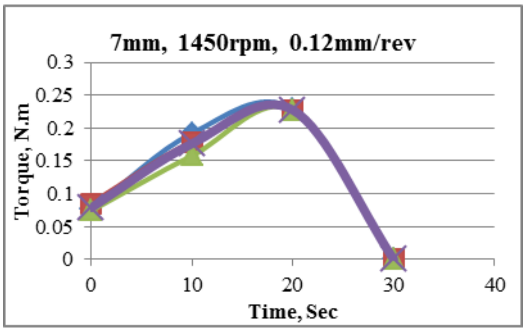
7mm, 1450rpm, 0.12mm/rev
Torque, N.m
0 0.05 0.1 0.15 0.2 0.25 0.3
0 10 20 30 40
Time, Sec

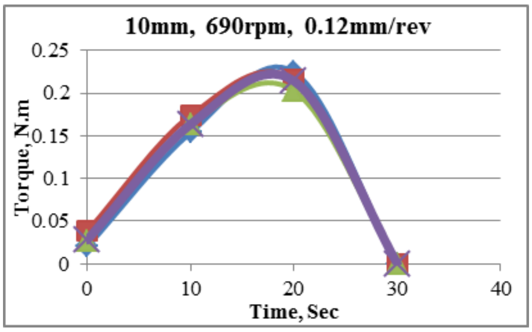
10mm, 690rpm, 0.12mm/rev
Torque, N.m
0 0.05 0.1 0.15 0.2 0.25
0 10 20 30 40
Time, Sec

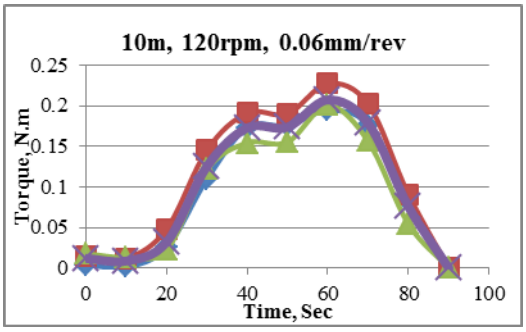
10m, 120rpm, 0.06mm/rev
Torque, N.m
0 0.05 0.1 0.15 0.2 0.25
0 20 40 60 80 100
Time, Sec

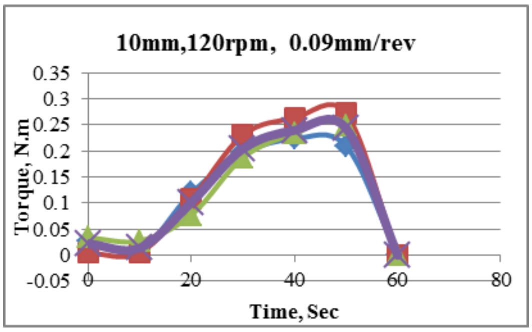
10mm,120rpm, 0.09mm/rev
Torque, N.m
-0.05 0 0.05 0.1 0.15 0.2 0.25 0.3 0.35
0 20 40 60 80
Time, Sec

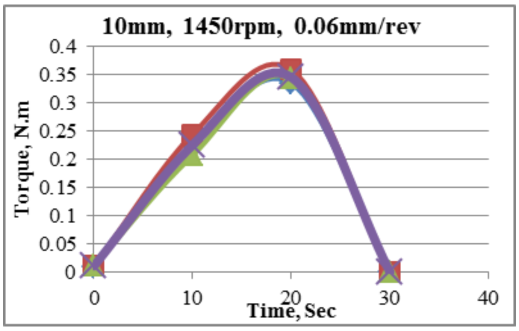
10mm, 1450rpm, 0.06mm/rev
Torque, N.m
0.4
0.35
0.3
0.25
0.2
0.15
0.1
0.05
0
0
10
20
30
40
Time, Sec

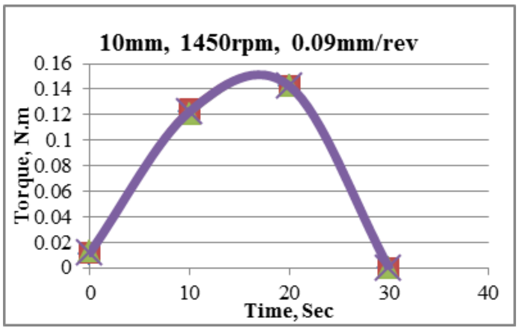
10mm, 1450rpm, 0.09mm/rev
Torque, N.m
0.16
0.14
0.12
0.1
0.08
0.06
0.04
0.02
0
0
10
20
30
40
Time, Sec

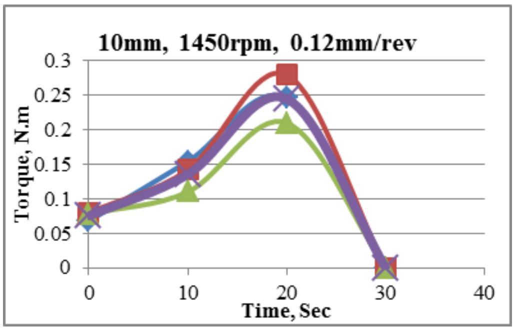
10mm, 1450rpm, 0.12mm/rev
Torque, N.m
0.3
0.25
0.2
0.15
0.1
0.05
0
0
10
20
30
40
Time, Sec

B.2 GFEC

B.2.1 Raw collected Thrust forces data

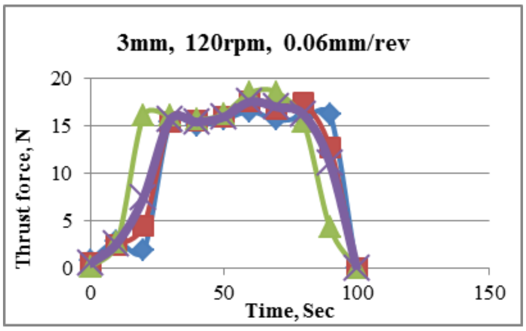

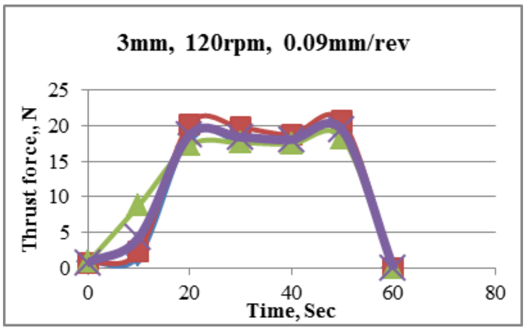

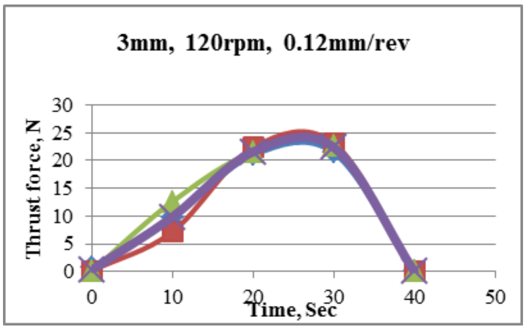

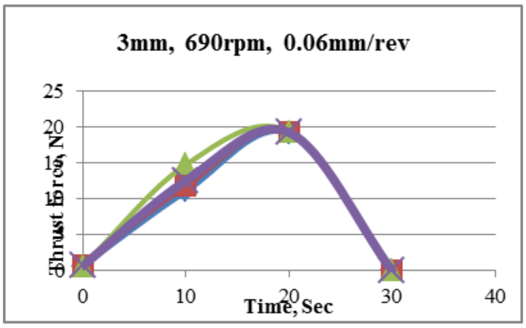

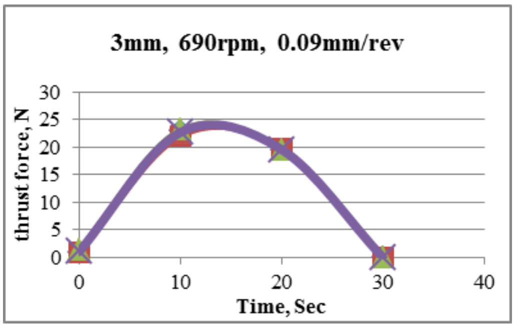

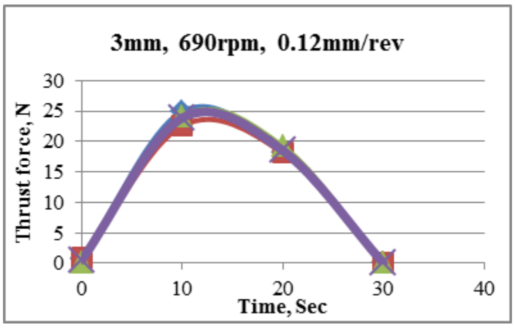

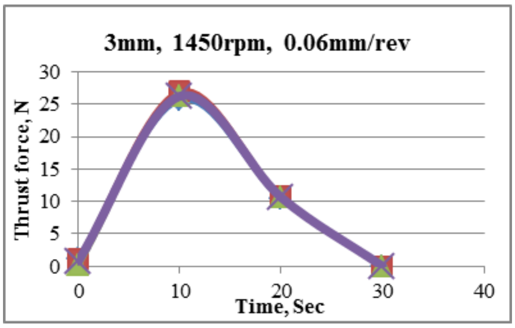

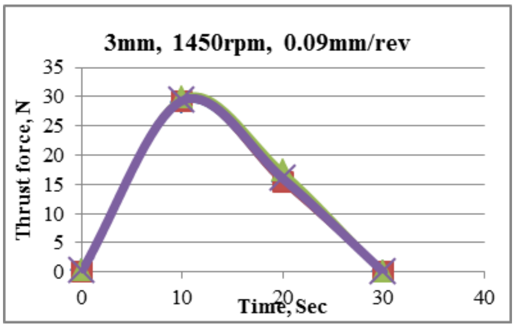

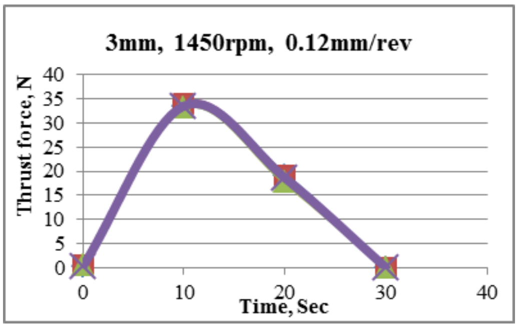
3mm, 1450rpm, 0.12mm/rev
Thrust force, N
Time, Sec
0
5
10
15
20
25
30
35
40
0 10 20 30 40

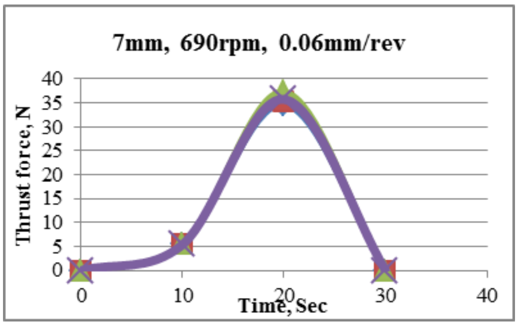
7mm, 690rpm, 0.06mm/rev
Thrust force, N
Time, Sec
0
5
10
15
20
25
30
35
40
0 10 20 30 40

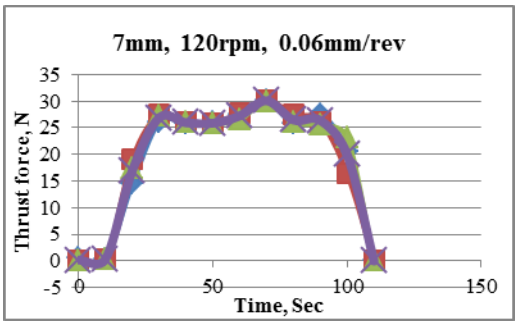
7mm, 120rpm, 0.06mm/rev
Thrust force, N
Time, Sec
-5
0
5
10
15
20
25
30
35
0 50 100 150

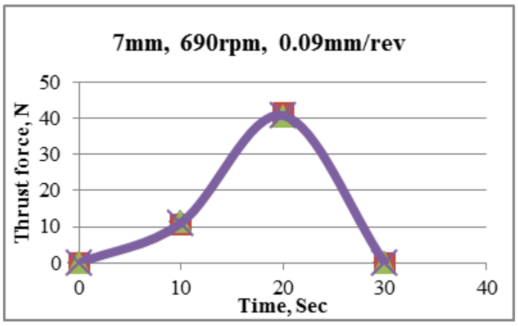
7mm, 690rpm, 0.09mm/rev
Thrust force, N
Time, Sec
0
10
20
30
40
50
0 10 20 30 40

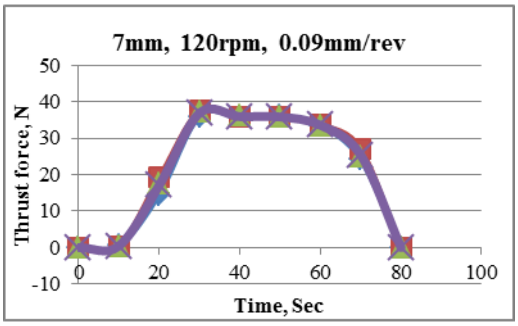
7mm, 120rpm, 0.09mm/rev
Thrust force, N
Time, Sec
-10
0
10
20
30
40
50
0 20 40 60 80 100

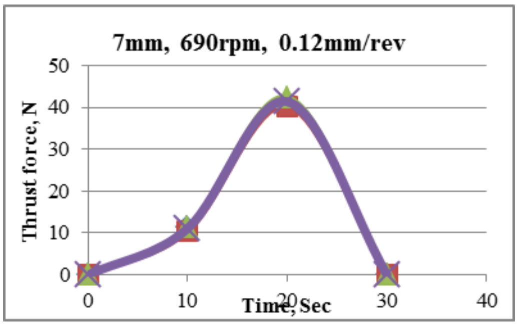
7mm, 690rpm, 0.12mm/rev
Thrust force, N
Time, Sec
0
10
20
30
40
50
0 10 20 30 40

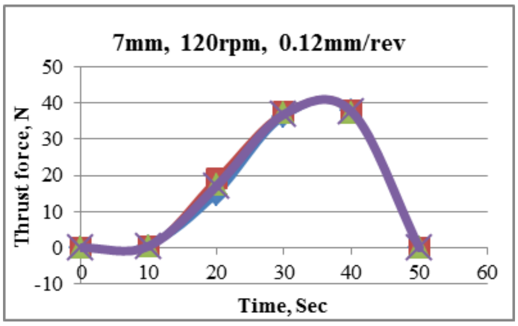
7mm, 120rpm, 0.12mm/rev
Thrust force, N
Time, Sec
-10
0
10
20
30
40
50
0 10 20 30 40 50 60

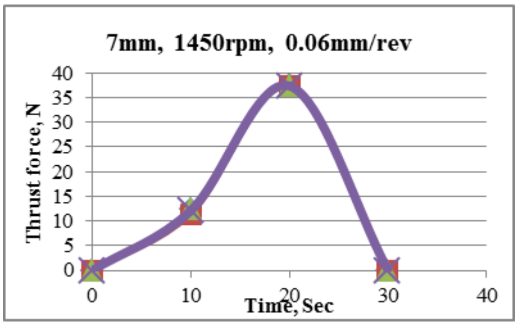
7mm, 1450rpm, 0.06mm/rev
Thrust force, N
Time, Sec
0
5
10
15
20
25
30
35
40
0 10 20 30 40

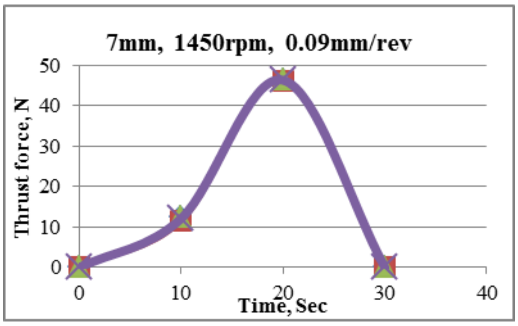
7mm, 1450rpm, 0.09mm/rev
Thrust force, N
Time, Sec
0
10
20
30
40
50
0
10
20
30
40

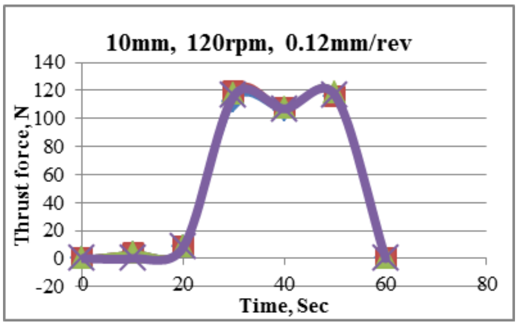
10mm, 120rpm, 0.12mm/rev
Thrust force, N
Time, Sec
-20
0
20
40
60
80
100
120
140
0
20
40
60
80

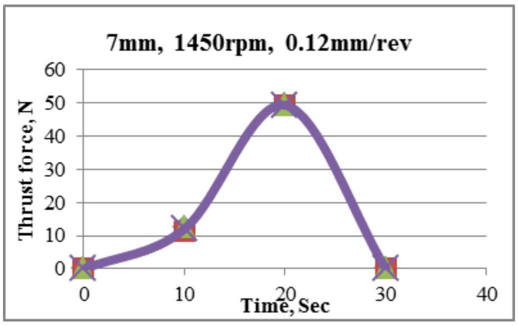
7mm, 1450rpm, 0.12mm/rev
Thrust force, N
Time, Sec
0
10
20
30
40
50
60
0
10
20
30
40

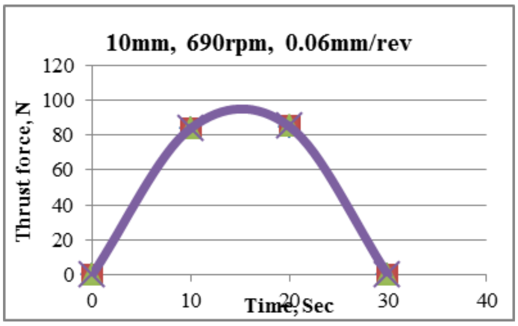
10mm, 690rpm, 0.06mm/rev
Thrust force, N
Time, Sec
0
20
40
60
80
100
120
0
10
20
30
40

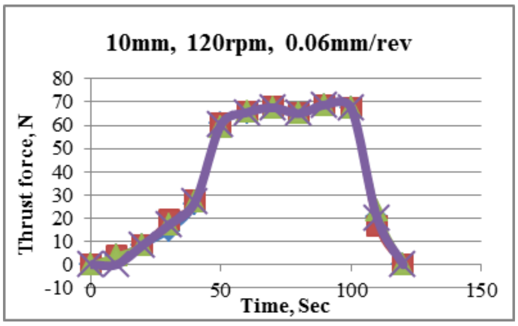
10mm, 120rpm, 0.06mm/rev
Thrust force, N
Time, Sec
-10
0
10
20
30
40
50
60
70
80
0
50
100
150

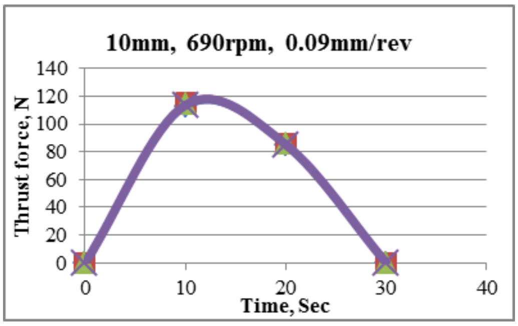
10mm, 690rpm, 0.09mm/rev
Thrust force, N
Time, Sec
0
20
40
60
80
100
120
140
0
10
20
30
40

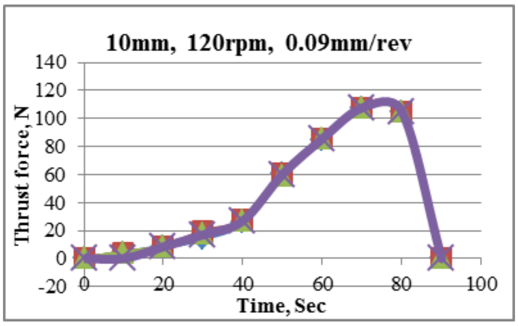
10mm, 120rpm, 0.09mm/rev
Thrust force, N
Time, Sec
-20
0
20
40
60
80
100
120
140
0
20
40
60
80
100

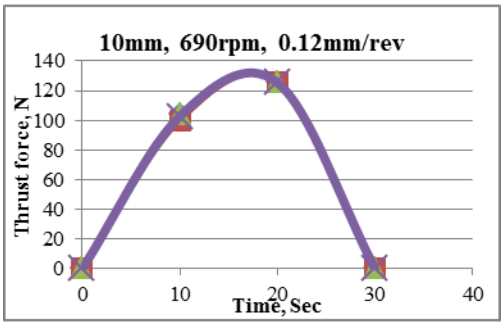
10mm, 690rpm, 0.12mm/rev
Thrust force, N
Time, Sec
0
20
40
60
80
100
120
140
0
10
20
30
40

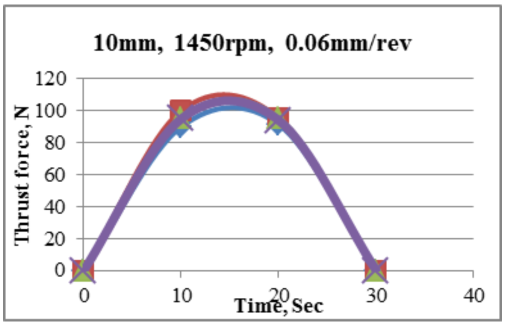
10mm, 1450rpm, 0.06mm/rev
Thrust force, N
Time, Sec
120
100
80
60
40
20
0
0
10
20
30
40

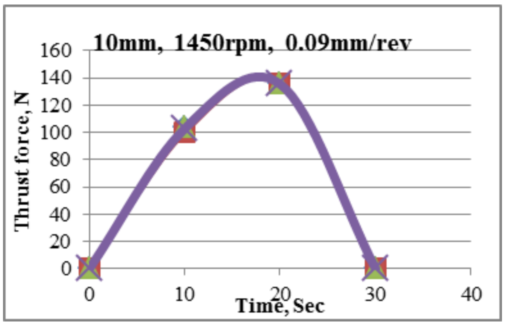
10mm, 1450rpm, 0.09mm/rev
Thrust force, N
Time, Sec
160
140
120
100
80
60
40
20
0
0
10
20
30
40

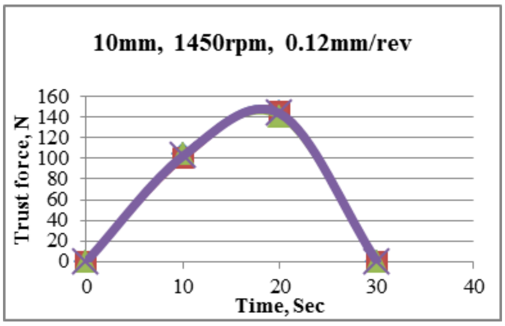
10mm, 1450rpm, 0.12mm/rev
Trust force, N
Time, Sec
160
140
120
100
80
60
40
20
0
0
10
20
30
40

B.2.2 Raw collected Torque data

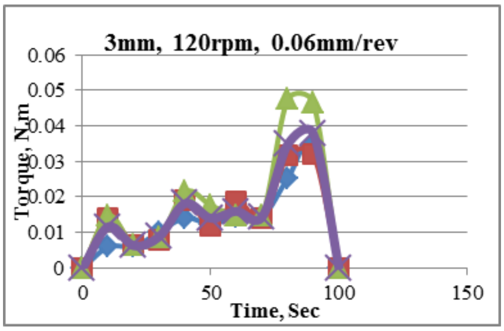

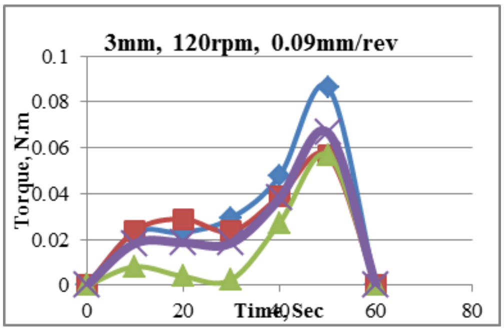

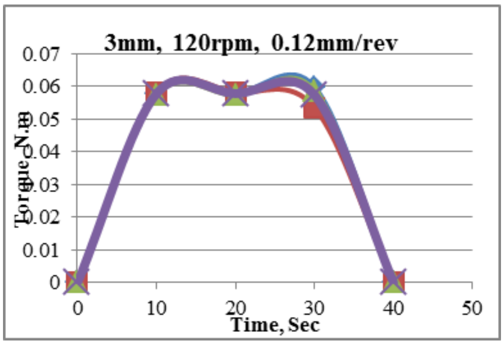

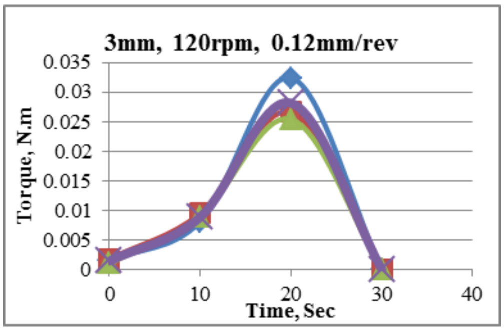

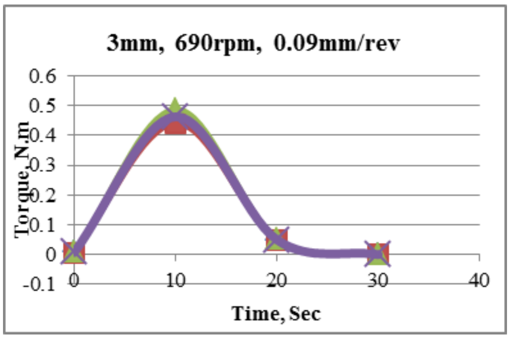

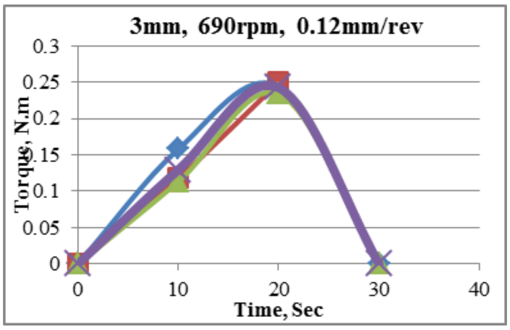

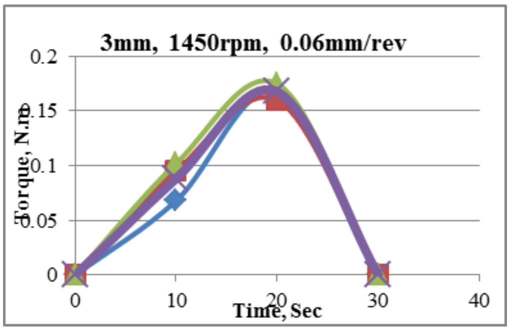

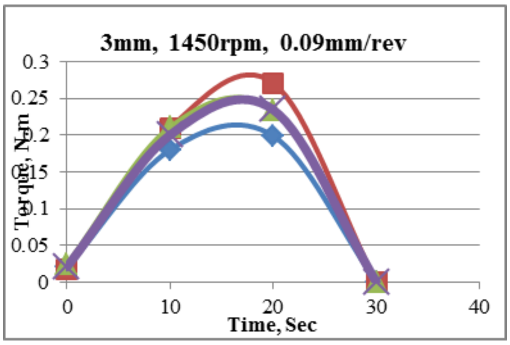

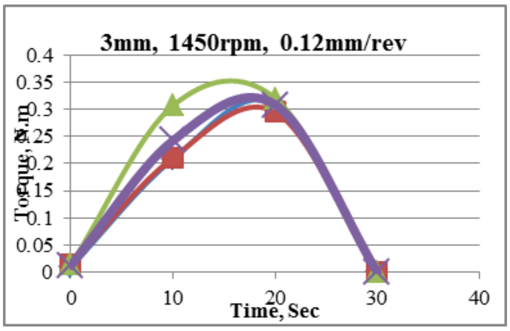
3mm, 1450rpm, 0.12mm/rev
Torque, N.m
Time, Sec

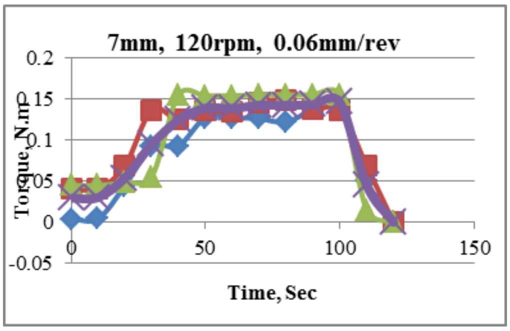
7mm, 120rpm, 0.06mm/rev
Torque, N.m
Time, Sec

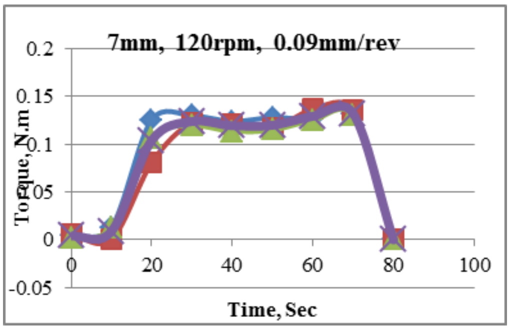
7mm, 120rpm, 0.09mm/rev
Torque, N.m
Time, Sec

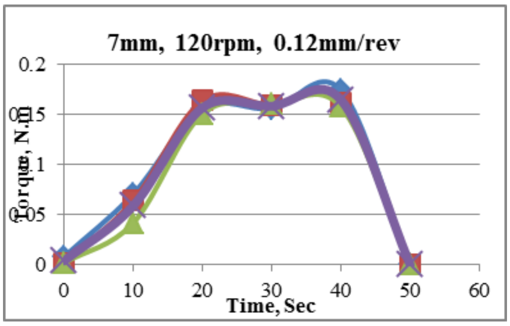
7mm, 120rpm, 0.12mm/rev
Torque, N.m
Time, Sec

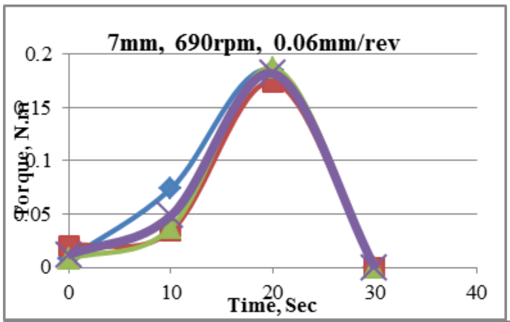
7mm, 690rpm, 0.06mm/rev
Torque, N.m
Time, Sec

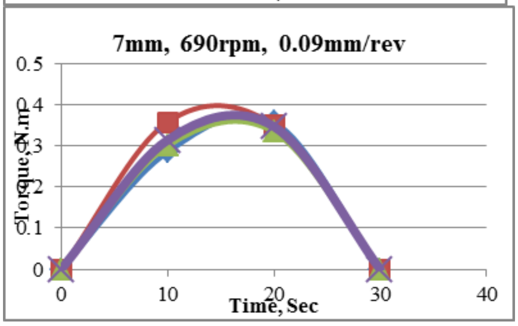
7mm, 690rpm, 0.09mm/rev
Torque, N.m
Time, Sec

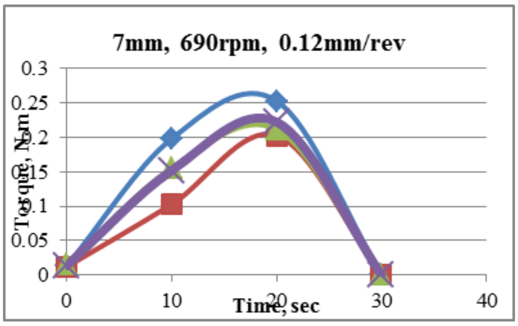
7mm, 690rpm, 0.12mm/rev
Torque, N.m
Time, sec

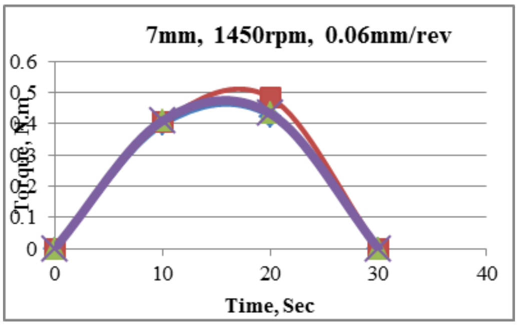
7mm, 1450rpm, 0.06mm/rev
Torque, N.m
Time, Sec

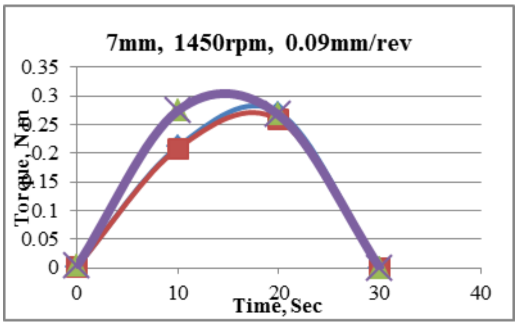
7mm, 1450rpm, 0.09mm/rev
Torque, N.m
Time, Sec

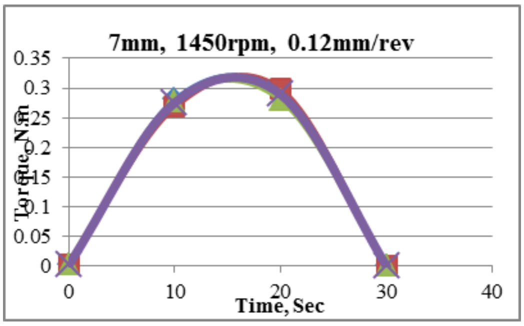
7mm, 1450rpm, 0.12mm/rev
Torque, N.m
Time, Sec

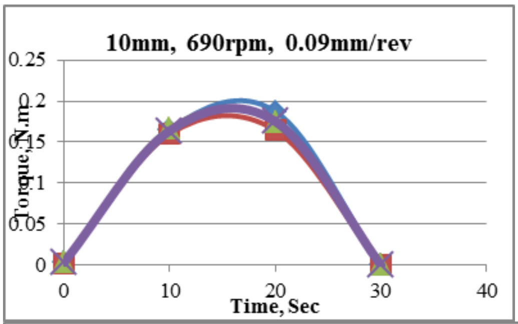
10mm, 690rpm, 0.09mm/rev
Torque, N.m
Time, Sec

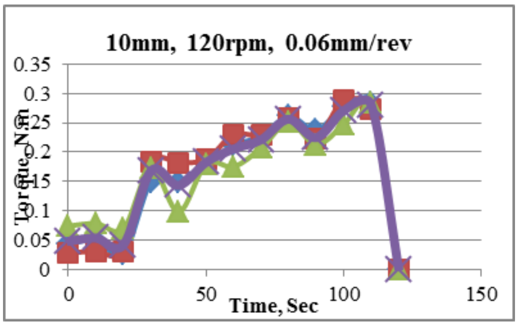
10mm, 120rpm, 0.06mm/rev
Torque, N.m
Time, Sec

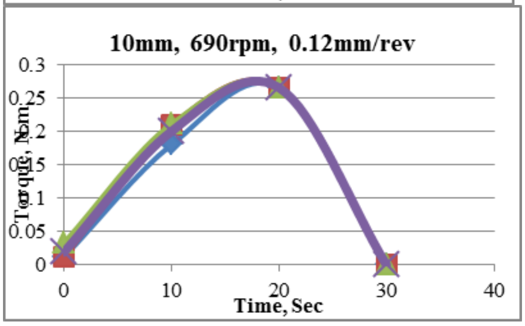
10mm, 690rpm, 0.12mm/rev
Torque, N.m
Time, Sec

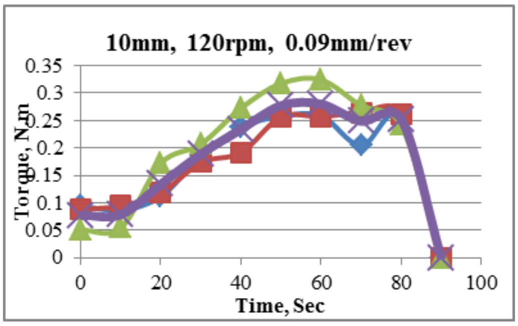
10mm, 120rpm, 0.09mm/rev
Torque, N.m
Time, Sec

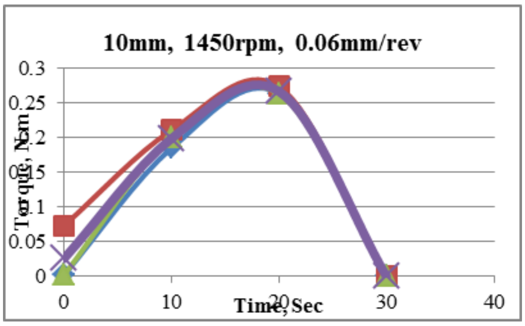
10mm, 1450rpm, 0.06mm/rev
Torque, N.m
Time, Sec

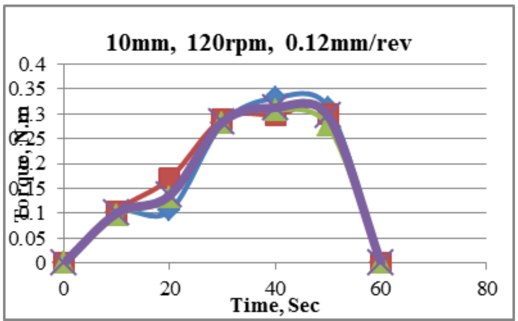
10mm, 120rpm, 0.12mm/rev
Torque, N.m
Time, Sec

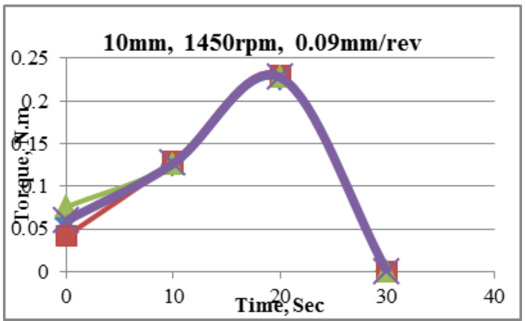
10mm, 1450rpm, 0.09mm/rev
Torque, N.m
Time, Sec

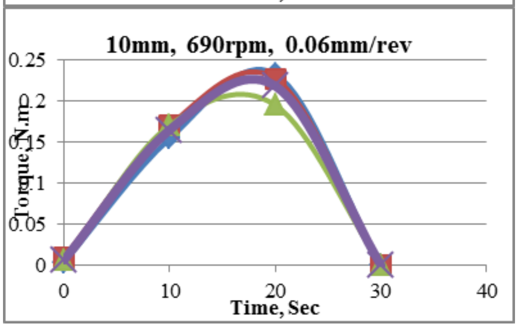
10mm, 690rpm, 0.06mm/rev
Torque, N.m
Time, Sec

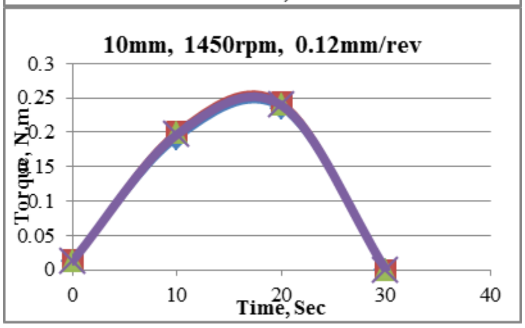
10mm, 1450rpm, 0.12mm/rev
Torque, N.m
Time, Sec

B.3 DPFEC

B.3.1 Raw collected Thrust forces data

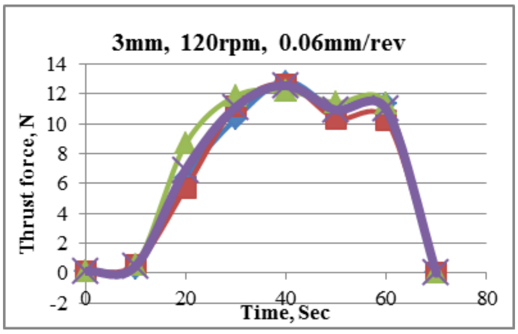

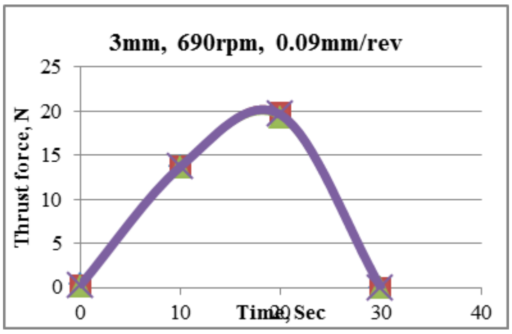

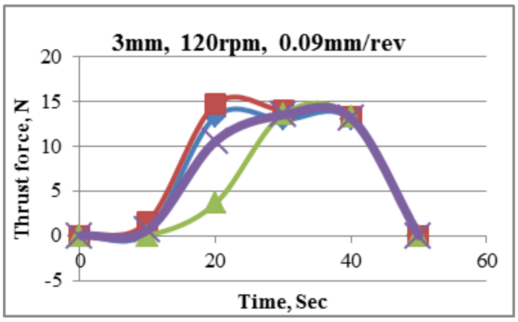

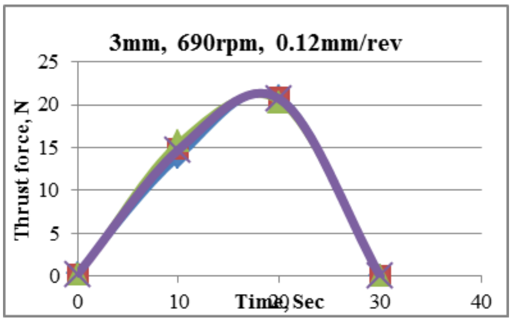

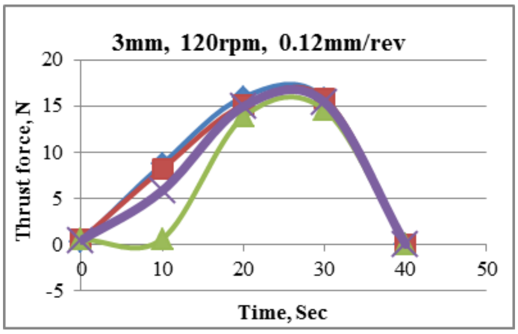

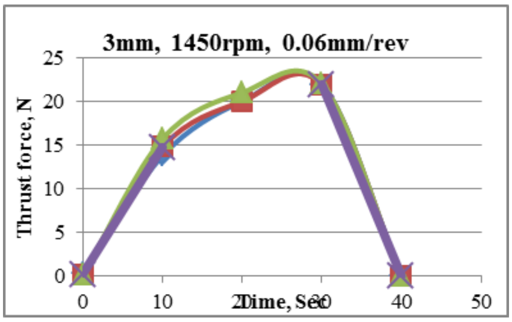

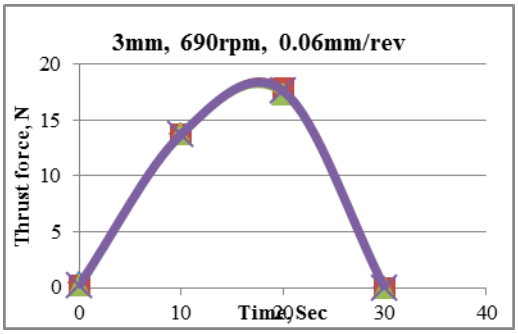

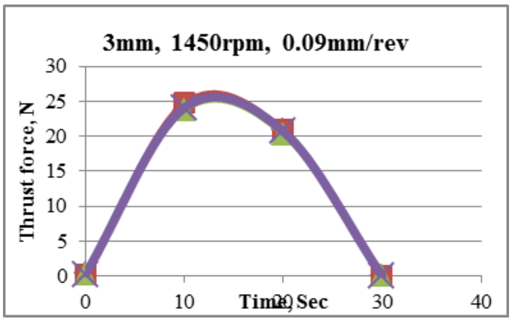

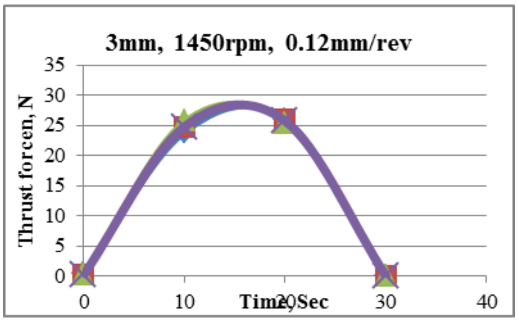
3mm, 1450rpm, 0.12mm/rev
Thrust forcen, N
Time, Sec

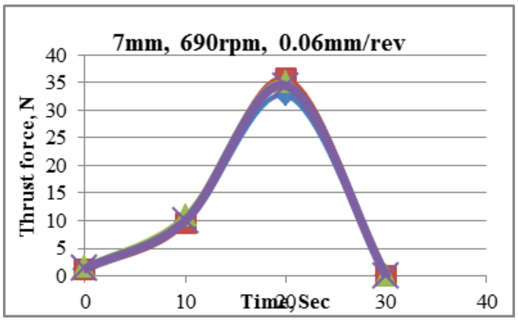
7mm, 690rpm, 0.06mm/rev
Thrust force, N
Time, Sec

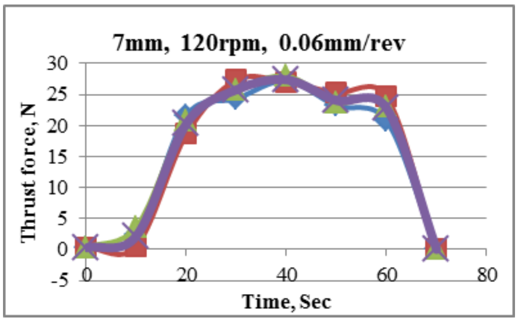
7mm, 120rpm, 0.06mm/rev
Thrust force, N
Time, Sec

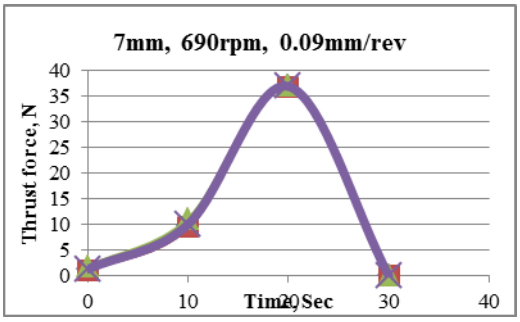
7mm, 690rpm, 0.09mm/rev
Thrust force, N
Time, Sec

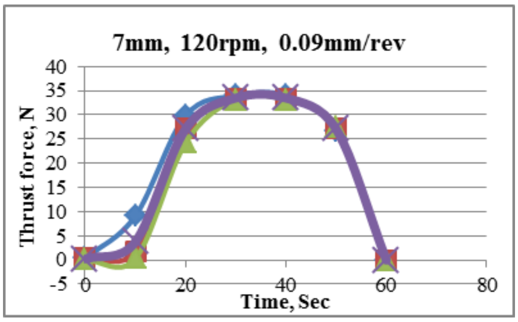
7mm, 120rpm, 0.09mm/rev
Thrust force, N
Time, Sec

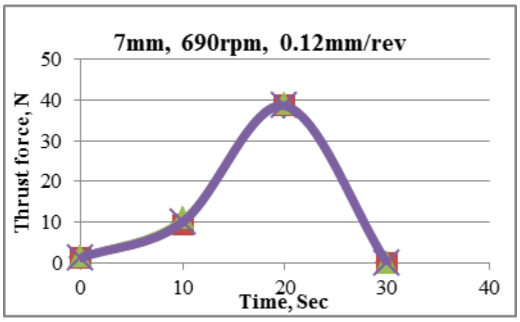
7mm, 690rpm, 0.12mm/rev
Thrust force, N
Time, Sec

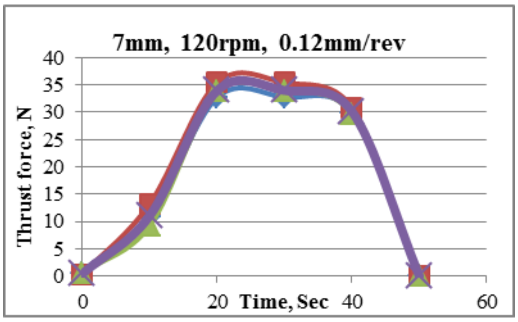
7mm, 120rpm, 0.12mm/rev
Thrust force, N
Time, Sec

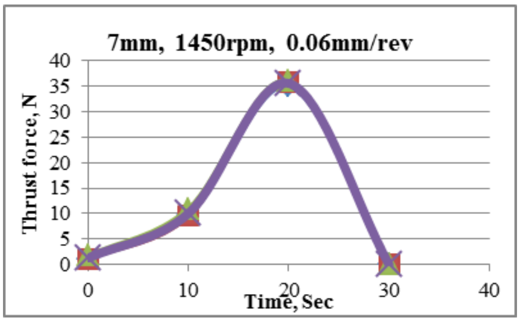
7mm, 1450rpm, 0.06mm/rev
Thrust force, N
Time, Sec

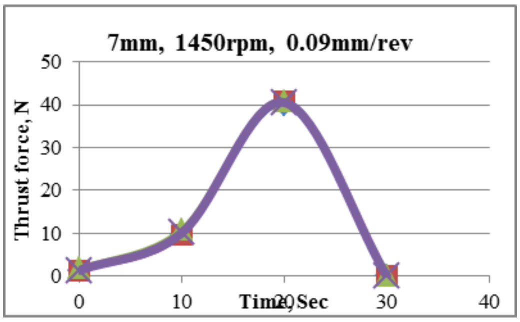
7mm, 1450rpm, 0.09mm/rev
Thrust force, N
Time, Sec

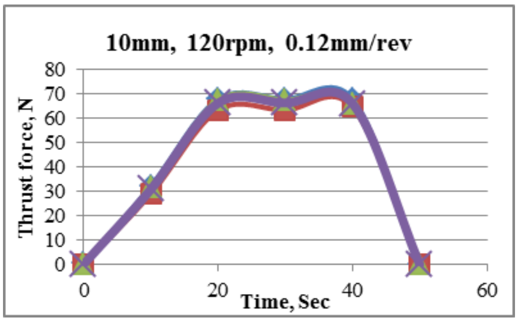
10mm, 120rpm, 0.12mm/rev
Thrust force, N
Time, Sec

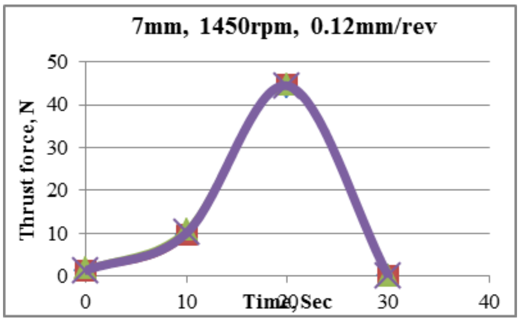
7mm, 1450rpm, 0.12mm/rev
Thrust force, N
Time, Sec

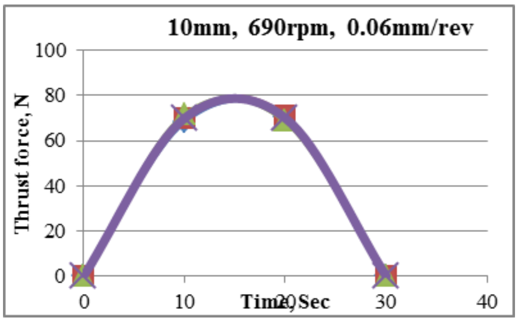
10mm, 690rpm, 0.06mm/rev
Thrust force, N
Time, Sec

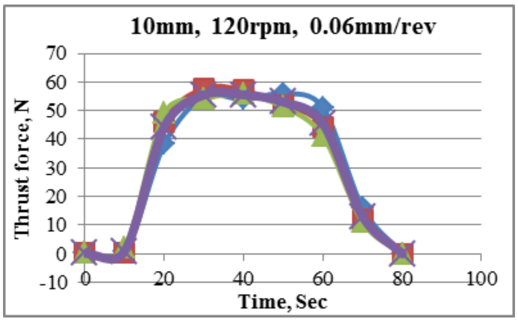
10mm, 120rpm, 0.06mm/rev
Thrust force, N
Time, Sec

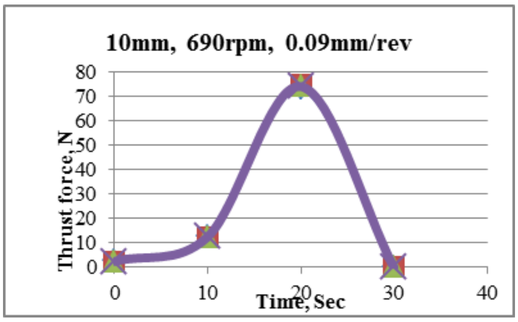
10mm, 690rpm, 0.09mm/rev
Thrust force, N
Time, Sec

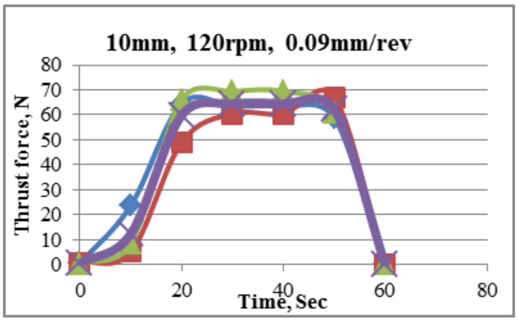
10mm, 120rpm, 0.09mm/rev
Thrust force, N
Time, Sec

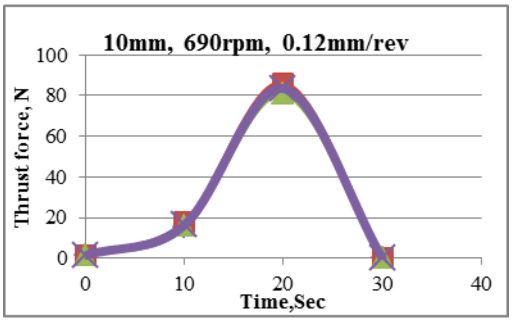
10mm, 690rpm, 0.12mm/rev
Thrust force, N
Time,Sec

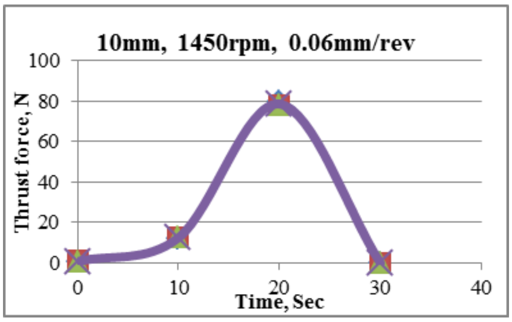

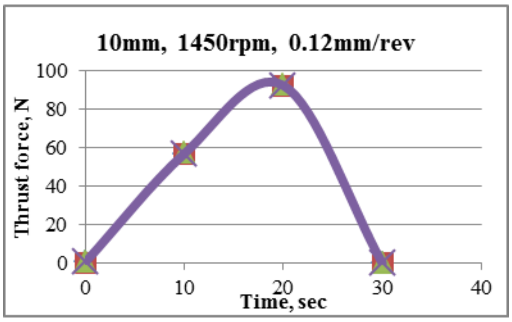

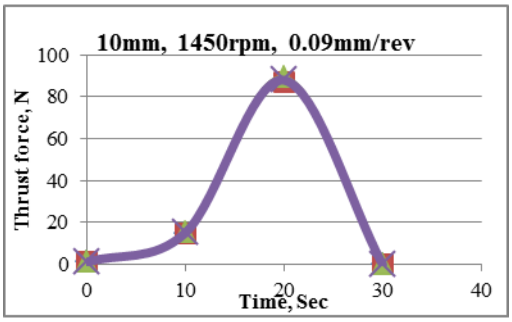

B.3.2 Raw collected Torque data

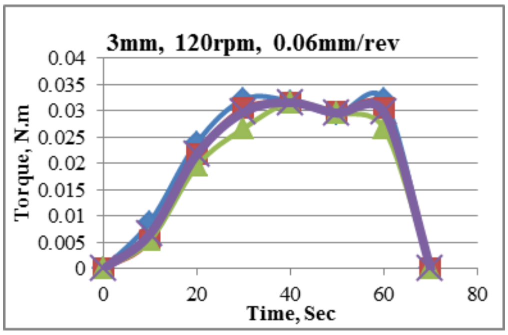

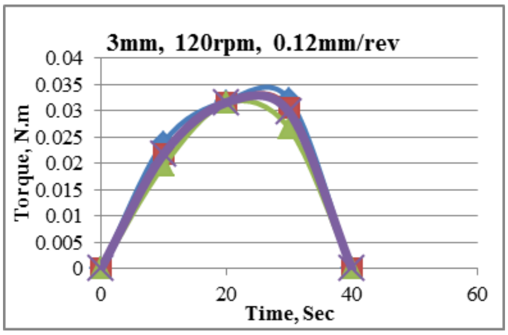

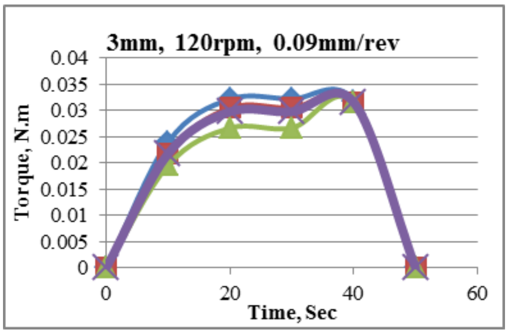

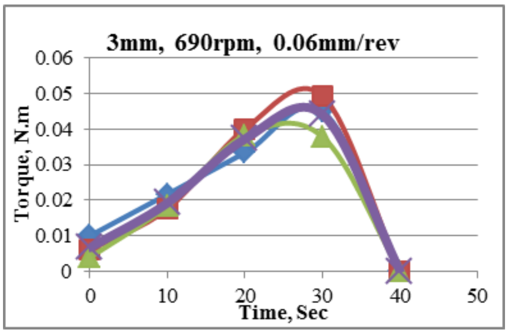

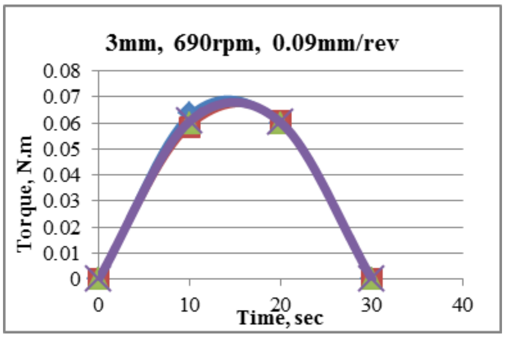
3mm, 690rpm, 0.09mm/rev
Torque, N.m
Time, sec

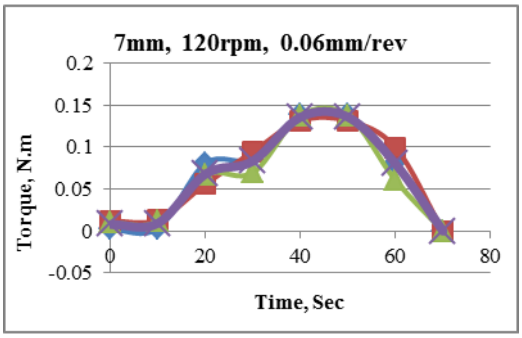
7mm, 120rpm, 0.06mm/rev
Torque, N.m
Time, Sec

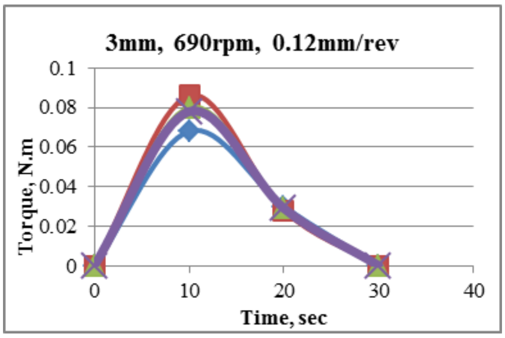
3mm, 690rpm, 0.12mm/rev
Torque, N.m
Time, sec

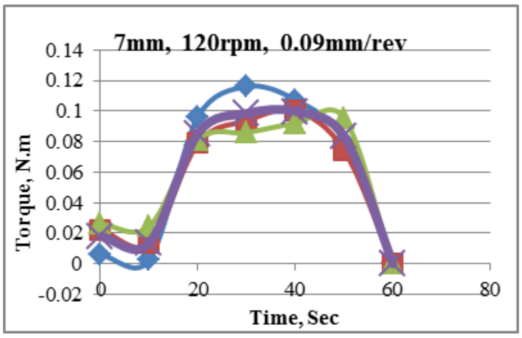
7mm, 120rpm, 0.09mm/rev
Torque, N.m
Time, Sec

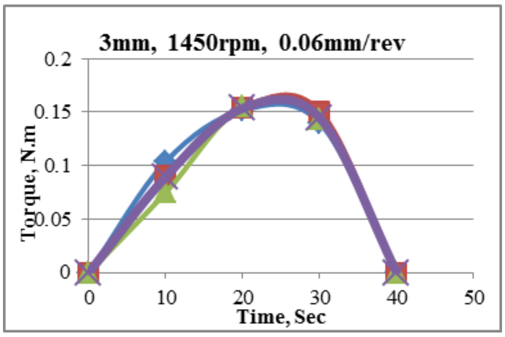
3mm, 1450rpm, 0.06mm/rev
Torque, N.m
Time, Sec

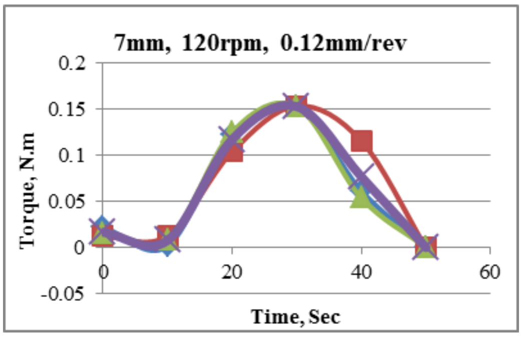
7mm, 120rpm, 0.12mm/rev
Torque, N.m
Time, Sec

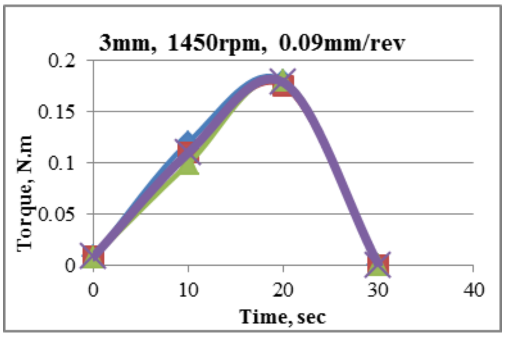
3mm, 1450rpm, 0.09mm/rev
Torque, N.m
Time, sec

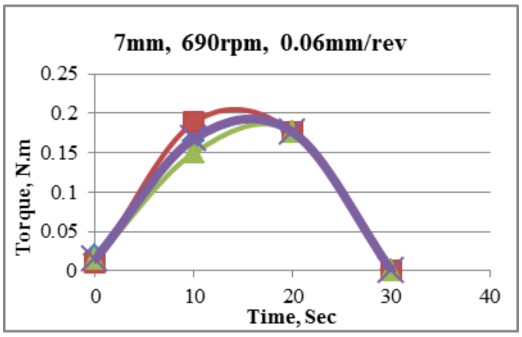
7mm, 690rpm, 0.06mm/rev
Torque, N.m
Time, Sec

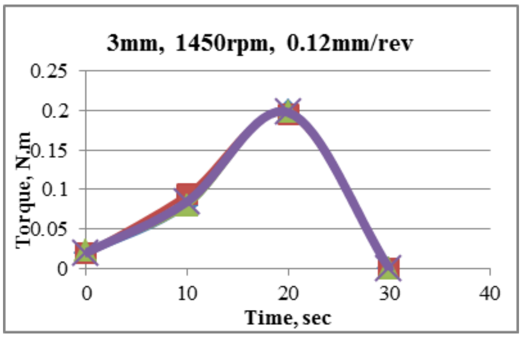
3mm, 1450rpm, 0.12mm/rev
Torque, N.m
Time, sec

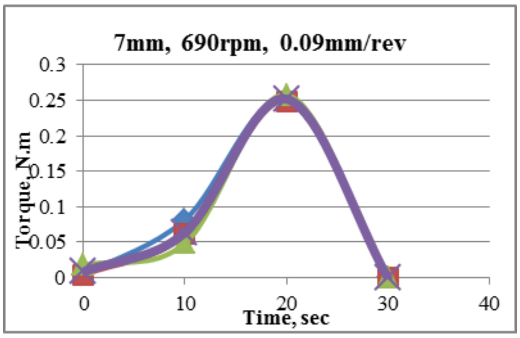
7mm, 690rpm, 0.09mm/rev
Torque, N.m
Time, sec

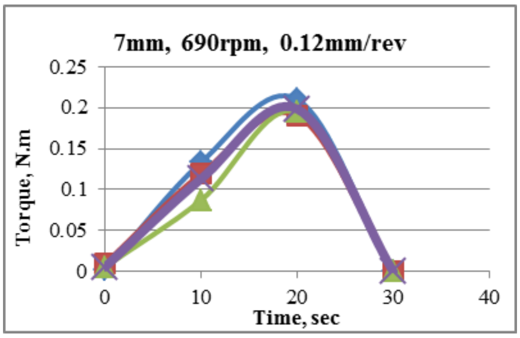
7mm, 690rpm, 0.12mm/rev
Torque, N.m
0 0.05 0.1 0.15 0.2 0.25
0 10 20 30 40
Time, sec

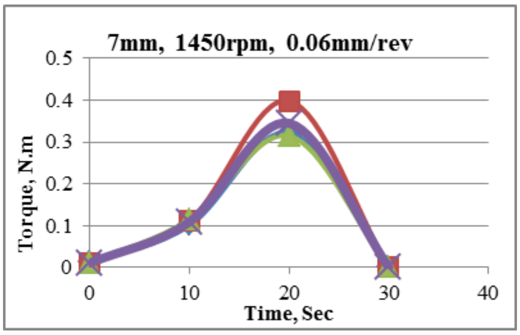
7mm, 1450rpm, 0.06mm/rev
Torque, N.m
0 0.1 0.2 0.3 0.4 0.5
0 10 20 30 40
Time, Sec

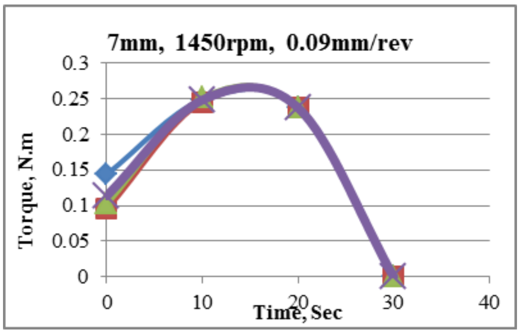
7mm, 1450rpm, 0.09mm/rev
Torque, N.m
0 0.05 0.1 0.15 0.2 0.25 0.3
0 10 20 30 40
Time, Sec

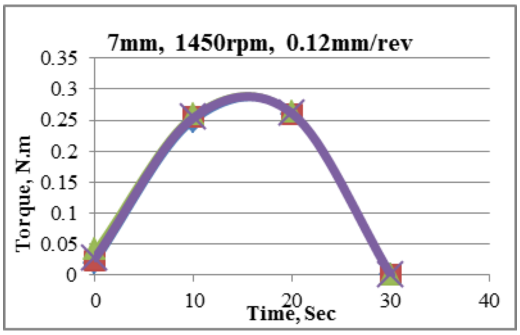
7mm, 1450rpm, 0.12mm/rev
Torque, N.m
0 0.05 0.1 0.15 0.2 0.25 0.3 0.35
0 10 20 30 40
Time, Sec

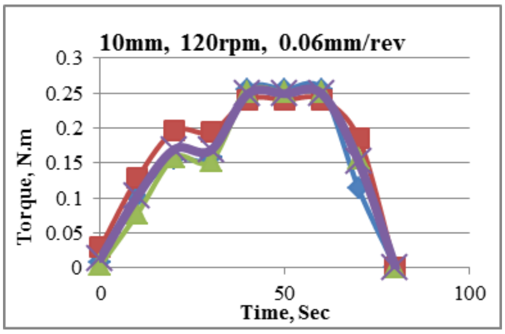
10mm, 120rpm, 0.06mm/rev
Torque, N.m
0 0.05 0.1 0.15 0.2 0.25 0.3
0 50 100
Time, Sec

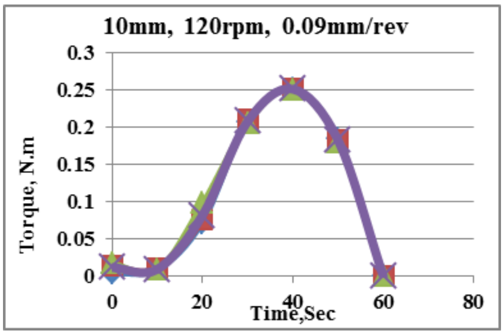
10mm, 120rpm, 0.09mm/rev
Torque, N.m
0 0.05 0.1 0.15 0.2 0.25 0.3
0 20 40 60 80
Time,Sec

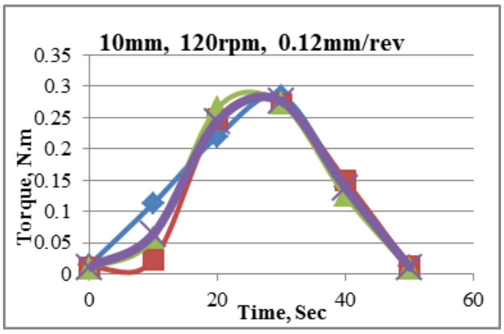
10mm, 120rpm, 0.12mm/rev
Torque, N.m
0 0.05 0.1 0.15 0.2 0.25 0.3 0.35
0 20 40 60
Time, Sec

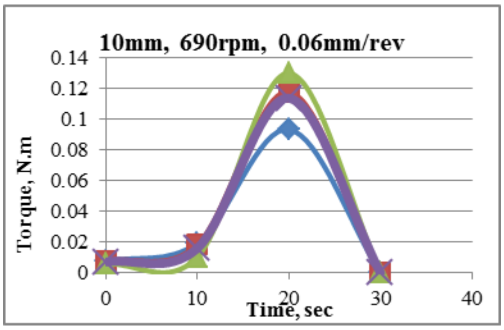
10mm, 690rpm, 0.06mm/rev
Torque, N.m
0 0.02 0.04 0.06 0.08 0.1 0.12 0.14
0 10 20 30 40
Time, sec

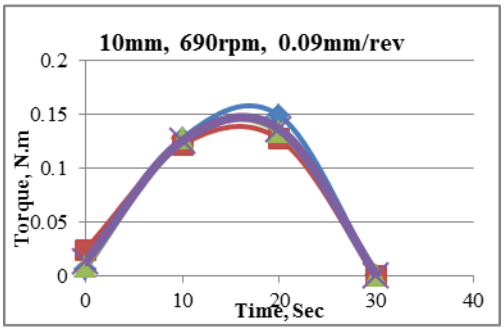
10mm, 690rpm, 0.09mm/rev
Torque, N.m
0 0.05 0.1 0.15 0.2
0 10 20 30 40
Time, Sec

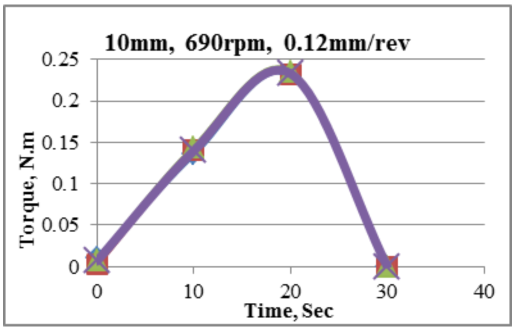
10mm, 690rpm, 0.12mm/rev
Torque, N.m
0 0.05 0.1 0.15 0.2 0.25
0 10 20 30 40
Time, Sec

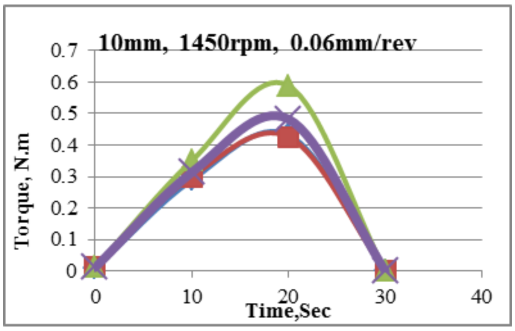
10mm, 1450rpm, 0.06mm/rev
Torque, N.m
Time,Sec
0
0.1
0.2
0.3
0.4
0.5
0.6
0.7
10
20
30
40

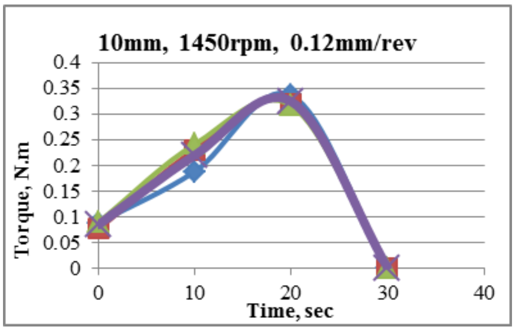
10mm, 1450rpm, 0.12mm/rev
Torque, N.m
Time, sec
0
0.05
0.1
0.15
0.2
0.25
0.3
0.35
0.4
10
20
30
40

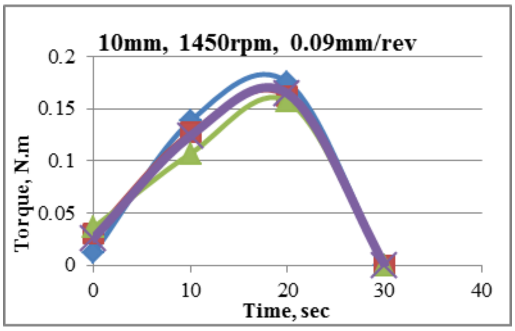
10mm, 1450rpm, 0.09mm/rev
Torque, N.m
Time, sec
0
0.05
0.1
0.15
0.2
10
20
30
40

APPENDIX C: OPTICAL MICROSCOPY IMAGES USED FOR MACHINABILITY

C.1 Neat

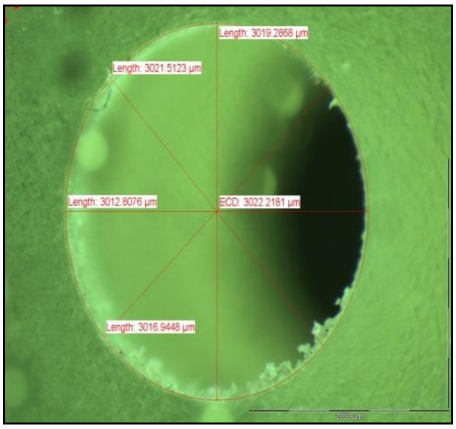

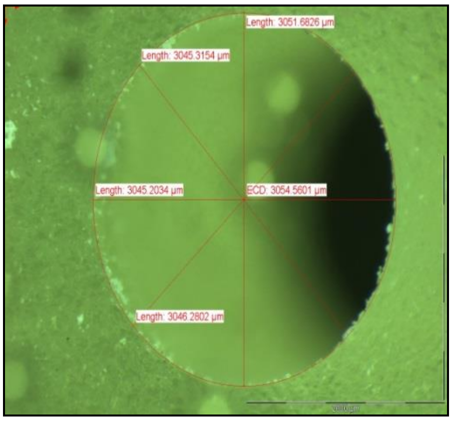

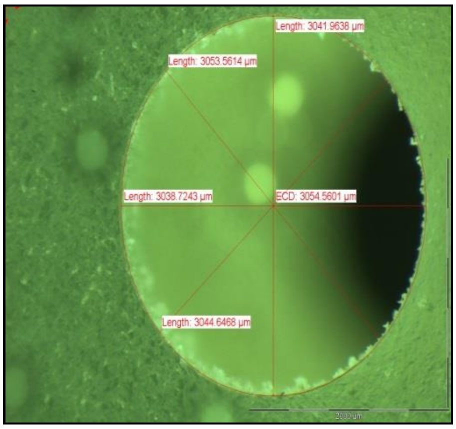

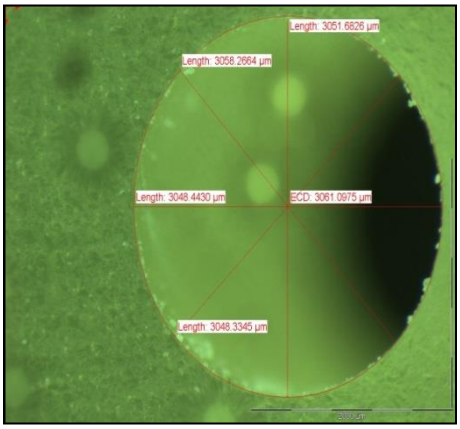

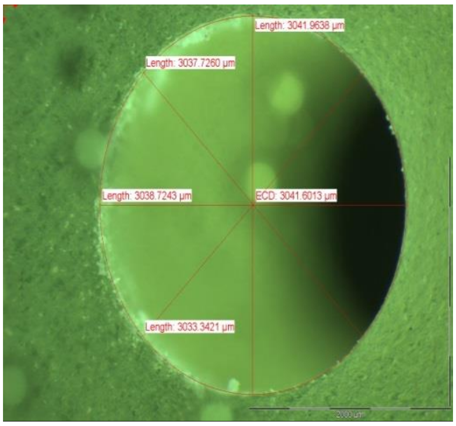

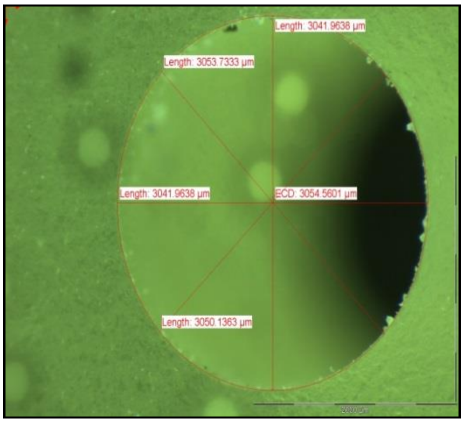

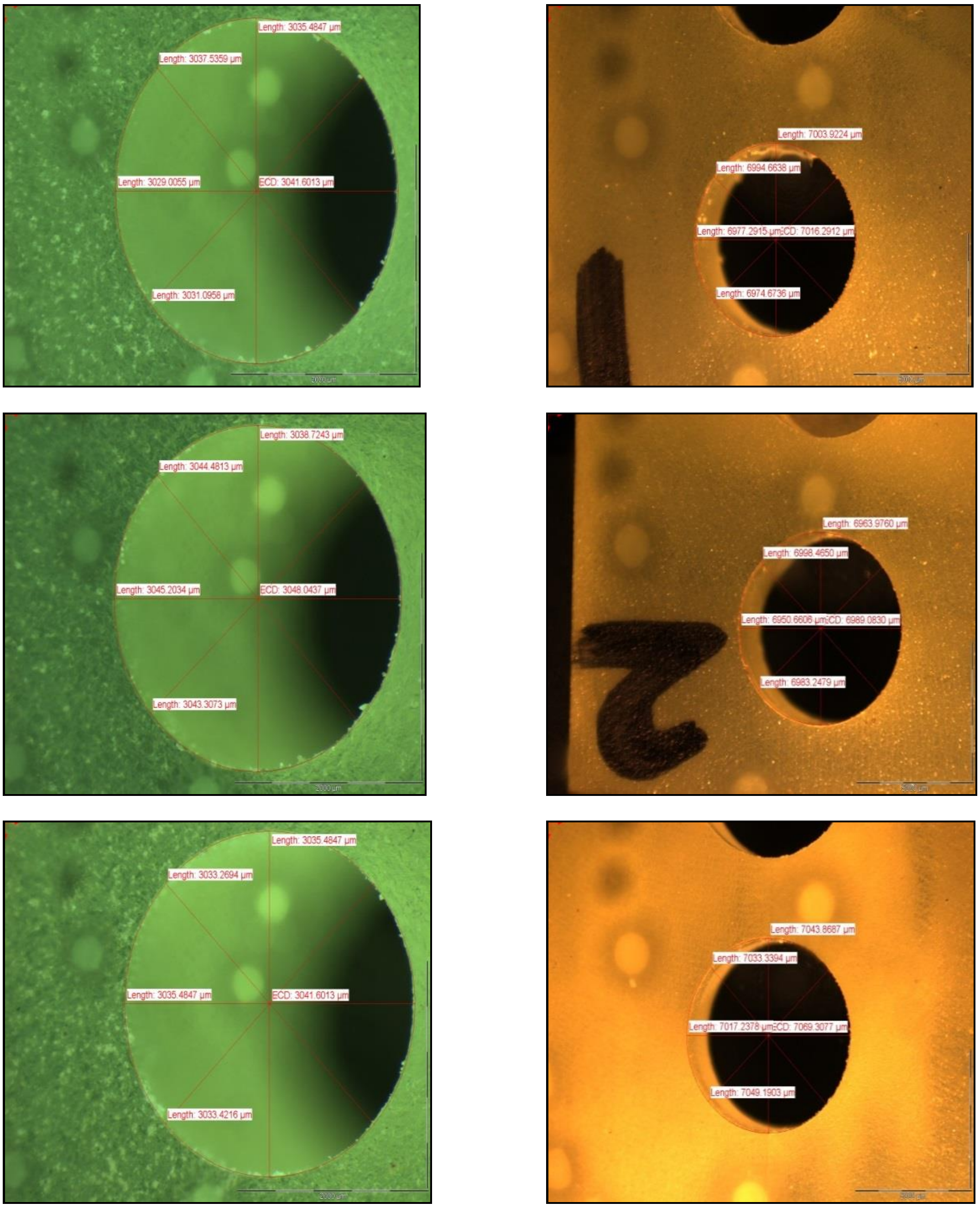
Length: 3035.4847 µm
Length: 3037.5359 µm
Length: 3029.0055 µm
ECD: 3041.6013 µm
Length: 3031.0958 µm
Length: 7003.9224 µm
Length: 6994.6638 µm
Length: 6977.2915 µm
ECD: 7016.2912 µm
Length: 6974.6736 µm
Length: 3038.7243 µm
Length: 3044.4813 µm
Length: 3045.2034 µm
ECD: 3048.0437 µm
Length: 3043.3073 µm
Length: 6963.9760 µm
Length: 6998.4650 µm
Length: 6950.6608 µm
ECD: 6989.0830 µm
Length: 6983.2479 µm
Length: 3035.4847 µm
Length: 3033.2694 µm
Length: 3035.4847 µm
ECD: 3041.6013 µm
Length: 3033.4216 µm
Length: 7043.8687 µm
Length: 7033.3394 µm
Length: 7017.2378 µm
ECD: 7069.3077 µm
Length: 7049.1903 µm

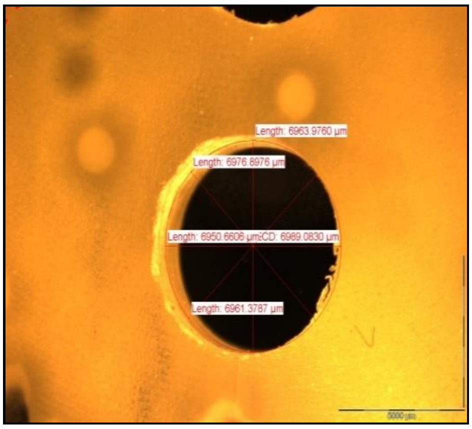
Length: 6963.9760 µm
Length: 6976.8976 µm
Length: 6950.6606 µm ECD: 6989.0830 µm
Length: 6961.3787 µm

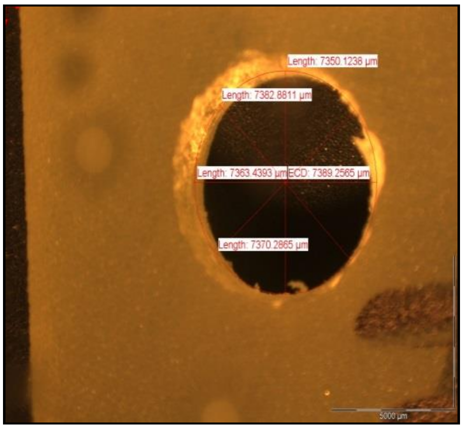
Length: 7350.1238 µm
Length: 7382.8811 µm
Length: 7363.4393 µm ECD: 7389.2565 µm
Length: 7370.2865 µm

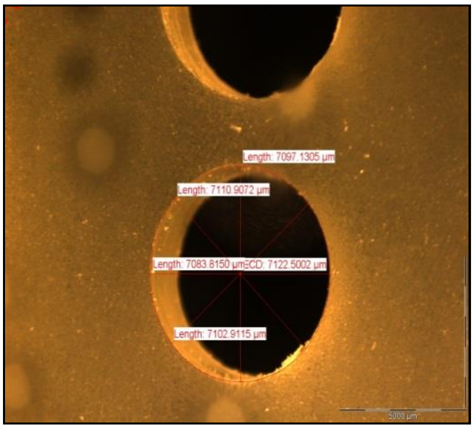
Length: 7097.1305 µm
Length: 7110.9072 µm
Length: 7083.8150 µm ECD: 7122.5002 µm
Length: 7102.9115 µm

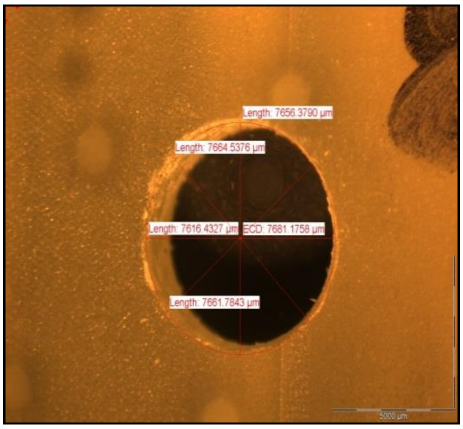
Length: 7656.3790 µm
Length: 7664.5376 µm
Length: 7616.4327 µm ECD: 7681.1758 µm
Length: 7661.7843 µm

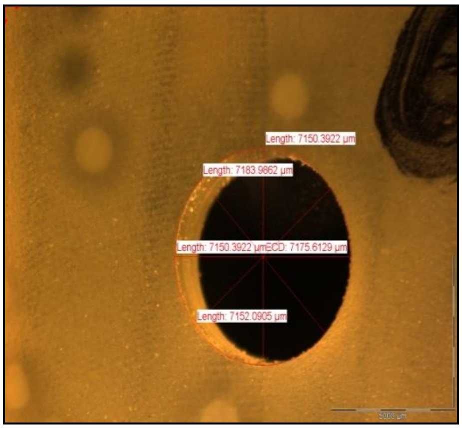
Length: 7150.3922 µm
Length: 7183.9862 µm
Length: 7150.3922 µm ECD: 7175.6129 µm
Length: 7152.0905 µm

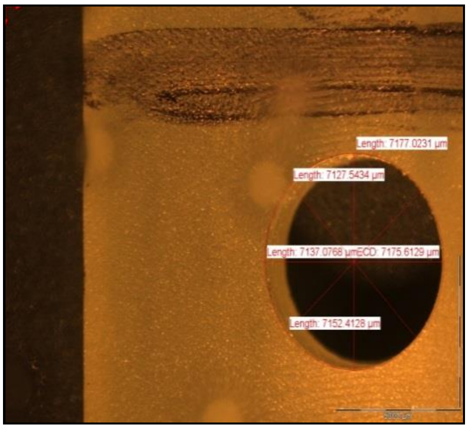
Length: 7177.0231 µm
Length: 7127.5434 µm
Length: 7137.0768 µm ECD: 7175.6129 µm
Length: 7152.4128 µm

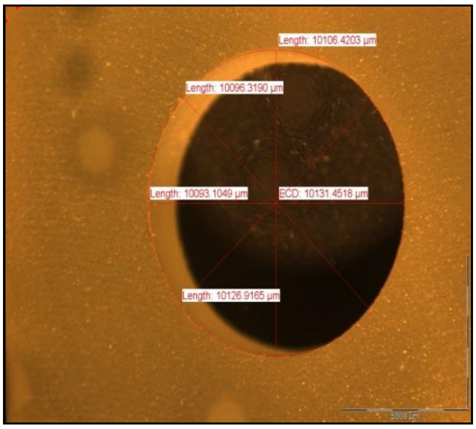
Length: 10106.4203 µm
Length: 10096.3190 µm
Length: 10093.1049 µm
ECD: 10131.4518 µm
Length: 10126.9165 µm

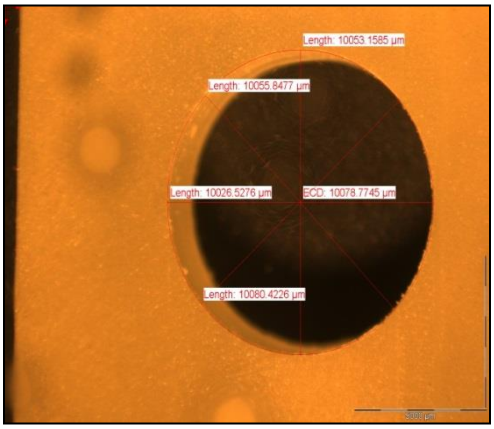
Length: 10053.1585 µm
Length: 10055.8477 µm
Length: 10026.5276 µm
ECD: 10078.7745 µm
Length: 10080.4226 µm

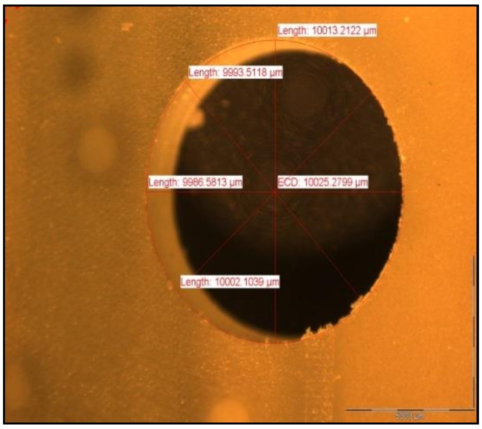
Length: 10013.2122 µm
Length: 9993.5118 µm
Length: 9986.5813 µm
ECD: 10025.2799 µm
Length: 10002.1039 µm

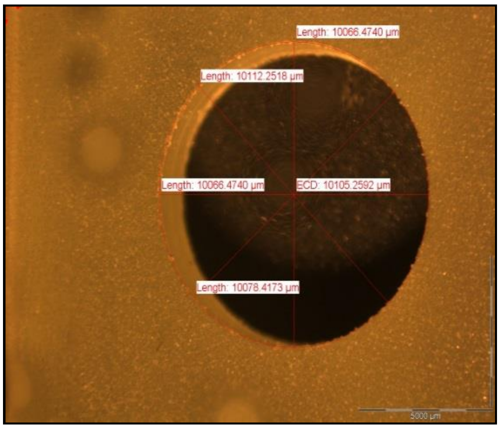
Length: 10066.4740 µm
Length: 10112.2518 µm
Length: 10066.4740 µm
ECD: 10105.2592 µm
Length: 10078.4173 µm
5000 µm

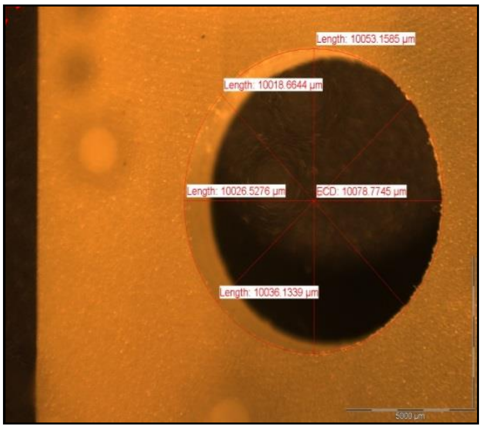
Length: 10053.1585 µm
Length: 10018.6644 µm
Length: 10026.5276 µm
ECD: 10078.7745 µm
Length: 10036.1339 µm

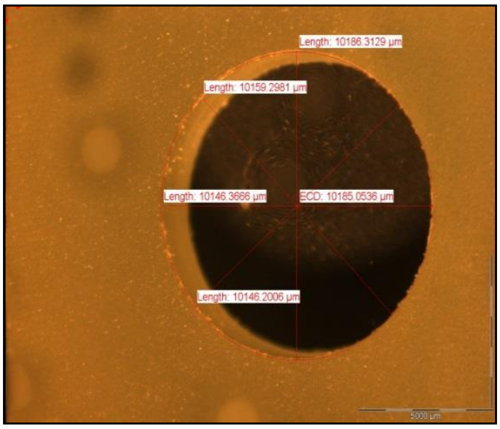
Length: 10186.3129 µm
Length: 10159.2981 µm
Length: 10146.3666 µm
ECD: 10185.0536 µm
Length: 10146.2006 µm

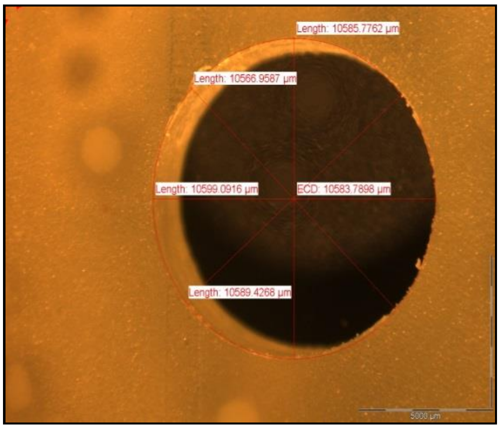
Length: 10585.7762 µm
Length: 10566.9587 µm
Length: 10599.0916 µm
ECD: 10583.7898 µm
Length: 10589.4268 µm

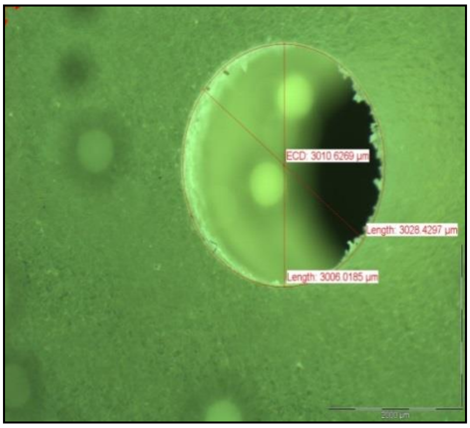
ECD: 3010.6269 µm
Length: 3028.4297 µm
Length: 3006.0185 µm

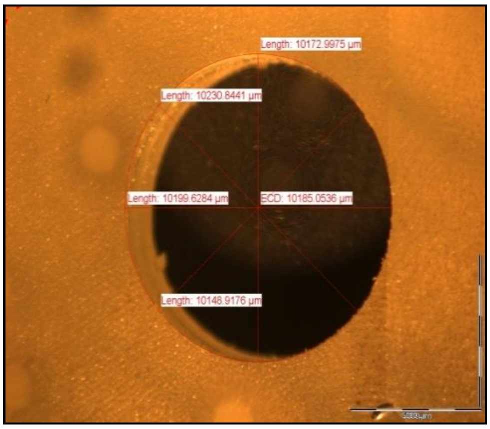
Length: 10172.9975 µm
Length: 10230.8441 µm
Length: 10199.6284 µm
ECD: 10185.0536 µm
Length: 10148.9176 µm

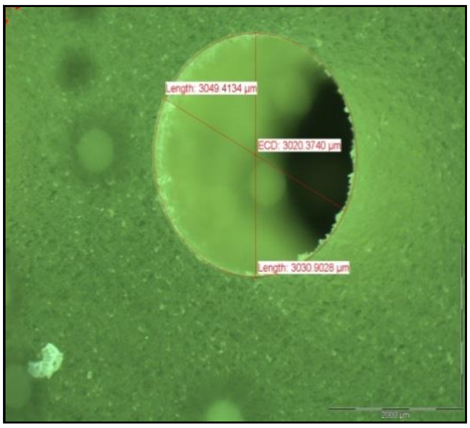
Length: 3049.4134 µm
ECD: 3020.3740 µm
Length: 3030.9028 µm

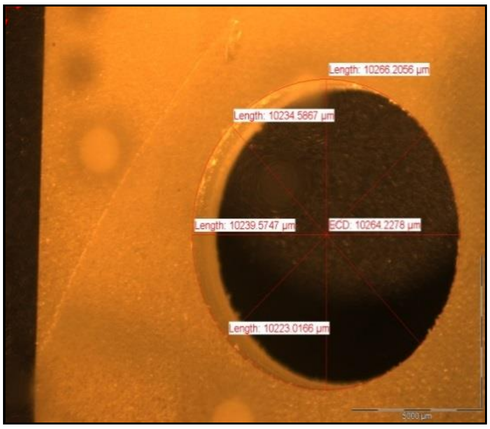
Length: 10266.2056 µm
Length: 10234.5867 µm
Length: 10239.5747 µm
ECD: 10264.2278 µm
Length: 10223.0166 µm

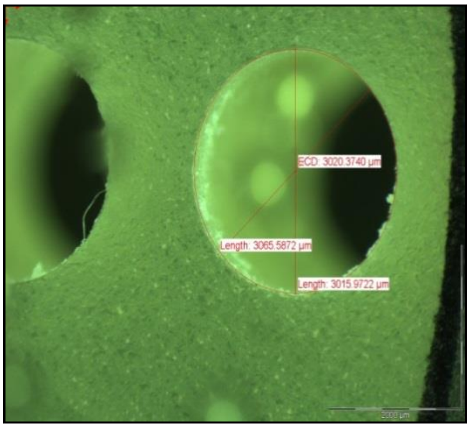
ECD: 3020.3740 µm
Length: 3065.5872 µm
Length: 3015.9722 µm

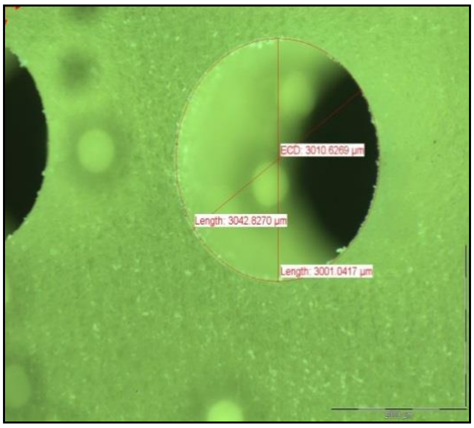
ECD: 3010.6269 µm
Length: 3042.8270 µm
Length: 3001.0417 µm

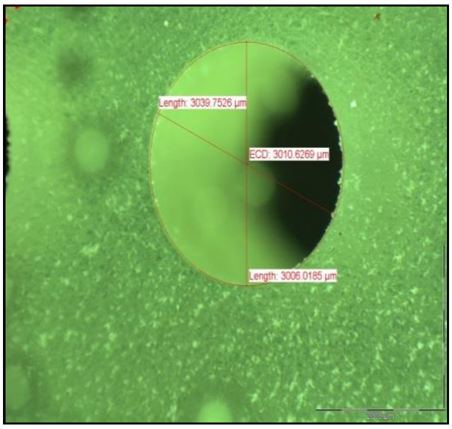
Length: 3039.7526 µm
ECD: 3010.6269 µm
Length: 3006.0185 µm

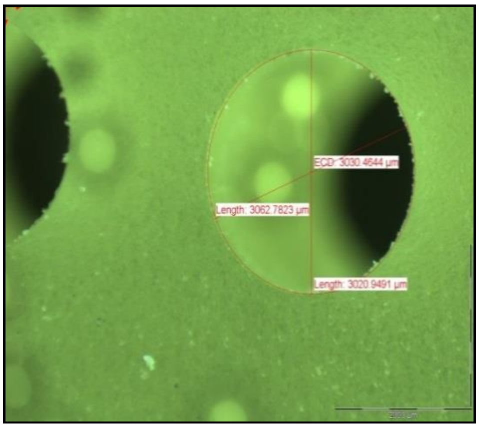
ECD: 3030.4644 µm
Length: 3062.7823 µm
Length: 3020.9491 µm

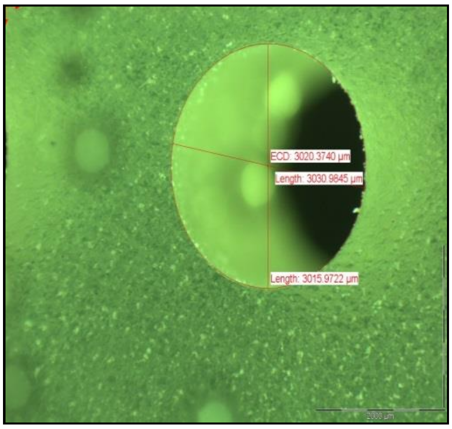
ECD: 3020.3740 µm
Length: 3030.9845 µm
Length: 3015.9722 µm

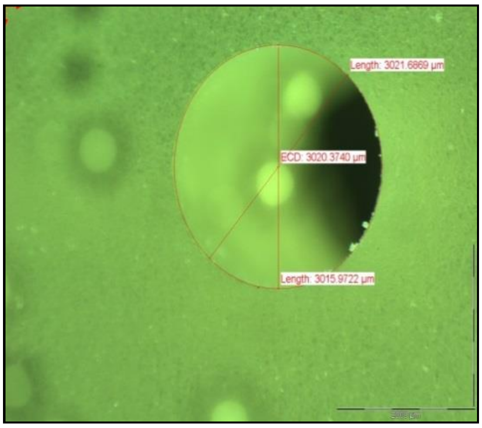
Length: 3021.6869 µm
ECD: 3020.3740 µm
Length: 3015.9722 µm

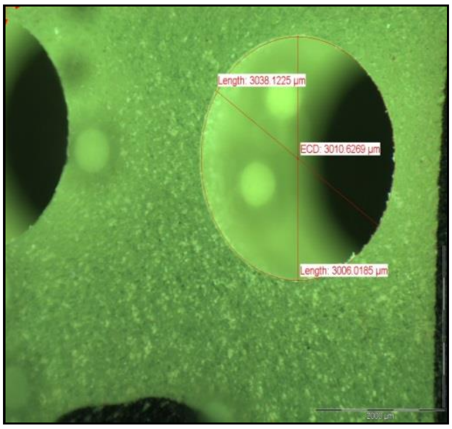
Length: 3038.1225 µm
ECD: 3010.6269 µm
Length: 3006.0185 µm

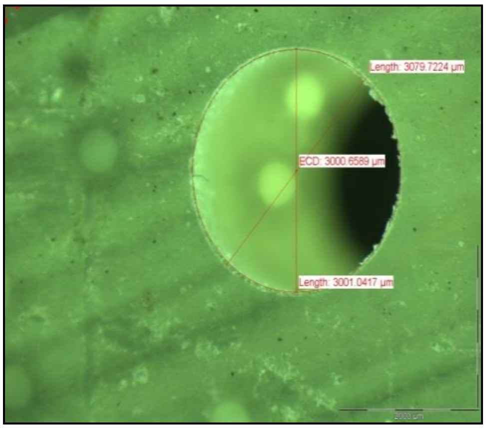
Length: 3079.7224 µm
ECD: 3000.6589 µm
Length: 3001.0417 µm

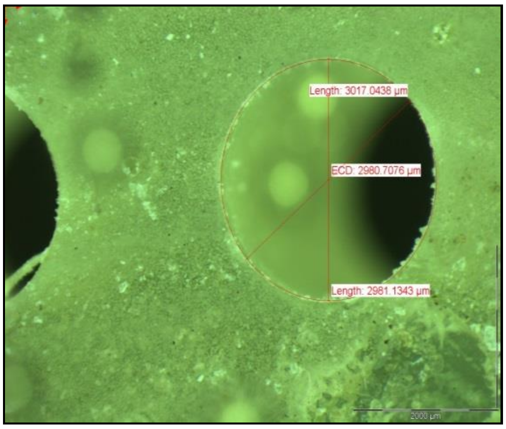
Length: 3017.0438 µm
ECD: 2980.7076 µm
Length: 2981.1343 µm

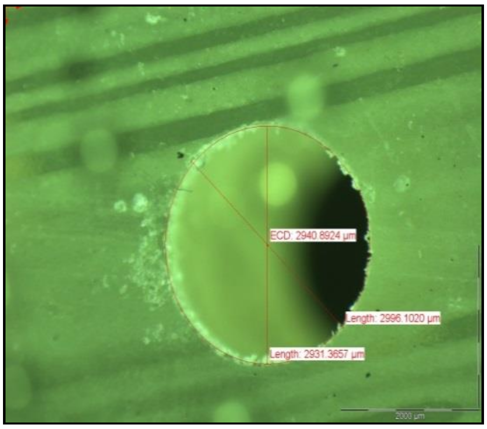
ECD: 2940.8924 µm
Length: 2996.1020 µm
Length: 2931.3657 µm

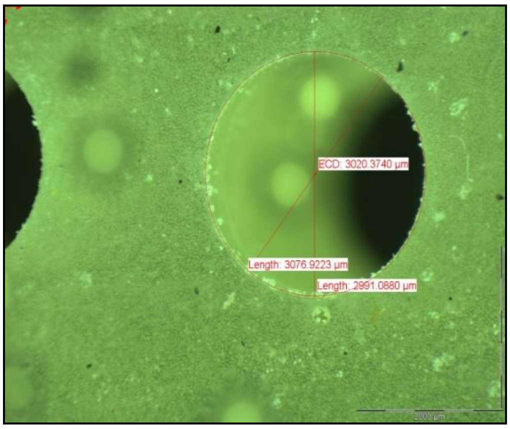
ECD: 3020.3740 µm
Length: 3076.9223 µm
Length: 2991.0880 µm

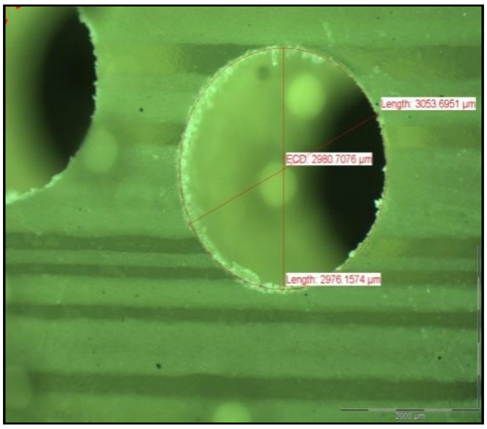
Length: 3053.6951 µm
ECD: 2980.7076 µm
Length: 2976.1574 µm

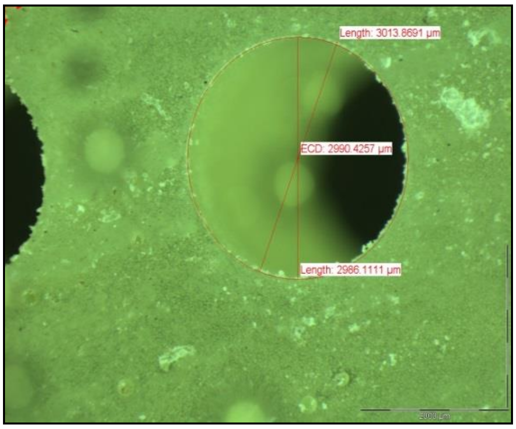
Length: 3013.8691 µm
ECD: 2990.4257 µm
Length: 2986.1111 µm

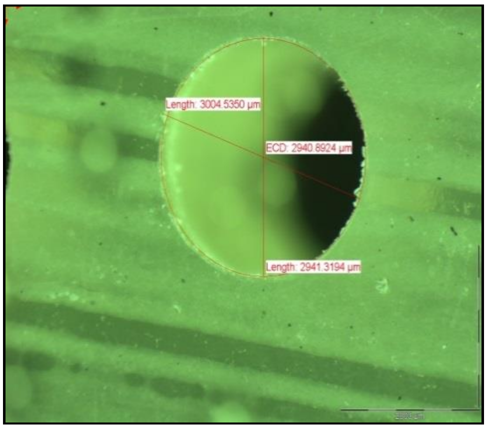
Length: 3004.5350 µm
ECD: 2940.8924 µm
Length: 2941.3194 µm

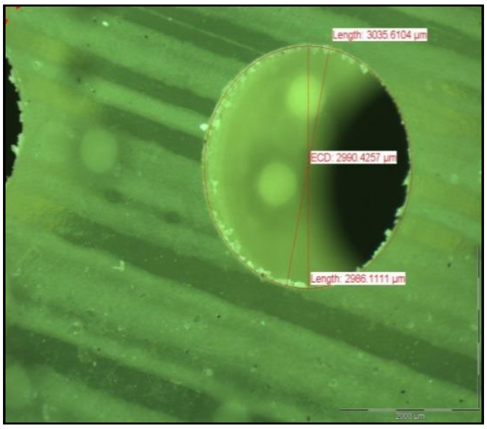
Length: 3035.6104 µm
ECD: 2990.4257 µm
Length: 2986.1111 µm

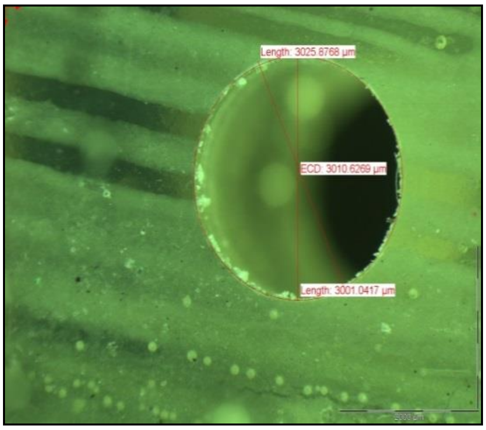
Length: 3025.8768 µm
ECD: 3010.6269 µm
Length: 3001.0417 µm

C.2 GFEC

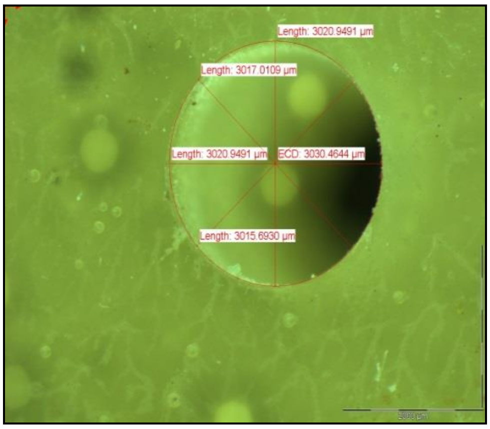
Length: 3020.9491 µm
Length: 3017.0109 µm
Length: 3020.9491 µm
ECD: 3030.4644 µm
Length: 3015.6930 µm

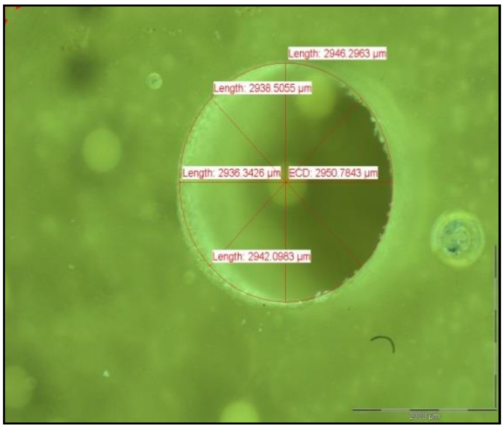
Length: 2946.2963 µm
Length: 2938.5055 µm
Length: 2936.3426 µm
ECD: 2950.7843 µm
Length: 2942.0983 µm

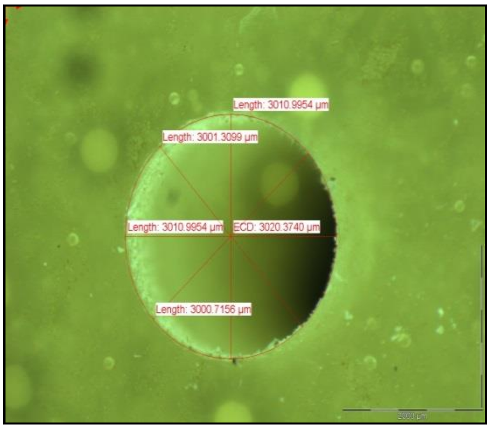
Length: 3010.9954 µm
Length: 3001.3099 µm
Length: 3010.9954 µm
ECD: 3020.3740 µm
Length: 3000.7156 µm

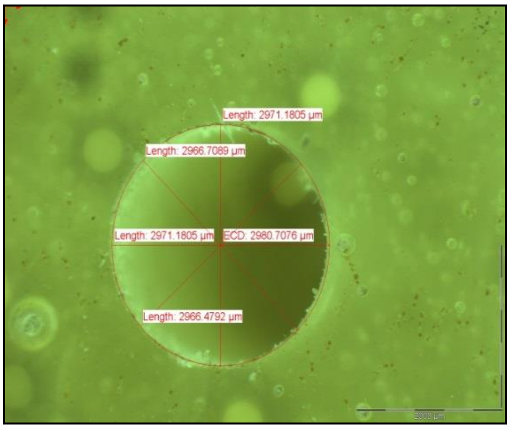
Length: 2971.1805 µm
Length: 2966.7089 µm
Length: 2971.1805 µm
ECD: 2980.7076 µm
Length: 2966.4792 µm

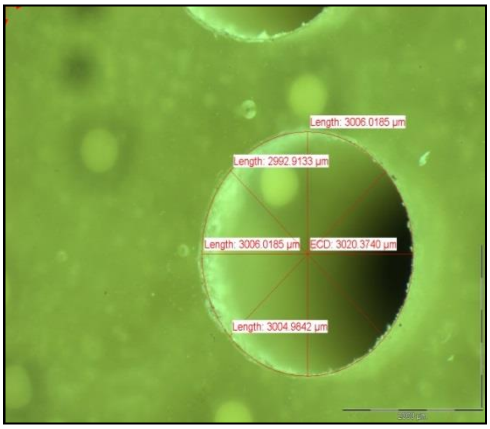
Length: 3006.0185 µm
Length: 2992.9133 µm
Length: 3006.0185 µm
ECD: 3020.3740 µm
Length: 3004.9842 µm

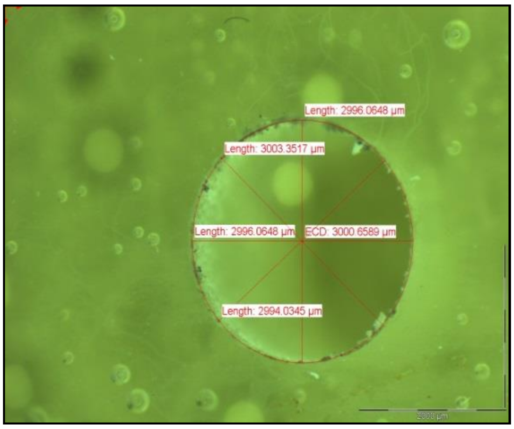
Length: 2996.0648 µm
Length: 3003.3517 µm
Length: 2996.0648 µm
ECD: 3000.6589 µm
Length: 2994.0345 µm

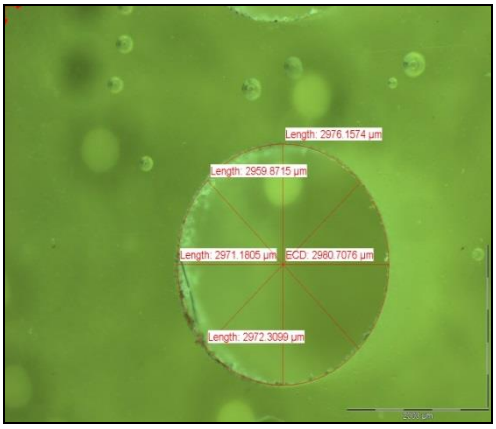
Length: 2976.1574 µm
Length: 2959.8715 µm
Length: 2971.1805 µm
ECD: 2980.7076 µm
Length: 2972.3099 µm

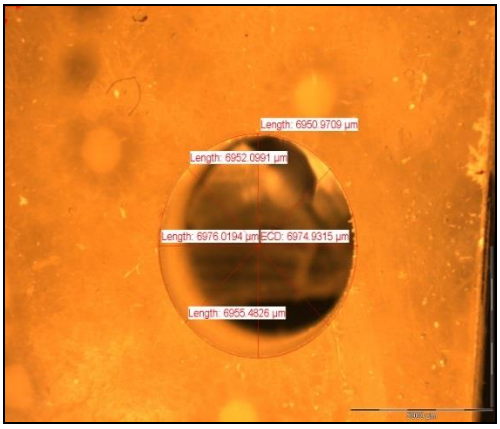
Length: 6950.9709 µm
Length: 6952.0991 µm
Length: 6976.0194 µm
ECD: 6974.9315 µm
Length: 6955.4826 µm

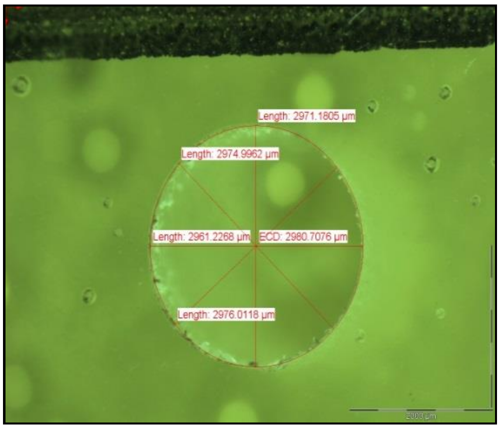
Length: 2971.1805 µm
Length: 2974.9962 µm
Length: 2961.2268 µm
ECD: 2980.7076 µm
Length: 2976.0118 µm

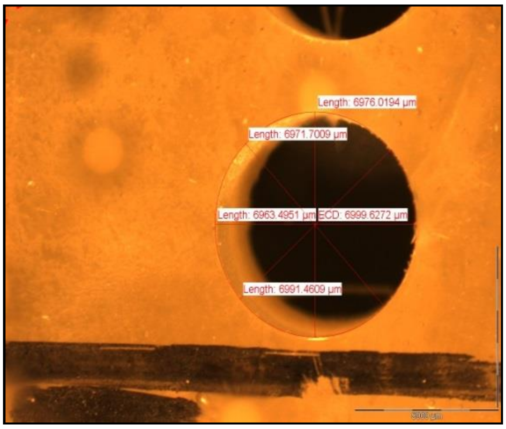
Length: 6976.0194 µm
Length: 6971.7009 µm
Length: 6963.4951 µm
ECD: 6999.6272 µm
Length: 6991.4609 µm

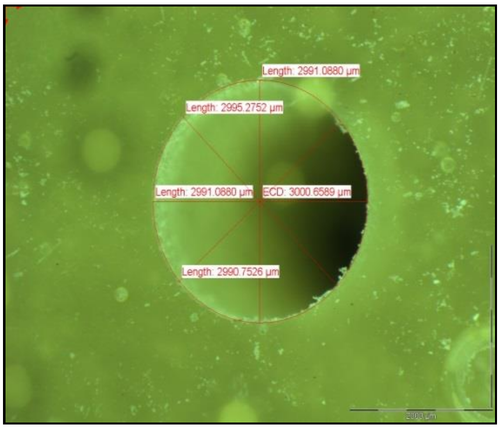
Length: 2991.0880 µm
Length: 2995.2752 µm
Length: 2991.0880 µm
ECD: 3000.6589 µm
Length: 2990.7526 µm

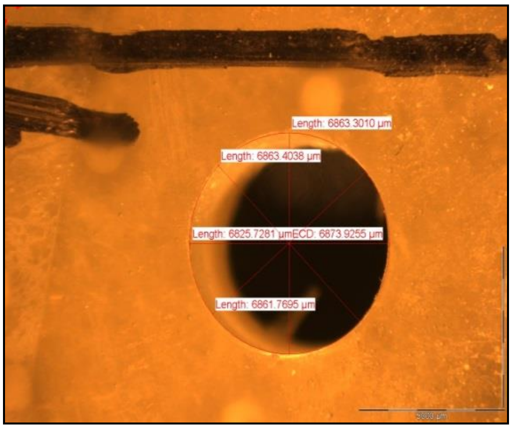
Length: 6863.3010 µm
Length: 6863.4038 µm
Length: 6825.7281 µm
ECD: 6873.9255 µm
Length: 6861.7695 µm

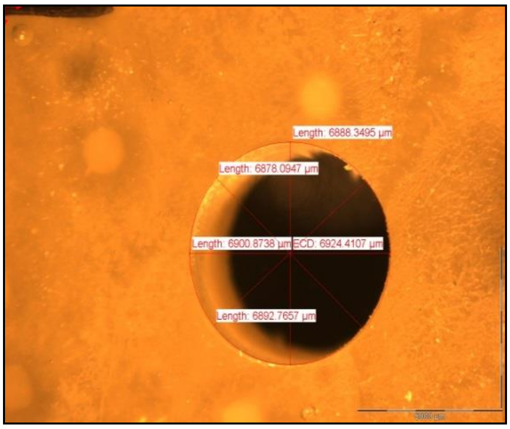
Length: 6888.3495 µm
Length: 6878.0947 µm
Length: 6900.8738 µm
ECD: 6924.4107 µm
Length: 6892.7657 µm

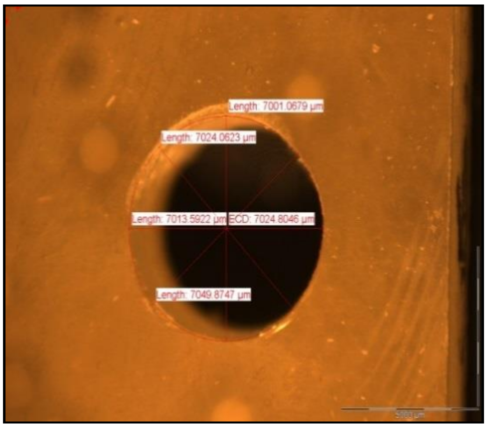
Length: 7001.0679 µm
Length: 7024.0623 µm
Length: 7013.5922 µm
ECD: 7024.8046 µm
Length: 7049.8747 µm

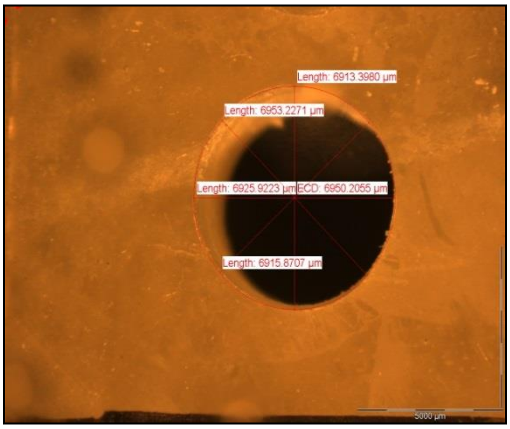
Length: 6913.3980 µm
Length: 6953.2271 µm
Length: 6925.9223 µm
ECD: 6950.2055 µm
Length: 6915.8707 µm
5000 µm

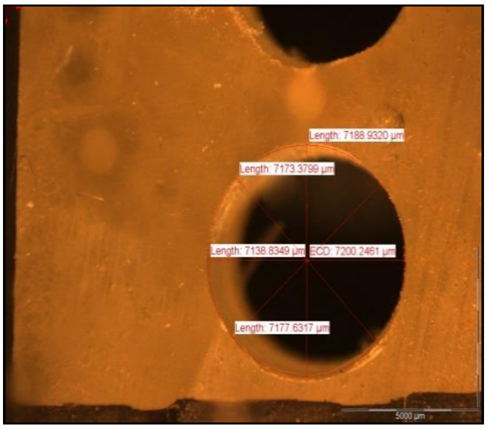
Length: 7188.9320 µm
Length: 7173.3799 µm
Length: 7138.8349 µm
ECD: 7200.2461 µm
Length: 7177.6317 µm
5000 µm

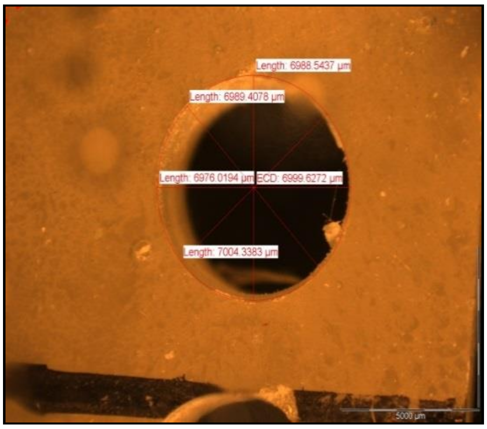
Length: 6988.5437 µm
Length: 6989.4078 µm
Length: 6976.0194 µm
ECD: 6999.6272 µm
Length: 7004.3383 µm
5000 µm

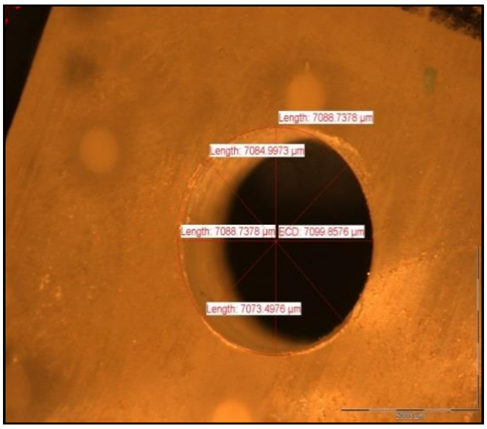
Length: 7088.7378 µm
Length: 7084.9973 µm
Length: 7088.7378 µm
ECD: 7099.8576 µm
Length: 7073.4976 µm

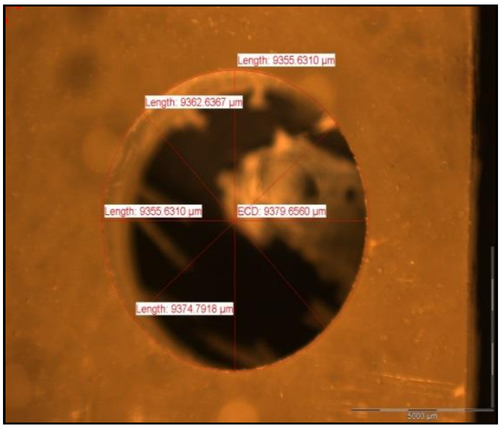
Length: 9355.6310 µm
Length: 9362.6367 µm
Length: 9355.6310 µm
ECD: 9379.6560 µm
Length: 9374.7918 µm
5000 µm

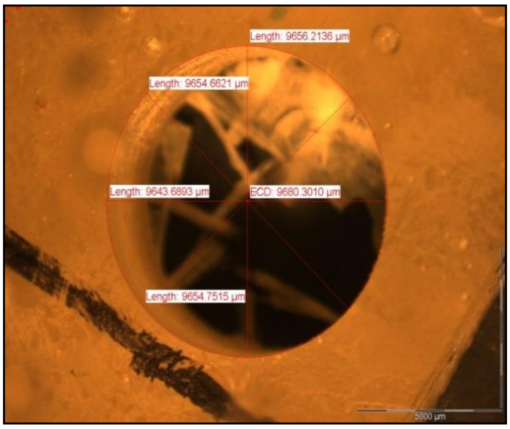
Length: 9656.2136 µm
Length: 9654.6621 µm
Length: 9643.6893 µm
ECD: 9680.3010 µm
Length: 9654.7515 µm
5000 µm

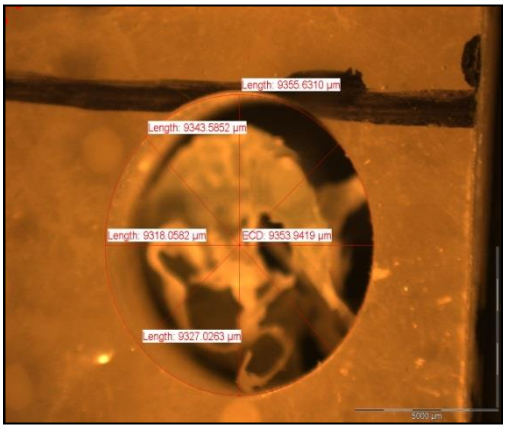
Length: 9355.6310 µm
Length: 9343.5852 µm
Length: 9318.0582 µm
ECD: 9353.9419 µm
Length: 9327.0263 µm
5000 µm

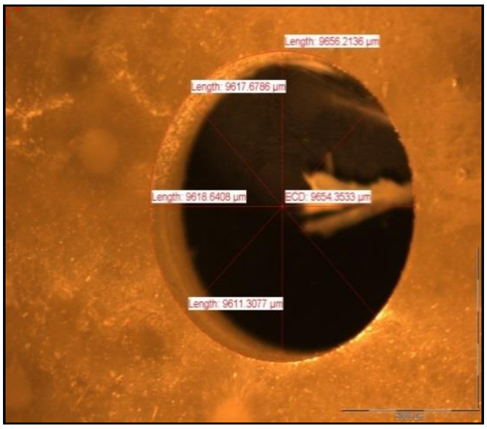
Length: 9656.2136 µm
Length: 9617.6786 µm
Length: 9618.6408 µm
ECD: 9654.3533 µm
Length: 9611.3077 µm

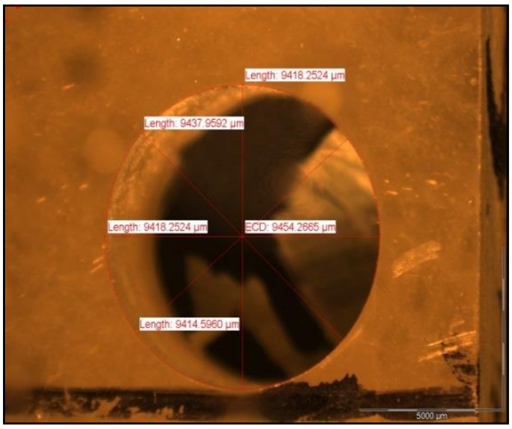
Length: 9418.2524 µm
Length: 9437.9592 µm
Length: 9418.2524 µm
ECD: 9454.2665 µm
Length: 9414.5960 µm
5000 µm

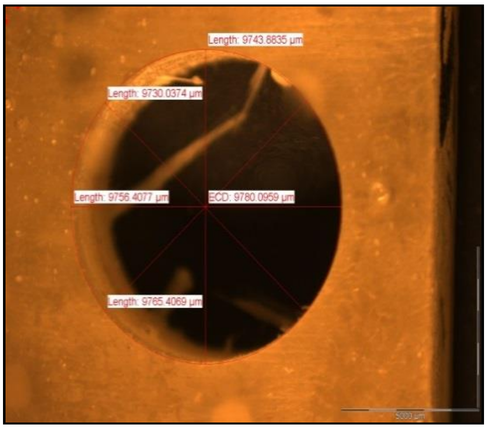
Length: 9743.8835 µm
Length: 9730.0374 µm
Length: 9756.4077 µm
ECD: 9780.0959 µm
Length: 9765.4069 µm

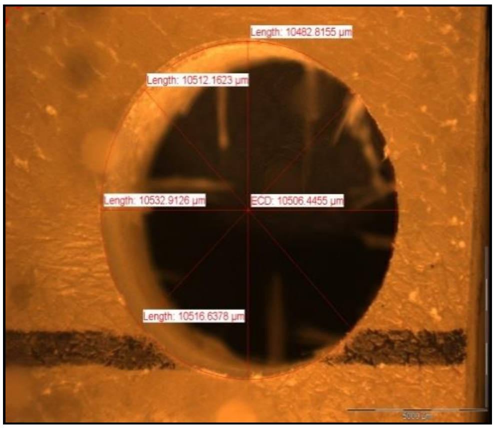
Length: 10482.8155 µm
Length: 10512.1623 µm
Length: 10532.9126 µm
ECD: 10506.4455 µm
Length: 10516.6378 µm

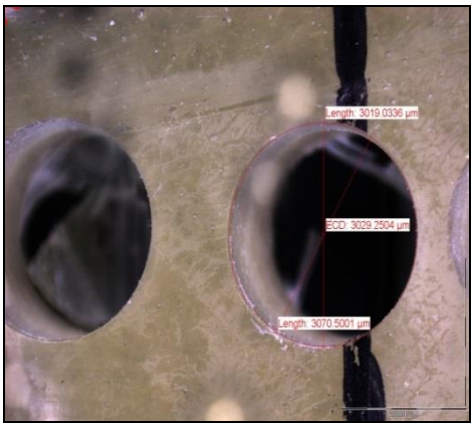
Length: 3019.0336 µm
ECD: 3029.2504 µm
Length: 3070.5001 µm

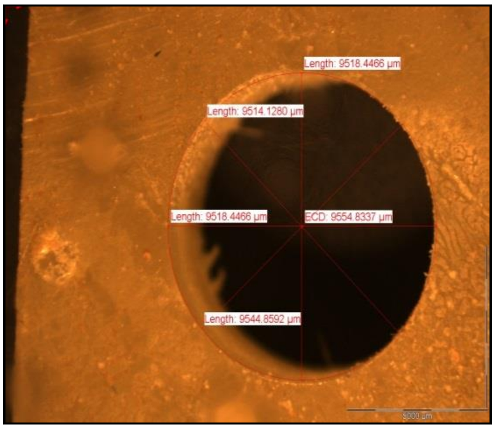
Length: 9518.4466 µm
Length: 9514.1280 µm
Length: 9518.4466 µm
ECD: 9554.8337 µm
Length: 9544.8592 µm

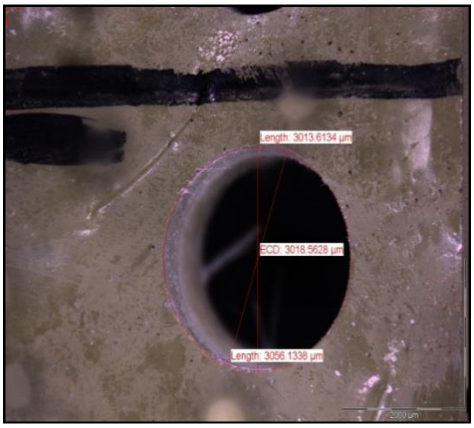
Length: 3013.6134 µm
ECD: 3018.5628 µm
Length: 3056.1338 µm

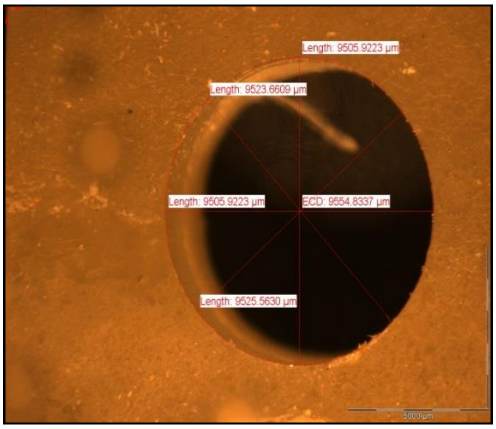
Length: 9505.9223 µm
Length: 9523.6609 µm
Length: 9505.9223 µm
ECD: 9554.8337 µm
Length: 9525.5630 µm

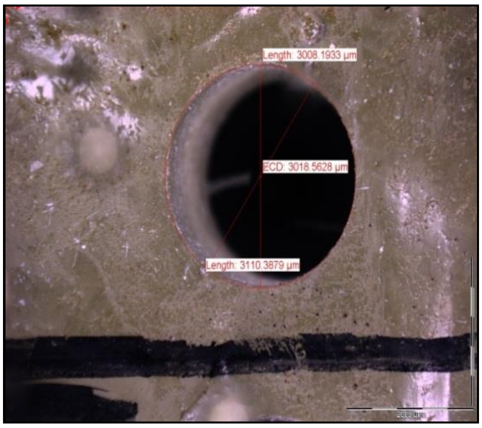
Length: 3008.1933 µm
ECD: 3018.5628 µm
Length: 3110.3879 µm

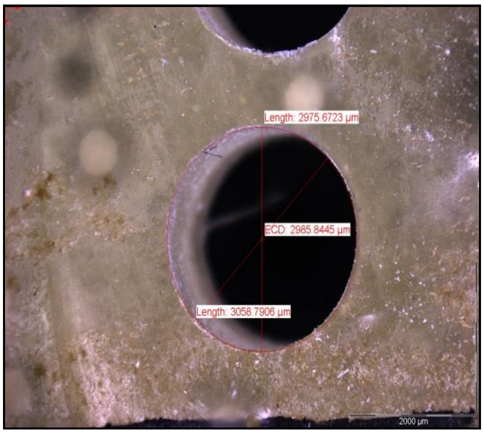
Length: 2975.6723 µm
ECD: 2985.8445 µm
Length: 3058.7906 µm
2000 µm

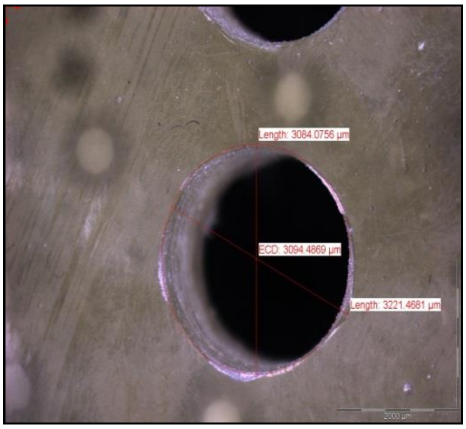
Length: 3084.0756 µm
ECD: 3094.4869 µm
Length: 3221.4681 µm
2000 µm

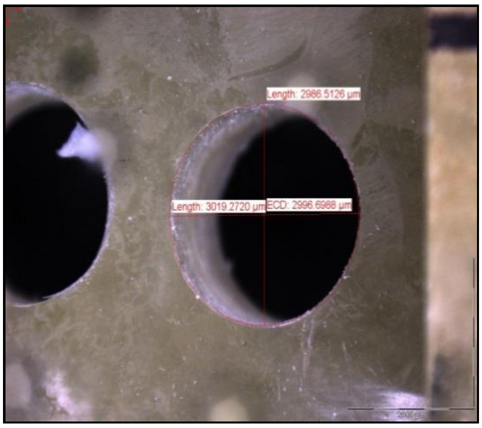
Length: 2986.5126 µm
Length: 3019.2720 µm
ECD: 2996.6988 µm

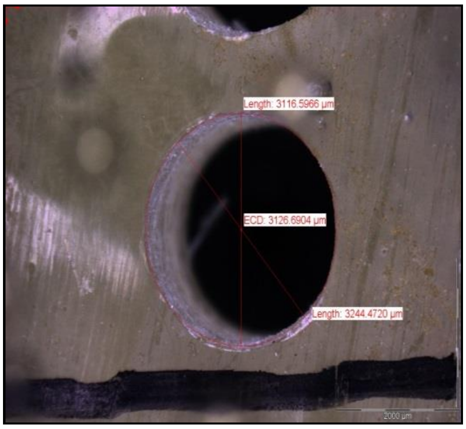
Length: 3116.5966 µm
ECD: 3126.6904 µm
Length: 3244.4720 µm
2000 µm

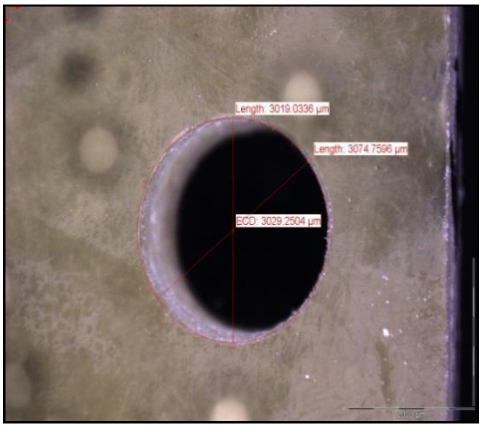
Length: 3019.0336 µm
Length: 3074.7596 µm
ECD: 3029.2504 µm

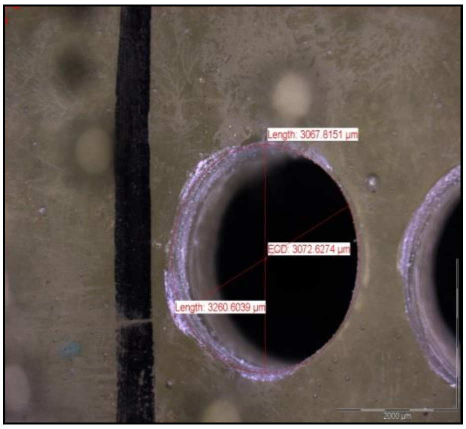
Length: 3067.8151 µm
ECD: 3072.6274 µm
Length: 3260.6039 µm
2000 µm

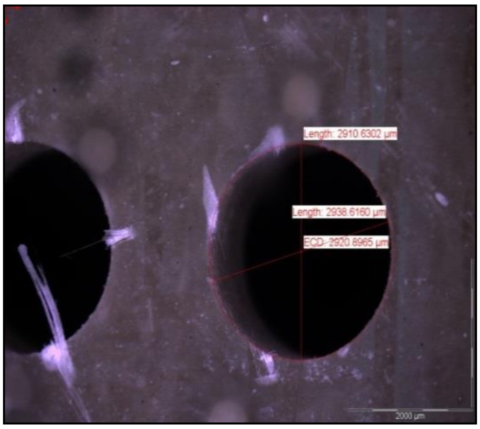
Length: 2910.6302 µm
Length: 2938.6160 µm
ECD: 2920.8965 µm
2000 µm

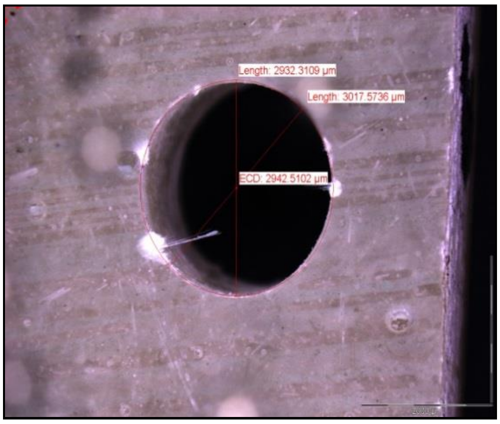
Length: 2932.3109 µm
Length: 3017.5736 µm
ECD: 2942.5102 µm

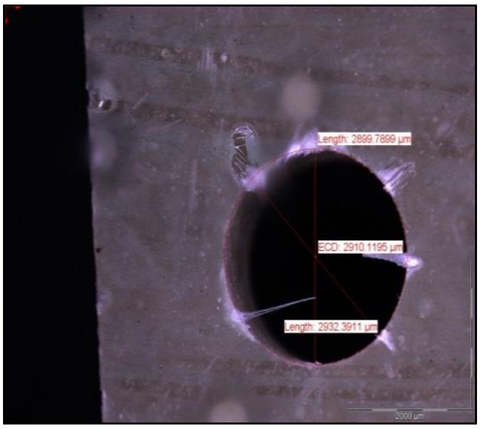
Length: 2899.7899 µm
ECD: 2910.1195 µm
Length: 2932.3911 µm
2000 µm

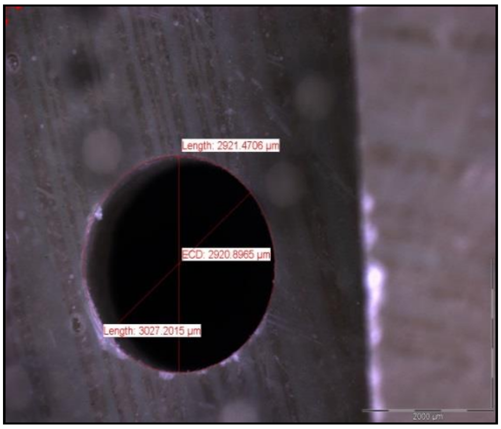
Length: 2921.4706 µm
ECD: 2920.8965 µm
Length: 3027.2015 µm
2000 µm

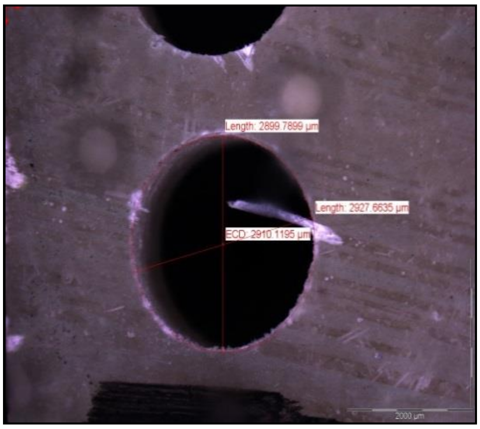
Length: 2899.7899 µm
Length: 2927.6635 µm
ECD: 2910.1195 µm
2000 µm

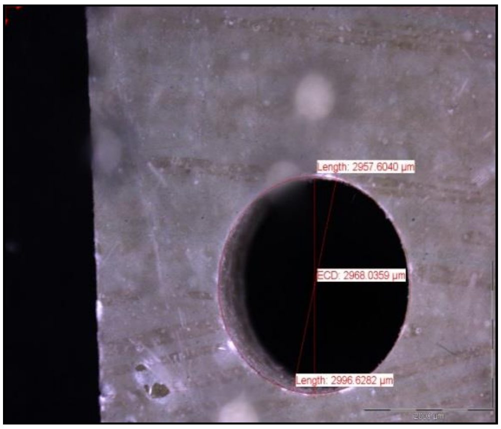
Length: 2957.6040 µm
ECD: 2968.0359 µm
Length: 2996.6282 µm

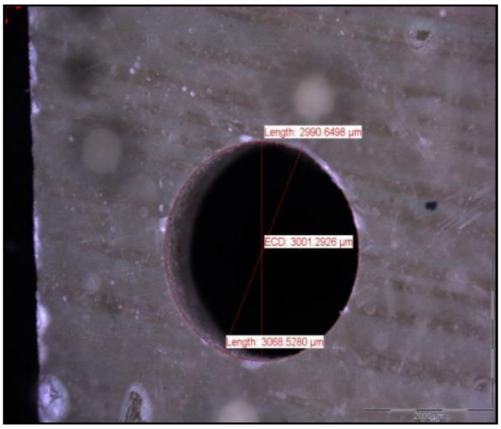
Length: 2990.6498 µm
ECD: 3001.2926 µm
Length: 3068.5280 µm
2000 µm

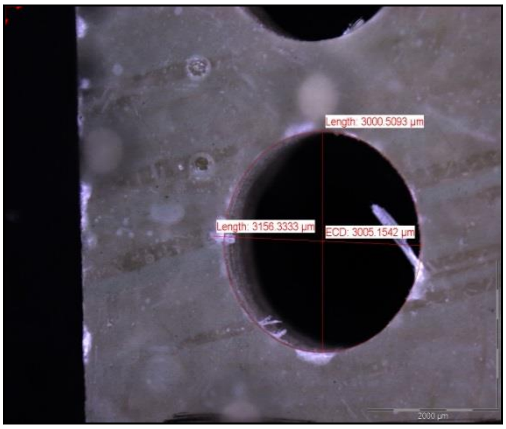
Length: 3000.5093 µm
Length: 3156.3333 µm
ECD: 3005.1542 µm
2000 µm

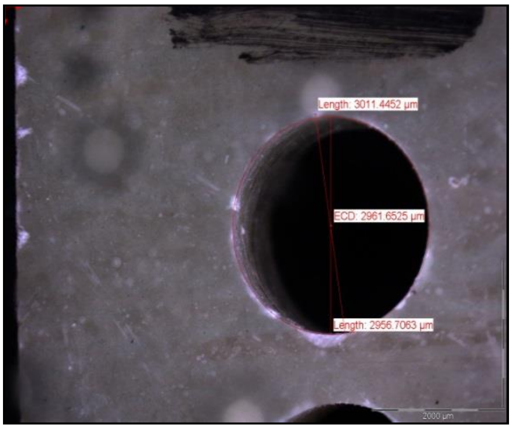
Length: 3011.4452 µm
ECD: 2961.6525 µm
Length: 2956.7063 µm
2000 µm

C.3 DPFEC

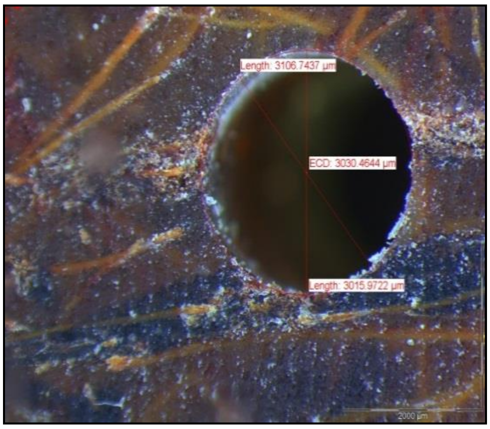
Length: 3106.7437 µm
ECD: 3030.4644 µm
Length: 3015.9722 µm
2000 µm

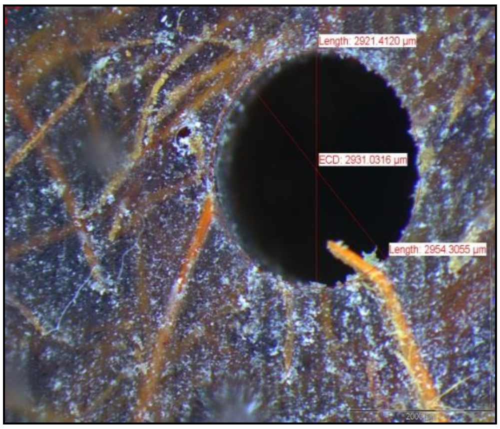
Length: 2921.4120 µm
ECD: 2931.0316 µm
Length: 2954.3055 µm

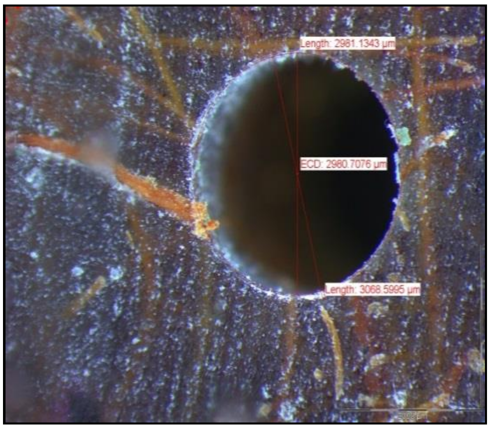
Length: 2981.1343 µm
ECD: 2980.7076 µm
Length: 3068.5995 µm

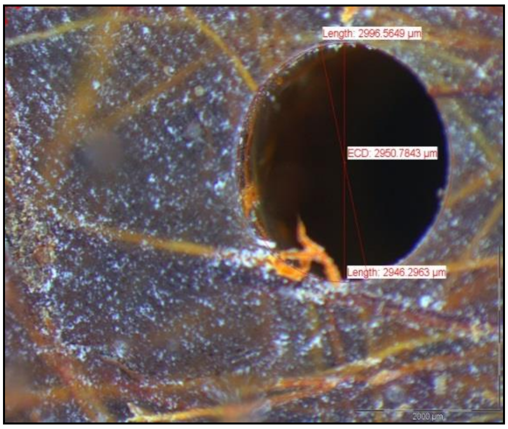
Length: 2996.5649 µm
ECD: 2950.7843 µm
Length: 2946.2963 µm
2000 µm

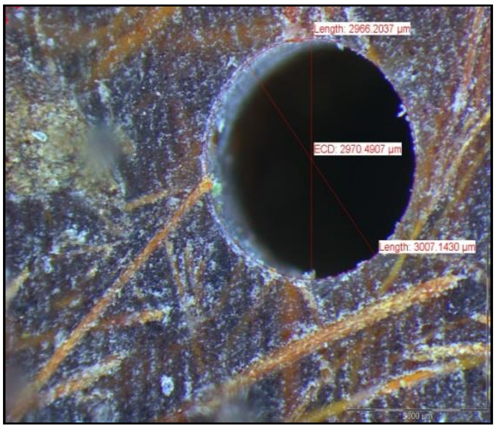
Length: 2966.2037 µm
ECD: 2970.4907 µm
Length: 3007.1430 µm

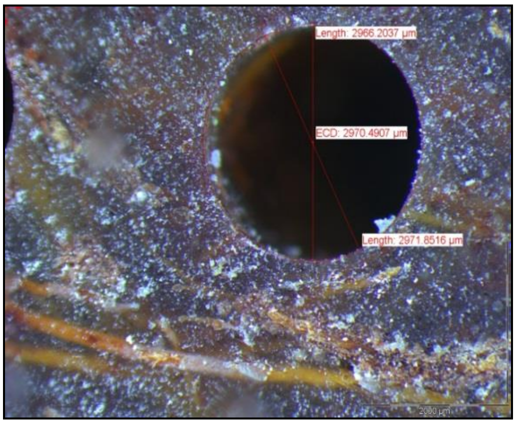
Length: 2966.2037 µm
ECD: 2970.4907 µm
Length: 2971.8516 µm
2000 µm

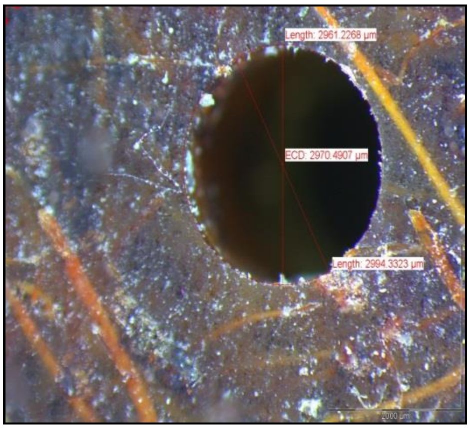
Length: 2961.2268 µm
ECD: 2970.4907 µm
Length: 2994.3323 µm
2000 µm

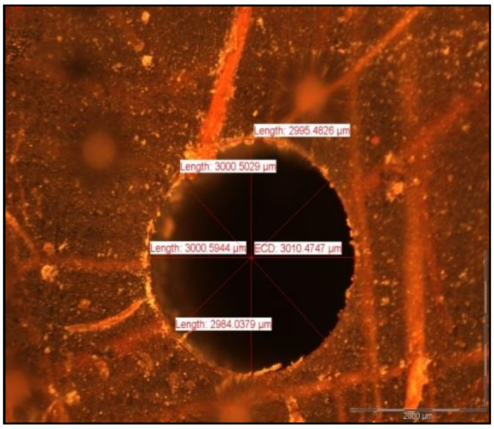
Length: 2995.4826 µm
Length: 3000.5029 µm
Length: 3000.5944 µm
ECD: 3010.4747 µm
Length: 2984.0379 µm
2000 µm

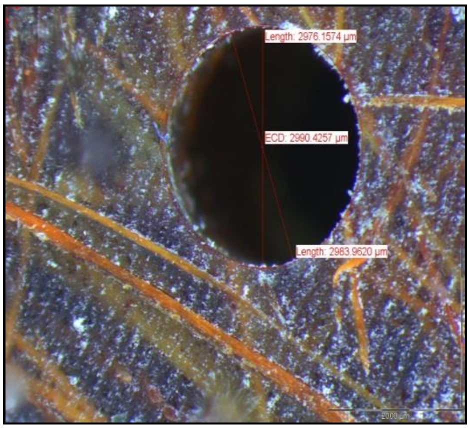
Length: 2976.1574 µm
ECD: 2990.4257 µm
Length: 2983.9620 µm
2000 µm

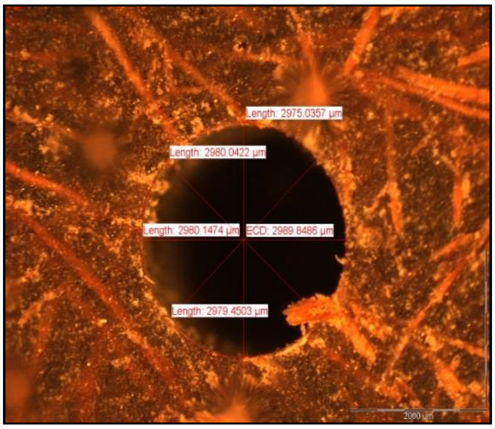
Length: 2975.0357 µm
Length: 2980.0422 µm
Length: 2980.1474 µm
ECD: 2989.8486 µm
Length: 2979.4503 µm
2000 µm

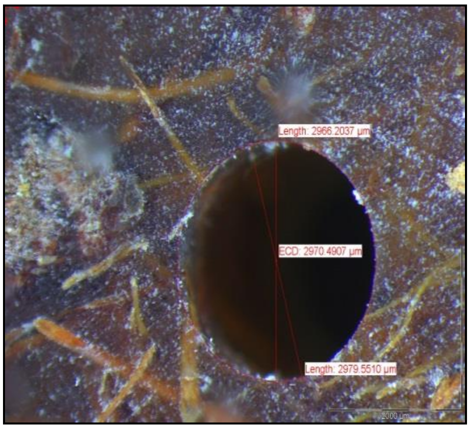
Length: 2966.2037 µm
ECD: 2970.4907 µm
Length: 2979.5510 µm
2000 µm

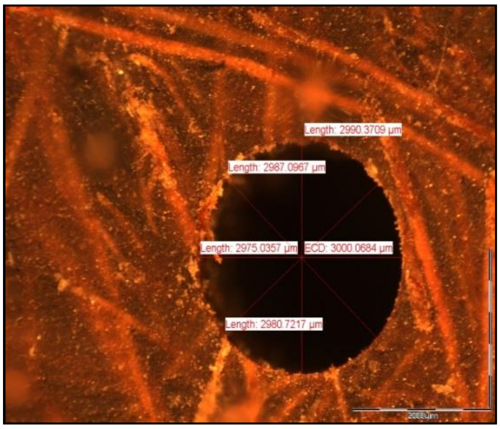
Length: 2990.3709 µm
Length: 2987.0967 µm
Length: 2975.0357 µm
ECD: 3000.0684 µm
Length: 2980.7217 µm

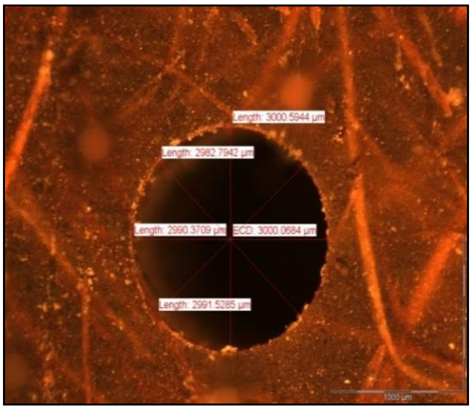
Length: 3000.5944 µm
Length: 2982.7942 µm
Length: 2990.3709 µm
ECD: 3000.0684 µm
Length: 2991.5285 µm
1000 µm

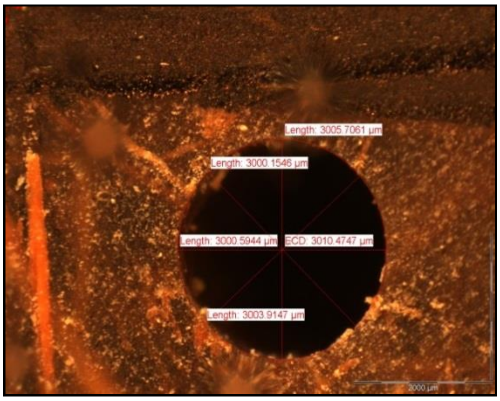
Length: 3005.7061 µm
Length: 3000.1546 µm
Length: 3000.5944 µm
ECD: 3010.4747 µm
Length: 3003.9147 µm
2000 µm

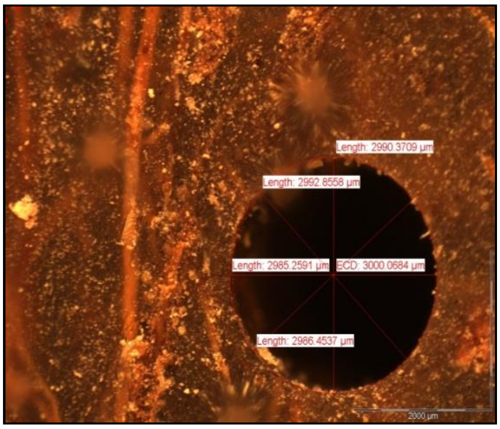
Length: 2990.3709 µm
Length: 2992.8558 µm
Length: 2985.2591 µm
ECD: 3000.0684 µm
Length: 2986.4537 µm

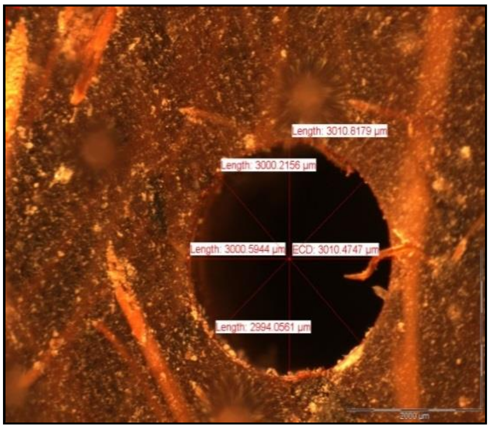
Length: 3010.8179 µm
Length: 3000.2156 µm
Length: 3000.5944 µm
ECD: 3010.4747 µm
Length: 2994.0561 µm

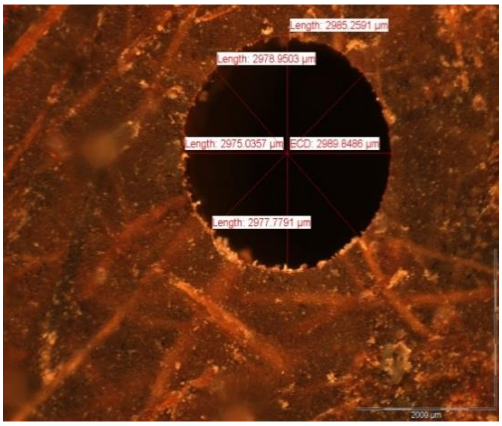
Length: 2985.2591 µm
Length: 2978.9503 µm
Length: 2975.0357 µm
ECD: 2989.8486 µm
Length: 2977.7791 µm

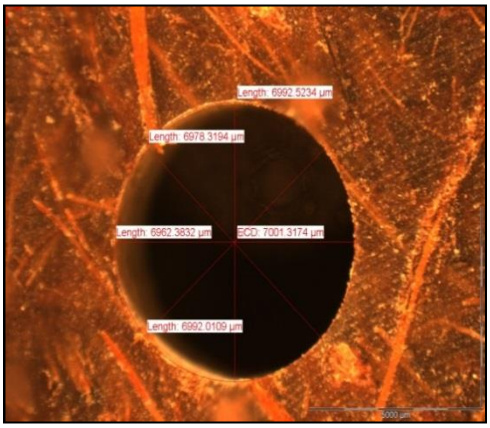
Length: 6992.5234 µm
Length: 6978.3194 µm
Length: 6962.3832 µm
ECD: 7001.3174 µm
Length: 6992.0109 µm

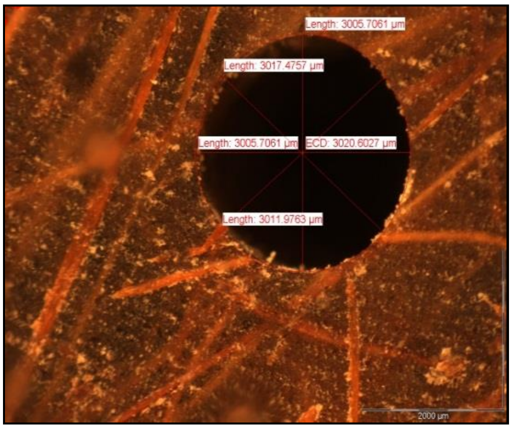
Length: 3005.7061 µm
Length: 3017.4757 µm
Length: 3005.7061 µm
ECD: 3020.6027 µm
Length: 3011.9763 µm

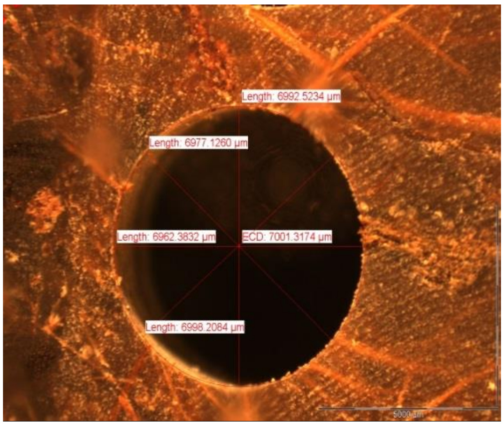
Length: 6992.5234 µm
Length: 6977.1260 µm
Length: 6962.3832 µm
ECD: 7001.3174 µm
Length: 6998.2084 µm

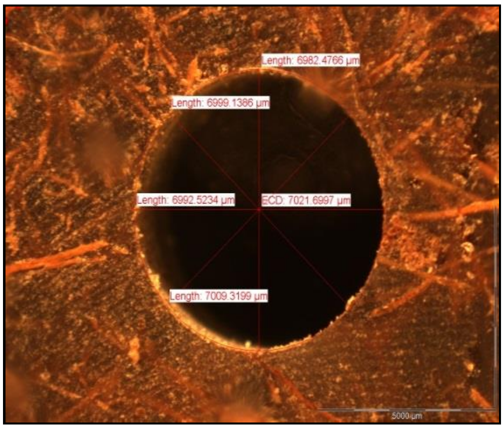
Length: 6982.4766 µm
Length: 6999.1386 µm
Length: 6992.5234 µm
ECD: 7021.6997 µm
Length: 7009.3199 µm
5000 µm

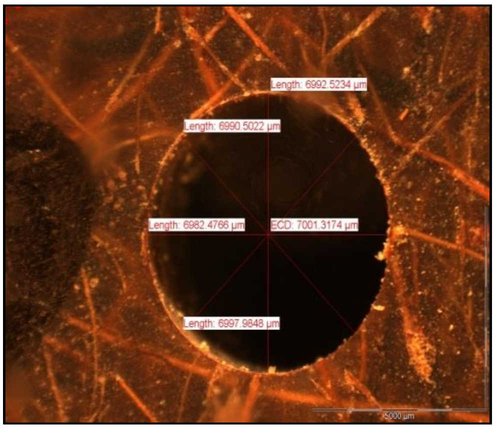
Length: 6992.5234 µm
Length: 6990.5022 µm
Length: 6982.4766 µm
ECD: 7001.3174 µm
Length: 6997.9848 µm
5000 µm

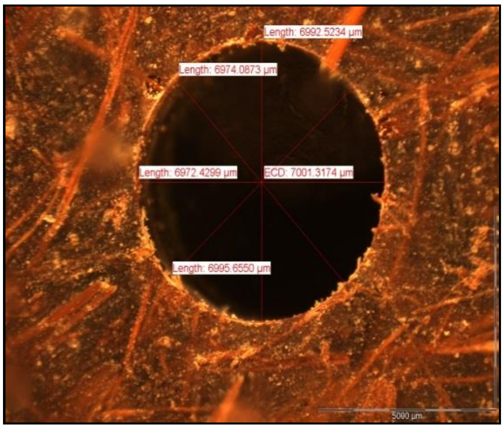
Length: 6992.5234 µm
Length: 6974.0873 µm
Length: 6972.4299 µm
ECD: 7001.3174 µm
Length: 6995.6550 µm
5000 µm

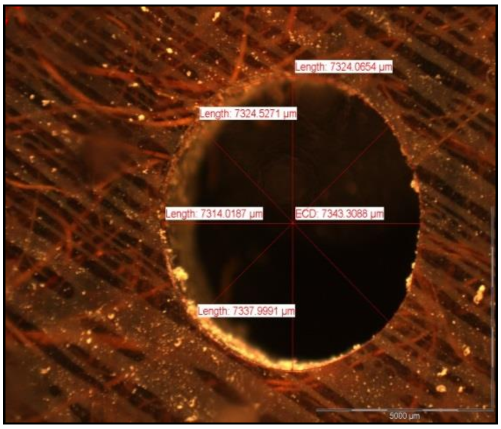
Length: 7324.0654 µm
Length: 7324.5271 µm
Length: 7314.0187 µm
ECD: 7343.3088 µm
Length: 7337.9991 µm
5000 µm

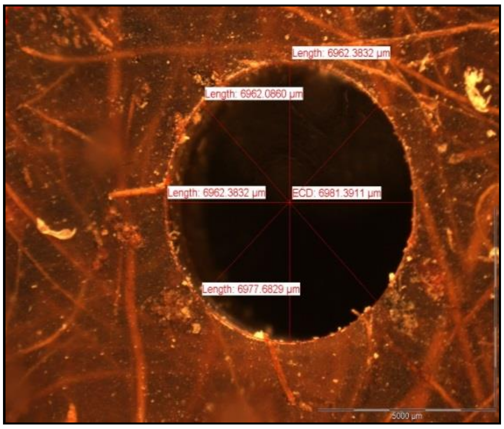
Length: 6962.3832 µm
Length: 6962.0860 µm
Length: 6962.3832 µm
ECD: 6981.3911 µm
Length: 6977.6829 µm
5000 µm

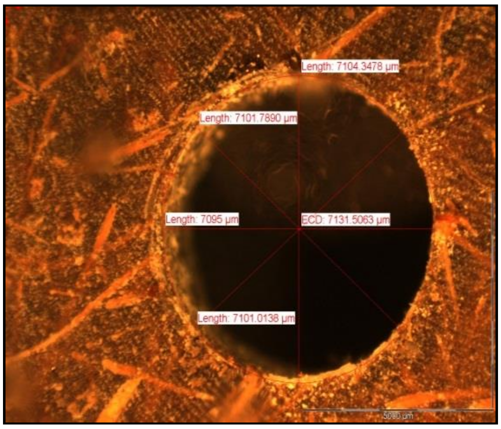
Length: 7104.3478 µm
Length: 7101.7890 µm
Length: 7095 µm
ECD: 7131.5063 µm
Length: 7101.0138 µm
5000 µm

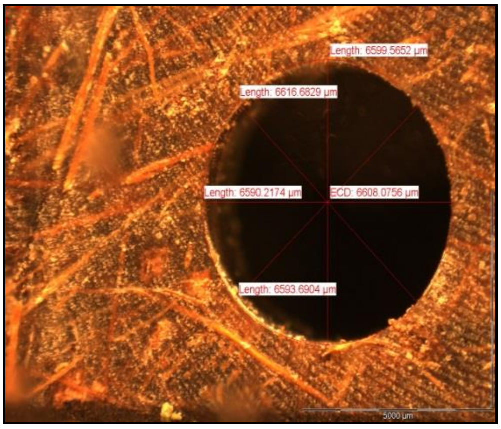
Length: 6599.5652 µm
Length: 6616.6829 µm
Length: 6590.2174 µm
ECD: 6608.0756 µm
Length: 6593.6904 µm
5000 µm

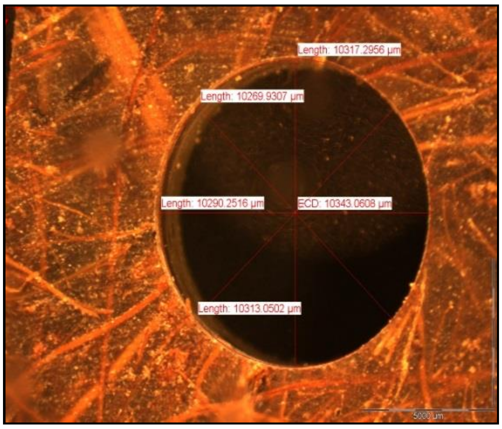
Length: 10317.2956 µm
Length: 10269.9307 µm
Length: 10290.2516 µm
ECD: 10343.0608 µm
Length: 10313.0502 µm
5000 µm

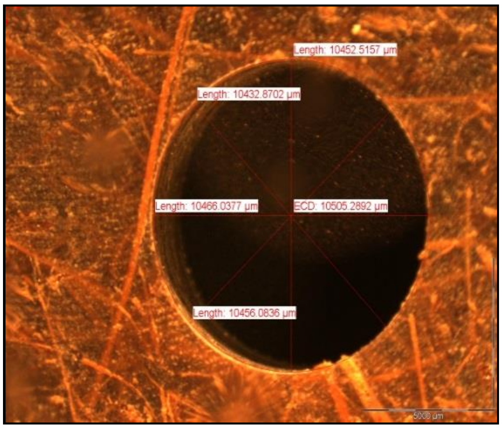
Length: 10452.5157 µm
Length: 10432.8702 µm
Length: 10466.0377 µm
ECD: 10505.2892 µm
Length: 10456.0836 µm
5000 µm

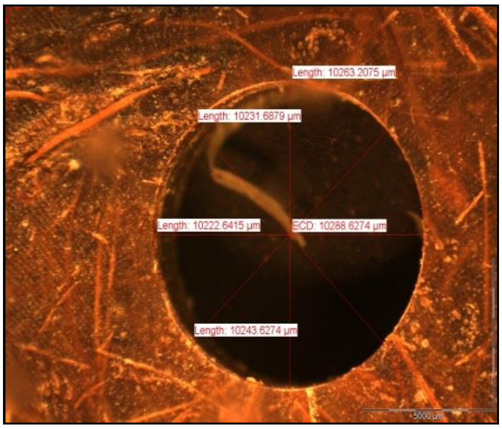
Length: 10263.2075 µm
Length: 10231.6879 µm
Length: 10222.6415 µm
ECD: 10288.6274 µm
Length: 10243.6274 µm
5000 µm

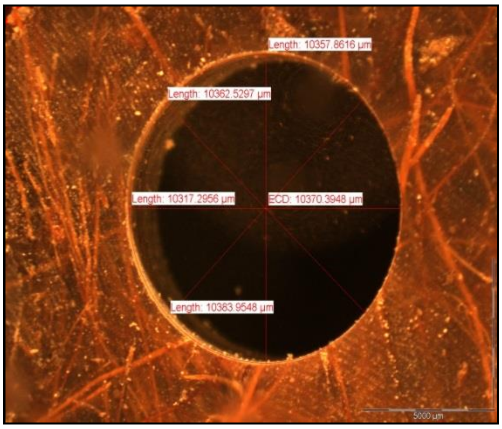
Length: 10357.8616 µm
Length: 10362.5297 µm
Length: 10317.2956 µm
ECD: 10370.3948 µm
Length: 10383.9548 µm
5000 µm

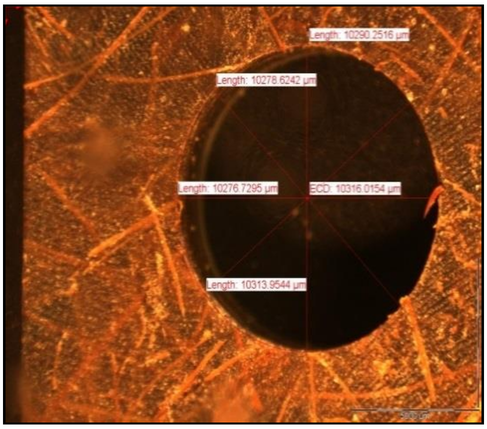
Length: 10290.2516 µm
Length: 10278.6242 µm
Length: 10276.7295 µm
ECD: 10316.0154 µm
Length: 10313.9544 µm

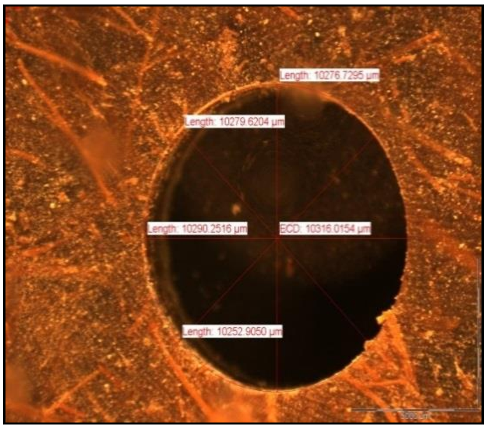
Length: 10276.7295 µm
Length: 10279.6204 µm
Length: 10290.2516 µm
ECD: 10316.0154 µm
Length: 10252.9050 µm

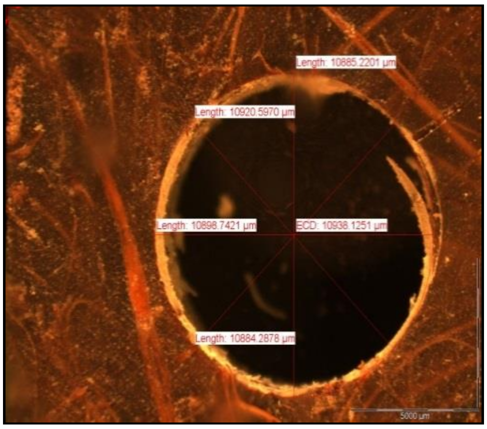
Length: 10885.2201 µm
Length: 10920.5970 µm
Length: 10898.7421 µm
ECD: 10938.1251 µm
Length: 10884.2878 µm
5000 µm

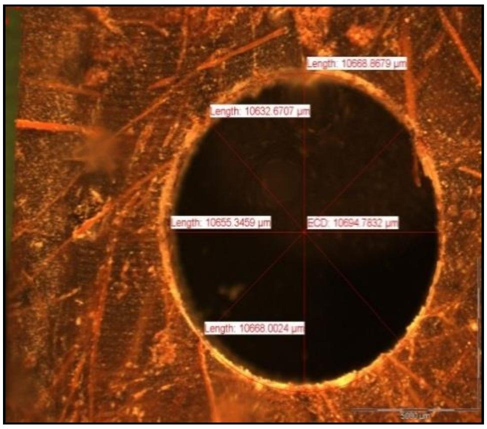
Length: 10668.8679 µm
Length: 10632.6707 µm
Length: 10655.3459 µm
ECD: 10694.7832 µm
Length: 10668.0024 µm

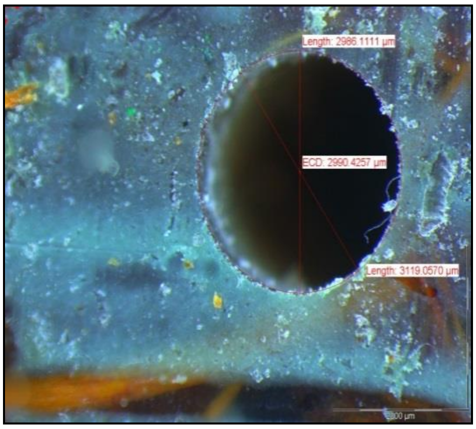
Length: 2986.1111 µm
ECD: 2990.4257 µm
Length: 3119.0570 µm

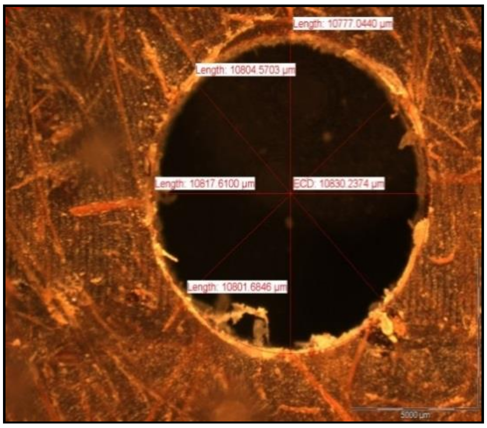
Length: 10777.0440 µm
Length: 10804.5703 µm
Length: 10817.6100 µm
ECD: 10830.2374 µm
Length: 10801.6846 µm
5000 µm

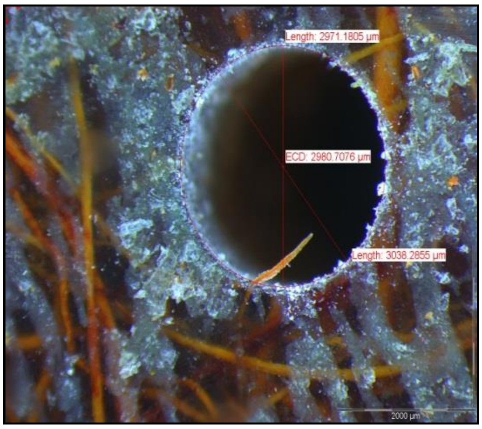
Length: 2971.1805 µm
ECD: 2980.7076 µm
Length: 3038.2855 µm
2000 µm

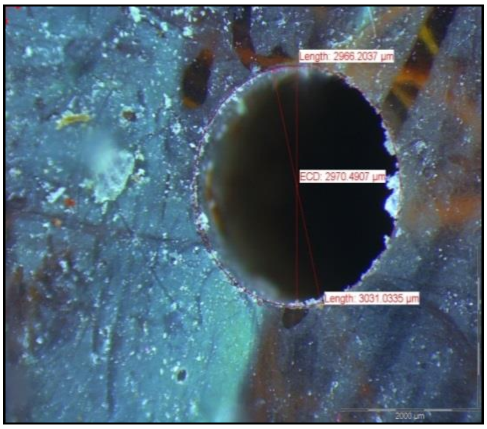
Length: 2966.2037 µm
ECD: 2970.4907 µm
Length: 3031.0335 µm
2000 µm

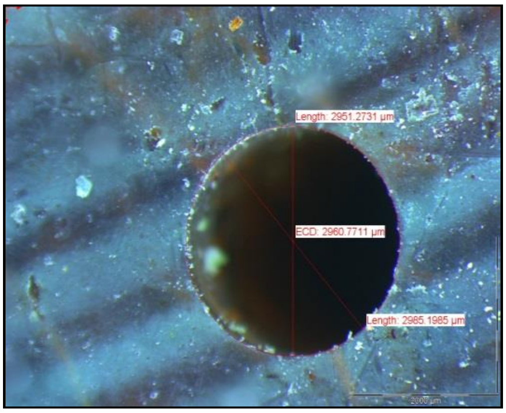
Length: 2951.2731 µm
ECD: 2960.7711 µm
Length: 2985.1985 µm
2000 µm

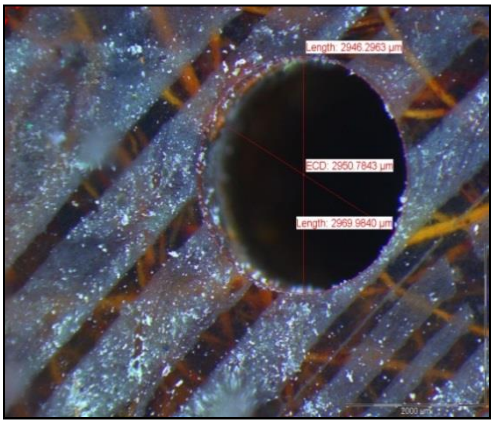
Length: 2946.2963 µm
ECD: 2950.7843 µm
Length: 2969.9840 µm
2000 µm

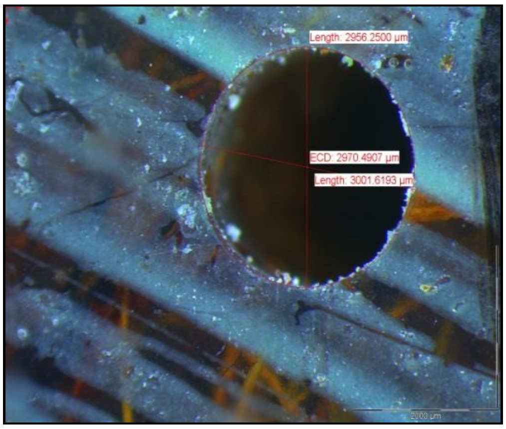
Length: 2956.2500 µm
ECD: 2970.4907 µm
Length: 3001.6193 µm
2000 µm

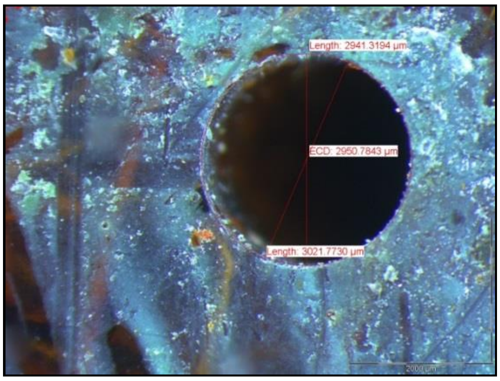
Length: 2941.3194 µm
ECD: 2950.7843 µm
Length: 3021.7730 µm
2000 µm

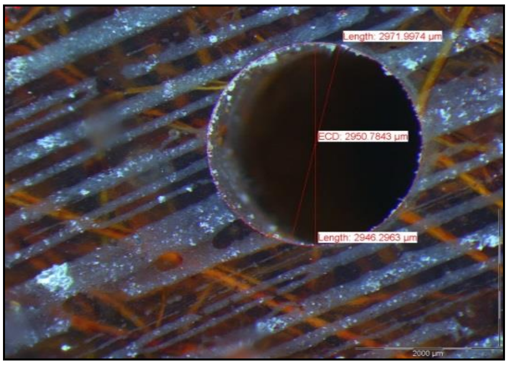
Length: 2971.9974 µm
ECD: 2950.7843 µm
Length: 2946.2963 µm
2000 µm

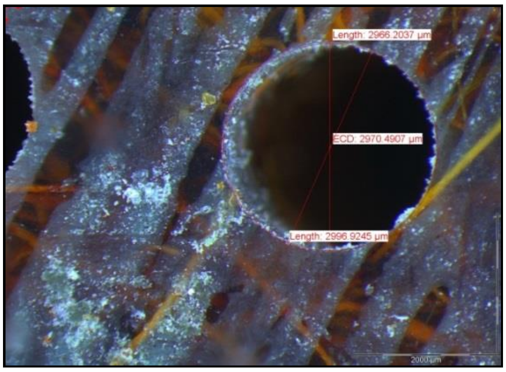
Length: 2966.2037 µm
ECD: 2970.4907 µm
Length: 2996.9245 µm
2000 µm